Kumamoto Journal of Science

Series A (Mathematics, Physics and Chemistry)

Vol. 3, No. 1, February 1957

Published by the
Faculty of Science, Kumamoto University
Kumamoto, Japan

熊本大學理學部紀要　第一部　第三卷　第一號　昭和三十二年二月
熊　本　大　學　理　學　部

CONTENTS

A METHOD OF EXPLORATION ON THE SEISMIC PROSPECTING

(When the curvature of travelling-time curve is small concerning refraction method)

Ryuzo ADACHI

(Received November 30, 1956)

In the previous Journal I discussed a problem for the exploration on the refraction method when the travelling-time curve is a parabola near to a straight line. In this paper I treated of a method of exploration when the travelling-time curve is any curve which has small curvature, and by this method we can calculate the velocity of wave in the under layer and the form of separation curve provided that the velocity of wave in the first layer and the form of the travelling-time curve are known without to know the functional expression of the travelling-time curve, and two examples were shown.

1. Introduction.

As shown in Fig. 1, let

$$y = y(x) \quad \cdots\cdots (1)$$

be the equation of the curve of separation, where y-axis is taken towards underground, and let

$$t = \varphi(X) \quad \cdots\cdots (2)$$

be the travelling-time curve. Then we have following relations[1]

$$t = \frac{v_1\sqrt{1+y'(x)^2}}{v_1(v_1 - Vy'(x_0))} + \frac{1}{v_2}\int_{x_0}^{x}\sqrt{1+y'(x)^2}\,dx + \frac{v_2\sqrt{1+y'(x)^2}}{v_1 - v_1 y'(x)} = \varphi(X) \quad \cdots\cdots (3)$$

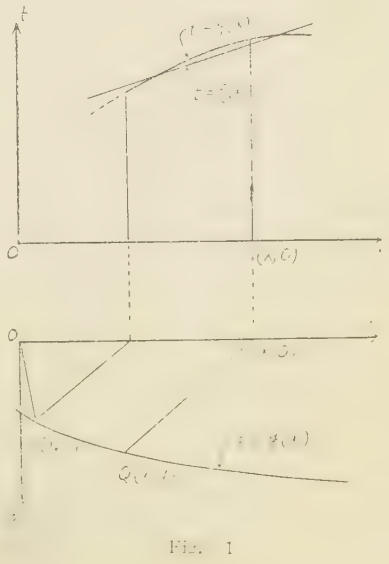

Fig. 1

$$X = x + \frac{v_1 + Vy'(x)}{V - v_1 y'(x)}\,y(x) \quad \cdots\cdots (4)$$

$$v_1 + Vy'(x) - v_1 v_2 \sqrt{1 + y'(x)^2}\,\frac{d}{dX}\varphi(X) = 0\ * \quad \cdots\cdots (5)$$

$$x_0 = \frac{v_1 - Vy'(x_0)}{V + v_1 y'(x_0)}\, y(x_0) \quad \cdots\cdots (6)$$

where v_1 and v_2 are the velocities of wave in the first layer and the second layer respectively, and $v_1 < v_2$, $V = \sqrt{v_2^2 - v_1^2}$, $y'(x) = \dfrac{d}{dx}y(x)$.

2. Determination of the Form of $y(x)$.

Let the curvature of $y = y(x)$ be very small, then the curvature of $t = \varphi(X)$ becomes very small also and it is near to a straight line and let it be

$$t = \varphi_0(X) = bX + c' \quad \cdots\cdots (7)$$

and put to

$$\varphi(X) = \Psi(X) + \varphi_0(X) = \Psi(X) + bX + c' \quad \cdots\cdots (8)$$

then

$$\Psi(X) = 0(h),\ \ \Psi'(X) = 0(h),\ \ \Psi''(X) = 0(h) \quad \cdots\cdots (9)$$

where h is a small positive value.
Next, let

$$y_0(x) = \beta x + c_0 \quad \cdots\cdots ((10$$

be the solution of Eq. (7), then from Eq. (5) we get

$$\alpha + \beta = \alpha\gamma\ \ b; \quad \cdots\cdots (11)$$

where $\gamma = \sqrt{1 + \beta^2}$, $\alpha = v_1/V$. Now we supposed that $\Psi(X)$ is very small, therefore the solution of Eq. (2) may be near to (10), and by first supposition, its curvature is very small, hence if we put to

$$y(x) = \tau(x) + \beta x + c'' \quad \cdots\cdots (12)$$

$$c_0 - c'' = 0(h)$$

$\tau(x)$ and $\tau'(x)$ may be very small, therefore we can suppose to

* One easily can prove Eq. (5) as follows.
Let the exit angle at R be α and put $\sin\theta = v_1/v_2$, $\tan\omega = y'$, then we have

$$\sin\alpha = v_1 \frac{d}{dX}\varphi(X),\ \ \alpha = \theta + \omega$$

$$\therefore\ \ v_1 \frac{d}{dX}\varphi(X) = \sin(\theta + \omega) = \frac{v_1 + Vy'}{v_2\sqrt{1 + y'^2}}$$

$$\tau(x) = 0(h), \quad \tau'(x) = 0(h) \quad \cdots\cdots (13).$$

Under these assumptions and neglecting $0(h^2)$, we have

$$\sqrt{1 + y'^2} = \sqrt{1 + (\tau' + \beta)^2} = \frac{1}{\gamma}(\gamma^2 + \beta\tau') = \frac{1}{\gamma}(1 + \beta y')$$

$$X = x + \frac{\alpha + y'}{1 - \alpha y'} y = x + \frac{\alpha + \beta}{1 - \alpha\beta} y + \frac{1 + \alpha^2}{(1 - \alpha\beta)^2} y\tau' \ *$$

Therefore putting to

$$U = x + \frac{\alpha + \beta}{1 - \alpha\beta} y \quad \cdots\cdots (14)$$

gives $X = U + 0(h)$ and by Eqs. (9), we get

$$\Psi(X) = \Psi(U), \quad \Psi'(X) = \Psi'(U) \quad \cdots\cdots (15)$$

therefore

$$\begin{aligned}\sqrt{1 + y'^2}\frac{d}{dX}\varphi(X) &= \frac{1}{\gamma}(\gamma^2 + \beta\tau')\left\{\frac{d}{dU}\Psi(U) + b\right\} \\ &= \gamma\frac{d}{dU}\Psi(U) + \frac{b}{\gamma}(1 + \beta y') \quad \cdots\cdots (16).\end{aligned}$$

Consequently, from the fundamental formula (5), we get

$$\frac{dy}{dx} = \frac{\gamma^3\alpha v_2}{1 - \alpha\beta}\frac{d}{dU}\Psi(U) + \beta \quad \cdots\cdots (17)$$

and from Eq. (14)

$$\frac{dU}{dx} = 1 + \frac{\alpha + \beta}{1 - \alpha\beta}\frac{dy}{dx} \quad \cdots\cdots (18)$$

(i) When $\alpha + \beta \neq 0$

Substituting Eq. (18) in Eq. (17), we get

$$\frac{dx}{dU} = \left[\frac{\gamma^2}{k}\left\{1 + \frac{\gamma\alpha v_2(\alpha + \beta)}{k} - \frac{d}{dU}\Psi(U)\right\}\right]^{-1} =$$

$$\frac{k}{\gamma^2}\left[1 - \frac{\gamma\alpha v_2(\alpha + \beta)}{k}\frac{d}{dU}\Psi(U)\right]$$

* When $1 - \alpha\beta = 0$, from Eq. (11) we get

$$\alpha + \frac{1}{\alpha} = \alpha v_2 b\sqrt{1 + \frac{1}{\alpha^2}} \quad \therefore \quad 1 = v_1 b.$$

This means that the irrational equation (11) with respect to β has no root, hence we suppose to $1 - \alpha\beta \neq 0$.

where $k = 1 - \alpha\beta$, therefore

$$x + e = \frac{k}{\gamma^2}\left[U - \frac{\gamma\alpha v_2(\alpha+\beta)}{k}\Psi(U)\right] \quad \cdots\cdots (19)$$

where $e =$ *an integrating constant.* Solving Eq. (19) with respect to U gives**

$$U = U_1 + \frac{\gamma\alpha v_2(\alpha+\beta)}{k}\Psi(U_1)$$

and substituting Eq. (14), we get

$$y(x) = \gamma\alpha v_2\,\Psi(U_1) + \beta x + \frac{\gamma^2}{\alpha+\beta}e \quad \cdots\cdots (20)$$

where $U_1 = \frac{\gamma^2}{k}(x - e)$ $\cdots\cdots (21)$.

Now let us suppose to $y(m) = c$, where m, c are given constants, then we get

$$\gamma\alpha v_2\,\Psi\left(\frac{\gamma^2}{k}(m+e)\right) + \beta m + \frac{\gamma^2}{\alpha+\beta}e = c \quad \cdots\cdots (22)$$

and solving this equation with respect to e gives***

$$e = \frac{\alpha+\beta}{\gamma^2}(c - \beta m) - \frac{\alpha v_2(\alpha+\beta)}{\gamma^2}\Psi(B) \quad \cdots\cdots (23),$$

therefore

$$U_1 = \frac{\gamma^2}{k}x + A - \frac{\gamma\alpha v_2(\alpha+\beta)}{k}\Psi(B)$$

** ***

From Eq. (19) we get

$$U = \frac{\gamma^2}{k}(x+e) + \frac{\gamma\alpha v_2(\alpha+\beta)}{k}\Psi(U)$$

and consider to solve this equation with respect to U by iterative method, that is, by the relations

$$U_1 = \frac{\gamma^2}{k}(x+e), \quad U_2 = U_1 + \frac{\gamma\alpha v_2(\alpha+\beta)}{k}\Psi(U_1)$$

$$U_3 = U_1 + \frac{\gamma\alpha v_2(\alpha+\beta)}{k}\Psi(U_2), \quad \cdots\cdots$$

$$\cdots\cdots$$

$$U_i = U_1 + \frac{\gamma\alpha v_2(\alpha+\beta)}{k}\Psi(U_{i-1}), \quad \cdots\cdots$$

calculate $U_2, U_3, U_4, \cdots\cdots$ successively and as $|\Psi|$ is very small, $\lim_{i\to\infty} U_i$ converges to a definite function uniformly and this limitting function is the solution of Eq. (19). But in this case $U - U_2 = 0(h)$ and we can put to $U = U_2$.

Similarly Eq. (23) is obtained from Eq. (22).

and

$$\Psi(U_1) = \Psi\left(\frac{\gamma^2}{k}x + A + 0(h)\right) = \Psi\left(\frac{\gamma^2}{k}x + A\right) \quad \cdots\cdots (24)$$

where

$$A = \frac{\alpha+\beta}{k}(c - \beta m),\ B = m + \frac{\alpha+\beta}{k}c \quad \cdots\cdots (25).$$

Consequently we get

$$y(x) = \gamma\alpha v_2\left[\Psi\left(\frac{\gamma^2}{k}x + A\right) - \Psi(B)\right] + \beta(x - m) + c \cdots\cdots (26).$$

By substituting Eq. (8) in Eq. (26), we have

$$y(x) = \gamma\alpha v_2\left[\varphi\left(\frac{\gamma^2}{k}x + A\right) - \varphi(B)\right] + \frac{\alpha + 2\alpha\beta + \beta}{k}(m - x) + c \cdots (27).$$

(ii) When $\alpha + \beta = 0$

In this case, we have $U = x$ and $k = \gamma^2$, therefore Eq. (17) becomes

$$\frac{dy}{dx} = \gamma\alpha v_2 \frac{d}{dx}\Psi(x) + \beta$$

and

$$y(x) = \gamma\alpha v_2\ \Psi(x) + \beta x + const$$

while $y(m) = c$ and $const = c - \beta m - \gamma\alpha v_2\ \Psi(m)$, therefore we get

$$y(x) = \gamma\alpha v_2[\Psi(x) - \Psi(m)] + \beta(x - m) + c$$

that is

$$y(x) = \gamma\alpha v_2[\varphi(x) - \varphi(m)] + \beta(x - m) + c \cdots\cdots (28).$$

This means that Eq. (27) is satisfied when $\alpha + \beta = 0$.

Consequently Eq. (27) is generally true and it is our required solution, and by this formula we can find each value of $y(x)$ corresponding to each value of x provided that the form of travelling-time curve and the values of v_0, v_1, b, c, m are given. Here it is not necessary to know the functional expression and it is sufficient to know the form of the travelling-time curve only.

Experimentally the values of $\varphi(X)$ when $X = X_1, X_2, X_3, \cdots\cdots$ are given and by interpolation we can calculate the value of $\varphi(X)$ for any value of X, or more practically plot the points $(X_1, \varphi(X_1))$, $(X_2, \varphi(X_2))$, $\cdots\cdots$ in a section paper with a scale as large as

we can and draw a curve passing through these points and then round the unevenness of this curve and from this curve we can find the value of $\varphi(X)$ for any value of X.

3. Modification of the Formula (27)

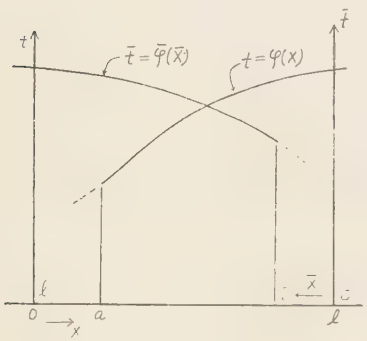

Fig. 2

In practice, as shown in Fig. 2, generally the travelling-time curve does not exist for small value of X, and let a be the least value of X when $\varphi(X)$ exists, then if $\frac{\gamma^2}{k}x + A < a$ in Eq. (27) we can not find the value of $y(x)$, and we take following procedure.

Let us experiment from the opposite direction taking the origin at $(l, 0)$ as shown in Fig. 2, and let the travelling-time curve be

$$t = \bar{\varphi}(X) \quad \cdots\cdots (29).$$

Then similarly as above, as the solution of (29) we get

$$\bar{y}(\bar{x}) = \gamma\alpha v_2\left[\bar{\varphi}\left(\frac{\gamma^2}{k}\bar{x} + \bar{A}\right) - \bar{\varphi}(B)\right] + \frac{\alpha + 2\alpha\beta^2 - \beta^3}{k}(m - \bar{x}) + c \quad \cdots\cdots (30)$$

where

$$\left.\begin{aligned} &\bar{y}(\bar{m}) = \bar{c}, \quad \bar{A} = \frac{\alpha - \beta}{k}(\bar{c} + \beta m) \\ &\bar{k} = 1 + \alpha\beta, \; B = m + \frac{\alpha - \beta}{k}c \end{aligned}\right\} \quad \cdots\cdots (31).$$

While $y(x)$ and $\bar{y}(\bar{x})$ must express same curve and we get

$$y(x) \equiv \bar{y}(l - x)$$

that is

$$\gamma\alpha v_2\left[\varphi\left(\frac{\gamma^2}{k}x + A\right) - \varphi(B)\right] + \frac{\alpha + 2\alpha\beta^2 + \beta^3}{k}(m - x) + c =$$

$$\gamma\alpha v_2\left[\bar{\varphi}\left(\frac{\gamma^2}{k}\overline{l - x} + A\right) - \bar{\varphi}(B)\right] + \frac{\alpha + 2\alpha\beta^2 - \beta^3}{k}(m - l + x) + c \quad \cdots\cdots (32).$$

When $\frac{\gamma^2}{k}x + A < a$, if $B \geqq a$, $\frac{\gamma^2}{k}(l - x) + \bar{A} \geqq \bar{a}$, $\bar{B} \geqq \bar{a}$, we can find the

value of $\bar{\varphi}\left(\frac{\gamma^2}{k}x + A\right)$ from *Eq.* (32).

Putting to $m = l - m$ gives $\bar{c} = c$, and Eq. (32) becomes as follows

$$\varphi\left(\frac{\gamma^2}{k}x + A\right) = \varphi(B) + \bar{\varphi}\left(\frac{\gamma^2}{\bar{k}}\overline{l-x} + \bar{A}\right) - \bar{\varphi}(\bar{B}) + \frac{2\gamma^3}{v_2 k\bar{k}}(x - m) \quad \cdots\cdots (33)$$

where

$$\left.\begin{aligned} A &= \frac{\alpha+\beta}{k}(c - \beta m), \qquad B = m + \frac{\alpha+\beta}{k}c \\ \bar{A} &= \frac{\alpha-\beta}{\bar{k}}\{c + \beta(l-m)\}, \quad \bar{B} = l - m + \frac{\alpha-\beta}{\bar{k}}c \end{aligned}\right\} \quad \cdots\cdots (34).$$

When $a \leqq B$, $\bar{a} \leqq \bar{B}$ and $k > 0$, $\bar{k} > 0$, we get

$$ka \leqq km + (\alpha+\beta)c, \quad \bar{k}\bar{a} \leqq \bar{k}(l-m) + (\alpha-\beta)c$$

$$\therefore \quad \bar{k}\bar{a} \leqq \bar{k}l + 2\alpha c - 2\alpha\beta m - ka,$$

and moreover if $\frac{\gamma^2}{k}x + A < a$ we obtain

$$\bar{a} < \frac{1}{\bar{k}}\left[\bar{k}l + 2\alpha c - 2\alpha\beta m - (\gamma^2 x + kA)\right] = \frac{\gamma^2}{\bar{k}}(l - x) + \bar{A},$$

that is, when

$$k > 0, \quad \bar{k} > 0, \quad a < B, \quad \bar{a} < \bar{B} \quad \cdots\cdots (35)$$

and

$$\frac{\gamma^2}{k}x + A < a \quad \cdots\cdots (36)$$

we get

$$\bar{a} < \frac{\gamma^2}{\bar{k}}(l - x) + \bar{A} \quad \cdots\cdots (37).$$

Accordingly, when inequalities (35) and (36) are satisfied, inequality (37) is satisfied also, and the value of $\varphi\left(\frac{\gamma^2}{k}x + A\right)$ is computable by Eq. (33), hence we have following formulas.

When $\frac{\gamma^2}{k}x + A \geqq a$

$$y(x) = v_1\gamma\kappa\left[\varphi\left(\frac{\gamma^2}{k}x + A\right) - \varphi(B)\right] + \frac{1}{k}(\alpha + 2\alpha\beta^2 + \beta^3)(m - x) + c \quad \cdots\cdots (27)_1$$

when $\dfrac{\gamma^2}{k}x + A < a$

$$y(x) = v_1\gamma\kappa\left[\bar{\varphi}\left(\frac{\gamma^2}{\bar{k}}\sqrt{l - x} + \bar{A}\right) - \bar{\varphi}(\bar{B})\right] + \frac{1}{\bar{k}}(\beta^3 - \alpha - 2\alpha\beta)(m - x) + c \quad \cdots\cdots (27)_2$$

Similarly

when $\dfrac{\gamma^2}{\bar{k}}\bar{x} + \bar{A} \geqq \bar{a}$

$$\bar{y}(\bar{x}) = v_1\gamma\kappa\left[\bar{\varphi}\left(\frac{\gamma^2}{\bar{k}}\bar{x} + \bar{A}\right) - \bar{\varphi}(\bar{B})\right] + \frac{1}{k}(\alpha + 2\alpha\beta^2 - \beta^3)(l - m - \bar{x}) + c \quad \cdots\cdots (27)_3$$

when $\dfrac{\gamma^2}{\bar{k}}\bar{x} + A < \bar{a}$

$$\bar{y}(\bar{x}) = v_1\gamma\kappa\left[\varphi\left(\frac{\gamma^2}{k}\sqrt{l - \bar{x}} - A\right) - \varphi(B)\right] - \frac{1}{k}(\alpha + 2\alpha\beta - \beta^3)(l - m - \bar{x}) + c \quad \cdots\cdots (27)_4$$

where $\kappa = \sqrt{1 + \alpha^2}$ and $v_1\kappa = \alpha v_2$ and by these formulas, $y(x)$ and $\bar{y}(\bar{x})$ are all computable from the travelling-time curve provided that $a \leqq B$, $\bar{a} \leqq B$, $k > 0$ and $\bar{k} > 0$.

In practice, it is usual that the values of v_2 and c are unknown, therefore at first we must consider how to determine them.

4. Determination of v_2 and c.

When Eqs. (12) and (13) are given, we get following relations

$$t_1 = \frac{v_2\sqrt{1 + y_0'^2}}{v_1(v_1 - Vy_0')}x_0 = \frac{v_2 x_0}{\gamma v_1 T^2}\{\gamma^2 T + (V + \beta v_1)\tau_0'\} \quad \cdots\cdots (38)$$

$$t_2 = \frac{1}{v_2}\int_{x_0}^{x}\sqrt{1 + y'^2}\,dx = \frac{1}{\gamma v_2}\{\beta\tau(x) + \gamma^2 x - \beta\tau_0 - \gamma^2 x_0\} \quad \cdots\cdots (39)$$

$$t_3 = \frac{v_2\sqrt{1 + y'^2}}{v_1(V - v_1 y')}y = \frac{v_2}{\gamma v_1 s^2}[\gamma^2 s\{\tau(x) + \beta x + c''\} + (v_1 + V\beta)(\beta x + c'') + \tau'(x)] \quad \cdots\cdots (40)$$

where

$$T = V(\alpha - \beta),\ s = Vk,\ y_0' = y'(x_0),\ \tau_0 = \tau(x_0),\ \tau_0' = \tau'(x_0) \cdots\cdots (41).$$

From Eq. (6) we get

$$x_0 = a_0 + \frac{\alpha - \beta}{\gamma^2}\tau(a_0) - \frac{v_2^2 c''}{V^2\gamma^4}\tau'(a_0) \cdots\cdots (42)$$

where

$$a_0 = \frac{\alpha - \beta}{\gamma^2} c'' \cdots\cdots (43).$$

Substituting Eqs. (42) (43) in Eqs. (38) (39), we get

$$\begin{aligned} t &= t_1 + t_2 + t_3 \\ &= -\frac{1}{\gamma\alpha v_2 k}\left[(\alpha^2 + \alpha\beta + \beta^2 + 1)\tau(x) + \frac{\kappa^2(\alpha + \beta)}{k^2}(\beta x + c'')\tau'(x)\right. \\ &\qquad \left. + \gamma^2(\alpha + \beta)x + k\tau(a_0) + (\alpha^2 + \beta^2 + 2)c''\right] \cdots\cdots (44). \end{aligned}$$

From Eq. (4) we get

$$x = x_1 - \frac{\kappa^2}{\gamma^4}(\beta x + c'')\tau'(x_1) - \frac{\alpha + \beta}{\gamma^2}\tau(x_1) \cdots\cdots (45)$$

where

$$x_1 = \frac{1}{\gamma^2}\{kX - (\alpha + \beta)c''\} \cdots\cdots (46)$$

and substituting Eqs. (45) (46) in Eq. (44) gives

$$\begin{aligned} t &= \frac{1}{\gamma\alpha v_2}[\tau(x_1) + \tau(a_0) + (\alpha + \beta)X + 2c''] \\ &= \frac{1}{\gamma\alpha v_2}\left[y(x_1) + \frac{\alpha + 2\alpha\beta^2 + \beta^3}{\gamma^2}X + y(a_0) + \frac{2\beta^2}{\gamma^2}c''\right] \cdots\cdots (47).* \end{aligned}$$

If we put to

$$\left.\begin{aligned} \tau(x) &= \gamma\alpha v_2\left[\Psi\left(\frac{\gamma^2}{k}x + A\right) - \Psi(B)\right] \\ c'' &= c - \beta m \end{aligned}\right\} \cdots\cdots (48)$$

we get

$$\frac{\gamma^2}{k}x + A = X,\quad \frac{\gamma^2}{k}a_0 + A = \frac{2\alpha}{k}(c - \beta m)$$

* we derived Eq. (47) under the condition $T \neq 0$ that is $\alpha \neq \beta$. But we can easily show that Eq. (47) is satisfied when $\alpha = \beta$ too.

and Eq. (47) becomes

$$t = \varphi(X) = \varphi(X) + bX + \Psi\left(\frac{2\alpha}{k}(c - \beta m)\right) - 2\Psi(B) + \frac{2}{\gamma\alpha v_2}(c - \beta m) \quad \cdots\cdots (49).$$

The equations (49) and (2) must coinside, therefore we get

$$\Psi\left(\frac{2\alpha}{k}(c - \beta m)\right) - 2\Psi(B) + \frac{2}{\gamma\alpha v_2}(c - \beta m) = c'$$

that is

$$\varphi\left(\frac{2\alpha}{k}(c - \beta m)\right) - 2\varphi(B) + \frac{2b}{k}(m + \beta c) + \frac{2(c - \beta m)}{\gamma\alpha v_2} = 0 \quad \cdots\cdots (50).$$

In most cases we have $\frac{\gamma^2}{k}(c - \beta m) > a$, hence we modify Eq. (50) as follows.

Put to $\frac{\gamma^2}{k}x + A = \frac{2\alpha}{k}(c - \beta m)$ that is $x = \frac{1}{\gamma^2}(\alpha - \beta)(c - \beta m)$,

then $\frac{\gamma^2}{k}(l - x) + A = l$ and from (33) we get

$$\varphi\left(\frac{\gamma^2}{k}(c - \beta m)\right) = \varphi(B) - \bar{\varphi}(l) - \bar{\varphi}(B) + \frac{2\gamma}{v_1 k k}\{(\alpha - \beta)c - \bar{k}m\},$$

and applying this relation to (50), we get

$$\bar{\varphi}(l) - \varphi(B) - \bar{\varphi}(\bar{B}) + \frac{2\gamma\kappa}{v_1 k k}c = 0 \quad \cdots\cdots (51).$$

Next, let n be a given value which satisfies that

$$\frac{\gamma^2}{k}n + A > a, \quad \frac{\gamma^2}{k}(l - n) + A > \bar{a} \text{ and } n \neq m$$

and putting to $x = n$ in Eq. (33), we get

$$\varphi\left(\frac{\gamma^2}{k}n + A\right) + \bar{\varphi}(B) = \varphi(B) + \bar{\varphi}\left(\frac{\gamma^2}{k}\overline{l - n} + \bar{A}\right) + \frac{2\gamma^3}{v_2 k\bar{k}}(n - m).$$

Consequently we have following equations

$$\begin{aligned} \varphi(D) + \bar{\varphi}(B) &= \varphi(B) + \bar{\varphi}(\bar{D}) + \frac{2\alpha\gamma^3(n - m)}{v_1\kappa k k} \cdots\cdots \text{(i)} \\ \bar{\varphi}(l) - \varphi(B) - \bar{\varphi}(\bar{B}) + \frac{2\gamma\kappa}{v_1 k k}c &= 0 \cdots\cdots \text{(ii)} \\ \alpha + \beta &= v_1 b\gamma\kappa \cdots\cdots \text{(iii)} \end{aligned} \quad \cdots\cdots (52)$$

where $D = \frac{\gamma^2}{k} n + A$, $D = \frac{\gamma^2}{\bar{k}} (l - n) + \bar{A}$.

The equations (52) are simultaneous equations with respect to α, β, c and solving them we can obtain the values of v and c provided that the forms of the travelling-time curves $t = \varphi(X)$, $t = \bar{\varphi}(X)$ and the values of v_1, b, l, m, n are known.

Here, we can give the value of b arbitrarily provided that $t = \varphi(X) = bX + c$ expresses a straight line which is approximated to $t = \varphi(X)$, that is $\Psi(X) = 0(h)$, while β and b are related by Eq. (2), therefore we can give the value of β arbitrarily provided that $\Psi(X) = 0(h)$, and in this case we have

$$\left.\begin{aligned} \varphi(D) + \bar{\varphi}(B) &= \varphi(B) + \bar{\varphi}(D) + \frac{2\alpha\gamma^3(n-m)}{v_1\kappa k\bar{k}} \quad \cdots\cdots \text{(i)} \\ \bar{\varphi}(l) - \varphi(B) - \bar{\varphi}(B) &+ \frac{2\gamma\kappa}{v_1 k\bar{k}} c = 0 \quad \cdots\cdots \text{(ii)} \end{aligned}\right\} \quad \cdots\cdots (53).$$

Solving Eqs. (53) with respect to α, c we get the values of v_2 and c provided that the forms of the travelling-time curves $t = \varphi(X)$, $t = \bar{\varphi}(X)$ and the values of v_1, β, l, m, n are given, and this procedure is simpler than the former.

Of course it is difficult to solve Eqs. (52) or (53) analytically, but to find their numeriaal approximate solutions is not so difficult. For this purpose, iterative method is very usefull one. For example from Eq. (53), we have

$$\left.\begin{aligned} \alpha &= \frac{v_1\kappa k\bar{k}}{2\gamma^3(n-m)} \cdot [\varphi(D) + \bar{\varphi}(B) - \varphi(B) - \bar{\varphi}(D)] \\ c &= \frac{v_1 k\bar{k}}{2\gamma\kappa} \cdot [\varphi(B) + \bar{\varphi}(B) - \bar{\varphi}(l)] \end{aligned}\right\} \quad \cdots\cdots (54)$$

and starting from any one pair (α_0, c_0) which are approximate values of (α, c) we compute (α_1, c_1), (α_2, c_2), (α_3, c_3), $\cdots\cdots$ successively by the relations

$$\left.\begin{aligned} \alpha_{i+1} &= \frac{v_1\kappa_i k_i \bar{k}_i}{2\gamma_i^3(n-m)} \cdot [\varphi(D_i) + \bar{\varphi}(B_i) - \varphi(B_i) - \bar{\varphi}(D_i)] \\ c_{i+1} &= \frac{v_1 k_i \bar{k}_i}{2\gamma_i\kappa_i} [\varphi(B_i) + \bar{\varphi}(B_i) - \bar{\varphi}(l)] \end{aligned}\right\} \quad \cdots\cdots (55)$$

where

$$\kappa_i = \sqrt{1 + \alpha_i^2}, \quad k_i = 1 - \alpha_i\beta, \quad \bar{k}_i = 1 + \alpha_i\beta$$

$$B_i = m + \frac{\alpha_i + \beta}{k_i} c_i, \quad D_i = \frac{\gamma_i n}{k_i} + \frac{\alpha_i + \beta}{k_i} (c_i - \beta m)$$

$$\bar{B}_i = l - m + \frac{\alpha_i - \beta}{\bar{k}_i} c_i, \quad \bar{D}_i = \frac{\gamma^2}{k_i}(l-n) + \frac{\alpha_i - \beta}{\bar{k}_i}\{c_i + \beta(l-m)\}.$$

and if α_i, c_i converge to definite values when $i \to \infty$, these limitting values are our required solutions. In practice, when $\alpha_{i+1} = \alpha_i$, $c_{i+1} = c_i$ are satisfied within required accuracy, we take these values as the solutions. Of course it may occur that α_i, c_i do not converge, and in this case, it means that starting formulas as Eqs. (55) are not suitable and another forms must be emploied. In order to converge some condition must be satisfied. But we can assert that when they converge, the limitting values are really our required solutions. Therefore in any case try above iteration and if $\alpha^{i+1} = \alpha_i$, $c_{i+1} = c_i$ are reached, they are our solutions, and really in most cases they converge well.

In order that α, c are computable from Eqs. (52) or (53), besides inequalities (36), following inequalities must be satisfied

$$D = \frac{1}{k}\left[\gamma^2 n + (\alpha+\beta)(c-\beta m)\right] \geqq a,$$

$$\bar{D} = -\frac{1}{\bar{k}}\left[\gamma^2(l-n) + (\alpha-\beta)\{c+\beta(l-m)\}\right] \geqq \bar{a} \cdots\cdots\cdots (56).$$

If k, $\bar{k}$ are positive (in most cases they are so), (56) becomes

$$L_2 \leqq n \leqq L_1 \cdots\cdots (57)$$

where

$$L_1 = l + \frac{1}{\gamma^2}\left[(\alpha-\beta)\{c+\beta(l-m)\} - \bar{k}\bar{a}\right], \quad L_2 = \frac{1}{\gamma^2}\left[ka - (\alpha+\beta)(c-\beta m)\right]$$

Next, in Eq. (54), if $v_1 \kappa k \bar{k}/2\gamma^3(n-m)$ is large, $\varphi(D) + \bar{\varphi}(B) - \varphi(B) - \bar{\varphi}(D)$ is very small and the error of α becomes large, therefore we should take $|n-m|$ as large as possible. While we have

$$L_1 - m = \frac{k}{\gamma^2}(B - \bar{a}) \geqq 0, \quad m - L_2 = \frac{k}{\gamma^2}(B - a) \geqq 0.$$

Consequently put to

$$n = L_1 \quad when \quad \bar{k}(\bar{B} - \bar{a}) \geqq k(B-a)$$

$$n = L_2 \quad when \quad \bar{k}(\bar{B} - \bar{a}) < k(B-a).$$

But really, we know approximate values of L_1, L_2 etc only, therefore we must put to

$n =$ (*known approximate value of* L_1) $-$ (*small positive value*)

or

$n =$ (*known approximate value of* L_2) $+$ (*small positive value*)

in order to avoid that $n > L_1$ or $n < L_2$.

5. When $\beta = 0$

Let $t = \varphi_0(X) = bX + c'$, $t = \bar{\varphi}_0(\bar{X}) = \bar{b}\bar{X} + \bar{c}'$ be approximate straight lines of $t = \varphi(X)$, $\bar{t} = \bar{\varphi}(X)$ respectively and if $b \fallingdotseq \bar{b}$, it means that the curve $y = y(x)$ is nearly parallel to x-axis. Therefore in this case we can put to $\beta = 0$ and the computation becomes very simple as follows.

$$\gamma = k = \bar{k} = 1, \quad A = \bar{A} = \alpha c, \quad B = m + \alpha c, \quad \bar{B} = l - m + \alpha c$$

$$y(x) = v_1\kappa\,[\varphi(x + \alpha c) - \varphi(m + \alpha c)] + \alpha(m - x) + c \cdots\cdots (27)'_1$$

$$\text{when } x + \alpha c \geqq a$$

$$y(x) = v_1\kappa\,[\bar{\varphi}(l + \alpha c - x) - \bar{\varphi}(l - m + \alpha c)] - \alpha(m - x) + c \cdots\cdots (27)'_2$$

$$\text{when } x + \alpha c < a$$

$$\bar{y}(\bar{x}) = v_1\kappa\,[\bar{\varphi}(\bar{x} + \alpha c) - \bar{\varphi}(l - m + \alpha c)] + \alpha(l - m - \bar{x}) + c \cdots\cdots (27)'_3$$

$$\text{when } \bar{x} + \alpha c \geqq \bar{a}$$

$$\bar{y}(\bar{x}) = v_1\kappa\,[\varphi(l + \alpha c - \bar{x}) - \varphi(m + \alpha c)] - \alpha(l - m - \bar{x}) + c \cdots\cdots (27)'_4$$

$$\text{when } \bar{x} + \alpha c < \bar{a}$$

$$\alpha = \frac{v_1\kappa}{2(n - m)}\,[\varphi(n + \alpha c) + \bar{\varphi}(l - m + \alpha c) - \varphi(m + \alpha c) - \bar{\varphi}(l + \alpha c - n)] \cdots\cdots (54)'$$

$$c = \frac{v_1}{2\kappa}\,[\varphi(m + \alpha c) + \bar{\varphi}(l - m + \alpha c) - \bar{\varphi}(l)]$$

6. Examples.

Example 1.

Following data and $v_1 = 490m/sec$, $l = 200m$ are given. Find the value of v_2 and each value of $y(x)$ corresponding to $x = 0m$, $20m$, $40m$, ·····, $2000m$.

$X, \bar{X}(m)$	40	50	60	80	100	120	140	160	180	200	210	220
$\varphi(X)(sec)$	0.163	0.172	0.180	0.196	0.210	0.224	0.237	0.251	0.264	0.274	0.278	0.281
$\bar{\varphi}(X)(sec)$	0.144	0.154	0.163	0.181	0.199	0.216	0.234	0.250	0.265	0.275	[illegible]	[illegible]

Solution:-

The graphs of $t = \varphi(X)$ and $t = \bar{\varphi}(X)$ are shown in Fig. 3, and their curvatures

are both small, and straight lines drawn approximately to them are

$$t = \varphi_0(X) = 0.000725X + 0.132 \cdots\cdots \text{(i)}$$

$$t = \bar{\varphi}_0(X) = 0.000860\bar{X} + 0.107 \cdots\cdots \text{(ii)}$$

where units of length, time are taken meter, second respectively.

Solving these equations with ordinary method which is used at present, we get $y_0(x) = -0.036x + 35.1$ and 1.26×10^3 *m/sec* as an approximate value of v_2.
Therefore we put to

$$\alpha_0 \fallingdotseq 490/\sqrt{(1.26 \times 10^3)^2 - (490)^2} \fallingdotseq 0.422, \quad c_0 \fallingdotseq -0.036 \times 100 + 35.1 \fallingdotseq 31.5$$

and $\beta_0 \fallingdotseq -0.036 \fallingdotseq 0$, therefore we take the formulas when $\beta = 0$. Hence putting to $m = \frac{l}{2}$ we get $B = B = \frac{l}{2} + \alpha c \fallingdotseq 113$, $a = \bar{a} = 40$, $\therefore\ B - a = B - \bar{a}$, $L_1 \fallingdotseq 173$ and putting to $n = 170$ in Eqs. (54), we get following equations

$$\left.\begin{aligned} \alpha &= \frac{49\kappa}{14}\left[\varphi(170 + \alpha c) + \bar{\varphi}(100 + \alpha c) - \varphi(100 + \alpha c) - \bar{\varphi}(30 + \alpha c)\right] \\ c &= \frac{245}{\kappa}\left[\varphi(100 + \alpha c) + \bar{\varphi}(100 + \alpha c) - \bar{\varphi}(200)\right] \end{aligned}\right\} \text{(iii).}$$

Solving these equations by iteration we get following result

i	0	1	2	3	4
α_i	0.422	0.418	0.4165	0.4163	0.4163
C_i	31.5	34.9	35.38	35.44	35.44

Consequently $\alpha = 0.4163$, $c = 35.44$ and $\kappa = 1.0831$, $v_2 = v_1\kappa/\alpha = 1.28 \times 10^3 m/sec$
$\alpha c = 14.75$, $B = B = 114.75$, therefore we get following relations

when $x \geqq 25$

$$y(x) = 530.8\varphi(x + 14.8) - (0.4163x + 39.75) \cdots\cdots \text{(iv)}$$

when $x < 25$

$$y(x) = 530.8\bar{\varphi}(214.8 - x) - (118.50 - 0.4163x) \cdots\cdots \text{(v)}$$

Similarly we get

when $\bar{x} \geqq 25$

$$\bar{y}(\bar{x}) = 530.8\bar{\varphi}(\bar{x} + 14.8) - (0.4163\bar{x} + 35.24) \cdots\cdots \text{(vi)}$$

when $\bar{x} < 25$

$$\bar{y}(\bar{x}) = 530.8\varphi(214.8 - \bar{x}) - (123.01 - 0.4163\bar{x}) \quad \cdots\cdots\cdots\cdots\cdots\cdots\cdots\cdots \text{(vii)}$$

and from these relations we got following result

$x, \bar{x}(m)$	0	20	40	60	80	100	120	140	160	180	200
$y(x)(m)$	30.3	34.5	37.1	37.1	36.5	35.4	34.4	33.3	32.0	29.8	25.6
$\bar{y}(\bar{x})(m)$	25.6	29.8	32.1	33.3	34.4	35.4	36.5	37.0	36.8	34.5	30.3

and these show that $y(x) \fallingdotseq \bar{y}(200 - x)$.

Here the values of $\varphi(54.8)$, $\varphi(74.8)$, etc. are obtained from the graphs shown in Fig. 3 (actually it is drawn in a section paper-1 *division=2.5m.m and 1 division expresses 1m in abscissa and 0.001 sec in ordinate*).

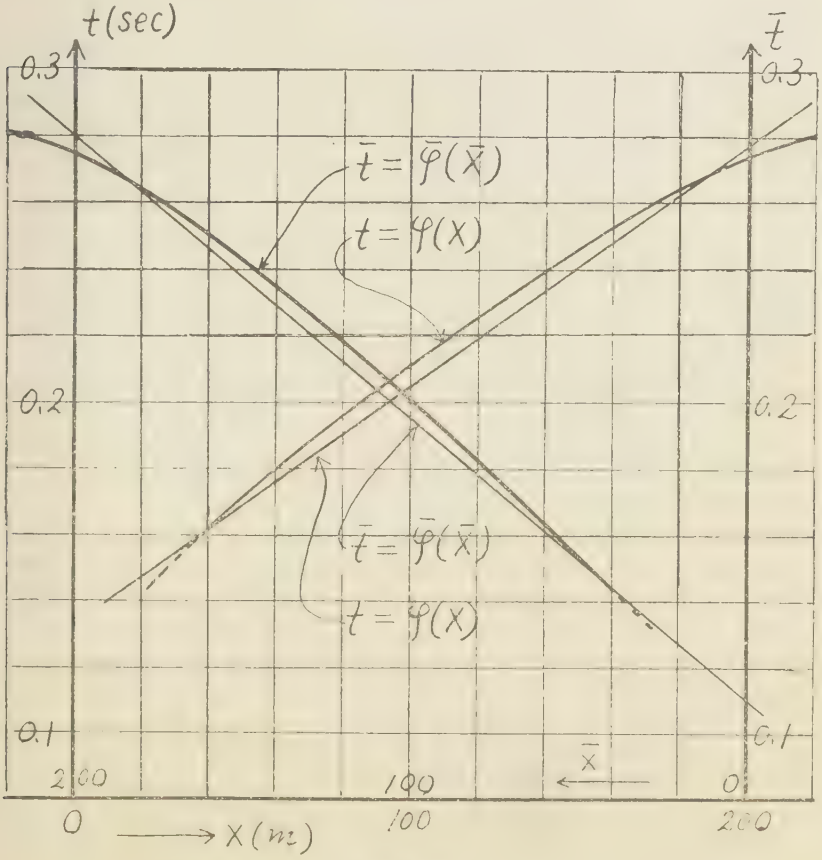

Fig. 3

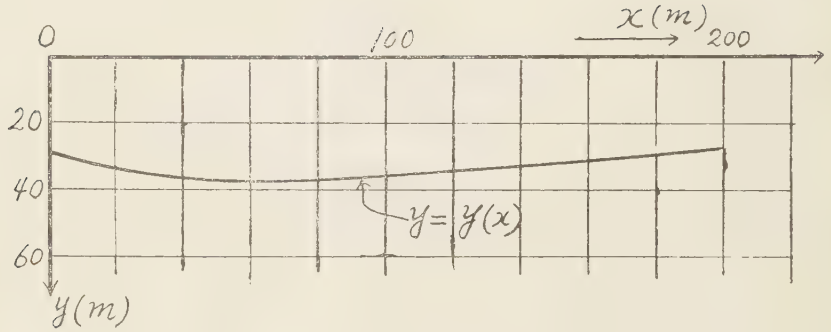

Fig. 4

Example 2.

$v_1 = 540m/sec$, $l = 320m$ and following data are given. Find the value of v_2 and the numerical values of $y(x)$ corresponding to $x = 0, 30, 60, \cdots\cdots, 300, 320(m)$.

$X, \bar{X}(m)$	30	60	90	120	150	180	210	240	270	300	320	350	380
$\varphi(X)(sec)$	0.096	0.129	0.160	0.190	0.219	0.248	0.275	0.300	0.325	0.347	0.360	0.379	0.397
$\bar{\varphi}(X)(sec)$	—	0.331	0.341	0.349	0.355	0.359	0.362	0.363	0.364	0.363	0.361	0.357	—

Solution :-

The graphs of two travelling-time curves are shown in Fig. 5, and their curvatures are both small, and

$$t = \varphi_0(X) = 0.000920X + 0.075 \quad \cdots\cdots \text{(i)}$$

$$t = \bar{\varphi}_0(X) = 0.000125X + 0.330 \quad \cdots\cdots \text{(ii)}$$

where units were taken meter, second.

Solving these equations, we get $y_0(x) = 0.230x + 21.7$

and $1.87 \times 10^3 m/sec$ as an approximate value of v_2. Therefore we get $\alpha_0 = 0.303, c_0 = 58.6$ and put to $\beta = 0.2300$, $m = \frac{1}{2}l$. Then we can easily show that $k(B-a) > \bar{k}(B-\bar{a})$ and $L_2 \fallingdotseq 15$. Hence putting to $n = 25$ (it may be good to put $n = 20$, but for the sake of safety we put to so) we get

$$\alpha = -1.851\kappa k\bar{k}\,[\varphi(D) + \bar{\varphi}(B) - \varphi(B) - \bar{\varphi}(D)] \quad \cdots\cdots \text{(iii)}$$

$$c = 263.13\,\frac{k\bar{k}}{\kappa}\,[\varphi(B) + \bar{\varphi}(B) - \bar{\varphi}(l)] \quad \cdots\cdots \text{(iv)}$$

where

$$\kappa = \sqrt{1+\alpha^2},\quad k = 1 - 0.23\alpha,\quad \bar{k} = 1 + 0.23\alpha$$

$$\left.\begin{aligned} A &= \frac{1}{k}(\alpha + 0.2300)(c - 36.8),\quad B = 160 + \frac{c}{k}(\alpha + 0.2300) \\ \bar{A} &= \frac{1}{k}(\alpha - 0.2300)(c + 36.8),\quad B = 160 + \frac{c}{k}(\alpha - 0.2300) \end{aligned}\right\} \cdots\cdots (v)$$

$$D = \frac{26.32}{k} + A \qquad , \bar{D} = \frac{310.6}{k} + \bar{A}$$

Solving Eqs. (iii) and (iv) by iteration we get

i	0	1	2	3	4	5
α_i	0.303	0.289	0.3000	0.3008	0.3007	0.3007
$C_i(m)$	58.6	64.4	65.18	65.24	65.28	65.28

Consequently we get

$$\alpha = 0.3007,\quad c = 65.28(m)$$

and

$$\kappa = 1.0442,\quad \gamma = 1.0261,\quad k = 0.9308,\quad \bar{k} = 1.0692,\quad A = 16.23$$

$$A = 6.75,\quad B = 197.2,\quad B = 164.3,\quad v_2 = 1.88 \times 10^3 (m/sec)$$

$$\gamma^2/k = 1.1311,\quad \gamma^2/\bar{k} = 0.9848,\quad v_1\gamma\kappa = 578.6,\quad \varphi(B) = 0.2632,\quad \bar{\varphi}(B) = 0.3575$$

$$\frac{1}{k}(\alpha + 2\alpha\beta^2 + \beta^3) = 0.3696,\quad \frac{1}{k}(\alpha + 2\alpha\beta^2 - \beta^3) = 0.2989,$$

therefore

when $x \geqq 12$

$$y(x) = 578.6\varphi(1.1311x + 16.23) - (27.87 + 0.3696x) \cdots\cdots (vi)$$

when $x < 12$

$$y(x) = 578.6\bar{\varphi}(321.89 - 0.9848x) - (189.39 - 0.2989x) \cdots\cdots (vii)$$

and similarly

when $\bar{x} \geqq 54$

$$\bar{y}(\bar{x}) = 578.6\bar{\varphi}(0.9848\bar{x} + 6.75) - (0.2989\bar{x} + 93.75) \cdots\cdots (viii)$$

when $\bar{x} < 54$

$$\bar{y}(\bar{x}) = 578.6\varphi(378.18 - 1.1311\bar{x}) - (146.15 - 0.3696\bar{x}) \cdots\cdots (ix).$$

From these relations we obtain following result

$x, \bar{x}(m)$	0	30	60	90	120	150	180	210	240	270	300	320
$y(x)(m)$	19.1	29.5	39.3	47.7	55.8	63.0	69.5	74.7	78.8	81.2	82.6	82.7
$\bar{y}(l-\bar{x})(m)$	19.1	29.7	39.2	47.7	55.7	63.2	69.5	74.8	79.0	81.2	82.6	82.8

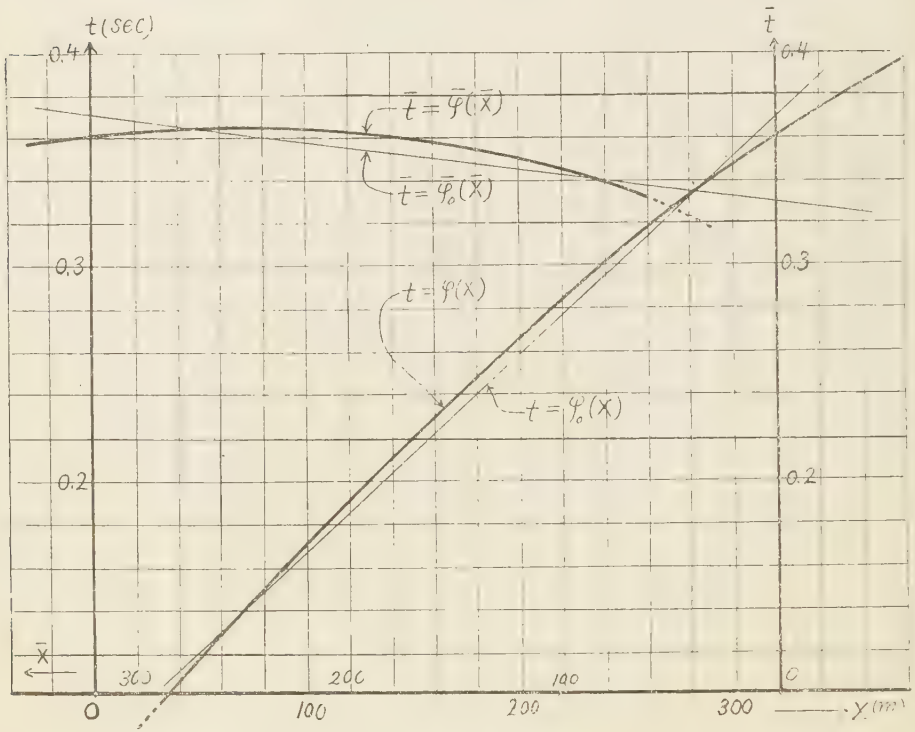

Fig. 5

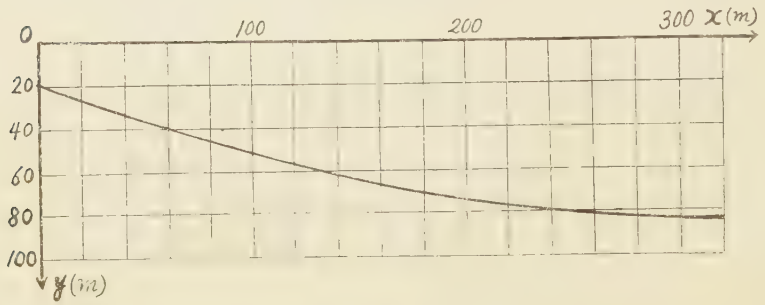

Fig. 6

6. Comments.

The method discussed here is applicable to a case when $\varphi(X)$ is any curve which has small curvature, and is generarization of the method discussed in the previous Journal, and moreover the method of computation became very simple and less laborious.

In practice, *the accuracy of the solution mainly depends on the accuracy of the measurement of travelling-time.*

It is obvious that if the values of v_2 and c are known by any way, we can calculate $y(x)$ from Eqs. (27) immediately.

The computation of $y(x)$, $\bar{y}(\bar{x})$ and the relation $y(x) = \bar{y}(l - x)$ can be used for the estimation of the correctness of experimental data and computation.

References

(1) R. Adachi : Fundamental Relations on the Seismic Prospecting. Kumamoto Journal of Science Vol. 2, No. 3.

(2) R. Adachi ; A Problem on the Seismic Prospecting. Kumamoto Journal of Science Vol. 2, No. 4.

A METHOD OF EXPLORATION ON THE SEISMIC PROSPECTING

(General case concerning the refraction method)

Ryuzo ADACHI

(Received November 30, 1956)

On the refraction method, I tried to find the form of separation curve when the travelling-time curve is any curve, and obtained accurate solution which has no approximation and no abbreviation.

1. Introduction

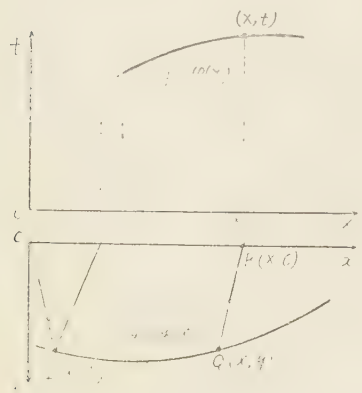

Fig. 1

In Fig. 1, let ox be a straight line along which travelling-time is observed and

$$y = y(x) \qquad (1)$$

be the curve of separation and consider a refracted wave which runs along $OPQR$ and its travelling-time be t. In this case, if

$$t = \varphi(X) \qquad (2)$$

is the travelling-time curve, we have

$$X = x + \frac{\alpha + \dfrac{dy}{dx}}{1 - \alpha \dfrac{dy}{dx}} y \qquad (3)$$

$$\frac{dy}{dx} + \alpha = \kappa v_1 \sqrt{1 + \left(\frac{dy}{dx}\right)^2} \frac{d}{dX} \varphi(X) \qquad (4)$$

where $V = \sqrt{v_2^2 - v_1^2}$, $\alpha = v_1/V$, $\kappa = \sqrt{1 + \alpha^2} = v_2/V$ and v_1, v_2 are the velocities of the wave in the first layer and the second layer respectively. (*)

When Eq. (2) is known, substituting (3) in (4), we get a differential equation of the first order with respect to $y(x)$ and if we can solve it, the form of separation curve will be determined.

2. Solution of $y(x)$.

At first, by solving the irrational equation (4) with respect to dy/dx we get

(*) See Reference (1)

$$\frac{dy}{dx} = \frac{\alpha - \kappa^2 B\sqrt{1-B^2}^{(**)}}{\kappa^2 B^2 - 1} = \frac{B - \alpha\sqrt{1-B^2}}{\alpha B + \sqrt{1-B^2}} \quad \cdots\cdots (5)$$

where $B = v_1 \frac{d}{dX}\varphi(X)$. Applying (5) to (3) gives

$$y = -\frac{\sqrt{1-B^2}}{B}(x - X) \quad \cdots\cdots (6).$$

Now, let us suppose that x, y are functions of X, and differentiate (6) with respect to X, then we get

$$\frac{dy}{dX} = -\frac{1}{B(1-B^2)}\frac{dB}{dX}y - \frac{\sqrt{1-B^2}}{B}\left(\frac{dx}{dX} - 1\right) \quad \cdots\cdots (7).$$

From (5) we get

$$\frac{dy}{dX} = \frac{B - \alpha\sqrt{1-B^2}}{\alpha B + \sqrt{1-B^2}}\frac{dx}{dX} \quad \cdots\cdots (8),$$

and eliminating $\frac{dx}{dX}$ from (7) and (8) gives

$$\frac{dy}{dX} + \frac{B - \alpha\sqrt{1-B^2}}{1-B^2}\frac{dB}{dX}y = (B - \alpha\sqrt{1-B^2})\sqrt{1-B^2} \quad \cdots\cdots (9),$$

while $B = v_1 \frac{d}{dX}\varphi(X)$ is a known function of X, therefore Eq. (9) is a linear differential equation of the first order with respect to y taking X as an independent variable and its general solution is

$$y = \sqrt{1-B^2}\, e^{\alpha \sin^{-1} B}\left[\int_a^X (B - \alpha\sqrt{1-B^2})e^{-\alpha \sin^{-1} B}dX + c'\right] \quad \cdots\cdots (10),$$

and substituting (10) in (6) gives

$$x = X - Be^{\alpha \sin^{-1} B}\left[\int_a^X (B - \alpha\sqrt{1-B^2})e^{-\alpha \sin^{-1} B}dX + c'\right] \quad \cdots\cdots (11),$$

where c' is integrating constant and a is a constant which satisfies that the travelling-time curve is known when $a \leqq X$.

Eqs. (10) and (11) are a parametric expression of the curve $y = y(x)$, and we can calculate the numerical values of $x(X)$ and $y(X)$ provided that $\varphi(X)$, v_1, α and c' are

(**) One easily may find that when $|B| < 1$ and $1 < \kappa B$, equation (4) has two roots

$$y' = \frac{\alpha - \kappa^2 B\sqrt{1-B^2}}{\kappa^2 B^2 - 1}, \quad y' = \frac{\alpha + \kappa^2 B\sqrt{1-B^2}}{\kappa^2 B^2 - 1}$$

but the latter does not satisfy our problem.

known.

3. Determination of v_2 and c'.

By boring or other suitable method, if we know the value of v_2 and the value of $y(x)$ when $x = f$, that is $y(f) = c$ where f, c are known values, and in this case let a_0 be the value of X, then we have

$$\phi(v_1\varphi'(a_0))(f - a_0) = c \quad \cdots\cdots (12)$$

where $\phi(B) = -\sqrt{1 - B^2}\, B$ and α may be obtained as a root of this equation. Then putting to $B_0 = v_1\varphi'(a_0)$, we have

$$\sqrt{1 - B_0^2}\, e^{\alpha \sin^{-1} B_0}\left[\int_a^{a_0} (B - \alpha\sqrt{1 - B^2})e^{-\alpha \sin^{-1} B}\, dX + c'\right] = c \quad \cdots\cdots (13)$$

and from this equation, we can get the value of c'.

As usual, when we get two travelling-time curve $t = \varphi(X)$, $t = \varphi(\bar{X})$ by experiment and if these two curves have some parts which have small curvatures, we can compute the values of v_2 and c by the method which is discussed *in preceding article of this Journal.*

4. Example.

$v_1 = 4.4 \times 10^3 m/sec$ and following data are given. Find the value of v_2 and the curve of $y = y(x)$.

$X, \bar{X}(m)$	20	40	60	80	100	120	140	160	180	200	220	240	260	280	300
$\varphi(X)(sec)$	0.133	0.155	0.175	0.195	0.214	0.231	0.248	0.264	0.278	0.289	0.295	0.297	0.292	0.283	0.270
$\bar{\varphi}(X)(sec)$	0.080	0.113	0.144	0.171	0.194	0.212	0.225	0.235	0.244	0.251	0.258	0.263	0.266	0.269	0.270

Solution :

At first draw the curves of $t = \varphi(X)$ and $t = \bar{\varphi}(X)$ plotting aboved data in a section paper and from the parts which have small curvature, we get $v_2 = 1.68 \times 10^3 m/sec$ and $y(150) = 49.6m$, $\alpha = 0.272$.

Next, find each value of $\varphi(X)$ graphically and then compute the values of B. From these data, we can calculate each value of $e^{\alpha \sin^{-1} B}$, $(B - \alpha\sqrt{1 - B^2})\, e^{-\alpha \sin^{-1} B}$ etc. corresponding to $X = 20, 40, \cdots\cdots, 300$ and the value of

$$I(X) = \int_{\cdot}^{X} (B - \alpha\sqrt{1 - B^2})\, e^{-\alpha \sin^{-1} B}\, dX$$

by numerical integration, and following table is obtained

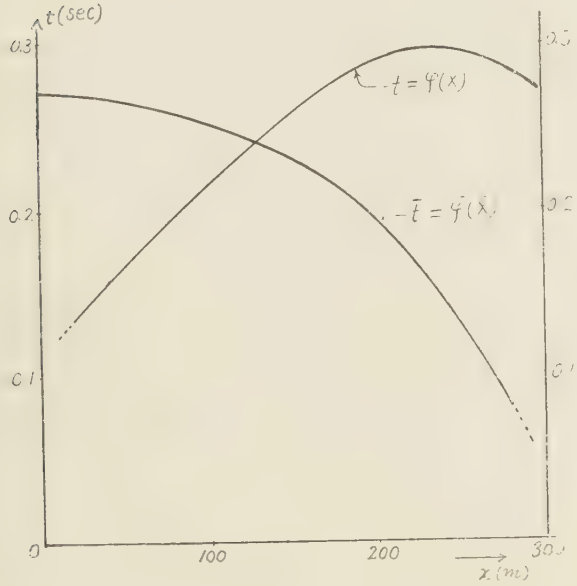

Fig. 2

Table. 1

$X, \bar{X}^{(m)}$	$B(X)$	$e^{\alpha \sin^{-1} B}$	$(B-\alpha\sqrt{1-B^2}) \times e^{-\alpha \sin^{-1} B}$	$I(X)^{(m)}$	$\phi(B)(150-X)^{(m)}$	$I(X)+c'^{(m)}$	$x^{(m)}$ $y^{(m)}$	$\bar{B}(\bar{X})$	$\bar{x}^{(m)}$ $\bar{y}^{(m)}$
20	0.49	1.15	0.223	0.0		27.7	4 28	0.74	4 15
40	0.45	1.14	0.185	4.0		31.7	24 32	0.71	17 23
60	0.44	1.13	0.177	7.6		35.3	42 36	0.65	33 32
80	0.42	1.12	0.152	11.0		38.7	62 40	0.55	54 40
100	0.39	1.11	0.122	13.7		41.4	82 43	0.45	77 46
120	0.37	1.11	0.110	16.0	−74.4	43.7	102 45	0.34	102 50
140	0.37	1.11	0.101	18.1	−25.5	45.8	122 47	0.26	127 50
160	0.33	1.10	0.071	19.9	28.2	47.6	143 49	0.20	150 50
180	0.28	1.08	0.019	20.8	102.0	48.5	165 50	0.17	172 48
200	0.20	1.06	−0.065	20.4	247.5	48.1	190 50	0.15	193 46
220	0.10	1.03	−0.169	18.0		45.8	215 47	0.12	215 43
240	−0.03	0.99	−0.306	13.4		41.2	241 41	0.10	236 40
260	−0.17	0.96	−0.455	5.7		33.4	265 32	0.066	258 35
280	−0.25	0.94	−0.546	−4.4		23.3	285 21	0.044	279 31
300	−0.29	0.92	−0.596	−15.9		11.9	303 11	0.022	299 26

where we get $a_0 = 166.4m$ from $\phi(B_0)\,(150m - a_0) = 49.6m$ and $I(a_0) = 20.2m$, $\sqrt{1-B_0^2}\; e^{\alpha \sin^{-1} B_0} = 1.034$ by interpolation, and then $c' = 27.7m$ from Eq. (13).

Similarly from $\bar{t} = \bar{\varphi}(X)$ we can calculate the values of $\bar{x}(X), \bar{y}(X)$ and the result of my computation is shown in the last part of the table 1. Fig. 3 shows the curves of $y = y(x)$ and $\bar{y} = \bar{y}(\bar{x})$ which were plotted above data and they nearly coincide each other.

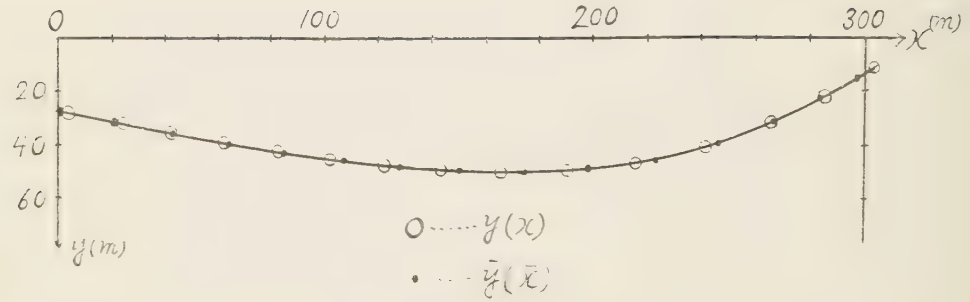

Fig. 3

5. Some Comments.

Eqs. (10) and (11) are analytically accurate solutions which have no approximation and no abbreviation, but practically they are not sufficient enough because of the fact that in most cases v_2 and c' are unknown.

Generally if we get two travelling-time curves $t = \varphi(X)$, $\bar{t} = \bar{\varphi}(\bar{X})$ by experiment, we ought to be able to find the values of v_2 and c'. At this point of view, I obtained one method, but there can exist so large errors in this method that it is yet worthless in practice, and only in the case when the curves of $t = \varphi(X)$ and $\bar{t} = \bar{\varphi}(X)$ have some parts near to straight lines, I can compute the values of v_2 and c'.

It is obvious that when $y = y(x)$ and the values of v_1 and v_2 are given the travelling-time curve is determined uniquely. Inversely, when the travelling-time curve and the values of v_1 are given the curve of separation $y = y(x)$ is determined by Eqs. (10) and (11), hence if the values of v_2 and c' are given uniquely, the solution of $y = y(x)$ is also determined uniquely. But, generally, I can not yet assert the uniqueness of v_2 and c'.

The computation of $y(x)$, $\bar{y}(\bar{x})$ and the relation $y(x) = \bar{y}(l - x)$ can be used for the estimation of the correctness of experimental data and computation.

References

(1) R. Adachi : Fundamental Relations on the Seismic Prospecting. Kumamoto Journal of Science Vol. 2, No. 3.
(2) R. Adachi : A Problem on the Seismic Prospecting. Kumamoto Journal of Science Vol. 2, No. 4.

FUNDAMENTAL RELATIONS NO THE SEISMIC PROSPECTING AND A METHOD OF EXPLORATION

(general case concerning the reflection method)

Ryuzo ADACHI

(Received November, 15. 1956)

On the reflection method, I derived some fundamental relations between the curve of separation and the travelling-time curve in general case, and tried to find the form of separation curve when the travelling-time curve is given, and obtained an accurate solution which has no approximation and no abbraviation.

1. Relations between Curve of Separation and Travelling-time Curve.

In Fig. 1, let Ox de a straight line along which travelling-time is odserved and

$$y = y(x) \quad \cdots\cdots (1)$$

bn the curve of separation, and consider a reflected wave which runs along OPR and its travelling-time be t. Then we can easily find that

$$X = \overline{OR} = \frac{2(x + yy')(y - xy')}{y - 2xy' - yy'^2},$$

$$\overline{OP} + \overline{PR} = \frac{2\sqrt{x^2 + y^2}\,(y - xy')}{y - 2xy' - yy'^2}$$

where $y' = dy/dx$. Therefore, if

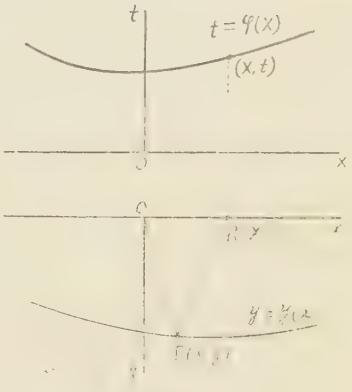

Fig. 1

$$t = \varphi(X) \quad \cdots\cdots (2)$$

is travelling-time curve, and v is the velocity of wave, we get

$$t = \frac{1}{v}\,\frac{2\sqrt{x^2 + y^2}\,(y - xy')}{y - 2xy' - yy'^2} = \varphi(X) \quad \cdots\cdots (3)$$

$$X = \frac{2(x + yy')(y - xy')}{y - 2xy' - yy'^2} \quad \cdots\cdots (4)$$

and these are fundamental relations.

If $y = y(x)$ is given, solving (4) with respect to x, we can express x by a funcion of X and sudstituting it to (3) we get the travelling-time curve. Of course we can consid-

er that Eqs. (3), (4) express the travelling-time curve taking x as a parameter.

When $\varphi(X)$ is given, substitute (4) into (3) and we get a functional equation with respect to $y(x)$, and solving this equation we get $y(x)$.

2. Solution of $y = y(x)$ when $\varphi(X)$ is given.

Let us suppose that $\varphi(X)$ is a well behaved function of X, then from Eqs. (3) and (4) we get

$$E(X)(x + yy') = X\sqrt{x^2 + y^2} \qquad (5)$$

or

$$y = \frac{1}{y}\left(\frac{X}{E}\sqrt{x^2 + y^2} - x\right) \qquad (5)'$$

where

$$E(X) = v\varphi(X) \qquad (6)$$

Then applying (5)', we get

$$y - xy' = \frac{\sqrt{x^2 + y^2}}{y}\left(\sqrt{x^2 + y^2} - \frac{X}{E}x\right)$$

$$y - 2xy' - yy'^2 = \frac{1}{y}(x^2 + y^2)\left(1 - \frac{X^2}{E^2}\right)$$

and

$$X = \frac{2EX}{E^2 - X^2}\left(\sqrt{x^2 + y^2} - \frac{X}{E}x\right)$$

therefore

$$\frac{E^2 - X^2}{2E} + \frac{X}{E}x = \sqrt{x^2 + y^2} \qquad (7)$$

Taking X as a parameter, consider that x, y are functions of X, and differentiating (7) with respect to X, we get

$$\frac{-2XE + (E^2 + X^2)E'}{2E^2} + \frac{E - XE'}{E^2}x + \frac{X}{E}\frac{dx}{dX} = \frac{x + yy'}{\sqrt{x^2 + y^2}}\frac{dx}{dX}$$

and substituting (5) gives

$$\frac{-2XE + (E^2 + X^2)E'}{2E^2} + \frac{E - XE'}{E^2}x = 0, \text{ where } E' = \frac{dE}{dX},$$

therefore

$$x = \frac{2XE - (E^2 + X^2)E'}{2(E - XE')} \qquad \cdots\cdots (8).$$

Substituting (8) in (7) we get

$$y^2 = \frac{(E^2 - X^2)^2}{4E^2} + \frac{X(E^2 - X^2)}{E^2}x + \frac{X^2}{E^2}x^2 - x^2 = \frac{(1 - E'^2)(E^2 - X^2)^2}{4(E - XE')^2}$$

that is

$$y = \frac{\sqrt{1 - E'^2}\,(E^2 - X^2)}{2(E - XE')} \qquad \cdots\cdots (9).$$

(*)

(8) *and* (9) *are a parametric expression of the solution curve* $y = y(x)$ *taking* X *as a parameter.* We considered that $\varphi(X)$ is given, hence $E(X) = v\varphi(X)$ is a known function of X and the right sides of (8) and (9) are both known functions of X, and we can compute the values of them corresponding to any value of X.

For example, when

$$E(X) = \sqrt{X^2 + 4hX\ sin\ \omega + 4h^2} \quad \text{where} \quad h,\ \omega = consts$$

is given, we have

$$E' = \frac{X + 2h\ sin\ \omega}{E}, \quad E - XE' = \frac{2h}{E}(X\ sin\ \omega + 2h)$$

and

$$x = \frac{h(X\ cos\ 2\omega - 2h\ sin\ \omega)}{X\ sin\ \omega + 2h}, \quad y = \frac{2h\ cos\ \omega(X\ sin\ \omega + h)}{X\ sin\ \omega + 2h}$$

therefore

$$y = x\ tan\ \omega + \frac{h}{cos\ \omega}$$

and this is well known result.

3. Examples.

Example 1.

$E(X) = aX + b$, (where a, b are constants and $|a| < 1$, $0 < b$) is given. Find the curve $y = y(x)$.

Solution:-

From Eqs. (8) and (9) we get

(*) We can easily show that E and X must satisfy $E > |X|$, $1 > |E'|$, therefore $E - XE' > 0$, $E^2 - X^2 > 0$.

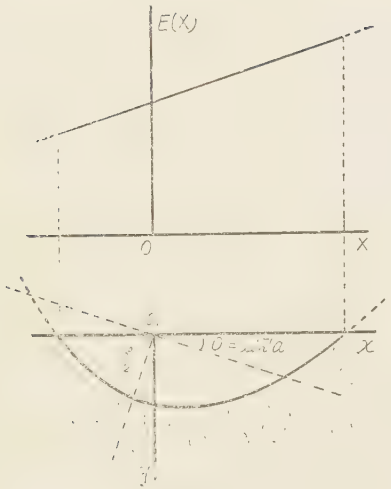

Fig. 2

$$\left.\begin{aligned} x &= \frac{1}{2b}\left[a(1-a^2)X^2 + 2b(1-a^2)X - ab^2\right] \\ y &= \frac{1}{2b}\sqrt{1-a^2}\left[(a^2-1)X^2 + 2abX + b^2\right] \end{aligned}\right\} \quad \cdots\cdots\cdots\cdots\cdots\cdots \text{(i)}.$$

Eliminating X from (i) gives

$$(1-a^2)x^2 + 2a\sqrt{1-a^2}\,xy + a^2y^2 - 2abx + 2b\sqrt{1-a^2}\,y - b^2 = 0 \cdots\cdots\cdots\cdots \text{(ii)}.$$

Rotating the co-ordinate axes by an angle $\theta = sin^{-1}\ a$ gives

$$y = \frac{1}{2b}(b^2 - x^2) \quad \cdots\cdots\cdots\cdots\cdots\cdots \text{(iii)}.$$

This is a parabola whose focus is $(0,0)$, focal length is $b/2$ and axis is $y = -\dfrac{\sqrt{1-a^2}}{a}x$.

Example 2.

Following values of $E(X)$ shown in the table 1 are given. Find the curve $y = y(x)$.

Solution:-

At first, we must find the values of $E'(X)$ corresponding to each value of X. By using approximate formulas for differential coefficients derived from interpolation formula(*) I obtained the values of $E'(X)$ shown in the table 1, and by applying these data in the Eqs. (8) and (9) we got the values of x and y shown in the table 1, and the curve $y = y(x)$ was shown in the Fig. 3, b.

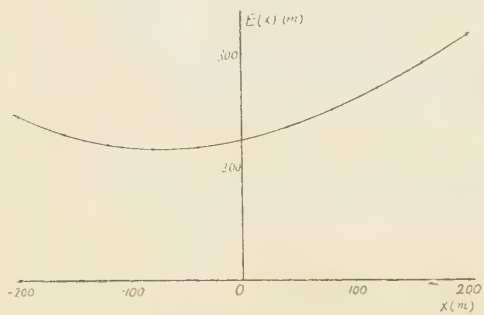

Fig. 3. a

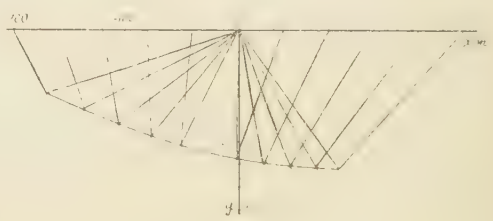

Fig. 3. b

(*)See reference (1).

Table 1

$X_{(m)}$	$E(X)^{(m)}$	$E'(X)$	$x^{(m)}$	$y^{(m)}$
−200	245	−0.458	−170	58
−180	236			
−160	229	−0.311	−137	71
−140	224			
−120	220	−0.160	−107	83
−100	217			
−80	216	−0.023	−78	94
−60	216			
−40	218	0.111	−52	102
−20	221			
20	230			
40	236	0.338	−1	114
60	243			
80	252	0.435	23	118
100	261			
120	271	0.520	47	121
140	281			
160	293	0.598	69	122
180	305			
200	318	0.669	89	124

Table 2,

$X_{(m)}$	$E(X)_{(m)}$	$E'(X)$	$x_{(m)}$	$y^{(m)}$
−180	374			
−170	368	−0.562	−60	162
−150	357	−0.561	−42	159
−130	346	−0.563	−24	156
−110	335	−0.525	−15	154
−90	325	−0.477	−8	152
−70	316	−0.413	−2	151
−50	309	−0.337	4	149
−30	303	−0.260	10	148
35	295	0.022	32	146
55	297	0.135	35	145
75	300	0.213	43	145
95	305	0.323	46	146
105	309			

Example 3.

The values of $E(X)$ shown in the table 2, are given. Find the curve $y = y(x)$.

Solution:-

In this case, the values of $E'(X)$ were obtained from the graph of $E(X)$ by drawing tangents and shown in the table 2. Then the values of x, y were calculated by Eqs. (8), (9) and the graph $y = y(x)$ was shown in the Fig. 4, b.

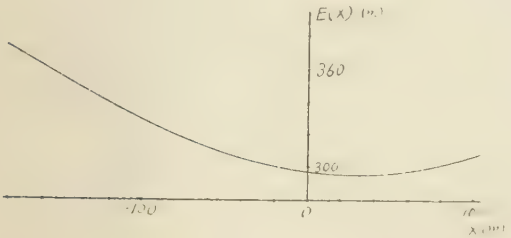

Fig. 4, a

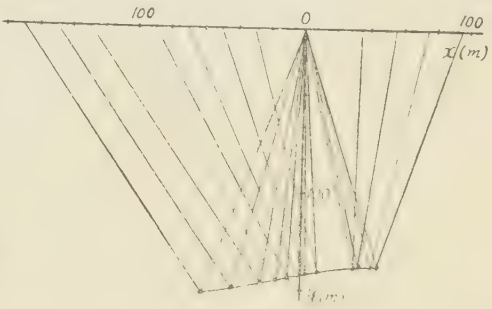

Fig. 4, b

4. Errors.

In practice, we must find the values of v and $\varphi(X)$ by experiment and then the values of $\varphi(X)$ may be found from the values of $\varphi(X)$ numerically. Hence there occur some errors in $v, \varphi(X)$ and $\varphi'(X)$.

Let δv, $\delta\varphi$, $\delta\varphi'$ be errors of v, φ, φ' respectively and δx, δy be that of x, y caused by δv, $\delta\varphi$, $\delta\varphi'$ then we have

$$\begin{aligned}\delta x &= \frac{\partial x}{\partial v}\delta v + \frac{\partial x}{\partial \varphi}\delta\varphi + \frac{\partial x}{\partial \varphi'}\delta\varphi' \\ &= \left(v\frac{\partial x}{\partial v}\right)\frac{\delta v}{v} + \left(\frac{1}{v}\frac{\partial x}{\partial \varphi}\right)\delta\bar{E} + \left(\frac{1}{v}\frac{\partial x}{\partial \varphi'}\right)\delta\bar{E}' \\ \delta y &= \frac{\partial y}{\partial \delta}\partial v + \frac{\partial y}{\partial \varphi}\delta\varphi + \frac{\partial y}{\partial \varphi'}\delta\varphi' \\ &= \left(v\frac{\partial y}{\partial v}\right)\frac{\partial v}{v} + \left(\frac{1}{v}\frac{\partial y}{\partial \varphi}\right)\partial E + \left(\frac{1}{v}\frac{\partial y}{\partial \varphi'}\right)\partial E'\end{aligned} \quad \cdots\cdots (10)$$

where $\delta\bar{E} = v\delta\varphi$, $\delta E' = v\delta\varphi'$.(*)
While from Eqs. (8) and (9), we get

$$\begin{aligned} v\frac{\partial x}{\partial v} &= \frac{-E^2E'}{E-XE'} & v\frac{\partial y}{\partial v} &= \frac{E^2+X^2-2E^2E'}{2(E-XE')\sqrt{1-E'^2}} \\ \frac{1}{v}\frac{\partial x}{\partial \varphi} &= \frac{-(E^2+X^2-2XEE')E'}{2(E-XE')^2} & & \\ & & \frac{1}{v}\frac{\partial y}{\partial \varphi} &= \frac{\sqrt{1-E'^2}(E^2+X^2-2XEE')}{2(E-XE')^2} \\ \frac{1}{v}\frac{\partial x}{\partial \varphi'} &= \frac{-(E^2-X^2)E}{2(E-XE')^2} & \frac{1}{v}\frac{\partial y}{\partial \varphi'} &= \frac{(E^2-X^2)(X-EE')}{2(E-XE')^2\sqrt{1-E'^2}} \end{aligned} \quad (11).$$

By these formulas, we can estimate the errors of x and y.

For instance, in example 3, computing by above equations we get following result.

X	$v\frac{\partial x}{\partial v}$	$v\frac{\partial y}{\partial v}$	$\frac{1}{v}\frac{\partial x}{\partial \varphi}$	$\frac{1}{v}\frac{\partial y}{\partial \varphi}$	$\frac{1}{v}\frac{\partial x}{\partial \varphi'}$	$\frac{1}{v}\frac{\partial y}{\partial \varphi'}$
−170m	28 10m	18 10m	0.36	0.50	−26 10m	32m
−110 〃	21 〃	13 〃	0.29	0.47	−22 〃	48 〃
−30 〃	8 〃	14 〃	0.12	0.43	−16 〃	32 〃
35 〃	−0.7 〃	14 〃	−0.01	0.43	−15 〃	14 〃
95 〃	−11 〃	14 〃	−0.18	0.50	−17 〃	−5 〃

if

$$|\delta v/v| \leqq 0.02, \quad |\delta E'| \leqq 0.01,$$

$$|\delta\bar{E}| \leqq 2^m \text{ (therefore the error of time } |\delta\varphi| \leqq 2^m/v)$$

and let $[\alpha]$ be a upper bound of $|\alpha|$, where α is any one of $\frac{\partial x}{\partial v}\delta v$, $\frac{\partial y}{\partial v}\partial v$, ... $\frac{\partial y}{\partial \varphi'}\delta\varphi'$, δx, δy we get following result

(*) $\delta E, \delta E'$ do not mean the errors of E, E'.

X	$\left(\frac{\partial x}{\partial v}\delta v\right)$	$\left(\frac{\partial x}{\partial \varphi}\delta\varphi\right)$	$\left(\frac{\partial x}{\partial \varphi'}\delta\varphi'\right)$	$[\delta x]$	$\left(\frac{\partial y}{\partial v}\delta v\right)$	$\left(\frac{\partial y}{\partial \varphi}\delta\varphi\right)$	$\left(\frac{\partial y}{\partial \varphi'}\delta\varphi'\right)$	$[\delta y]$
−170m	5.6m	0.8m	2.6m	9.0m	3.6m	1.0m	0.4m	5.0m
−110	4.2	0.6	2.2	7.0	2.6	1.0	0.4	4.0
−30	1.6	0.2	1.6	3.4	2.8	0.8	0.4	4.0
35	0.2	0.0	1.6	1.8	2.8	0.8	0.2	3.8
95	2.2	0.4	1.8	4.4	2.8	1.0	0.0	3.8

This example shows that the influence fo the error of v is greatest.

5. Comments.

It is obvious that when $y = y(x)$ is given, the travelling-time curve is determined uniquely. Inversely, when the travelling-time curve is given the curve of separation $y = y(x)$ is determined by Eqs. (8) and (9), hence it is also determined uniquely. Accordingly $y = y(x)$ *and* $t = \varphi(X)$ *are related by one to one correspondence.*

The Eqs. (8) and (9) are analytically *accurate solution* of $y = y(x)$ when $t = \varphi(X)$ is given and it has no approximation and no abbraviation.

But in practice, it is very difficult to find the functional form of $\varphi(X)$ and in most cases, we are obliged to explorate $y(x)$ from the numerical values of $\varphi(X)$ directly as shown in example 2 and 3, and there occur some errors caused by the errors of v, φ and φ' and they are expressed by Eqs. (10) and (11).

References

(1) R. Adachi: Approximate Formulas for Definite Integrals and Differential Coefficients. Kumamoto Journal of Science Vol. 2, No. 2 (1955)

(2) R. Adachi: Fundamental Relations on the Seismic Prospecting. Kumamoto Journal of Science Vol. 2, No. 3 (1955)

ASCENSION OF A SMALL MASS OF AIR AND THE CHANGES IN ITS STATE (II) WET AIR

Shigeichi FUJITA

(Received November 30, 1956)

The ascending motion of wet air and the changes in its state are more complex than in the case of dry air. We have attempted here to solve the problem theoretically under the same assumptions as used in the case of dry air, and have obtained some results. As the results are nearly in accord with practical cases, we can use them to know nearly the practical motion and the changes in state of a small mass of wet air.

1. Introduction

It is assumed as in the previous paper[1] that there is a small mass of wet air in the atmosphere at rest, the temperature of the mass of air is heigher than that of the surrounding atmosphere. The mass of air will then move upwards and its state will be changed. It is assumed also, that the surrounding atmosphere is always at rest and keeps its own states in spite of the motion of the ascending mass of air. The temperature of the atmosphere varies with height in a constant lapse rate, and the pressure changes with height corresponding to the changes in the temperature. The pressure in the moving mass of air is safely assumed to be always equal to that of the surrounding atmosphere as the mass of air is not very large, and also assumed that the mass of air has a distinct boundary with the surrounding atmosphere and accepts no resistance from the surrounding. It is assumed, more over, that there is no heat exchange between the mass of air and the surrounding atmosphere.

The change in state of the mass of air which contains saturated vapour is quite different from the change in state of the mass of air which contains unsaturated vapour. Accordingly, we have studied, firstly, the changes in state and the ascending motion of the mass of air which contains unsaturated vapour, and obtained the height at which the condensation begines, and studied, in the next, the changes in state and the ascending motion of the mass of air which contains saturated vapour, especially the relation between the ascending velocity and the height of the mass of air.

2. Reversible Adiabatic Process of Mixed Gases

The gas 1 of ν_1 moles and the gas 2 of ν_2 moles are mixed thoroughly. The molar heats at constant volume and the partial pressures of the two gases are C_{v1}, C_{v2} and p_1, p_2 respectively. The total pressure, volume and temperature of the mixed gases are p, V and T respectively. If it is supposed that a very small reversible adiabatic change occurs in the

state of mixed gases, in which T and V change by dT and dV respectively, then

$$0 = (\nu_1 C_{v1} + \nu_2 C_{v2})\, dT + (\nu_1 + \nu_2)\frac{RT}{V} dV \quad \cdots\cdots (1)$$

or $$C_v \log T + R \log V = const., \quad \cdots\cdots (2)$$

where $$C_v = \frac{\nu_1 C_{v1} + \nu_2 C_{v2}}{\nu_1 + \nu_2} \quad \cdots\cdots (3)$$

From (2) we get

$$T^{C_v} V^R = const., \quad p^{C_v} V^{C_p} = const., \quad p^{-R} T^{C_p} = const., \quad \cdots\cdots (4)$$

where $C_p = C_v + R$.

For each gas, the relations

$$\left.\begin{aligned} p_1^{C_v} V^{C_p} &= const., \quad p_1^{-R} T^{C_p} = const., \\ p_2^{C_v} V^{C_p} &= const., \quad p_2^{-R} T^{C_p} = const. \end{aligned}\right\} \quad \cdots\cdots (5)$$

must be satisfied.

As a special case, if $\nu_1 \gg \nu_2$, we can put $C_v \fallingdotseq C_{v1}$, $p \fallingdotseq p_1$, so that the gas 2 changes by

$$p_2^{C_{v1}} V^{C_{p1}} = const., \quad p_2^{-R} T^{C_{p1}} = const. \quad \cdots\cdots (6)$$

as if the gas 2 has the molar heats C_{v1}, C_{p1} of the principal gas 1.

The same relations are satisfied in the case of the mixture of many gases 1, 2, ……, n whose quantities are $\nu_1, \nu_2, \cdots\cdots, \nu_n$ moles respectively. If the molar heats at constant volume and at constant pressure of each gases are $C_{v1}, C_{v2}, \cdots\cdots, C_{vn}$ and $C_{p1}, C_{p2} \cdots\cdots, C_{pn}$, the partial pressures are $p_1, p_2, \cdots\cdots, p_n$ and the total pressure, volume and temperature are p, V and T respectively, there exist the relations

$$T^{C_v} V^R = const., \quad p^{C_v} V^{C_p} = const., \quad p^{-R} T^{C_p} = const., \quad \cdots\cdots (7)$$

where $$C_v = \frac{\nu_1 C_{v1} + \nu_2 C_{v2} + \cdots\cdots + \nu_n C_{vn}}{\nu_1 + \nu_2 + \cdots\cdots + \nu_n}, \quad C_p = C_v + R. \quad \cdots\cdots (8)$$

For each gas, the following relations must be satisfied.

$$\left.\begin{aligned} p_1^{C_v} V^{C_p} &= const., \quad p_2^{C_v} V^{C_p} = const., \cdots\cdots, \quad p_n^{C_v} V^{C_p} = const., \\ p_1^{-R} T^{C_p} &= const., \quad p_2^{-R} T^{C_p} = const., \cdots\cdots, \quad p_n^{-R} T^{C_p} = const. \end{aligned}\right\} \quad \cdots\cdots (9)$$

If $\nu_1 \gg \nu_2 + \nu_3 + \cdots\cdots + \nu_n$, we can put $C_v \fallingdotseq C_{v1}$, $C_p \fallingdotseq C_{p1}$, and therefore, the relations

$$\left.\begin{aligned} p_1^{C_{v1}} V^{C_{p1}} &= const., \quad p_2^{C_{v1}} V^{C_{p1}} = const., \cdots\cdots, \quad p_n^{C_{v1}} V^{C_{p1}} = const., \\ p_1^{-R} T^{C_{p1}} &= const., \quad p_2^{-R} T^{C_{p1}} = const., \cdots\cdots, \quad p_n^{-R} T^{C_{p1}} = const., \end{aligned}\right\} \quad \cdots\cdots (10)$$

are applied, which means that the gases 2, 3, ……, n behave as if each of them has the molar heats of principal gas 1.

3. Change in Vapour Pressure by the Ascension of Wet Air

If the pressure of dry air only is p_1, the pressure of unsaturated water vapour contained in the air is f, and the temperature is T, we obtain by (6)

$$f^{-R}T^{C_{p1}} = const., \quad \cdots\cdots (11)$$

where C_{p1} is the molar heat at constant pressure of air. If the initial temperature of air and the initial partial pressure of the water vapour are T_0 and f_0 respectively, (11) becomes

$$f = f_0\left(\frac{T}{T_0}\right)^{\frac{C_{p1}}{R}} = f_0\left(\frac{T}{T_0}\right)^{3.5} \quad \cdots\cdots (11')$$

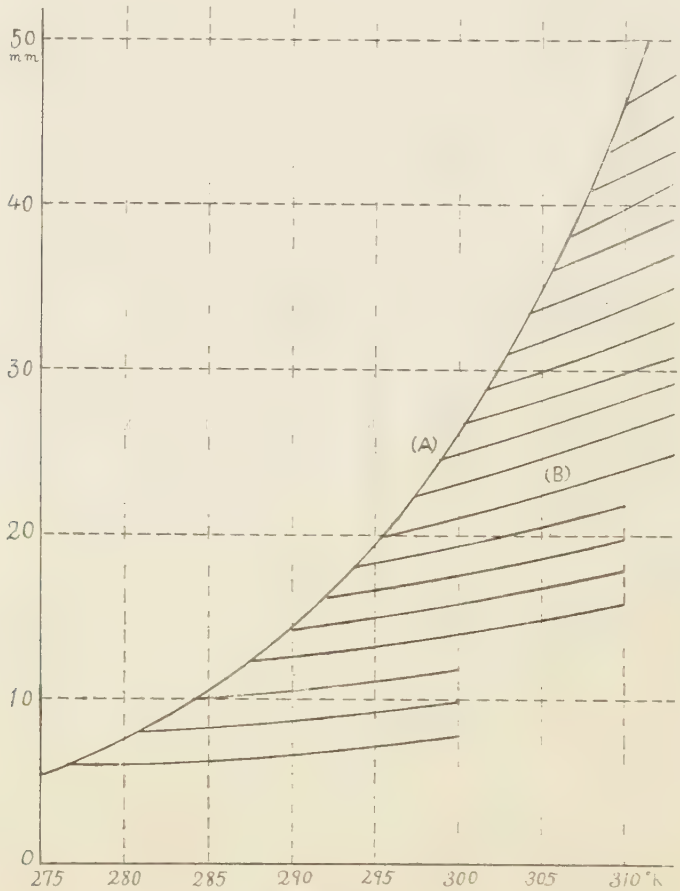

Fig. 1.

To obtain the temperature at which the vapour contained in the air becomes saturate by the reversible adiabatic expansion, we draw the curve which expresses the relation between the maximum vapour pressure and the temperature, and the curve which expresses the relation between f and T by (11'), for different values of f_0 and T. Then the intersection of the two curves gives the temperature T_s at which vapour becomes saturate. In Fig. 1, (A) shows the curve which expresses the relation between temperature and pressure of saturated vapour, and (B) shows the curves which are obtained by (11'). The intersections of (A) and (B) are the temperatures at which vapour becomes saturate. Table 1 shows the temperatures.

Table 1.

T_0 = 280						
f_0 = 7.47mm	6(80%)	5(67%)	4			
T_s = 280	276	273	267			
T_0 = 290						
f_0 = 14.4	12(83%)	10(69%)	8(55%)	6(42%)	4(28%)	
T_s = 290	286.5	283	279	274	267	
T_0 = 300						
f_0 = 26.47	24(90%)	22(83%)	20(75%)	18(68%)	16(60%)	14(53%)
T_s = 300	298	296	294	292	289.5	287
f_0 = 12(45%)	10(38%)	8(30%)				
T_s = 284	281	277				
T_0 = 310						
f_0 = 46.65	43(92%)	40(86%)	38(82%)	36(79%)	34(73)	32(68%)
T_s = 310	308	306.5	305.5	304.5	303	301.5
f_0 = 30(64%)	28(60%)	26(56%)	24(52%)	22(47%)	20(43%)	
T_s = 300	298.5	297	295.5	293.5	292	
f_0 = 18(39%)	16(34%)					
T_s = 290	287.5					
T_0 = 320						
f_0 = 79.07	75(95%)	70(89%)	65(82%)	60(76%)	55(70%)	50(63%)
T_s = 320	318.5	317	315.2	313.2	311.3	309.1
f_0 = 45(57%)	40(51%)	35(44%)	30(38%)			
T_s = 306.7	304.1	301.2	297.7			

4. The Height of the Condensation Level

The temperature at which the vapour contained in the mass of air begines condensation by reversible adiabatic expansion is obtained by the method written in 3., assuming initial temperature and initial vapour pressure. We can treat wet air similarly as dry air while the vapour is unsaturated. Thence, the changes in temperature of air which

contains unsaturated vapour can be obtained by the same procedure given in the previous paper[1]. Thus if the temperatures of the atmosphere at height 0 and at height h are T_{10} and $T_1 = T_{10} - \gamma h$ respectively, where γ is the constant lapse rate, and the temperature of the mass of air is $T_0\ (> T_{10})$ at height 0, and T at height h, there is the relation

$$\frac{T}{T_0} = \left(\frac{T_1}{T_{10}}\right)^{\frac{\Gamma}{\gamma}} = \left(1 - \frac{\gamma h}{T_{10}}\right)^{\frac{\Gamma}{\gamma}}, \quad \cdots\cdots (12)$$

in the adiabatic case, where Γ is the dry adiabatic lapse rate. If the values of $\frac{\Gamma}{\gamma}$, T_{10}, T_0 and T are given, we can obtain the height h. Accordingly, obtaining by Fig. 1 the temperature at which the vapour becomes saturate, and putting it in (12), the height of the condensation level can be obtained. After the condensation of vapour begines, the relation between temperature and height is quite different from (12).

5. Changes in Temperature by the Ascension of Air which contains Saturated Vapour

It is assumed that there is $x\ g$ of saturated vapour and $(x_0 - x)\ g$ of water drops in $1\ g$ of dry air, whose partial pressure, volume and temperature are p, v and T respectively, and that the partial pressure of vapour is f and the total pressure of the wet air is p. In a small adiabatic change, there exists for wet air the following relation[2],

$$R' d\log p = (C_p + Cx_0) d\log T + d\left(\frac{rx}{T}\right), \quad \cdots\cdots (13)$$

where R' and C_p are the specific gas constant and the specific heat at constant pressure of dry air respectively, and C and r are the specific heat and the latent heat of vaporisation of vapour respectively. If T_0 is the temperature at which whole the water evaporates and becomes saturated vapour, f_0 the maximum vapour pressure, p_0 the total pressure of the wet air, r_0 the latent heat of vaporisation at T_0, then (13) becomes

$$R' \log \frac{p - f}{p_0 - f_0} = (C_p + Cx_0) \log \frac{T}{T_0} + \left(\frac{rx}{T} - \frac{r_0 x_0}{T_0}\right)^{(2)}. \quad \cdots\cdots (14)$$

This is the expression of reversible adiabatic process of wet air which contains saturated vapour.

In (14), if T is given, f, r and x are determined, and hence p is determined. As p is intimately related to h, h is determined also. We can, therefore, obtain the relation between T and h by (14).

Dividing (13) by dh, we can obtain the adiabatic lapse rate. The approximate value of it is given by

$$-\frac{dT}{dh}=\Gamma\frac{1+\frac{rx}{R'T_1}}{1+\frac{x}{C_p}\left(C+\frac{dr}{dT}+\frac{r}{f}\frac{df}{dT}\right)} \quad \cdots\cdots (15)$$

or

$$-\frac{dT}{dh}=\Gamma\frac{1+\frac{rx}{R'T_1}}{1+\frac{rx}{c_pf}\frac{df}{dT}}. \quad \cdots\cdots (16)$$

This is the Brunt's well-known formura.

If the values of f_0 and f are very small compared to p_0 and p, (14) becomes

$$\frac{g}{\gamma}\log\frac{T_1}{T_{10}}=(C_p+Cx_0)\log\frac{T}{T_0}+\left(\frac{rx}{T}-\frac{r_0x_0}{T_0}\right) \quad \cdots\cdots (17)$$

where the relation $\frac{p}{p_0}=\left(\frac{T_1}{T_{10}}\right)^{\frac{g}{R'\gamma}}$ is used.

From (17) we can obtain

$$-\frac{dT}{dh}=\Gamma\frac{T}{T_1}\frac{1}{1+\frac{Cx_0}{C_p}+\frac{1}{\frac{T}{C_p}\frac{d}{dT}\left(\frac{rx}{T}\right)}} \quad \cdots\cdots (18)$$

If $Cx_0 \ll C_p$, (18) becomes

$$-\frac{dT}{dh}=\Gamma\frac{T}{T_1}\frac{1}{1+\frac{T}{C_p}\frac{d}{dT}\left(\frac{rx}{T}\right)} \quad \cdots\cdots (19)$$

6. Examples of the Numerical Relation between h and T

To obtain the numerical relation between h and T by (14), we put $x=\varepsilon\frac{f}{p-f}$, $\varepsilon=0.622$, and for simplicity's sake we put $\frac{p-f}{p_0-f_0}=\frac{p}{p_0}$ and $Cx_0 \ll C_p$. Some examples are given in the table 2.

7. A Graphical Method of obtaining the Relation between h and $\frac{dh}{dt}$

If the temperatures of the small mass of air and the surrounding atmosphere are T and T_1 respectively, then the ascending acceleration of the mass, in the case of no resistance, is expressed by

$$\frac{d^2h}{dt^2}=\frac{\triangle T}{T_1}g, \text{ where } \triangle T=T-T_1.$$

Table. 2.

$P_0 = 760$, $T_0 = 300$

T	300	295	290	285	280	275	270
P	760	658	571	500	441	390	347
T_1	290	284.1	278.4	273.2	268.3	263.6	259.3
h	0	1190	2320	3350	4340	5270	6140
T_1	280	274.3	268.8	263.8	259.0	254.6	250.4
h	0	1150	2240	3240	4190	5090	5920

$P_0 = 760$, $T_0 = 290$

T	290	285	280	275	270	265	260
P	760	673	600	538	486	438	399
T_1	285	280.0	275.4	271.2	267.3	263.5	260.0
h	0	1000	1910	2750	3550	4310	5010
T_1	280	275.1	270.6	266.5	262.5	258.5	255.4
h	0	986	1880	2700	3490	4240	4950
T_1	275	270.2	265.9	261.7	257.9	254.3	250.8
h	0	967	1850	2650	3420	4140	4840
T_1	270	265.2	261.0	257.0	253.2	249.7	246.3
h	0	950	1810	2600	3360	4060	4750

$P_0 = 760$, $T_0 = 310$

T	310	305	300	295	290	285	280
P	760	646	547	463	397	339	292
T_1	305	298.0	291.0	284.2	277.7	271.8	266.0
h	0	1400	2800	4170	5450	6640	7790
T_1	300	294.1	286.2	279.5	273.2	267.3	261.6
h	0	1380	2760	4100	5360	6540	7670
T_1	295	288.2	281.4	274.8	268.6	262.7	257.3
h	0	1360	2720	4030	5270	6430	7540
T_1	290	283.3	276.7	270.2	263.4	258.4	253.0
h	0	1335	2670	3960	5180	6320	7410

Integrating this expression, under the condition $\frac{dh}{dt} = 0$ at $h = 0$, we get

$$\int^{h} \frac{\triangle T}{T_1} g dh = \frac{1}{2}\left(\frac{dh}{dt}\right)^2. \qquad \cdots\cdots (16)$$

When the changes in T and T_1 with height h are given graphically as in Fig. 2. the value of the integral $\int_0^h \frac{\triangle T}{T_1} g dh$ can be graphically obtained approximately.

On the graph, $\triangle T dh$ is the element of the area between T-curve and T_1-curve. If the mean value of $\frac{1}{T_1}$ is expressed by $\frac{1}{T_{1m}}$, the integral becomes

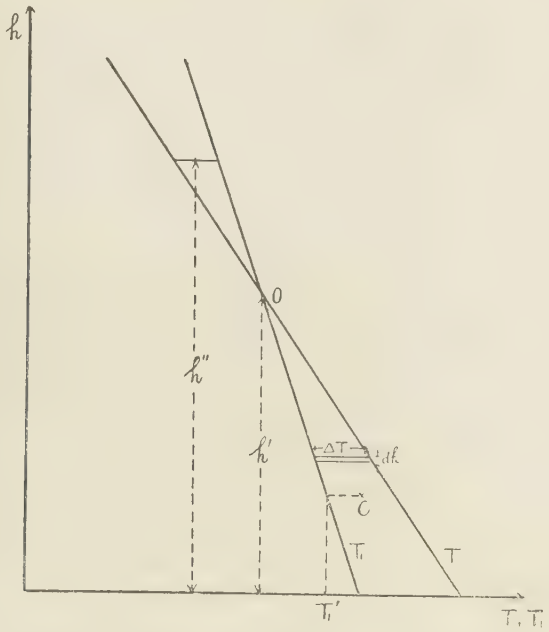

Fig. 2

$$\int_0^h \frac{\triangle T}{T_1}\,dh = \frac{1}{T_{1m}}\int_0^h \triangle T dh.$$

If the mean value of T_1 is expressed by, T_1', the difference between T_1' and T_{1m} is very small in the practical case, and we can put approximately

$$\int_0^h \frac{\triangle T}{T_1}\,dh = \frac{1}{T_1'}\int_0^h \triangle T dh.$$

T_1' is obtained easily as the temperature of the centre of the area, and so the approximate value of the integral is easily obtained graphically. $\left(\frac{dh}{dt}\right)^2$ is given by the integral multiplied by $2g$. For example, to get the ascending velocity of the mass of air at $h=h'$, the area between two curves lower than h' is divided by the temperature T_1' at the centre of the area, and multiplied by $2g$. The result gives the square of the velocity. The square of the velocity at the height h'', higher than the place of the intersection 0 of the two curves, is obtained similarly if the area above 0 is taken negative.

This method is not mathematically exact, but as shown in the next examples in the Table 3, the results obtained by this method agree fairly good with those obtained by exact numerical calculation. In the examples, the values of $\frac{dh}{dt}$ obtained by the above

graphical method and the values of $\frac{dh}{dt}$ of Table 2 of the previous paper [1] are given side by side for comparison. $\left(\frac{dh}{dt}\right)_g$ is the values obtained by the graphical method and $\left(\frac{dh}{dt}\right)_c$ is the values in the Table 2 of the previous paper which are obtained by the numerical calculation. In the examples, we take in the graphical method only the case where $T_1 = T_{10} - \frac{h}{200}$ and $T = T_0 - \frac{h}{100}$ are satisfied.

Table 3,

T_{10}	T_0	h	T_1	$\left(\frac{dh}{dt}\right)_g$	$\left(\frac{dh}{dt}\right)_c$
260°K	265°K	1000m	258°.3K	13.8$\frac{m}{sec}$	13.5 $\frac{m}{sec}$
	270	1000	257.8	23.8	23.5
		2000	256.7	27.6	26.8
260	275	1000	257.7	30.8	30.5
		2000	255.8	39.1	38.2
		3000	255.0	41.5	40.0(h=2836m)
260	280	1000	257.6	36.5	35.2
		2000	255.6	48.0	45.8
		3000	254.0	53.8	51.8
		4000	253.3	55.6	52.7(h=3714)
270	275	1000	268.3	13.5	13.3(h=982)
270	280	2000	266.7	27.1	26.4(h=1929)
270	285	3000	265.0	40.8	39.2(h=2842)
270	290	4000	263.3	54.5	51.9(h=3725)
280	285	1000	278.3	13.3	13.0(h=983)
280	290	2000	276.7	26.6	25.9(h=1931)
280	295	3000	275.0	40.0	38.6(h=2848)
280	300	4000	273.3	53.5	51.0(h=3734)
290	295	1000	288.3	13.0	
290	300	2000	286.7	26.1	
290	305	3000	285.0	39.3	
290	310	4000	283.3	52.6	

It is obvious from the examples that if the curves of T and T_1 are graphically given, we can easily obtain the reliable values of the ascending velocities.

When $\triangle T_0 = T_0 - T_{10}$ becomes large as 20°, and the height becomes considerably large, the values of $\left(\frac{dh}{dt}\right)_g$ and $\left(\frac{dh}{dt}\right)_c$ slightly differ. But it is considered that this difference is principally caused from the assumption in the graphical method that the lapse rate of T is always $\Gamma = \frac{1}{100}^{\circ} - \frac{1}{m}$, while the lapse rate of T in the Table 2 of the previous

paper is given by $-\frac{dT}{dh} = \Gamma\frac{T}{T_1}$. Thus when $T > T_1$, T has the lapse rate greater than Γ and $\triangle T$ becomes smaller than the case of the above assumption, and naturally we get $\left(\frac{dh}{dt}\right)_e < \left(\frac{dh}{dt}\right)_g$. From these considerations, it is concluded that the graphical method above mentioned can be applied in most cases with sufficient accuracy.

8. Ascending Velocity of Wet Air

For the simplicity's sake, we consider here only the case of no resistance to the ascension. The ascending acceleration of wet air depends not only on the difference of temperature with the surrounding atmosphere, but also on the quantity of water vapour contained in the air. We take the wet air of pressure p and temperature T. If the volume of the wet air, which contains the mass of the dry air of 1 g, is v, and the mass of water vapour contained in v is x g, and the partial pressure of water vapour is f, x is given by $x = \frac{0.622f}{p-f}$. If the temperature and the partial pressure of the vapour of the surrounding atmosphere are T_1 and f_1, and the quantities of dry air and water vapour contained in the volume v are $m\,g$ and $x_1 g$ respectively, x_1 is given by $x_1 = \frac{0.622f_1}{p-f_1} = m$.

Therefore the ascending force, acting on the wet air of volume v, which contains 1 g of dry air, is expressed by

$$\{m + x_1 - (1 + x)\}g = (m - 1 + x_1 - x)g$$

But from $(p-f)v = RT$, $(p-f_1)v = mRT_1$, we obtain $m = \frac{T}{T_1}\frac{p-f_1}{p-f}$ and $x_1 = \frac{0.622}{p-f}\frac{T}{T_1}f_1$, and the ascending force is given by

$$\left\{\left(\frac{T}{T_1}\frac{p-f_1}{p-f} - 1\right) + \frac{0.622}{p-f}\left(\frac{T}{T_1}f_1 - f\right)\right\}g.$$

If the temperatures T and T_1 are not so high, the principal term of the above expression is $\left(\frac{T}{T_1}\frac{p-f_1}{p-f} - 1\right)g$, as the following example shows.

As a special case, if we take $T = 290$, $T_1 = 280$, $p = 760$, $f = 14.4$, $f_1 = 7.5$, then $\frac{T}{T_1}\frac{p-f_1}{p-f} - 1$ is 0.045 and $\frac{0.622}{p-f}\left(\frac{T}{T_1}f_1 - f\right)$ is -0.0055. Thus if we can put $p \gg f$ and $p \gg f_1$, the ascending force can be expressed by

$$\left(\frac{T}{T_1} - 1\right)g = \frac{\triangle T}{T_1}\,g.$$

In this case the graphical method stated in 7. is available to obtain the ascending velociy of the wet air.

If the variations of T and T_1 with h are given graphically, the ascending velocity of wet air, in the case of no resistance, can be obtained easily by the graphical method. In the case of wet air which contains saturated vapour, the lapse rate of T becomes small compared to the case of dry air, it happens occasionally that the ascending acceleration keeps large value even at the considerable hieght when the temperature T is not low. When T becomes low, the quantity of water vapour contained in the wet air becomes small, change in T is nearly the same as in the case of dry air.

9. Conclusions

We have studied the ascension and the changes in state of a small mass of wet air under the assumptions as those taken in the case of dry air[1]. Here we have studied only the case where there is no resistance to the motion and no heat exchange between the mass of air and the surrounding atmosphere, and obtained the height of condensation layer, the change in temperature over the layer, and the ascending velocity in it. Concerning to the relation between the ascending velocity and the height, we have proposed a simple graphical method which can be used in the case of dry air and in the most cases of wet air.

In conclusions, the auther wishes to express his sincere thanks to professor S. T. Nakamura for his important suggestions, his guidance and encouragement.

References

(1) S. Fujita: Ascension of a Small Mass of Air (I).
Kumamoto J. Sc. Vol. 2. No. 4, (1956)
(2) See any Book written on the Meteorological Thermodynamics.

ANSWER TO MR. MATSUMAE'S CRITICISM GIVEN TO MY PAPERS ON THERMODYNAMICS

Shigeichi FUJITA

(Received November 30, 1956)

1. Introduction

Mr. S. Matsumae has given a severe criticism[3] to my papers[1],[2] on thermodynamics. He has used strong words, and without solid grounds, he has selfishly decided that I had grossly mistaken.

Some of the fundamental laws of thermodynamics were sometimes misunderstood by students and I wished always to remove the misunderstanding by clear explanation. The two mentioned papers on thermodynamics were written for the purpose of removing the misunderstanding about some of the fundamental laws of thermodynamics.

After reading Mr. Matsumae's criticism, I have been disappointed. It seems to me, I am sorry, that Mr. Matsumae also misunderstands on some points of the fundamental laws of thermodynamics. I shall state my opinion about his criticisms (1) and (2) in the following.

2. Answer to the Criticism (1)

In (1) he asserts, to sum up, "The expressions $dF=-pdV$ and $dF=-pdV-\sum_i X_i\,dx_i$ which are obtained by the reversible, isothermal process of the system, must be used only to the reversible isothermal process and must not be used to the irreversible isothermal processes".

Of course, if we want to obtain the change in entropy or the change in free energy of a system when it changes from one state to another state irreversibly, we assume a reversible process between the two states and calculate the change in entropy or the change in free energy on that reversible process. Hence, if the initial state and the final state of the system are given definitely, the change in entropy or the change in free energy is definitely determined, even though the process is irreversible.

From this reason, it is considered that Mr. Matsumae's assertion above mentioned will be erroneous.

For the purpose of clarifying the reason further, I shall consider, as a simple example, isothermal changes in state of ν moles of any ideal gas. We take as the independent state variables, the temperature T and the volume V, and consider the small change in state from (T,V) to $(T,V+dV)$. As the initial and the final states are given definitely, the changes in free energy must be definitely given by

$$dF = -pdV = -\nu RT\frac{dV}{V},$$

even though the change is irreversible. In the case of the finite change in state, reversible or irreversible, from (T, V_1) to (T, V_2), the change in free energy must be definitely given by

$$\triangle F = -\int_{V_1}^{V_2} pdV = \nu RT\ log\frac{V_1}{V_2}.$$

According to Mr. Matsumae's assertion, in the case of irreversible isothermal change in state, the change in free energy must be expressed by

$$dF < -pdV \text{ and } \triangle F < \nu RT\ log\frac{V_1}{V_2}.$$

It means that the change in free energy can not be determined by the initial and the final states only, but must be influenced by the process between the two states, which is considered erroneous.

3. Answer to the Criticism (2)

In (2) Mr. Matsumae gives two examples perhaps for denying the two examples which I mentioned for the purpose of proving my opinion that there are some cases where the entropy production of the stationary process under definite conditions is greater than the entropy productions of some of the non-stationary processes under the same conditions. But it is considered that his examples are out of focus and almost meaningless as shown in the following.

(a) For my statement "When a definite E.M.F. is applied to a circuit, the electric current increases from 0 to a stationary value. Accordingly, it can not be said that the entropy production of the stationary state becomes minimum.", Mr. Matsumae gives no reason of denying my statement, but gives the next sentence,

"The electirc current in the stationary state takes such a distribution that the total amount of the Joule's heat generated by the electric current is minimum. For example, when the electric current flows through a passive network, the electric current in the stationary state flows in accordance with the Kirchhoff's law and, in this case, the total amount of the Joule's heat is minimum, if compared with that in other cases. And the Kirchhoff's law is derived reciprocally from the principle of the minimum of the Joule's heat in the stationary state."

Here he takes up only the stationary current distrbiution given by the Kirchhoff's law and the other imaginary distributions of the stationary current. He does not notice, perhaps, that if we want to assert the minimum entropy production of the stationary state, we must consider the entropy production of the stationary state and all the entropy productions of the possible non-stationary states near the stationary state, and show that the

entropy production of the stationary state is the least among all these entropy productions. His understanding about the meaning of the minimum is very doubtful in this case.

(b) For my statement "When both ends of a homogeneous straight rod are kept at two constant temperatures T and T_1 ($T > T_1$) respectively, heat flows from T end to T_1 end, and if heat does not pass through lateral surface, the temperature T of the middle point of the rod is equal to $\frac{T + T_1}{2}$ in the stationary flow. But it is proved that if the temperature T of the middle point of the rod is slightly lower than $\frac{T + T_1}{2}$, the entropy production is slightly smaller than that of the case of $T = \frac{T_1 + T_2}{2}$.", Mr. Matsumae gives no reason of denying my statement, but gives a series of extremely special processes, and wants to say that the entropy production of the stationary flow is minimum in that series, and by this reason only he wants to decide that the entropy production of the stationary flow is minimum among all the entropy productions of the possible non-stationary flows near the stationary flow.

In my statement, a case, where the entropy production of non-stationary flow near the stationary one is smaller than the entropy production of the stationary flow, is given. By this case only, we can say that the entropy production of the stationary flow is not minimum.

As above stated, for the assertion of the minimum entropy production in the stationary process, it is necessary to show that among the entropy productions of stationary process and all the possible non stationary processes near the stationary one the entropy production of the stationary process is the least.

But for denying the minimum entropy production of the stationary process, it is sufficient to show only a case of the smaller entropy production of non-stationary process near the stationary process than the entropy production of the stationary process. Thus it is supposed that Mr. Matsumae misunderstands the meaning of the minimum in this case also.

4. Acknowledgement

The writer wishes to express his sincere thanks to Mr. R. Adachi for his detailed re examination about the writer's papers [1] and [2], in the proof of the typewrite of these papers.

References

(1) S. Fujita: Criticism on the Expressions of the Secood Law of Thermodynamics. Kumamoto J. Sc. Vol. 1. No. 4 (1954)
(2) S. Fujita: Quasi-Stationary Process (I) On Entropy Production. Kumamoto J. Sc. Vol. 2. No. 1 (1954)
(3) S. Matsumae: Criticism on the Fujita's Opinions on the Thermodynamics. Kumamoto J. Sc. Vol. 2. No. 4 (1956)

THE EXACT STELLAR MODEL OF THE PARTIALLY DEGENERATE ISOTHERMAL GAS SPHERE

Keisuke KAMINISI

(Received December 20, 1956)

Abstract

The internal structure of the exact model of the partially degenerate isothermal gas sphere in which the gas pressure consists of both the degenerate electron and the nondegenerate ion gas pressure is investigated. The values of density and pressure are, at $r \simeq 0.03\ R_{\odot}$, several times greater in this model (, whose central degeneracy $\psi_0 = 20$,) than in the approximate model in which the non-degenerate ion gas pressure is neglected.

1. Introduction

At present it is generally believed that a main-sequence star will evolve into the stage of a red giant in the following evolutionally process: A initially homogenous main-sequence star with a convective core and radiative envelope continues to exhaust its hydrogen fuel in its core by p-p or C N reactions. If the star possesses no appreciable mixing current between the core and envelope, hydrogen in the core is gradually converted into helium, but the material in the envelope retains in its original composition. After burning out of its hydrogen in its core, the star will evolve into the stage of a giant with a fuel-exhausted, isothermal core (whose energy generating zone will move outwards).

Stellar models with hydrogen exhausted isothermal cores in a partially degenerate state have been investigated by various authors [1], [2], [3], [4] and they found that these models could give very large radii—large enough to fit the red giants. In building up the inner core of the model, they used, as the pressure, only the partially degenerate pressure due to the degenerate electron gas and did not take account of the perfect gas pressure due to the non-degenerate ion gas, in order to facilitate the computation of these problems. Indeed, in the strong degenerate material the degenerate pressure is so huge that the proportion of non-degenerate pressure to the total pressure is negligible. But in the incipient degenerate state, the degenerate pressure is comparable with the non-degenerate pressure. In the usual partially degenerate isothermal core of giant, the contribution of non-degenerate ion gas pressure to the total pressure is not negligible. Furthermore in order to building up the stellar model, we must carry out the integration of differential equation involving the pressure gradient. Hence even small mathematical inexactitudes may lead to results which may be considerably incorrect.

In the present work we will integrate the more exact differential equation in which the gas pressure is expressed by the resultant of both degenerate electron gas pressure and

nondegenerate ion gas pressure, and show the considerably large discrepancy between the internal structures of our exact model and approximate model in which the non-degenerate gas pressure is neglected.

2. Partially Degenerate Isothermal Gas Sphere

The problem of the structure of partially degenerate isothermal stellar model was solved and tabulated by G. W. Wares [5], [6]. According to his theory, the equation of state of the partially degenerate isothermal model is

$$\left.\begin{aligned} \rho &= |B_1|\mu_e T^{3/2} F_{1/2}(\psi) \\ P &= p_e + p_r = |A_1| T^{5/2} \frac{2}{3} F_{3/2}(\psi) + \frac{a}{3} T^4 \end{aligned}\right\} \quad \cdots\cdots (1)$$

where

$$|B_1|\mu_e T^{3/2} = 9.11 \times 10^{-4}\ \mu_e T^{3/2}\ gr/cm^3 \quad \cdots\cdots (2)$$

$$|A_1| T^{5/2} = 7.42 \times 10^{-7}\ T^{5/2}\ \text{atm.} \quad \cdots\cdots (3)$$

and both $F_{1/2}(\psi)$ and $F_{3/2}(\psi)$ are the Fermi-Dirac functions defined by

$$F_v(\psi) = \int_0^\infty \frac{u^v\, du}{e^{-\psi+u}+1} \quad \cdots\cdots (4).$$

The fundamental differential equation for his model is

$$\frac{1}{\xi^2}\frac{d}{d\xi}\left(\xi^2 \frac{d\psi}{d\xi}\right) = -F_{1/2}(\psi) \quad \cdots\cdots (5)$$

where $r = \alpha_1 \xi$ $\cdots\cdots (6)$

and $$\alpha_1 = \left[\frac{|A_1| T^{5/2}}{4\pi G |B_1|^2 \mu_e^2 T^3}\right]^{1/2} = \frac{1.495}{\mu_e T^{1/4}} R_\odot \quad \cdots\cdots (7).$$

The results obtained by G. W. Wares have been used by various authors [1], [3], then the equation (5) obtained by using the equation of state (1) has been employed to build up the partially degenerate isothermal core of giand [2], [4]. However the equation of state is not rigorous from a physical point of view because of neglecting the non-degenerate ion gas pressure p_i, which is not a negligible small quantity.

The exact equation of state of the partially degenerate isothermal model is

$$P = p_e + p_i + p_r, \quad \rho = |B_1|\mu_e T^{3/2} F_{1/2}(\psi) \quad \cdots\cdots (8)$$

where

$$p_i = -\frac{\rho}{\mu_i H} kT$$
$$= \frac{4\pi}{h^3}\frac{\mu_e}{\mu_i}(2m)^{3/2}(kT)^{5/2} F_{1/2}(\psi)$$
$$= |A_1| T^{5/2}\frac{\mu_e}{\mu_i} F_{1/2}(\psi) \quad \cdots\cdots (9).$$

By making use of Eq. (8), we have the following fundamental differential equation of the partially degenerate isothermal model:

$$\frac{1}{\xi^2}\frac{d}{d\xi}\left\{\xi^2\frac{d\psi}{d\xi}\left(1+\frac{\mu_e}{\mu_i}\frac{1}{F_{1/2}(\psi)}\frac{dF_{1/2}(\psi)}{d\psi}\right)\right\} = -F_{1/2}(\psi) \quad \cdots\cdots (10)$$

This equation is tend to the Eq. (5) as the correction term $\frac{\mu_e}{\mu_i}\frac{1}{F_{1/2}(\psi)}\frac{dF_{1/2}(\psi)}{d\psi} \to 0$. In the correction term, both $\frac{\mu_e}{\mu_i} \fallingdotseq \frac{Z}{A} \fallingdotseq \frac{1}{2}$, where Z and A are the mean atomic number and weight respectively of the element in the hydrogen exausted core, and $\frac{F_{1/2}'(\psi)}{F_{1/2}(\psi)} = 0.79$ for $\psi = 0$ (incipient degeneracy), are not negligible quantities. In the case of rather strong degeneracy, for example, $\psi = 20$, $\frac{F_{1/2}'(\psi)}{F_{1/2}(\psi)} = 0.075$ is considerably small. However since the equation (10) is a differential equation, the even small discrepancy at the initial stage can lead to the great discrepancy because of the accumulation of small quantities, as we go on carrying out the numerical integration.

3. Numerical Integration

In the integration of Eq (10). we need to assume the values of μ_e and μ_i. The value of μ_e is computed to correspond to the number of free electrons, and depends upon the chemical composition and the degree of ionization of the material. In the completely ionized gas of hydrogen exhausted matter, $\mu_e = 2.00$. The estimation of the degree of ionization was given by T. D. Lee [7]. According to his results the helium and Russell mixture can be, over the region of pressure ionization and temperature ionization, regarded as completely ionized under the physical condition of the partially degenerate isothermal core of giant, where the temperature is cosiderably high. Hence we may adopt the value $\mu_e = 2.00$ throughout our hydrogen exhausted model. The value of μ_i is computed to correspond to the number of ions and depends upon the chemical composition. Under the circumstances in our hydrogen exhausted core we may assume that the chemical composition in our model consists of the uniform mixture of 0.924 He and 0.076 Russell mixture, then such a chemical composition gives the value $\mu_i = 4.24$ throughout our model. Hence we can get the value

$\frac{\mu_e}{\mu_i} = 0.472$, which is constant in the all region we are considering. The values of $F_\nu(\psi)$, Fermi-Dirac functions, are read from the table given by J. Mc Dougall and E. C. Stoner (8).

Now we can numerically integrate Eq. (10). The results obtained by iteration method are tabulated in the table (1), where the boundary conditions have been taken at the center ($\xi = 0$) of our model as follow:

$$\psi(0) = \psi_0 = 20, \quad \frac{d\psi}{d\xi} = 0 \qquad (11).$$

TABLE 1

ξ	ψ	$\rho\propto F_{1/2}(\psi)$	$\frac{2}{3}F_{3/2}(\psi)$	$p_g\propto\left(\frac{2}{3}F_{3/2}(\psi)+\frac{\mu_e}{\mu_i}F_{1/2}(\psi)\right)$	$-\frac{d\psi}{d\xi}$	$M(\xi)\propto-\xi_2\frac{d\psi}{d\xi}\left(1+\frac{\mu_e}{\mu_i}\frac{1}{F_{1/2}}\frac{dF_{1/2}}{d\psi}\right)$
0.0	20.000	59.813	484.379	512.611	0.000	0.000 00
0.1	19.904	59.384	478.657	506.686	1.917	0.019 85
0.2	19.618	58.114	461.855	489.285	3.783	0.156 77
0.3	19.151	56.061	435.196	461.657	5.550	0.517 87
0.4	18.513	53.295	400.314	425.469	7.172	1.191 2
0.5	17.722	49.933	359.493	383.061	8.613	2.238 9
0.6	16.797	46.095	315.088	336.845	9.845	3.692 6
0.7	15.761	41.922	269.506	289.293	10.847	5.552 1
0.8	14.636	37.544	224.821	242.542	11.607	7.785 5
0.9	13.447	33.099	182.843	.198.466	12.126	10.334
1.0	12.219	28.712	144.913	158.465	12.407	13.118
1.1	10.974	24.486	111.821	123.378	12.466	16.044
1.2	9.733	20.510	83.926	93.607	12.321	19.010
1.3	8.515	16.851	61.199	69.153	11.995	21.918
1.4	7.339	13.564	43.340	49.742	11.515	24.678
1.5	6.217	10.674	29.766	34.804	10.907	27.213
1.6	5.161	8.194	19.825	23.693	10.200	29.465
1.7	4.180	6.124	12.822	15.713	9.421	31.393
1.8	3.278	4.446	8.073	10.172	8.605	32.997
1.9	2.459	3.136	4.983	6.463	7.782	34.280
2.0	1.721	2.155	3.043	4.060	6.901	35.273
2.1	1.058	1.449	1.857	2.541	6.264	36.020
2.2	0.464	0.965	1.147	1.602	5.624	36.569
2.3	−0.070	0.640	0.721	1.023	5.072	36.970
2.4	−0.554	0.429	0.464	0.666	4.610	37.263

4. Comparison with the approximate model.

We illustrate the (ψ, r), (ρ, r) and (p_g, r) curves in the Figures 1, 2, and 3 respectively, in each of which two curves (the one is determined from the Table 1 given by the results of our exact model and the other from Wares Table (6)) are drawn in order to show the discrepancy between the internal constitution of our exact model and the approximate model given by Wares.

In the Fig. 1 we find that the discrepancy of two curves becomes larger and larger as we proceed apart from the center of a configuration, and at $r = 1.8 \times \left(\frac{10}{T}\right) \frac{R_\bullet}{100}$, the distance from the center, the discrepancy between two values of ψ, the degree of

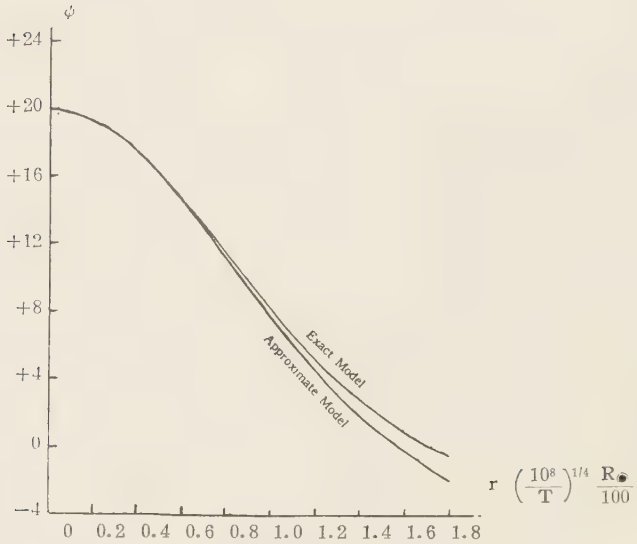

Fig. 1 The curves of the degree of degeneracy for two models

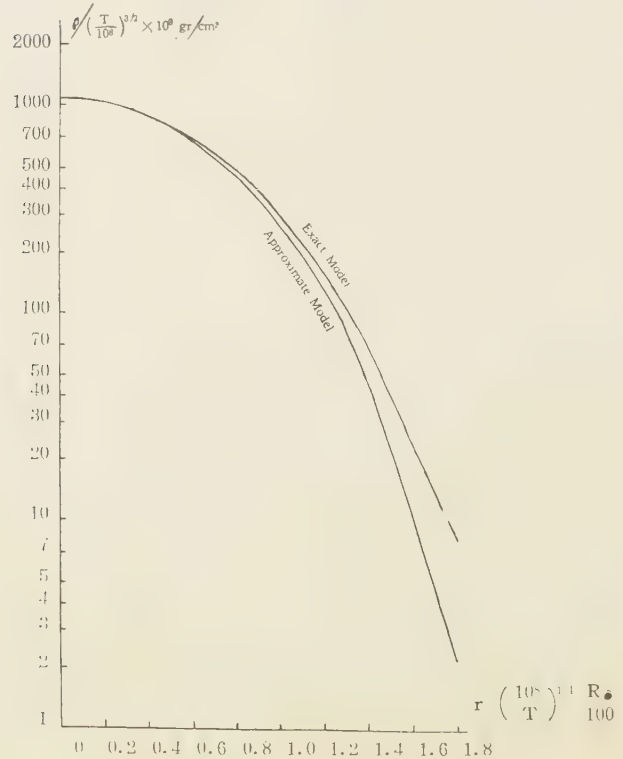

Fig. 2 Density distribution for two models

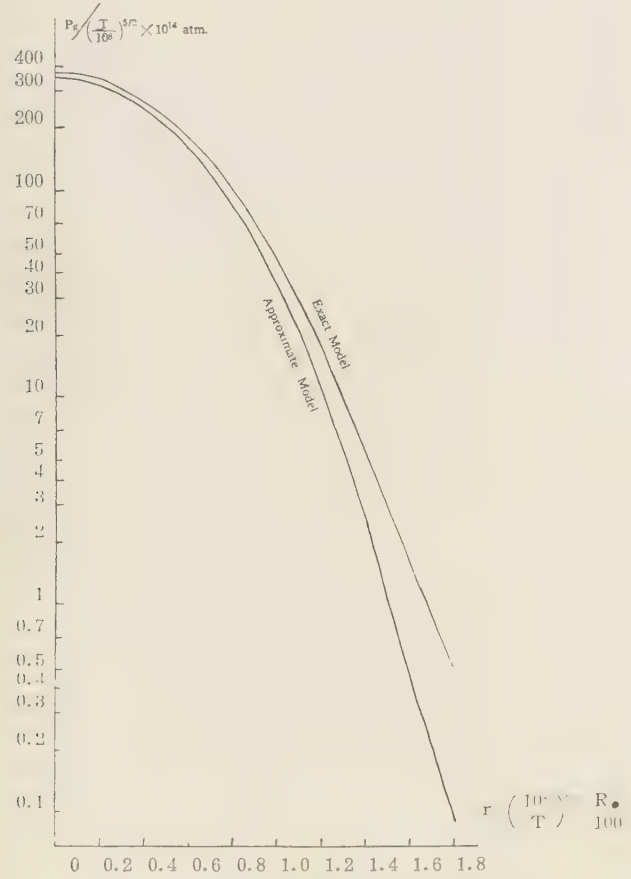

Fig. 3 Pressure distributions for two models

degeneracy, comes to about 1.7. In the Fig. 2 we find that since the decreasing of density is considerably slower in our exact model than in the approximate model, the ratio ρ_{exact}/ρ_{appr} runs up into about 4 at $r = 1.8 \times \left(\frac{10^8}{T}\right)^{1/4} \frac{R_\odot}{100}$. In the Fig. 3 we can also find that the ratio p_{exact}/p_{appr} reaches to about 5.6.

5. Conclusions

In almost all red giant models with partially degenerate isothermal core, the radius of core, $x_1 R$, falls within the rather narrow range from $0.05\ R_\odot$ to $0.08\ R_\odot$. Since it is considered that T, the temperature in core, may be about $2 \times 10^8\ K$, $r = 1.8 \times \left(\frac{10^8}{T}\right)^{1/4} \frac{R_\odot}{100}$ may be nearly equale to $0.027\ R_\odot$, which is much smaller than the radius of core. Even

at the small distance from the center $r = 0.027\ R_\odot$ the discrepancy between two models comes to considerably large, and practically speaking the density ratio $\rho_{exact}/\rho_{appr} \fallingdotseq 4$, and the gas pressure ratio $p_{exact}/p_{appr} \fallingdotseq 5.6$ (the radiation pressure is still negligible there). Since such a discrepancy will become larger and larger as we shall proceed from center to outer region, the physical condition such as pressure or density (or degree of degeneracy) will be very different from the one in our exact model at the surface of isothermal core.

Such a large discrepancy have serious effect on the fitting at the interface between core and radiative envelope. Hence for the more precise investigation of the structure of red giant we are obliged to deal with the exact model, in which the gas pressure consists of both the partially degenerate electron and the non-degenerate ion gas pressure.

This paper was read on May 2, 1956, at the annual meeting of the Astronomical Society of Japan.

The author wishes to express his thanks to the professors of the Department of Physics, Kumamoto University, for their constant encouragement.

References

1. G. Gamov and G. Keller: Rev. Mod. Phys., Vol. 17, p. 125, '45.
2. C. Hayashi: Prog. Theor. Phys., Vol. 2, p. 127, '47.
3. M. Schwarzschild. I. Robinowitz and R. Härm: Ap. J., Vol. 118, p. 326, '53.
4. F. Hoyle and M. Schwarzschild: Ap. J. Suppl. 2, No. 13, '55.
5. G. W. Wares: Ap. J., Vol. 100, p. 158, '44.
6. R. Härm and M. Schwarzschild: Ap. J. Suppl. 1, No. 10, '55.
7. T. D. Lee: Ap. J., Vol. 111, p. 625 '50
8. J. McDougall and E. C. Stoner: Phil. Trans., A, Vol. 257, p. 67, '38.

THE LONGITUDINAL MAGNETOSTRICTION OF Fe-Ni ALLOYS AND Fe-Co ALLOYS IN WEAK MAGNETIC FIELD

Tatuo TIKAZAWA and Shigeo MATSUMAE

(Received November 31, 1956)

[I] Introduction

One of the present writers studied the longitudinal magnetostriction of nickel in weak magnetic field.[1],[2],[3],[4] On further, we study the longitudinal magnetostriction of Fe–Ni alloys and Fe–Co alloys in weak magnetic field. The experimental results are as follows.

[II] Experimental results

Apparatus of the measurement and experimental method are the same as described in the previous papers.[1],[2],[3],[4]

The specimens are 21 cm long and 1.5 mm or 2 mm in diameter.

The specimens are annealed at 900°C for 2 hours and then cooled to the room-temperature with the furnace.

The specimens are, at first, demagnetized with the alternate magnetic field having the maximum amplitude of about 7 Oersted.

After demagnetizing, the tensive or compressive stresses are applied to the specimens, according to the positive or negative longitudinal magnetostriction of the specimen.

The experimental results are as follows.

(a) Fe–Ni alloys

(i) Fe

The specimens are 21 cm long and 1.5 mm in diameter.

The experimental results are shown in figure 1 and 2.

As shown in the figures, the longitudinal magnetostriction in weak magnetic field is unobservable, when the tensive stress is not applied to the specimen. But, under tensive stress, the longitudinal magnetostriction is detectable even in weak magnetic field. It increases, at first, with the increase of the tensive stress and then shows a maximum in the vicinity of the external stress of about 2.4 kg/mm² and finally decreases, on the contrary, with the increase of the tensive stress. The measurements are not taken, when the tensive stress is larger than 6 kg/mm².

This behavior was already found in nickel, as shown in previous papers[2],[3], and is also observed in Fe–Ni alloys and Fe–Co alloys, as described in the following.

And the longitudinal magnetostriction in weak magnetic field is almost direct proportional to the intensity of magnetization, as shown in the figures. This behavior is observed

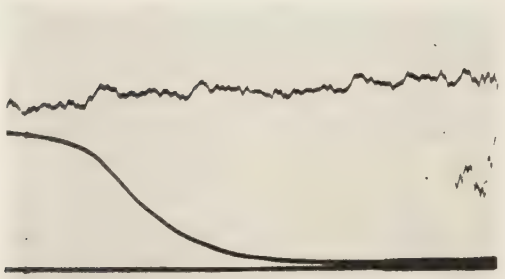

$\sigma = 0 \mathrm{kg/mm^2}$

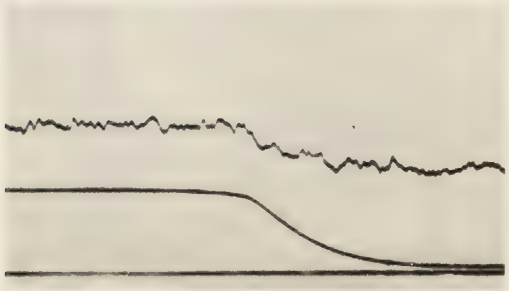

$\sigma = 1.2 \mathrm{kg/mm^2}$

$\sigma = 2.4 \mathrm{kg/mm^2}$

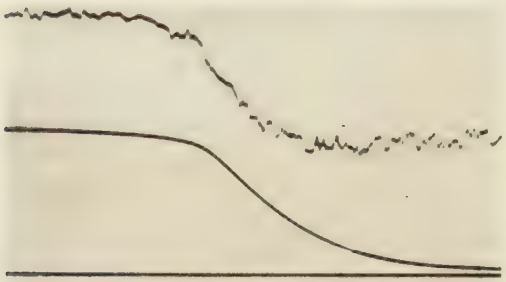

$\sigma = 3.6 \mathrm{kg/mm^2}$

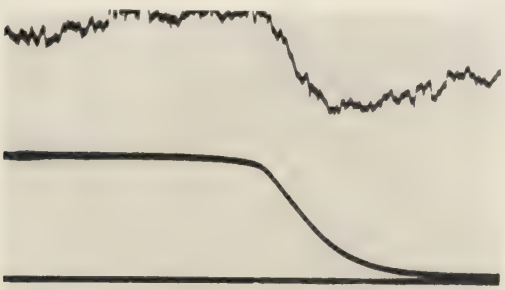

$\sigma = 4.8 \mathrm{kg/mm^2}$

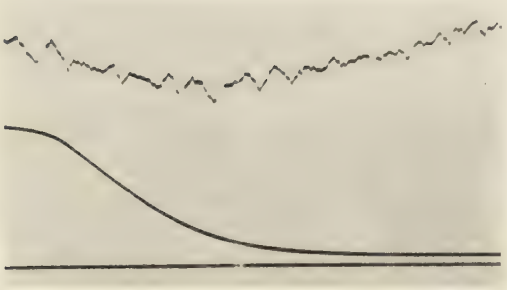

$\sigma = 6.0 \mathrm{kg/mm^2}$

Fig. 1. Oscillograph records of the longitudinal magnetostriction of iron under various tensive stresses in weak magnetic field.

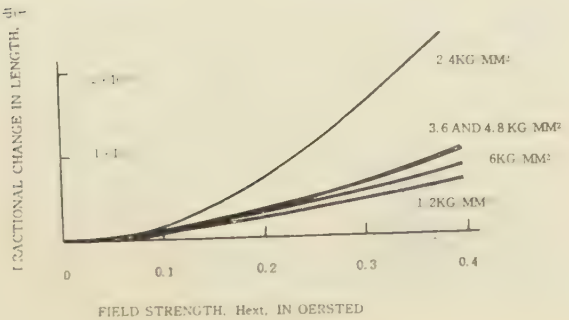

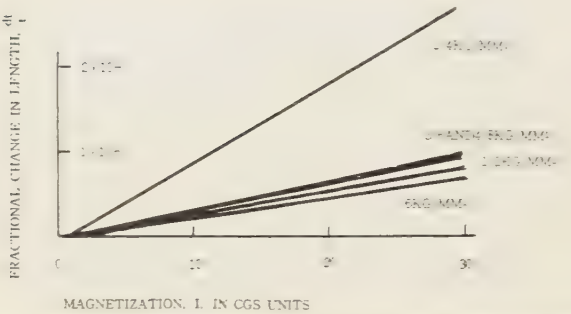

Fig. 2. dl/l–I and dl/l–Hext curves of iron under various tensive stresses in weak magnetic field.

in Fe–Ni alloys and Fe–Co alloys, as shown in the following.

(ii) Ni (70%)–Fe alloy

The specimens are 21 cm long and 1.5 mm in diameter.

The experimental results are shown in Fig. 3.

As shown in the figure, the longitudinal magnetostriction in weak magnetic field increases with the increase of the external tensive stress and shows a maximum in the

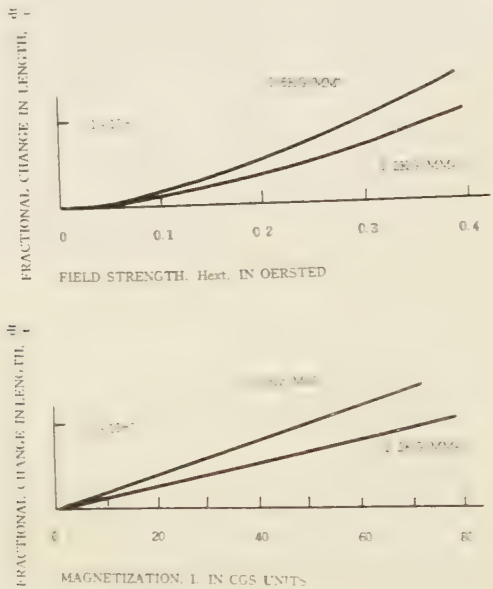

Fig. 3. dl/l–I and dl/l–Hext curves of Ni (70%) Fe alloy under various tensive stresses in weak magnetic field.

vicinity of about 0.6 kg/mm². Then, it decreases, on the contrary, with the increase of the external tensive stress and comes to be almost unobservable under the tensive stress of about 2 kg/mm².

(iii) Ni(50%)-Fe alloy

The specimens are 21 cm long and 1.5 mm in diameter.

The experimental results are shown in Fig. 4. and Fig. 5.

$\sigma = 0\text{kg/mm}^2$

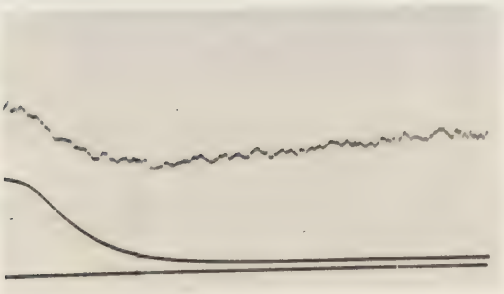

$\sigma = 0.6\text{kg/mm}^2$

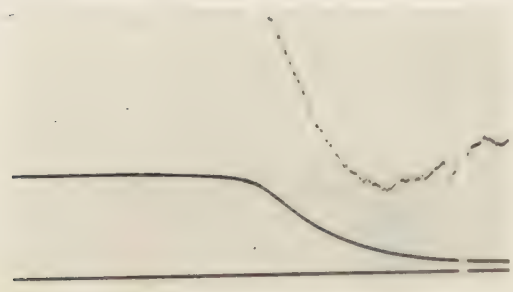

$\sigma = 1.8\text{kg/mm}^2$

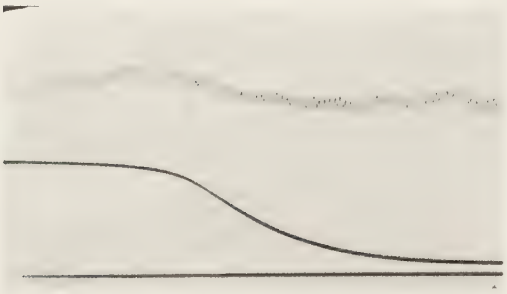

$\sigma = 3\text{kg/mm}^2$

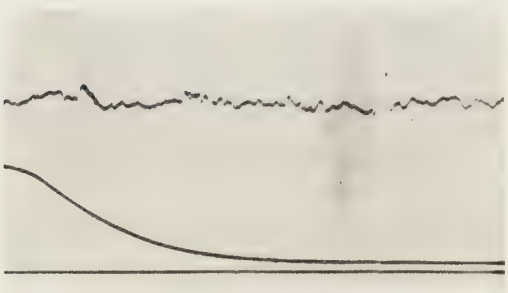

$\sigma = 4\text{kg/mm}^2$

Fig. 4. Oscillograph-records of the longitudinal magnetostriction of Ni (50%)-Fe alloy under various tensive stresses in weak magnetic field.

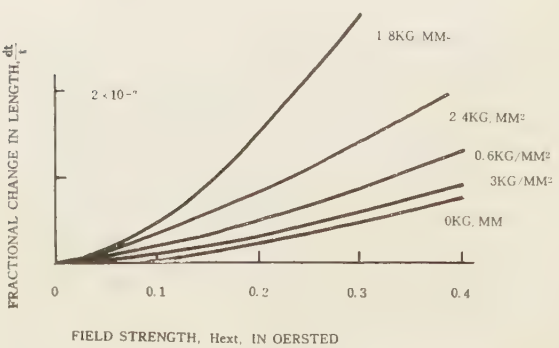

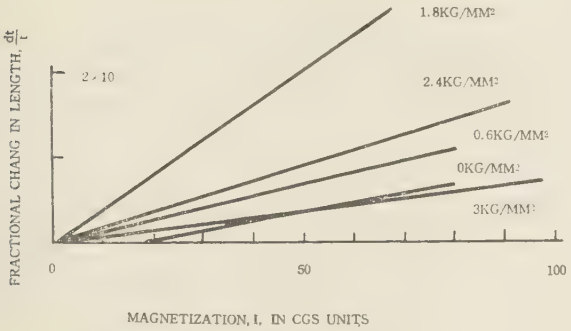

Fig. 5. dl/l–I and dl/l–Hext curves of Ni (50%)–Fe alloy under various tensive stresses in weak magnetic field.

As shown in the figure, the longitudinal magnetostriction in weak magnetic field increases with the increase of the external tensive stress and shows a maximum in the vicinity of about 1.8 kg/mm². Then, it decreases, on the contrary, with the increase of the external tensive stress and comes to be almost unobservable under the external tensive stress of about 4 kg/mm².

(iv) Ni (20%)–Fe alloy

The specimens are 21 cm long and 2 mm in diameter.

The longitudinal magnetostriction in weak magnetic field is small and is affected in a slight degree by the external tensive stress, smaller than about 2 kg/mm².

(b) Fe-Co alloys

(i) Co and Co (70%)–Fe alloy.

The specimens are 21 cm long and 2 mm in diameter.

In Co and Co (70%)-Fe alloy, the longitudinal magnetostriction in weak magnetic field is small and affected in a slight degree by the external stress, smaller than about 3 kg/mm².

(ii) Co (20%)–Fe alloy

The specimens are 21 cm long and 1.5 mm in diameter.

The experimental results are shown in Fig. 6.

As shown in the figure, the longitudinal magnetostriction in weak magnetic field increases with the increase of the external tensive stress and shows a maximum in the vicinity of about 1 kg mm⁻². Then, it decreases, on the contrary, with the increase of the

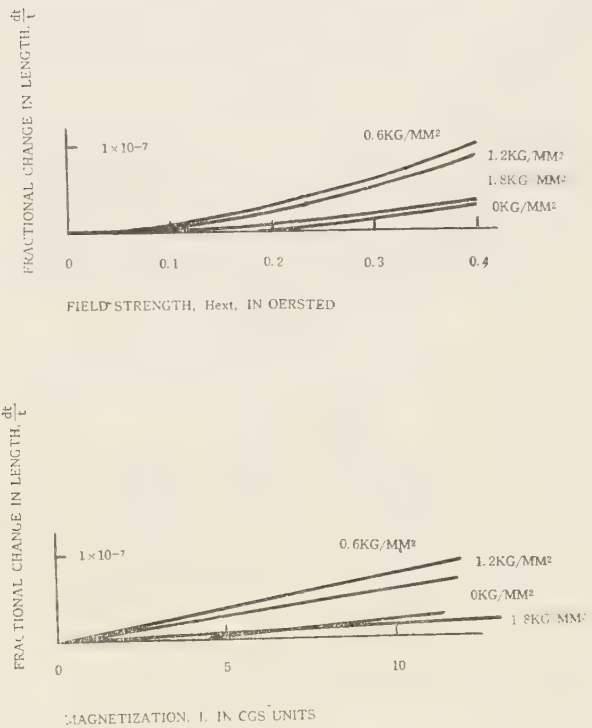

Flg. 6. dl/l–I and dl/l–Hext curves of Co(20%)–Fe alloy under various tensive stresses in weak magnetic field.

external tensive stress and comes to be almost unobservable under the external tensive stress of about 3 kg/mm².

According to the positive or negative longitudinal magnetostriction, the tensive or compressive external stress is applied to the specimen.

In this cases, the longitudinal magnetostriction in weak magnetic field increases at first and then shows a maximum and finally decreases, with the increase of the external stress. This behavior is observed in Ni, Fe, Fe–Ni alloys and Fe–Co alloys.

And the longitudinal magnetostriction in weak magnetic field is almost direct proportional to the intensity of magnetization. This behavior is also observed in Fe, Fe-Ni alloys and Fe–Co alloys and roughly in Ni.

References

(1) S. Matsumae : "The effect of the heat-treatment on the longitudinal magnetostriction in weak magnetic field (II)" Kumamoto Journal of Science, Vol. 2. No. 2. 1955.
(2) S. Matsumae : "The effect of the internal stress on the longitudinal magnetostriction in weak magnetic field." Kumamoto Journal of Science. Vol. 2. No. 2. 1955.
(3) S. Matsumae : "The effect of the internal stress on the longitudinal magnetostriction in weak magnetic field. (II)" Kumamoto Journal of Science. Vol. 2. No. 3. 1955.
(4) S. Matsumae : "The effect of demagnetization on the longitudinal magnetostriction in weak magnetic field." Kumamoto Journal of Science. Vol. 2. No. 4. 1956.

Correction

In the previous papers[1], [2], the maximum amplitude of the demagnetizing alternate magnetic field is 0.7 Oersted and, consequently, 7 Oersted are misprints.

LONGITUDINAL MAGNETOSTRICTION OF NICKEL IN WEAK MAGNETIC FIELD AT HIGH TEMPERATURE

Tatuo TIKAZAWA and Shigeo MATSUMAE

(Received November 30, 1956)

(1) Introduction

The longitudinal magnetostriction of nickel exists even in weak magnetic field, when the specimen is in the adequate condition, as already described in previous papers.

We studied the longitudinal magnetostriction of nickel in weak magnetic field at high temperature by the mutual-dynamic-impedance method. The experimental results are as follows.

(2) Experimental results

The experimental method is shown schematically in Fig. 1. The left hand side of the specimen is magnetized by the alternating-current which is supplied by the beat-oscillator but, on the other hand, the right hand side of the specimen is left in unmagnetized as the result of shielding. Near the frequency of the mechanical vibration of the specimen, the right hand side of the specimen begins to vibrate longitudinally and vibrates most intensly at the same frequency as that of the mechanical vibration of the specimen, due to the mechanical resonance. As the result of the Villari-effect, the electric voltage is induced in the coil Ns. The induced voltage is amplified by the amplifier and then measured by the valve-voltmeter.

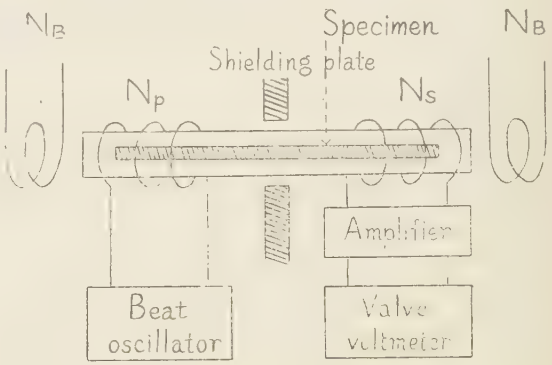

Fig. 1

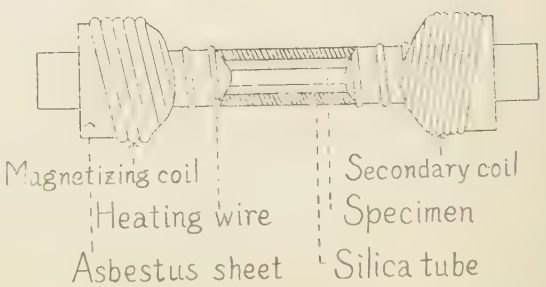

Fig. 2

As known from the thermodynamics, the induced voltages in the secondary coil are in proportion

to the magnitudes of the longitudinal magnetostriction of the specimen, when the proportional constants are same.

For an electric furnace, we wind a non-magnetic german-silver wire, 0.4 mm in diameter, on the outside of the silica-tube of 1.6 cm inside and 2.1 cm outside diameter and of 1 m length. Magnetizing coil, Np, and secondary coil, Ns, are wound on the asbestus-sheets on the outside of the german-silver wire, as shown in the Fig. 2.

The specimen is cold-worked and annealed at 750°C for one hour and then cooled to the room-temperature.

The specimen is set in the above-mentioned furnace and heated above the Curie-temperature. The measurement is taken when the specimen is cooling from above the Curie-temperature, without the heating-current.

The maximum amplitude of the exiting alternate magnetic field which floows through the primary coil is about 0.01 Oersted and the polarizing static magnetic field is about 0.03 Oersted.

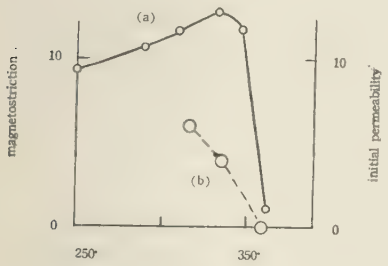

Fig. 3

In the Fig. 3, the curve (a) shows the relation between temperature and initial permeability which is denoted by the scale-readings of the galvanometer and the curve (b) shows the relation between temperature and scale-readings of the valve-voltmeter in a selected constant polarizing magnetic field.

As the proportional constants are considered to be different, the scale-readings of the valve-voltmeter are not strictly proportional to the longitudinal magnetostrictions at various temperatures. But, as seen from the figure, the longitudinal magnetostrion in weak magnetic field is observed even in the vicinity of the Curie-temperature, in nickel, when the specimen is in the adequate condition.

SOME STUDIES ON VOLCANIC ACTIVITY OF VOLCANO SAKURA-JIMA (PART 1)

THE INTERRELATION BETWEEN AIRA CALDERA AND TAISHO DEPRESSION AND THE DISTRIBUTION OF THE CENTRAL CONES AND HOT SPRINGS

Yasuhiro SUGIMOTO and Munetoshi NAMBA

(Received December 15th, 1956)

Abstract

Present writers determined the shape of Aira caldera on Kirishima Volcanic zone by a harmonic analysis, and then its result was applied to the distribution of the central cones and hot springs.

Then it will be understood that the process of volcanic activity in Aira caldera (old crater) has continued on to the present state, making cracks which can be classified in two types. And present writers have found out the interrelations between Aira caldera and Taishô depression which has occurred after the eruption in 1914.

1. Introduction.

After the vast outpourings of lava in quaternary age, Aira caldera was formed by the great depression, and afterward break out the volcanic islands (central cones) in its. Volcano Sakura-jima (1110.2m.) is one of the most active volcano next to Aso and Suwa-no-se. Sakura-jima Volcano is nothing more than a cone of central cones of the great Aira caldera as well as the central cones of Aso in its somma, not a simple volcano.

And depression occurred in regions surrounding the volcano after Taishô eruption in 1914. The writers understood particularly the active position of Sakura-jima Volcano, in addition to, interrelation of depressible form between Aira caldera and Taishô depression by harmonic analysis.

It may be understood easilly that the concentric and radiant cracks followed by the depression, which were mentioned in some reports on Volcano Aso.[1][2]

Where upon, the writers analysed the caldera and Tashô depression in 1914 which is reported by the Imperial Earthquake Investigation Committee.

2. On Aira Caldera.

The great Aira Volcano of caldera type has many central cones: craters, ventholes and elevated islets. But the later lavas spreded over the several craters or ventholes, and a few islets has depressed under the sea-level.[3][4]

The 8th year in An'ei (1779), not only there occurred the submarin eruption at the

northern sea of Sakura-jima, also nine volcanic islets was born at its regions, and has named; Inoko-jima, Naka-no-shima, Ioh-jima, Shin-shima, Doro-shima and etc..[5]

1). Harmonic Analysis of the Shape of Aira Caldera.

Avaling to yourself a topographical map on one fifty thousandth scale issued by the Geographical Investigation Institute, by which has been mapping the shape of Aira caldera by Prof. T. Matsumoto,[8] you can draw an east-west line for a base, passing through over the tentative origin (31°38′ N, 130°43′ E approximately) at near point between the Naka-no-shima and Ioh-jima isles off northern coast of Sakura-jima island, and more drew separating the radiant lines anticlockwise at every 15 degrees, and measured the distance of intersection with a radiant line and caldera rim (crater cliff), you will find 24 observed values.

These values analysed in the form

$$L = N_0 + N_1 + N_2 + N_3 + \cdots$$

$$= N_0 + R_1 \cos(\theta - \zeta_1) + R_2 \cos(\theta - \zeta_2) + R_3 \cos(3\theta - \zeta_3) + \cdots$$

where L: radious vector,

θ: degrees between the based line (east-west) and radiant line,

R, ζ: constans.

And the smaller term N_5 and downward are neglected, they will be

Table 1

Base Line	Observed Value	N_0+N_1	$N_0+N_1+N_2$	$N_0+N_1+N_2$	$N_0+N_1+N_2+N_3$	$N_0+N_1+N_3$	$N_0+N_1+N_2+N_3+N_4$
0	22.4	22.514	23.380	23.354	24.220	19.634	21.340
1	24.9	22.542	23.173	23.267	23.998	21.417	22.873
2	24.5	22.611	22.838	22.981	23.158	25.371	25.918
3	23.7	22.717	22.480	22.343	22.106	25.597	24.986
4	23.1	22.854	22.215	22.014	21.375	23.979	22.500
5	20.7	23.012	22.142	22.187	21.317	20.252	18.557
6	14.8	23.177	22.311	21.991	21.991	20.297	19.111
7	23.5	23.342	22.711	23.716	23.085	22.217	21.960
8	27.8	23.494	23.267	24.334	24.107	26.254	26.867
9	28.2	23.623	23.860	24.448	24.685	26.503	27.565
10	23.9	23.720	24.359	24.040	24.679	24.845	25.804
11	21.3	23.778	24.648	23.404	24.274	21.018	21.514
12	22.1	23.794	24.660	22.954	23.820	20.914	20.940
13	23.9	23.766	24.397	22.941	23.572	22.641	22.447
14	25.4	23.697	23.919	23.377	23.604	26.457	26.364
15	27.5	23.591	23.354	23.965	23.728	26.471	26.608
16	24.3	23.454	22.815	24.294	23.655	24.579	24.780
17	19.2	23.296	22.426	24.121	23.251	20.536	20.491
18	18.3	23.131	22.265	23.451	22.585	20.251	19.705
19	24.2	22.966	22.335	22.592	21.961	21.841	20.836
20	23.5	22.814	22.587	21.974	21.747	25.574	24.507
21	24.5	22.685	22.922	21.860	22.097	25.565	24.977
22	22.8	22.588	23.227	22.268	22.907	23.713	24.032
23	21.2	22.530	23.400	22.904	23.774	19.770	21.014
Probabl	Error	1.930	1.874	1.805	1.806	1.291	1.094
		8.3%	8.1%	7.8%	7.8%	5.6%	4.7%

$$L = 23.154cm + 0.614\ cos\ (\theta - 177°57') + 0.899\ cos\ (2\theta - 344°39') + 0.907\ cos\ (3\theta - 20°39') + 3.257\ cos\ (4\theta - 151°59') \pm 4.7\%,$$ in scale 1/50.000;

$$\therefore L = 11.577km + 0.307\ cos\ (\theta - 177°57') + 0.449\ cos\ (2\theta - 344°39') + 0.454\ cos\ (3\theta - 20°39') + 1.629\ cos\ (4\theta - 151°59') \pm 4.7\%,$$ in full scale;

in this equation, term N_4 is the greatest.

Therefore, observed values, calculated values, and probable error are tabulated in table 1.

According to the table 1, the shape of Aira caldera may be formed as

$$L = 11.577km + 0.307\ cos\ (\theta - 177°57') + 1.629\ cos\ (4\theta - 151°59') \pm 5.6\%$$
in full scale;

above equation is practically good presentation of the shape of the caldera as first approximation.

The center of distorted asteroid ($N_0 + N_1 + N_4$) is in position of about 2 km. NE off Sakura-jima, almost agrees with tentative origin (31°38'N, 130°43'E approximately), the diagonal line (from NE to SW) is 26.04 km, and area 421 sq. km..

Next, we applied the circle ($N_0 + N_1$) as second approximation.

$$L = 11.577km + 0.307\ cos\ (\theta - 177°57') \pm 8.3\%$$ in full scale

The center of this circle concides with that of the distorted asteroid ($N_0 + N_1 + N_4$), It has diameter of 23.15 km., about 73 km. in circumference and 415 sq. km. in area. (Fig. 1).

Thd position of the center, axis, area and circumference in each several shape may be tabulated approximately as in following table.

Table 2

Shape	Center	Axis	Circumference	Area
N_0+N_1 Circle	2km. NE off Sakura-jima 130°43'E, 31°38'N	23.15km in diameter	72.5km	415 sq. km
$N_0+N_1+N_4$ distorted asteroid	2km, NE off Sakura-jima 130°43'E, 31°38'N	26.04km. in diagonal line (NW-SE, NE-SW)	77.9km	420.9 sq. km
$N_0+N_1+N_2+N_3$			75.6km	419.8 sq. km
$N_0+N_1+N_2+N_3+N_4$			79.3km	430.2 sq. km

2). The Distribution of the Central Cones and Hot Springs.

The result of the analysis, may be discussed on the relations between the distribution of the central cones etc. on the caldera which may be seen as the distorted asteroid in

A_o Aoshiki
A_t Atago-yama
A_1 1st group of An'ei
A_2 2nd 〃 〃 〃
B_1 1st group of Bummei
B_2 2nd 〃 〃 〃
E_b Ebi-no-tsuka
G_o Gongen-yama
H_i Hiki-no-taira
H_u Hurihata
I_n Inoko-jima
I_o Ioh-jima
K_t Kita-dake (Ontake)
K_u Kurokawa
M_i Minami-dake
N_a Naka-dake
N_b Nabe-yama
N_e Nabekura
N_k Naka-no-shima
S_a Sambonkaki
S_h Shin-(moe)-shima
S_i Shigetomi
S_o Shôwa Crater
S_u Sumiyoshi-ike
T_1 1st group of Taishô
T_2 2nd 〃 〃 〃
Y_o Yonemaru
Y_u Yunohira

Fig. 1. Shape of Aira Caldera.

shape. The shape ($N_0 + N_1 + N_2$) may be considered as the crossed ellipses, therefore, the writers take up this crossed ellipses, and discuss.

You draw over the caldera of the shape $N_0 + N_1 + N_4$ (distorted asteroid) concentric figures, which each line passing through the points of trisection.

On the convenience of the discuss, the crossed ellipses classified in two types by the direction of the major axis, one of the SE–NW ellipse and SW–NE ellipse, so we call the former E_1 and the latter E_2, and further more E_1-1, E_1-2, E_1-3, and E_2-1, E_2-2, E_2-3 from outside of the concentric figures respectively. (Fig. 2).

(1) The extended line of major axis (from SE to NW) falls on Yonemaru, Sumiyoshiike and Aoshiki which is parasitic crater belonging to Aira Somma; Shin-shima islet; Doro-shima;

(2) On the $E_1 - 1$ line, Nabekura, Shigetomi and Kurokawa hot spring; Kita-dake and Nabe-yama craters; Second crater of An'ei; crater group of Taishô; Gongen-yama,

(3) On the $E_1 - 2$ line, first crater of Bummei;

(4) On the major axis (from NE to SW) of E_2, Kita-dake and Hiki-no-taira craters; Inoko-jima and Doro-shima (under the sea-level) which has yield caused by An'ei eruption (1779);

(5) On the $E_2 - 2$ line, Hiki-no-taira, Minami-dake, and Nabe-yama craters; crater groups of Taishô; first crater of An'ei (1779); Ebino-tsuka;

(6) On the $E_2 - 3$ line, first craters of Bummei, Shin-shima.

Next, you draw the concentric figures over the shape $N_0 + N_1$ (circle) which each line passing through the points which divides the radiant lines into three parts, and then you will see the bellowes:

(1) On the $C - 1$ (outside line), Shigetomi hot spring;

(2) On the $C - 2$ (middle line), Kita-dake, Naka-dake and Minami-dake craters; crater group of Taishô; Shôwa crater;

(3) On the $C - 3$ (inside line), first craters of Bummei.

Near the town of Kamo, 8 km. north-west of the bay, there are to be seen three craters; Yonemaru (1300m. in diameter, quite circular in form), Sumiyoshi-ike pond (300m. in diameter), and that of Mt. Aoshiki (pronounced Oshiki, 275.8m. in height) belonging to the Somma of Aira, probably they are something like the parasitic craters of Aira Volcano.[3]

Thus it may be considered that the process of the volcanic activity that cones and hotsprings along to the cracks in form of E_1 (NW–SE) ellipse might be equally belonging to the comparatively old period, and those on the E_2 (NE SW) elliptic cracks equally to the comparatively later on. All of them above mentioned can be gathered altogether on the lines of both of these above figures. Especially, major axis of each ellipse is chiefly active crack.

Thus, Aira Volcano has two radiant crack bands (SE–NW and SW–NE) when con-

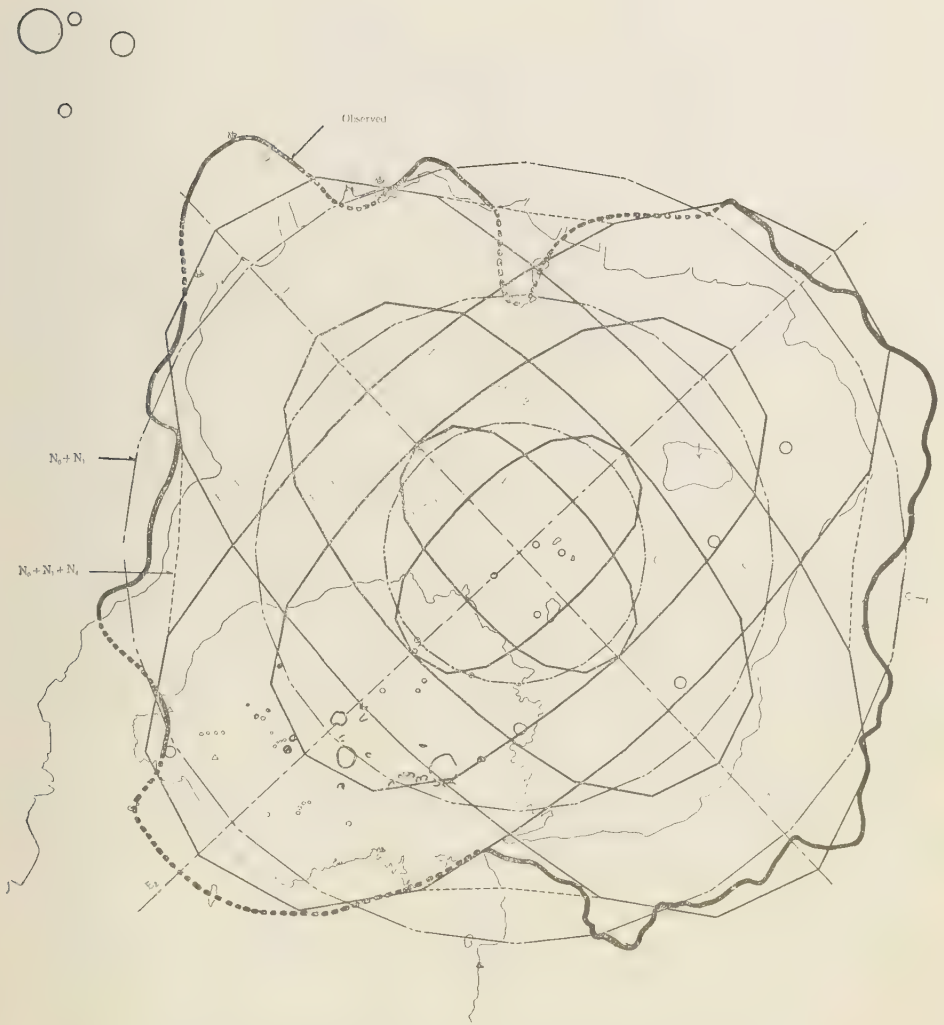

Fig. 2. Distribution of the Central cones and Hot springs.

cerning.

The line joining the bilateral craters of Bummei (1471–1476) parallels to the major axis (SW-NE) of ellipse, and also crater groups of Taishô (1914) nearly parallels to the concentric line $E_2 - 2$.

3. On Taishô Depression.

After the great eruption of Sakua-jima in 1914, a conspicious depression occurred in surrounding the volcano, and not withstanding the vastly outpourings of lava from the island,

Fig. 3. Equidepressions after Taishô eruption.

the main center of depression agrees with the form of the caldera. Since summer of 1914, the depression was surveyed by the Geographical Investigation Institute. The resulting altitude, it had comparatively depressed than its in 1894, as well be seen in Fig. 3.

It was estimated to be over about maximum 250cm. along the northern sea-bottom of Sakura-jima island.[5][6]

1). Harmonic Analysis of the Taishô Depression.

The writers tried the harmoinc analysis, take up the equidepression line (–50cm.) which is reconed to be near the caldera.

It may be assumed that the origin of depression is sea-bottom, about 3.5 km. to the northward of Kohmen village, and draw an east-west line for a base, from Ohsaki-ga-hana on western coast to Matsuo on the eastern coast of the bay.

Furthermore, you draw radiant lines at every 15 degrees anticlockwise, and observed it. You will find 24 values, these values analysed by the foregoing method, and the smaller term n_5 and downwards ignored, they will be,

$$l = 23.645cm + 2.381\ cos\ (\theta - 278°17') + 2.260\ cos\ (2\theta - 100°35') + 0.536\ cos\ (3\theta - 98°09') + 0.744\ cos\ (4\theta - 314°06') \pm 2.0\%,$$ in scale 1/50.000;

$$\therefore l = 11.823km + 1.191\ cos\ (\theta - 278°17') + 1.130\ cos\ (2\theta - 100°35') + 0.268\ cos\ (3\theta - 98°09') + 0.372\ cos\ (4\theta - 314°06') \pm 2.0\%$$ in full scale;

Observed values, calculated values and probable error are indicated in table 3.

According to the table 3

$$l = 11.823km + 1.191\ cos\ (\theta - 278°17') + 1.130\ cos\ (2\theta - 100°35') \pm 2.9\%$$ in full scale;

is best applicable, where the Taishô depression (-50cm.) is considered as almost ellipse $(n_0 + n_1 + n_2)$ in shape

Table 3

Base line	Obserred Value	n_0+n_1	n_0+n_2	$n_0+n_1+n_2$	$n_0+n_1+n_3$	$n_0+n_1+n_2+n_3+n_4$
0	23.6	23.988	23.230	23.573	23.912	24.015
1	24.3	23.366	24.397	24.118	23.688	24.236
2	24.3	22.765	25.364	24.484	23.295	24.287
3	24.1	22.223	25.865	24.443	22.652	24.354
4	24.0	21.775	25.775	23.905	21.851	24.185
5	23.1	21.460	25.115	22.930	21.138	23.329
6	21.5	21.285	24.060	21.700	20.755	21.688
7	20.3	21.280	22.893	20.528	20.851	19.895
8	19.9	21.435	21.926	19.716	21.359	18.919
9	19.3	21.735	21.425	19.515	22.057	19.319
10	20.0	21.172	21.515	20.040	22.702	20.776
11	22.1	22.704	22.175	21.234	23.133	22.384
12	25.4	23.302	23.230	22.887	23.378	23.481
13	23.9	23.924	24.397	24.672	23.602	24.060
14	23.6	24.525	25.364	26.244	23.995	24.993
15	26.3	25.067	25.865	27.287	24.638	26.340
16	28.0	25.515	25.775	27.645	25.439	27.773
17	29.7	25.830	25.115	27.300	26.152	28.343
18	26.8	26.005	24.060	26.420	26.535	27.468
19	24.5	26.010	22.893	25.258	26.439	25.483
20	24.0	25.855	21.926	24.130	25.931	23.491
21	23.5	25.555	21.425	23.335	25.233	22.495
22	22.6	25.120	21.515	22.990	24.590	22.664
23	22.7	24.586	22.175	23.116	24.157	23.408
Probable Error		1.136	1.246	0.685	1.136	0.474
		4.8%	5.3%	2.9%	4.8%	2.0%

The center of this ellipse is in the position of 2.5km. N from the northern coast of Sakura-jima which is 2.5km. NW from the center of Aira caldera. Major axis (from SW to NE) is 25.8km., and the minor axis (SE–NW) 21.4km..

Next, supposed the circle $(n_0 + n_1)$ as second approximation,

$$l = 11.823km + 1.191 \cos(\theta - 278°17') \pm 4.8\% \text{ in full scale;}$$

is beter, and it has diameter of 23.65km. (Fig. 4).

For each shape, the position of center, axis, area and circumference are tabulated in the following table.

Table 4

Shape	Center	Axis	Circumference	Area
circle n_0+n_1	2.5km. N off Sakura-jima 130°41′30″E, 31°38′30″N	23.65km in diameter	74.1km.	439.2 sq. km.
ellipse $n_0+n_1+n_2$	2.5km. N off Sakura-jima 130°41′30″E, 31°38′30″N	a=25.8km. b=21.4km.	74.8km.	432.5 sq. km.
distorted ellipse $n_0+n_1+n_2$			75.7km.	431.6 sq. km.
$n_0+n_1+n_2+n_3+n_4$			75.3km.	434.3 sq. km.

Fig. 4. Shape of Main Depression (−50cm.) and Distribution of the Central Cones etc.

2). The Distribution of the Central Cones and Hot Springs.

The distribution of the central cones and the hot springs in Aira caldera was pointed out the above being on the concentric and radiant cracks. However taking into considera-

tion the results of this case, compared the distribution of the central cones etc. with the former case.

The resulting shape are probable ellipse ($n_0 + n_1 + n_2$) and circle ($n_0 + n_1$), therefore, take up these shapes, and discuss. (Fig. 4).

Firstly, you draw over the Taishô depression (-50cm.) as is the shape $n_0 + n_1 + n_2$ (ellipse) concentric figures, which each line passing through the points dividing the radiant lines into three equallparts E′-1, E′-2, E′-3 in order from the outside.

(1) The E′-1 line falls on Shigetomi and Nabekura hot springs;

(2) On the E′-2 line, Hiki-no-taira, Nabe-Yama, Minami-dake craters; first crater of An'ei, Sambonkaki, Yunohira and Hurihata; crater groups of Taisho; Ebi-no-tsuka

(3) On the E′-3 line, Ioh-jima and Naka-no-shima volcanic isles; first craters of Bummei and Shin-shima.

Secondary, we considered the case of circle ($n_0 + n_1$), drew concentric figures by above method and called C′-1, C′-2, C′-3.

(1) On the C′-1 line, is sitting Nabekura hot spring;

(2) On the C′-2 line, Minami-dake, Nabe-yama, Naka-dake, first crater of An'ei, crater groups of Taishô, Sambonkaki. Hurihata, and Yunohira; Ebi-no-tsuka;

(3) On the C′-3 line, first craters of Bummei, Shin-shima, Ioh-jima and Naka-no-shima.

Following after the pattern of them can be gathered altogether on the lines of both of them above figures as well as the case of Aira caldera, especially, the C′-2 line is the most agreement with the crater groups of Taishô, Minami-dake and Shôwa craters.

4. On the Depression.

The writers considered on the depression of Aira caldera and Taishô depression, and discussed as followes:

1). The Vertical Structure of the Caldera.

As the caldera was formed causing by conical depression, it may be estimated the magma dome as the following pattern approximately, by taking into accounts V the volume of vastly outpouring of lava from Aira somma: 154.8 cub.km., h relative height of wall: 400-600m. (500m. average) which is calculated by Prof. T. Matsumoto [3], and 2R the diameter of circle: ($N_0 + N_1$) 23.15km..

The resulting values, H the depth of magma dome to above sea-level is about 10km., and θ the top angle of conical type is almost 95 degrees.

Thus we understood that the depth of magma dome of Sakura-jima Volcano is about 10km., and the depression of caldera wall occurred with inclination of about 45 degrees toward the vertical axis. (Fig. 5).

2). On Taishô Depression.

After the great eruption of bilateral craters in 1914, occurred the depression in the region surrounding the volcano, as well be seen in Fig. 3. The center of this depression

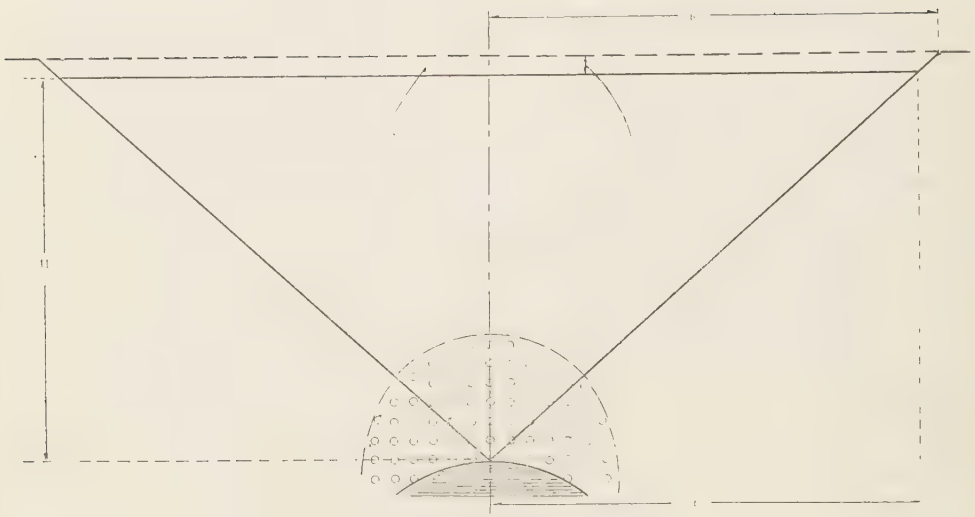

Fig. 5. Vertical section of Aira Volcano.

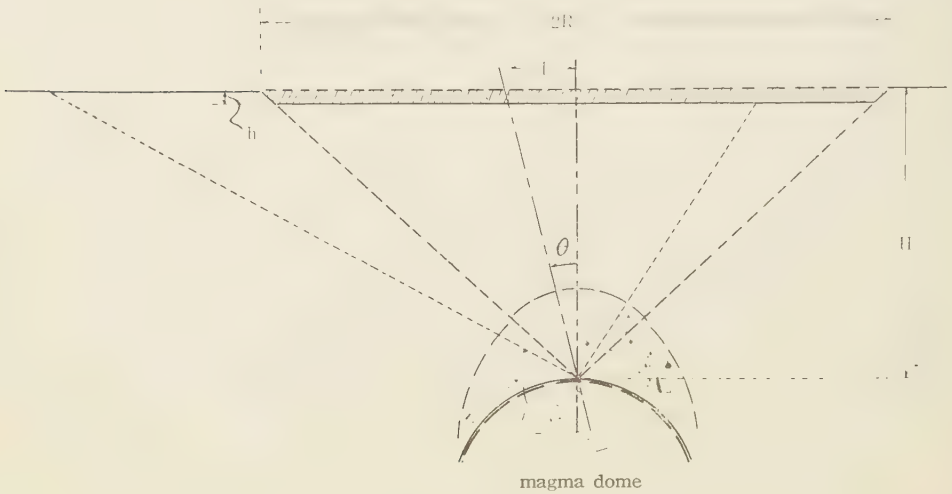

Fig. 6. Aira Caldera and Taisho depression.

(–50cm.) is 2.5 km. NW from the center of Aira caldera.

(a). From the results of harmonic analysis, it may be supposed that it had depressed with about 14 degrees to the vertical axis, including the center of Aira caldera, and we got the above pattern approximately. (Fig. 6).

(b). The writers assumed the following exponential equation for the relation between

the depressed depth η (in cm.) and the distance from the center to equidepression respectively x (in km.) where η_0 and λ are constants which shoud be determined, using the observed data[3][6][8] by the means of least square.

$$\eta = \eta_0 e^{1-\lambda x}$$

The resulting equations are:

on the direction of NW $\eta_1 = -82\ e^{1-0.128x_1}$ in full scale;

on the direction of SE $\eta_2 = -195\ e^{1-0.206x_2}$ in full scale;

where x_1, x_2 are positive respectively.

The observed values and calculated values are indicated as the following table and figure.

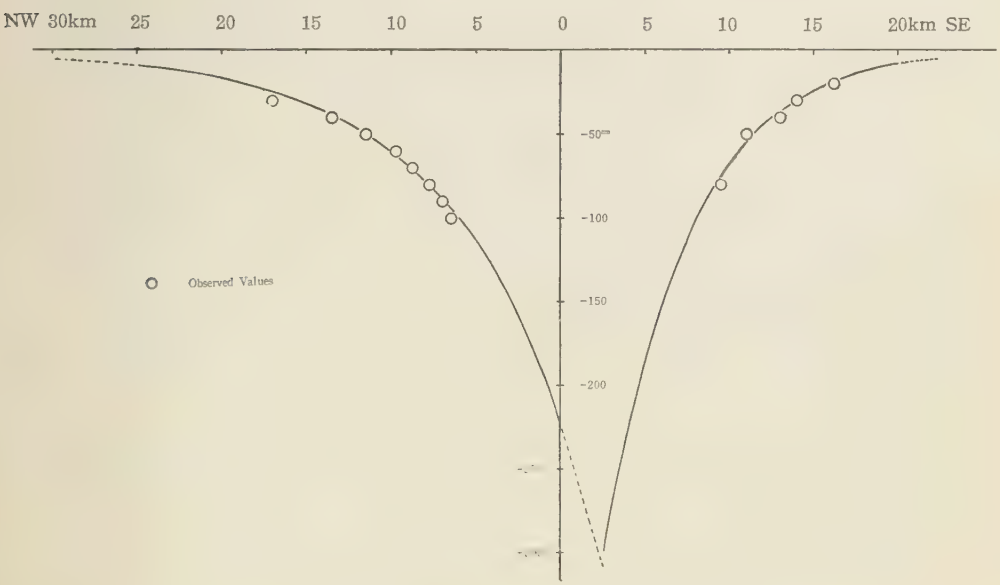

Fig. 7. Vertical section of Taishô depression.

From the above results, it may be estimated that the maximum depression was about 300cm. near the center of Aira caldera.

After the cosideration of aboves, the actual center of the Taishô depression agrees with the center of the caldera, and the lava originally came from a deep subterranean source underneath the center of it.

3). The Recent Crater of Mt. Minami-dake.

The recent feature of the crater (1955–1956) is seen in following figure which was observed by Mr. Y. Yasui, chief of the observing section of the Kagoshima Meteorological

Table 5

depression η^{cm}	observed NW	observed SE	calculated NW	calculated SE
			x km	x km
−5			30.5	21.3
−10			25.0	18.1
−20		16.3km	18.6	15.0
−30	17.0km	14.0	16.5	13.1
−40	13.5	13.0	14.3	11.8
−50	11.5	11.0	12.5	10.7
−60	9.5		11.1	10.0
−70	8.8		9.8	9.2
−80	7.8	9.5	8.8	8.6
−90	7.0		7.8	8.1
−100	6.5		7.1	7.5
−120			5.6	6.8
−140			4.5	6.1
−160			3.4	5.4
−180			2.5	4.9
−200			1.7	4.5
−250			−0.1	3.4
−300			−1.5	2.6

Observatory.

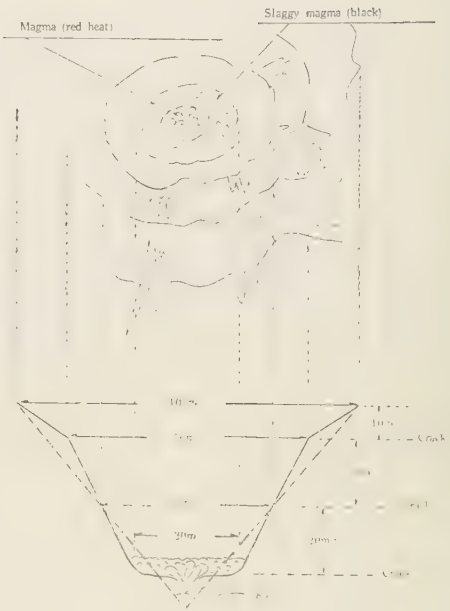

Fig. 8. Minami-dake new Crater (1955~1956)

5. Volcano Sakura-jima.

The Sakura-jima (1110.2m.) is nothing more than a group of central cones of the great Aira Volcano.

History records six lava outpouring from this volcano, of which three of them were great bilateral eruptions namely, during 1471–1476 (Bummei lava); during 1779–1780 (An'ei lava); in 1914 (Taishô lava); in 1946 (Shôwa lava).[4][6]

All of bilateral groups of the craters can be gathered altogether on the each streight line respectively which intersects with about 60 or 30 degrees on Minami-dake, and we pronounced those, "Bummei line", "An'ei line" and "Taishô line" repectively.

You will find the group of craters near the intersection with concentric line of $N_0 + N_1 + N_4$ or $N_0 + N_1$ and radiant lines belonging to Minamidake, especially, Bummei line is parallel to the major axis of E_2 ellipse (SW–NE), and the Taishô line is almost agrees with $E_2 - 2$ (concentric ellipse), and also Showa crater is sitting on it.

Further, extending An'ei line to northward, we find out the center of Taishô depresson. (Fig. 4, 9)

Let us suppose the another crack lines, draw one of line, from Kita-dake, to Minami-dake, and consider regular form of crack (every 60 degrees) like a tortoise shell belonging to Minami-dake or Kita-dake, except An'ei line. Further more, if you assumed a crack line, of from Kita-dake to Gongen-yama, you will easilly be able to describe that Gongen-yama and Hiki-no-taira are parasitic cones of Kita-dake[6] (fig. 9).

These active crack lines are classified into three, radiant and concentric crack bands

A_t Atago-yama
A_1 1st Craters of An'ei
A_2 2nd " " "
B_1 1st Craters of Bummei
B_2 2nd " " "
D_o Doroshima
E_b Ebi-no-tsuka
G_o Gongen-yama
H_i Hiki-no-taira
H_u Hurihata
I_n Inoko-jima
I_o Ioh-jima
K_i Kita-dake
M_i Minami-dake
N_a Naka-dake
N_b Nabe-yama
N_k Naka-no-shima
S_a Sambonkaki
S_h Shin-shima
S_o Showa Crater
T_1 1st Craters of Taishô
T_2 2nd " " "
Y_u Yunohira
A–A An'ei line
B–B Bummei line
T–T Taishô line

Fig. 9. Map of Volcano Sakura-jima

of the caldera, and radiant ones belonging to main central cones- Minami-dake and Kita-dake.

From above assumption, it may be discussed on active process of several cones as the follows:

(1) On Kita-dake (main central cone) begun its activity through the radiant crack major axis of E_2 of old crater (Aira caldera), and afterward Sakura-jima volcanic island was appeared on the active area at the first stage. And the stage ended causing by the activities of parasitic cones belonging to Kita-dake.

(2) Next, Minami-dake (main central cone) erupted, passing through the radiant crack of which is parallel crack to the major axis, and its activities made the radiant crack lines, it may be the second stage of construction the island.

(3) Eruptions in history, probably occurred near the intersections with the radiant line and concentric ellipse anticlockwisely at every about 60 degrees, except An'ei one which has lag of about 30 degrees from the regular line, passing through Kita-dake to Minami-dake.

(4) From the above mentioned results, Nabe-yama probably erupted during 1200–1300 A.D.

"In 8th year of Tempyo-Hoji (764 A.D), according to an old history (Zoku-Nihon-Ki), a submarine eruption was noticed off the coast of Shinini (信爾) village (the provinces Ohsumi and Satsuma), resulting in three new islets (conical form) of ash and pumice.

On this position, it has been recorded that the point is in about 4km. from Omura villge, now pronounces "Ko-jima" isle by old history (三國名稱圖會). Some recent writers has erroneously identified these historic islets as the foresaing islets."[5][6]

After the consideration to the above records and also the results of harmonic analysis, the writers estimated the position of eruption in 764 A.D. It is near the point between sea-coast of Shikine and An'ei islets which has more deep sea-bottom in around about 8km. NE of Sakura-jima (31°39′ N, 130°46′ E approximately).

Because the point is not only the Bummei line extended parallel to major axis of $N_0 + N_1 + N_2$, and also on about 5km. from the sea-coast of Omura, and call of Shinini has changed from generation to generation as following: Shigini→Shinini→Shikini→Shikine (敷根).

Next we may offer an other reference of depression phenomena, such islets caused. It was Uryuh-jima island that sitted in Beppu bay, 2km. N off the coast of Ohita.
The island had been getting depression slowly after the great earthquake of 1596 A.D. and now it is seen as deeper sea-bottom.[7]

6. Conclusions.

i). The shape of Aira caldera is distorted asteroid (crossed ellipses), the center is in

the position between Naka-no-shima isle and Inoko-jima isle in An'ei isles (31°38′ N, 130°43′ E approximately) off northern coast of Sakura-jima island. It has diagonal line of 26.04 km., and 421 sq. km. in area. But looking upon it as crossed ellipses, major axis (NW–SE, SW–NE) is 26.04km., and minor axis 13.02km..

ii). Sakura-jima island is sitting on major axis (SW–NE) which is active crck, and many central cones belonging to the island distributed on the intersections with concentric ellipse $N_0 + N_1 + N_4$ and radiant lines belonging to the main central cones.

iii). It may be cosidered that Taisho bilateral eruption (1914) occurred on the concentric ellipse $E_2 - 2$ of Aira caldera, Taishô line agrees with the second concentric circle of Taishô depression (–50cm.), and also the Showa crater (1946) is sitting on the Taisho line.

iv). It may be supposed that the volcanic activity has occurred anticlockwisely at every about 150 years in history on the three radiant crack lines belonging to Minami-dake, therefore, Nabe-yama and Ebi-no-tsuka (parasitic cones of Minami-dake) are on the position of second concentric ellipse $(E_2 - 2)$ belonging to the caldera. Thus it may be supposed that Nabe-yama was composed during 1200–1300 A. D.

v). The Bummei line parallels to the diagonal line (NE–SW) of distorted asteroid $(N_0 + N_1 + N_1)$ which is great and active crack of the caldera. Considering from the above mentioned, the writers estimated the eruptic position of 764 A. D had occurred between An'ei isles and sea coast of Shikine (31°39′ N, 130°46′ E approximately).

vi). Aira caldera had depressed as like conical type, top angle is about 90 degrees, probably 10km. in depth of magma dome, and volume of out pouring lava from Aira somma is eqivalent sphere of about 6.6km. in diameter.

Thus it may be considered that the volume of magma dome is about 150-200 cub. km..

vii). The values of depression after the eruption in 1914 (called Taishô depression) are caluculated by two exponential equations, and its maximum value is about 300cm. near the center of Aira caldera, not the center of Taishô depression (–50cm.) which is calculated by harmonic analysis, and is only an apparent center.

After all, the real center is in position agrees with the center of the caldera, the Taishô depression occurred in shape as shown in Fig. 7 in generally.

viii). The shape of Taishô depression (–50cm.) is neary ellipse, and its center is in position of 2.5km. NW from the center of Aira caldera (31°38′30″ N, 130°41′30″ E approximately). The major axis (from NE to SW) is 25.8km. and minor axis (from NE to SE) 21.4km..

References

1. Nomitsu, Karube and Kawaguchi: Electric Investigation of Crack Lines in the Aso Crater Plains, Geophysics Vol. VI, No. 3 (1942).
2. M. Namba and T. Murota: Some Studies on Volcano Aso and Kujiu (part 3), Kumamoto J. of Science, A, Vol. 1, No. 1 (1952).

3. T. Matsumoto: The Four Gigantic Caldera Volcanoes of Kuhshû, Japanese J. of Geology and Geography, Vol. XIX, Special Number (1943).
4. Report of Earthquake Investigation Committee, No. 86 (1918).
5. ditto, No. 87 (1918).
6. Report of Volcanologycal Society of Japan, Vol. 2, No. 3, (1935).
7. 吉田東伍: 大日本地名辭書 (1907).

PAPER CHROMATOGRAPHY OF INORGANIC IONS BY USING ORGANIC ANALYTICAL REAGENTS. III.

Precipitation Chromatography of Cations with 8-Quinolinol. (Part 2)

Hideo NAGAI

(Received Dec. 18, 1956)

In the foregoing paper[1], it has been pointed out that so far as Cu^{2+}, Fe^{3+}, Ni^{2+} and Co^{2+} were concerned, the precipitation chromatography, which was composed so as to precipitate the metal oxinates in the order of the degree of insolubility by reducing the dissolving power of the developing solvents to the metal oxinates, was superior in the separation of the cations to the usual type chromatography, which was intended to develop the metal oxinates in the soluble form in the developing solvent. In the developing solvents of the precipitation chromatography, *n*-butanol——water system gave the best results. But even in the best case, each cation zone was followed continuously by the next one, without any blank space between them, and in Cu^{2+} zone, a small amount of Fe^{3+} was found simultaneously. The explanation of no blank space may be as follows: as soon as the less soluble metal oxinate is almost completely precipitated, the next coming precipitation of the other oxinate commences, owing to the excess of the value of ion products over the solubility product. If we wish to suppress the value of the ion product under that of the solubility product, the oxine content per unit filter paper area must be so small that very large paper area is necessary. Moreover, then, the identification of the ions would become difficult and the mixing of the substances belonging to the neighbouring zones, which have the close solubility to the developing solvent, is liable to occur. Thus, the better separation of the ions may be obtained by applying the result of the study of the other factors, except the solubility product, which control the precipitation of the metal oxinates.

In this paper, the influence of *p*H of the developing solvent on the precipitation of the metal oxinates was studied and the experiments were undertaken to find the conditions to improve the separation of the zones of metal ions and, if possible, to find some blank spaces among the neighbouring zones.

Experimental

The experiment and apparatus used were almost the same as the previous paper[1]. In the previous paper, the developed chromatograms were not be surrendered to further treatments, but now in this paper the chromatograms, which were developed under the unstable *p*H range to the oxinates, were followed by the treatment in the atmosphere of the ammonia vapor in a closed vessel, so as to stabilize the precipitation of the oxinates. And

this revealed a phenomenon convenient for practice: the yellow ring zone of oxine which was appeared at the front of the development was discolored to almost colorless. Thereby, it is better to adopt this treatment with ammonia vapor in all experiments, even in the case of stable *p*H range development for the oxinates.

The room temperature in these experiments was 8°~13°C, and the care was taken to avoid the temperature change as much as possible during each experiment.

In the first series of the experiments, the developing solvents used were in the stable *p*H range for the oxinates as shown in table I. The aqueous solution of M/5 acetic acid and M/5 sodium acetate were mixed so as to get the buffer solutions of *p*H 4.4, 5.6, and

Table. I

Metal Ions	PH At Which Precipitation Begins	Range Through Which Precipitation Is Complete
Cu^{2+}	2.2	5.3~14.6
Fe^{3+}	2.4	2.8~11.2
Ni^{2+}	2.8	4.3~14.6
Co^{2+}	2.8	4.2~11.6

6.6. Then they were saturated with *n*-butanol and used as the developing solvents. The results of the use of these solvents were as follows: the higher the value of *p*H of the solvent, the worse was the separation of the cations. With the solvent of *p*H 6.6, all the cations were precipitated about the center of the filter paper and scarcely moved during the development. Thus, the separation of the cations was not sufficient: the identification of Cu^{2+} and Fe^{3+} was possible but in many cases Ni^{2+} and Co^{2+} were not detected. So the experiment of the development with the buffered solvents of higher *p*H than 6.6 was not executed. The result of the development with the solvent of *p*H 4.4 was the best in these buffered solvents, and the separability of the cations was almost the same as that of water saturated with *n*-butanol[1] (Figure 1A).

The experiments of the development in the unstable *p*H range for the metal oxinates was then tried. At first, aqueous acetic acid solutions of various concentrations were used as the developing solvents. The results of them were as follows.

a) 2% Acetic Acid. Though the separation of the metal ions was unsatisfactory and the pattern was somewhat broken, the identification of the four cations was possible, but with some difficulty. The order of the precipitation of the metal oxinates was Cu^{2+}, Fe^{3+}, Ni^{2+} and Co^{2+} from the center to the circumference of the filter paper (this order was kept unchanged in every solvent used in this paper).

b) 3% Acetic Acid. The result of the development was a little better than that of 2% acetic acid but Ni^{2+} and Co^{2+} were in some degree mixed together.

c) 4% Acetic Acid. At first, a fairly good precipitation chromatogram was obtained (the best separation of cations in all the acetic acid solvents mentioned above). But if the development was continued further, then, the once precipitated oxinates began to dissolve; the developing mechanisum changed to the soluble form chromatography, so the separation of the cations became worse. In the aqueous acetic acid solution series described above,

more dilute than 3% acetic acid may be used as a developing solvent of the precipitation chromatography, but its separability of the cations was not sufficient. This defect may be improved if the dissolving power of the solvent to the oxinates is increased because in the chromatograms developed with aqueous acetic acid, described above, some broken parts of the pattern was observed which appeared to be caused by the deficient dissolving power of the solvent. And before the sufficient dissolving power of the solvent was reached by increasing the proportion of the acetic acid, the lowering of *p*H of the solvent made the existence of the oxinates impossible. To increase the dissolving power of the solvent in a constant *p*H, the addition of a neutral organic solvent may be reasonable.

Under the consideration mentioned above, the experiment was conducted as followings: developing with an aqueous acetic acid solution, which was more dilute than 3%, and with *addition* of *n*-butanol. The latter substance showed the best result for developing solvent in the previous experiments[1].

a) 1% Acetic Acid Saturated With *n*-Butanol. The chromatogram obtained by this developing solvent was showed in figure 1B. Though in the center region of Cu^{2+} a little amount of Fe^{3+} was found, the amount was far less than the case of figure 1A or the case of developing by water saturated with *n*-butanol[1]. Between the zones of Fe^{3+} and Ni^{2+}, a little blank space was found. Ni^{2+} and Co^{2+} were also separated satisfactorily.

b) 2% Acetic Acid Saturated With *n* Butanol. The chromatogram obtained by this developing solvent was showed in figure 1C. This figure was better than the figure 1B: Cu^{2+} and Fe^{3+} were separated more satisfactorily than the case of figure 1B, Fe^{3+} and Ni^{2+} were separated with clear blank canal space and Ni^{2+} and Co^{2+} were also very clearly separated.

c) 3% Acetic Acid Saturated With *n* Butanol. The chromatogram obtained by this developing solvent was showed in figure 1D. The disturbance of the zone of Fe^{3+} was very remarkable and the separation of the other cations was all inferior to that of figure 1B and 1C.

Discussion

From the results described above, 2% acetic acid saturated with *n* butanol was the best developing solvent in acetic acid——water *n*-butanol system. But it is reasonable to doubt in the case that *n*-butanol was adequately added, even if 3% acetic acid were used, the result would be comparable to figure 1B and 1C. But 3% acetic acid to which various amount of *n*-butanol added could not be used as a good developing solvent. A fear may arise that some part of the cations might be carried to the developing front without perfectly precipitated at the position as illustrated in the figures, because the *p*H of the developing solvents was out of the stable range for the metal oxinates (1% acetic acid: *p*H 2.75, 2% acetic acid: *p*H 2.60). The following phenomena may resolve this fear: after the development, the chromatogram was exposed in the ammonia gas, the zones of the precipi

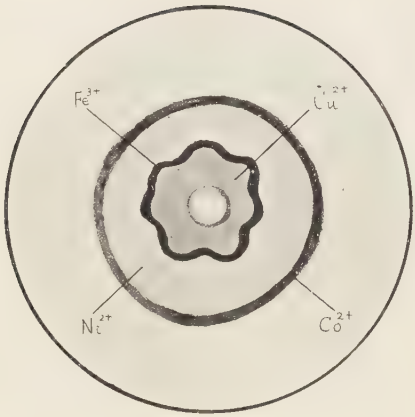

Figure 1A

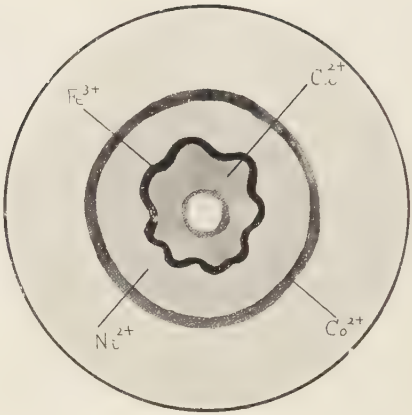

Figure 1B

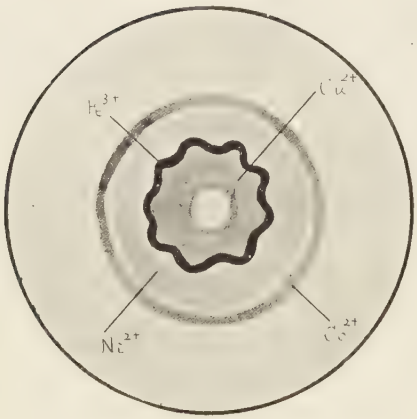

Figure 1C

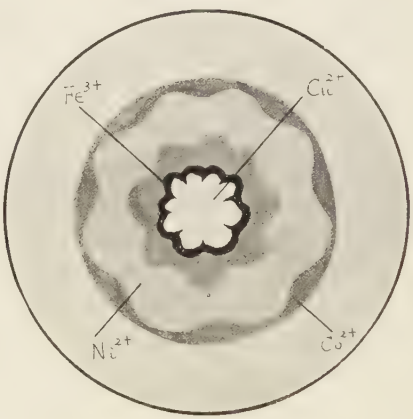

Figure 1D

tated cations were colored intensively but the yellow ring zone of oxine in the developing front was discolored to almost colorless. However, the discolored front zone was observed under the ultraviolet light, the faint fluorescence was so frequently seen that very little amount of ions might exist there.

Conclusion

1. The precipitation chromatography developed on the circular filter paper treated with oxine was able to separate Cu^{2+}, Fe^{3+}, Ni^{2+} and Co^{2+} sufficiently by controling the *p*H of the developing solvent. Though in sometimes, Cu^{2+} and Fe^{3+} were not separated completely, Fe^{3+}, Ni^{2+}, and Co^{2+} were separated with blank spaces among them. In the developing solvent of acetic acid—— water——*n*-butanol system, 2% acetic acid saturated with *n*-butanol gave the best result.

2. The yellow ring zone of oxine at the developing front was discolored with ammonia gas almost to the colorless. Thereby, in these experiments mentioned above even though the *p*H of the developing solvent were out of the stable range for the metal oxinates, the cations in the test sample were scarcely carried to the developing front.

The contents of this paper have mainly been published in J. Chem. Soc. Japan, Pure Chem. Sect. **77**, 1267 (1956).

Literature Cited

(1) H. Nagai, Kumamoto Journal of Science Series A, **2**, 304 (1955).
(2) F. J. Welcher, "Organic Analytical Reagents" (1947).

DETECTION OF POLONIUM IN VOLCANIC ASHES

Daisei YAMAMOTO

(Recieved 19 December 1956)

Detection of polonium in hot spring water has been reported by several chemical analysts[1] but as to it in volcanic ashes none of papers has been found.

The present author succeeded to separate a minute quantity of polonium by Erbacher-Phillip's method[2] in a volcanic ash gathered at the botton of 2nd crater of Volcano Aso in 1952 and in the next year, also found and separated it in a ash gathered at the yard of Aso meteorological observatory (ca. 1 km from the crater).

The origin of polonium may has some relationship to a radon in volcanic gas, in atmosphere, and in rain drops etc.

Descriptions in detail are given in Journal of the Chemical Society of Japan Vol. 75 P. 349 (1954) and Vol. 75 P. 717 (1954).

About these works, this author thanks Prof. Ohara for his encouragement and Prof. Namba for his advice on the volcanism of Aso.

1) K. Kimura K. Kuroda Y. Yokoyama J. Chem. Soc. Japan Vol. 69 p. 34 (1948), Vol. 70 p. 399 (1949) T. Ishimori I. Hataye Ibid Vo. 77 p. 122 (1956).

2) O. Erbacher K. Phillip Z. Phisik Vol. 51 p. 309 (1928).

A NEW DEDUCTION OF SINGULARITY CRITERIA FOR THE FIRST ORDER DIFFERENTIAL EQUATIONS

Katsumasa MATSUMOTO

(Received Jan. 30, 1957)

§ 1. The author, having been engaged in investigation of higher order singularities of differential equations, was, once on his way of study, struck with an idea to prove the singularity criteria hitherto known for the first order differential equations in a far easier way than those usually done. Until present, it seems to have been a tradition to deduce the criteria by the aid of matrices, transformations, characteristic equations, etc[1]. The author believes the methods adopted are too circuitous and seem awful for beginners, who will think it something mysterious. If it concerns only with the classification of singularities and with the criteria for distinguishing different types of them, there is no need of such circuitousness nor even necessity, for the most part, to soive the differential equations. As the differentiatiation is easier and always possible while the integration is not, we prefer the former to the latter in examining the properties of the solution curves. We shall develop here our idea mainly for the first order differential equations.

§ 2. Suppose that there is given a first order differential equation of the type

$$\frac{dy}{dx} = \frac{\alpha x+\beta y}{\gamma x+\delta y}\ ,\quad \alpha\delta-\beta\gamma\neq 0. \qquad \cdots\cdots (1)$$

The origin is a singular point. As any other first order differential equations, the singular point of which lies at any other point than the origin, may be reduced to the form (1) by simple translation. we always consider the differential equation in the form (1). Let $y=f(x)$ be its solution, if any, satisfying the initial condition $x=0$, $y=0$. Imagine that we follow along the solution curve until we reach the origin. We examine the slope of the curve how it changes along it. We shall inspect preliminarily a few special cases and compare with the solutions themselves already known in the purpose of explaining our ider and making clear how simple it is.

(a)
$$\frac{dy}{dx} = \frac{y}{x}\ . \qquad \cdots\cdots (2)$$

Solving it gives $y=Cx$. There are an infinite number of straight lines through the origin, which is a node. But if we try to infer the property of the origin without solving the equation, we proceed as follows. $\frac{y}{x}$ is an indeterminate form if $x\to 0$, $y\to 0$. In both members of (2), passing to the limit as $x\to 0$, especialiy applying L'Hospital's rule to the right member, we obtain

[1] Cf., e. g., Bieberbach, L.: Differentialgleichungen; Niemytzki, V. V. and Stepanov, V. V.: Qualitative theory of differential equations.

$$\left(\frac{dy}{dx}\right)_0 = \left(\frac{dy}{dx}\right)_0.$$

This means that any value whatever of $\left(\frac{dy}{dx}\right)_0$ may be had by the solution curves of (2), i. e., solution curves may enter into the origin along any direction. The origin is thus a node. Differentiating (2) again, we have $\frac{d^2y}{dx^2} = 0$, which means that the solution curves are straight lines.

(b)

$$\frac{dy}{dx} = a\frac{y}{x}. \quad \cdots\cdots (3)$$

Solving (3) yields $y = Cx^a$. All integral curves either (i) pass through the origin and are tangent to the y-axis there except $y = 0$ $(0 < a < 1)$ or (ii) pass through the origin and are tangent to the x-axis there except $x = 0$ $(a > 1)$ or (iii) are asymptotic to the axes, only $x = 0$ and $y = 0$ passing through the origin, which all others pass by $(a < 0)$. But we prefer to proceed as follows, not integrating (3) but differentiating it. Passing to the limit as $x \to 0$ in (3), we obtain

$$\left(\frac{dy}{dx}\right)_0 = a\left(\frac{dy}{dx}\right)_0,$$

which is satisfied by $\left(\frac{dy}{dx}\right)_0 = 0$ or ∞, indicating that infinitely many solution curves touch the coordinate axes at the origin or no curves pass through it except $x = 0$ and $y = 0$. Differentiating (3) again, we have

$$\frac{d^2y}{dx^2} = \frac{a(a-1)y}{x}. \quad \cdots\cdots (4)$$

Taking (3) – the slope – and (4) – the curvature – into account, and considering the uniqueness theorem, we obtain the following possible distributions of curves (Figs. 1, 2 and 3), indicating that the origin is either a node or a saddle point. In the figures, the marks ／ and ＼ signify that the slopes are positive and negative there respectively and the marks ∪ and ∩ that the curvatures are positive and negative there, respectively.

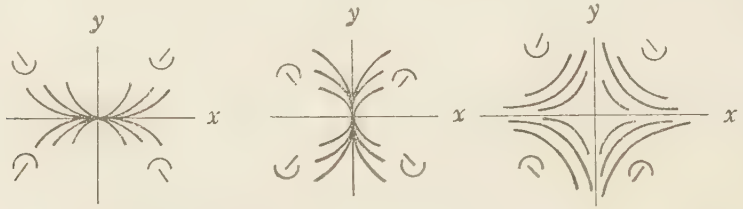

$a > 1$ Fig. 1 $0 < a < 1$ Fig. 2 $a < 0$ Fig. 3

(c)

$$\frac{dy}{dx} = \frac{x+y}{x}. \quad \cdots\cdots (5)$$

Solving (5) yields $y=x\log|x|+Cx$, which is a little hard to be graphed at a glance. Let us graph it not integrating (5) but differentiating it. Firstly, passing to the limit as $x\to 0$ in (5), we obtain

$$\left(\frac{dy}{dx}\right)_0=1+\left(\frac{dy}{dx}\right)_0,$$

which is satisfied by $\left(\frac{dy}{dx}\right)_0=\infty$. Next, differentiating (5), gives $\frac{d^2y}{dx^2}=\frac{1}{x}$. Noting the signs of slopes and curvatures, we easily obtain the possible distribution of curves near the origin as shown in Fig. 4, indicating that the origin is a node. See how simple it is as compared with the integration method.

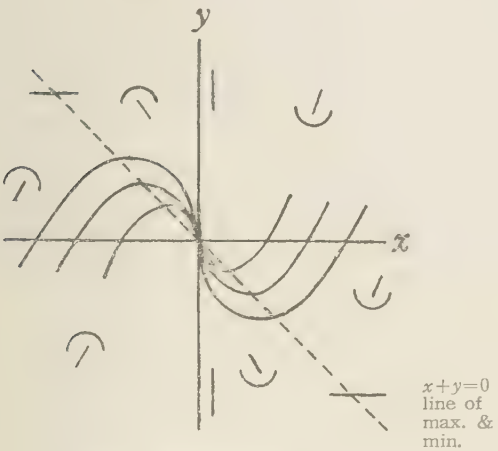

Fig. 4

(d)

$$\frac{dy}{dx}=-a^2\frac{x}{y}. \quad \cdots\cdots (6)$$

Solving (6) gives $y^2+a^2x^2=C$, which are ellipses. If we proceed as in the previous cases, making $x\to 0$ as well as $y\to 0$, we obtain

$$\left(\frac{dy}{dx}\right)_0^2=-a^2,$$

which no real directions satisfy. This means that we cannot make $y\to 0$ as $x\to 0$, i. e., no real curves pass through the origin. Combining the two imaginary straight lines entering the origin, which have the imaginary slopes $\pm ia$, we obtain $y^2+a^2x^2=0$, i. e., a point ellipse, which hints at the fact that the ellipse-like solution curves pack the neighborhood of the origin, which must therefore be either a center or a focus. We shall discuss this case in more general form later.

(e)

$$\frac{dy}{dx}=\frac{x-dy}{ax-y}. \quad \cdots\cdots (7)$$

Solving (7) in polar coordinates gives $r=Ce^{a\theta}$, which are logarithmic spirals. Proceeding as in (d), we obtain

$$\left(\frac{dy}{dx}\right)_0=1.$$

Remark is the same as in (d).

§ 3. Now we shall turn to the general case (1). Assuming that $y\to 0$ as $x\to 0$, making use of L'Hospital's rule and arranging in $\left(\frac{dy}{dx}\right)_0$, we obtain the following quadratic

equation in $\left(\frac{dy}{dx}\right)_0$:

$$\delta\left(\frac{dy}{dx}\right)_0^2-(\beta-\gamma)\left(\frac{dy}{dx}\right)_0-\alpha=0,$$

the discriminant of which is

$$\triangle=(\beta-\gamma)^2+4\alpha\delta.$$

We distinguish the following three cases.

(i) $\triangle>0$. We have two real distinct directions in which the solution curves enter the origin. Differentiating (1), we obtain

$$\frac{d^2y}{dx^2}=(\alpha\delta-\beta\gamma)\frac{\delta y^2-(\beta-\gamma)xy-\alpha x^2}{(\gamma x+\delta y)^3}. \quad \cdots\cdots\cdots\cdots\cdots\cdots (8)$$

$$m_{1,2}=\frac{\beta-\gamma\pm\sqrt{(\beta-\gamma)^2+4\alpha\delta}}{2\delta}$$

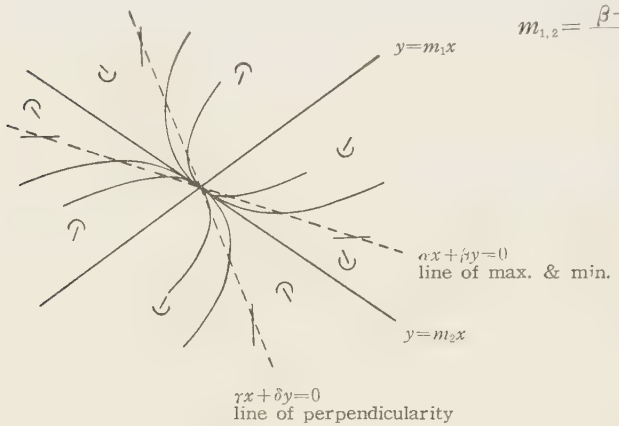

Fig. 5

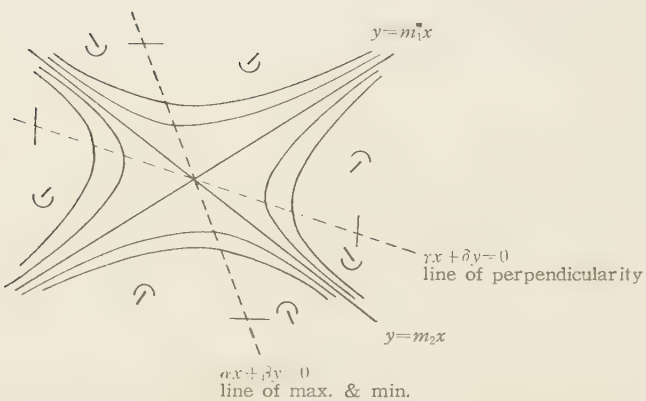

Fig. 6

Considering the slopes and curvatures, we draw all possible distributions of integral curves near the origin as shown in Figs. 5 and 6, which indicate that the origin is either a node $(\alpha\delta-\beta\gamma<0)$ or a saddle point $(\alpha\delta-\beta\gamma>0)$.

(ii) $\triangle=0$. We have one real direction in which the solution curves enter the origin. Regardless of the sign of $\alpha\delta-\beta\gamma$, we obtain a figure indicating that the origin is a node (Fig. 7).

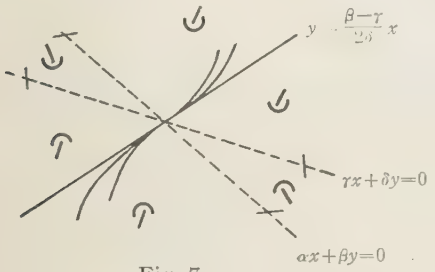

Fig. 7

(iii) $\triangle<0$. Combining into one the two imaginary straight lines

$$y=\frac{\beta-\gamma\pm i\sqrt{-\triangle}}{2\delta}x$$

which enter the origin, we obtain

$$\delta y^2-(\beta-\gamma)xy-\alpha x^2=0,$$

which is a point ellipse, indicating that the neighborhood of the origin is packed with ellipse-like integral curves. Integral curves appear to surround the origin in this case. To see how they surround the origin, we imagine a point moving along them, introduce time concept, rewriting (1) in the form of simultaneous equations

$$\begin{cases}\dfrac{dx}{dt}=\gamma x+\delta y\\[2ex] \dfrac{dy}{dt}=\alpha x+\beta y\end{cases} \qquad \cdots\cdots (9)$$

the characteristic equation of which is

$$\begin{vmatrix} D-\gamma & \delta \\ \alpha & D-\beta \end{vmatrix}=0$$

having the roots

$$D=\frac{\beta+\gamma\pm i\sqrt{-\triangle}}{2}$$

The solutions of (9) are

$$\begin{cases} x=e^{\frac{\beta+\gamma}{2}t}\left(C_1\cos\dfrac{\sqrt{-\triangle}}{2}t+C_2\sin\dfrac{\sqrt{-\triangle}}{2}t\right)\\[2ex] y=e^{\frac{\beta+\gamma}{2}t}\left\{C_1\left(\dfrac{\beta-\gamma}{2\delta}\cos\dfrac{\sqrt{-\triangle}}{2}t-\dfrac{\sqrt{-\triangle}}{2\delta}\sin\dfrac{\sqrt{-\triangle}}{2}t\right)\right.\\[2ex] \qquad \left.+C_2\left(\dfrac{\sqrt{-\triangle}}{2\delta}\cos\dfrac{\sqrt{-\triangle}}{2}t+\dfrac{\beta-\gamma}{2\delta}\sin\dfrac{\sqrt{-\triangle}}{2}t\right)\right\}\end{cases} \qquad \cdots\cdots (10)$$

where C_1 and C_2 are arbitrary constants.

We see from (10) that the solution curves encircle the origin either periodically

$(\beta+\gamma=0)$ or spirally $(\beta+\gamma\neq 0)$. The origin is thus a center $(\beta+\gamma=0)$ or a focus $(\beta+\gamma\neq 0)$.

§ 4. In conclusion, a few words about Poincaré's theorem. Let the equation be of the form:

$$\frac{dy}{dx}=\frac{\alpha x+\beta y+P(x,y)}{\gamma x+\delta y+Q(x,y)}$$

where $P(x,y)$ and $Q(x,y)$ are $O(x^2+y^2)$.

Proceeding in the previous way, we have, when $x\to 0$, $y\to 0$,

$$\left(\frac{dy}{dx}\right)_0=\frac{\alpha+\beta\left(\frac{dy}{dx}\right)_0}{\gamma+\delta\left(\frac{dy}{dx}\right)_0}$$

showing that the terms of higher order than the first do not affect the character of singularity of the origin, which hints at Poincaré's theorem. Case when $\beta+\gamma=0$ must be considered separately as one sees clearly from the fact that the nonlinear form like

$$\frac{dy}{dx}=\frac{\alpha x^2+\beta xy+\gamma y^2}{\alpha' x^2+\beta' xy+\gamma' y^2}$$

belongs to this case, which will not be touched here.

SOLUTIONS ON THE REFLECTION METHOD OF THE SEISMIC PROSPECTING

(General Case when 3 Dimensions)

Ryuzo ADACHI

(Received April. 30, 1957)

This paper is an extension of the paper discussed in the preceding Journal (Vol., 3, No. 1, 1957), and we got accurate solutions.

1. Relations between Surface of Separation and Travelling-time Surface

In Fig. 1, let travelling-time be observed along the xoy-plane, and the shot point be at the origin 0, and let

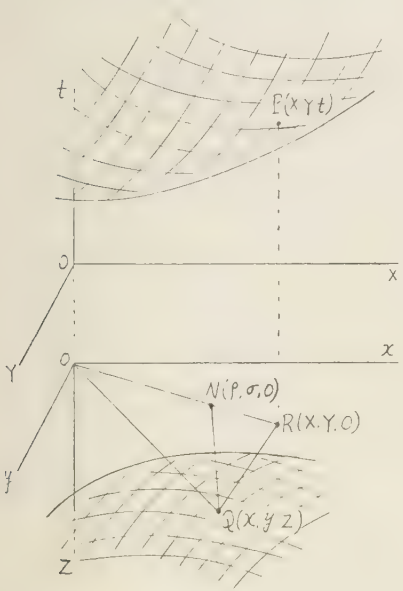

Fig. 1

$$z = z(x, y) \quad \cdots\cdots (1),$$

be the surface of separation, and consider a reflected wave which runs along OQR and let t be its travelling-time, and

$$t = \varphi(X, Y) \quad \cdots\cdots (2)$$

be the travelling-time surface, where R is on the xoy-plane.

Let $N(\rho, \sigma, o)$ be the intersection of the normal of (1) at Q with the xoy-plane, then we have

$$\rho = x + zz_x, \quad \sigma = y + zz_y.$$

While O, N, R must lay on a straight line and N must lay between O and R, therefore we have

$$\frac{X}{x + zz_x} = \frac{Y}{y + zz_y} = \lambda\,(say) > 1 \quad \cdots\cdots (i).$$

Next, QN must be the bisector of $\angle OQR$, and putting to

$$\sqrt{x^2 + y^2 + z^2} = OQ = r, \quad \sqrt{\rho^2 + \sigma^2} = \overline{ON} = l \quad \cdots\cdots (ii)$$

we have

$$r^2 : l^2 = [(X-x)^2 + (Y-y)^2 + z^2] : [(X-\rho)^2 + (Y-\sigma)^2]$$

that is

$$(2M - zL)(\lambda - 2) = zL - M \quad \cdots\cdots (iii)$$

where

$$M = z - xz_x - yz_y, \quad L = z_x^2 + z_y^2 + 1.$$

Evidently $\gamma > l$ and $\gamma^2 - l^2 = z\,(2M - zL) > 0$, that is

$$2M - zL = z\,(1 - z_x^2 - z_y^2) - 2\,(xz_x + yz_y) > 0 \quad \cdots\cdots \text{(iv)}.$$

From (iii), we get

$$\lambda = \frac{2M}{2M - zL}$$

therefore

$$\lambda - 1 = \frac{zL}{2M - zL} > 0$$

that is, actually $\lambda > 1$ when (iv) is satisfied.

Next

$$(X-x)^2 + (Y-y)^2 + z^2 = \gamma^2 + \lambda^2(\rho^2 + \sigma^2) - 2\lambda(x\rho + y\sigma) = \gamma^2(\lambda - 1)^2,$$

therefore

$$\overline{QR} = \sqrt{(X-x)^2 + (Y-y)^2 + z^2} = (\lambda - 1)\gamma$$

and

$$t = \frac{1}{v}\,(OQ + QR) = \frac{\lambda}{v}\,\gamma \quad \cdots\cdots \text{(v)}$$

where v is the velocity of wave in the first layer.

Accordingly we get

$$z = z\,(x, y) \quad \cdots\cdots \text{(1)}$$

$$t = \varphi\,(X, Y) \quad \cdots\cdots \text{(2)}$$

$$X = \lambda\,(x + zz_x) \quad \cdots\cdots \text{(3)}$$

$$Y = \lambda\,(y + zz_y) \quad \cdots\cdots \text{(4)}$$

$$t = \frac{\lambda}{v}\sqrt{x^2 + y^2 + z^2} \quad \cdots\cdots \text{(5)}$$

where

$$\lambda = \frac{2(z - xz_x - yz_y)}{z(1 - z_x^2 - z_y^2) - 2(xz_x + yz_y)} \quad \cdots\cdots \text{(6)}$$

$$\left.\begin{aligned} z\,(1 - z_x^2 - z_y^2) - 2\,(xz_x + yz_y) &> 0 \\ z &> 0 \end{aligned}\right\} \quad \cdots\cdots \text{(7)}.$$

These are fundamental relations between surface of separation and travelling-time surface.

2. Solution of $t = \varphi\,(X, Y)$ when $z\,(x, y)$ is given

When $z\,(x, y)$ is given, z, z_x, z_y become known functions of x, y, and (3) (4) (5) are a parametric expression of the travelling-time surface, where x, y are parameters.

3. Solution of $z = z(x, y)$ when $\varphi(X, Y)$ is given

Let us suppose that $\varphi(X, Y)$ is a well behaved function of X and Y, and put

$$E(X, Y) = r\varphi(X, Y) \quad \cdots\cdots (5),$$

then $E(X, Y)$, $E_X(X, Y)$, $E_Y(X, Y)$ are known well behaved functions of X, Y. From (5) we get $E(X, Y) = \lambda\gamma$, and applying (3) (4) gives

$$x + zz_x = \frac{X}{E}\gamma, \quad y + zz_y = \frac{Y}{E}\gamma \quad \cdots\cdots (\mathrm{i})$$

that is

$$z_x = \frac{1}{z}\left(\frac{X}{E}\gamma - x\right), \quad z_y = \frac{1}{z}\left(\frac{Y}{E}\gamma - y\right) \quad \cdots\cdots (\mathrm{i})'$$

and we get

$$\lambda = \frac{2E(E\gamma - xX - yY)}{\gamma(E^2 - X^2 - Y^2)} \quad \cdots\cdots (\mathrm{ii})$$

therefore from (3)

$$E^2 - X^2 - Y^2 = 2(E\gamma - xX - yY) \quad \cdots\cdots (\mathrm{iii})$$

where $X \neq 0$.

Now, let us suppose that z is a function of x, y; x, y are functions of X, Y, and differentiating (iii) with respect to X, we get

$$EE_X - X = E_X\gamma + \frac{E}{\gamma}\left\{(x + zz_x)\frac{\partial x}{\partial X} + (y + zz_y)\frac{\partial y}{\partial X}\right\} - x - X\frac{\partial x}{\partial X} - Y\frac{\partial y}{\partial X}$$

and applying (i) gives

$$EE_X - X = E_X\gamma - x \quad \cdots\cdots (\mathrm{iv}).$$

Eliminating γ from (iii) (iv), we get

$$2(E - XE_X)x - 2YE_X y = 2EX - E_X(E^2 + X^2 + Y^2) \quad \cdots\cdots (\mathrm{v})$$

similarly

$$-2XE_Y x + 2(E - YE_Y)y = 2EY - E_Y(E^2 + X^2 + Y^2) \quad \cdots\cdots (\mathrm{vi}).$$

Solving these equations with respect to x, y simultaneously gives

$$\left.\begin{aligned} x &= \frac{2X(E - YE_Y) - E_X(E^2 + X^2 - Y^2)}{2(E - XE_X - YE_Y)} \\ y &= \frac{2Y(E - XE_X) - E_Y(E^2 - X^2 + Y^2)}{2(E - XE_X - YE_Y)} \end{aligned}\right\} \quad \cdots\cdots (\mathrm{vii})$$

Next, from (iii)

$$\gamma = \frac{1}{E}\left\{xX + yY + \frac{1}{2}(E^2 - X^2 - Y^2)\right\}$$

and applying (vii), we get

$$r = \frac{E^2+X^2+Y^2-2E(XE_X+YE_Y)}{2(E-XE_X-YE_Y)} \quad \cdots\cdots \text{(viii)}.$$

Substituting (vii) (viii) in the relation $z^2=r^2-x^2-y^2$, we have

$$z^2 = \frac{(1-E_X^2-E_Y^2)(E^2-X^2-Y^2)^2}{4(E-XE_X-YE_Y)^2} \quad \cdots\cdots \text{(ix)}.$$

At first, from (ix), $1-E_X^2-E_Y^2$ must be positive and moreover

$$E=\overline{OQ}+QR>\overline{OR}=\sqrt{X^2+Y^2}$$

that is

$$1-E_X^2-E_Y^2>0, \quad E^2>X^2+Y^2 \quad \cdots\cdots \text{(x)}$$

hence

$$E^2-(XE_X+YE_Y)^2-X^2+Y^2-(XE_X+YE_Y)^2>(YE_X-XE_Y)^2>0$$

therefore

$$E-XE_X-YE_Y>0 \quad \cdots\cdots \text{(xi)}$$

Consequently we have

$$\left.\begin{aligned} x &= \frac{2X(E-YE_Y)-E_X(E^2+X^2-Y^2)}{2(E-XE_X-YE_Y)} \\ y &= \frac{2Y(E-XE_X)-E_Y(E^2-X^2+Y^2)}{2(E-XE_X-YE_Y)} \\ z &= \frac{\sqrt{1-E_X^2-E_Y^2}\,(E^2-X^2-Y^2)}{2(E-XE_X-YE_Y)} \end{aligned}\right\} \quad \cdots\cdots (9)^*$$

these are a parametric expression of the surface of separation, where X, Y are parameters, and these are our required solution.

There is no condition or no approximation except the existences of E_X and E_Y, therefore (9) is an accurate solution in general case.

For example, ***when*** $z=ax+by+c$ ***is given***, from Eqs. (3) (4) (5), we get

$$\left.\begin{aligned} X &= \frac{2c}{2c-(a^2+b^2+1)(ax+by+c)}\left\{(1+a^2)x+aby+ac\right\} \\ Y &= \frac{2c}{2c-(a^2+b^2+1)(ax+by+c)}\left\{abx+(1+b^2)y+bc\right\} \\ t &= \frac{2c}{v\{2c-(a^2+b^2+1)(ax+by+c)\}}\left\{x^2+y^2+(ax+by+c)^2\right\}^{\frac{1}{2}} \end{aligned}\right\} \quad \cdots\cdots \text{(a)}$$

* Let Q, Q' be two points whose coordinates are (X, y, z), (x, Y, z) respectively and put $\angle QRQ=\alpha$, $\angle QRQ'=\beta$, then we have $\sin\alpha=E_X$, $\sin\beta=E_Y$. Moreover we have

$$\sqrt{x^2+y^2+z^2}+\sqrt{(X-x)^2+(Y-y)^2+z^2}=E$$
$$X-x=\sqrt{(Y-y)^2+z^2}\tan\alpha$$
$$Y-y=\sqrt{(X-x)^2+z^2}\tan\beta$$

and solving these equations simultaneously with respect to x, y, z, we can also obtaine the equations (9).

and eliminating x, y gives

$$t = \varphi(X, Y) = \frac{1}{v}\sqrt{X^2+Y^2+\frac{4c}{a^2+b^2+1}}\,(aX+bY+c) \quad \cdots\cdots (b).$$

Inversely, if (b) ***is given***, from (9), we get

$$\left.\begin{aligned} x &= \frac{2c}{a^2+b^2+1}\cdot\frac{\frac{b^2+1-a^2}{2}X-abY-ac}{aX+bY+2c} \\ y &= \frac{2c}{a^2+b^2+1}\cdot\frac{-abX+\frac{a^2+1-b^2}{2}Y-bc}{aX+bY+2c} \\ z &= \frac{2c}{a^2+b^2+1}\cdot\frac{aX+bY+c}{aX+bY+2c} \end{aligned}\right\} \cdots\cdots (c)$$

and eliminating X, Y gives

$$z = ax + by + c \quad \cdots\cdots (d).$$

4. Uniqueness of the Solution

When $z(x, y)$ is given, the travelling-time surface is expressed by Eqs. (3) (4) (5) and is determined uniquely.

Inversely, when $\varphi(X, Y)$ is given, the surface of separation is expressed by Eqs. (9) and also is determined uniquely.

Therefore in any case, we can assert that there exists the uniqueness of the solution.

Reference

R. Adachi : Fundamental Relatinns on the Seismic Prospecting (general case in 2 dimensions concerning reflection method), Kumamoto Journalf of Science Vol. 3, No. 1, 1957.

ON THE SINGULAR POINT OF TRAVELLING-TIME CURVE

Ryuzo ADACHI

(Received April, 30, 1957)

1. Introduction

On the seismic prospecting, it is well known result that the travelling-time curve is a simple curve when the separation curve is a straight line or nearly straight. But when the curvature of the separation curve is great or the inclination is discontinuous at some point, the travelling-time curve is very complex and it may posses some singular points and the function which expresses the travelling-time may be many valued function of the distance.

I discussed some properties of the singular point of such travelling-time curve.

2. Some Properties of Singular Point

In the two dimentional space, let

$$y = y(x) \quad \cdots\cdots\cdots\cdots\cdots\cdots \quad (1)$$

be the equation of a separation curve, and let a wave-ray starts from O and travells along

$OPQR$ (Fig. 2) ····· when refraction method

OQR (Fig. 3) ····· when reflection method

and let t be its travelling-time, and

$$t = \varphi(X) \quad \cdots\cdots\cdots\cdots\cdots\cdots \quad (2)$$

be the travelling-time curve. Next, let v_1, v_2 be the velocities of the wave in the upper and lower layers respectively.

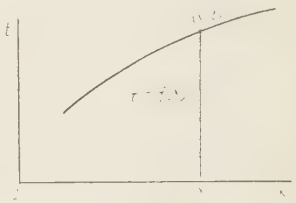

Fig. 1

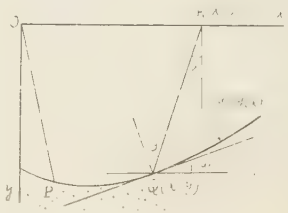

Fig. 2

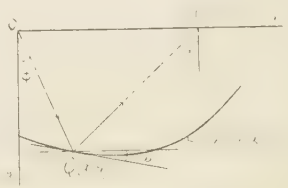

Fig. 3

Now, *we suppose that* $y(x)$ *and its derivative* dy/dx *are one valued continuous function of* x, *that is, the separation curve has no singular point and is continuous curve.*

Let α be the emergent angle at R and ω be the angle of inclination of the separation curve at Q, then

$\alpha = \theta + \omega$ ····· (when refraction method) ··· (3)

where $\theta = sin^{-1}(v_1/v_2) = const$

$\alpha = \phi + 2\omega$ ····· (when reflection method) ··· (4)

where ϕ = the angle shown in Fig. 3.

While by our assumption ω is a continuous function of x, of course ϕ is a continuous function of x, therefore α becomes also a continuous function of x when any case of above two.

Moreover we have a relation

$$v_1 \frac{d\varphi}{dX} = \sin \alpha \quad \cdots\cdots (5)$$

hence $d\varphi/dX$ is a continuous function of x, and

$$\left| \frac{d\varphi}{dX} \right| = \left| \frac{1}{v_1} \sin \alpha \right| < \frac{1}{v_1} \quad \cdots\cdots (6)$$

that is $|d\varphi/dX|$ has an upper bound.

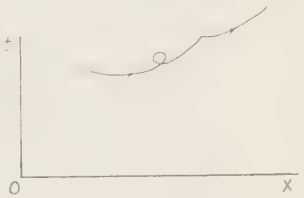

Fig. 4

Therefore, *the travelling-time curve never has a loop or a salient point such as shown in Fig. 4, and return point must be a cuspidal point at which two branches of the curve have common tangent.*

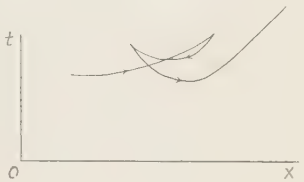

Fig. 5

Accordingly, *generally the singular point of a travelling-time curve must be any one of cuspidal point or nodal point such as shown in Fig. 5.*

Of course, above discussion needs the condition $dX/dx \neq 0$. When $dX/dx \equiv 0$ in the neighbourhood of R, emergent wave rays in the neighbourhood of R all must meet at R. The curve which satisfies this condition is found easily as follows,

ellipse whose foci are O *and* R ····· when reflection method

equiangular spiral whose center is R[(2)] ····· when refraction method,

and in both cases, the travelling-time from O to R is constant independently of the position of Q.

Hence if the curve of separation is above curve or includes some part of them, there may occur a case that the travelling-time curve has some isolated point or salient point, and since many wave rays meet at R at the same time, the energy of wave at this point is very strong. But this case is so rare that it scarcely occurs in practice.

3. Conclusion

In above discussion, we get a theoritical result. But at present, in practice, the observation points are not arranged closely, and the estimation of the travelling-time arrived not initially is difficult, therefore it is not easy to estimate the existence of a cuspidal point or a nodal point,

It is my delight that above discussion is of use in some aspects at present or in the future.

References

(1) See any book written on the seismic prospecting.

(2) R. Adachi : Fundamental Relation on the Seismic Prospecting.

THE APPLICATION OF THE DIFFUSION EQUATIONS

Akira ONUKI

(Received on 30th, April 1957)

1) Introduction

It seems that the Fick's diffusion eqnations are applicable for the various problems which we meet in the chemical engineering laboratories, even for the case in which we hesitate to use the word "diffusion" in its proper molecular theoretical meaning. For instance, in problems such as the washing or leaching of any substances mechanically contained in any other solid, what we have to consider is merely the rate of extraction of substances, and very frequently this is far from the true molecular diffusion. But, I believe, it is not totally useless to see these problems as the application of the diffusion equations, and compare the calculated results with the experimental data, so long as the suitable interpretations are made of the terminology used in the equations which may not be strictly exact in the physical or chemical sense. For example, we say "solute" and "solvent". It is only a matter of convenience to say so, and it is not necessarily understood in the usual sense. Some times "solute" means only substances mechanically contained in any other liquids or solids which are "solvent". The diffusion equations depend upon the well known Fick's first law, which says that the flux of the solute substances in the solvent is proportional to the concentration gradient of itself. This proportional coefficient is denoted by D and as usual is called diffusion coefficient. As stated above, D sometimes loses its molecular theoretical meaning, and might in some cases be understood simply as a mobility of substances within other liquids or solids, while in other cases as an average "diffusional constant" of two or more vaguely defined boundary layers of the solid.

2) The zero surface concentration.

The one-dimensional equation of diffusion is

$$\frac{\partial C}{\partial t} = D \frac{\partial^2 C}{\partial x^2} \qquad (2,1)$$

where C is the concentration of the "solute" substance in the "solvent" and has the dimension $\frac{gr}{cm^3}$. The flux of the "solute" through unit area perpendicular to the moving direction per unit time is denoted by J and is given as follows

$$J = -D \frac{\partial C}{\partial x} \qquad (2,2)$$

We take a line perpendicular to the surface of the "solvent" as x-coordinate axis, whose origin is at this surface, with the "solvent" being in the positive side of the x-coordinate. First we consider the case with concentration function $C(x.\ t)$ satisfying the following conditions,

$$C(0,\ t) = 0 \text{ for all positive } t. \qquad (2,3)$$

$$C(x, 0) = \phi_0(x) \text{ for all positive } x. \quad \cdots\cdots (2,4)$$

where $\phi_0(x)$ is a known function.

These conditions correspond to a situation that, while initial distribution of the solute in the solvent is arbitrary, the surface concentration, that is the concentration of the solute immediately outside of the solvent, is kept always to zero.

We assume that $\phi_0(x)$, together with $C(x, t)$ is the function which has the Laplace transform with respect to t, and is subject to the condition;

$$\lim_{x\to\infty} \phi_0(x) = \lim_{x\to\infty} C(x, t) = C_0 = const. \quad \cdots\cdots (2,5)$$

The Laplace transforms of any function $f(t)$ with respect to t will be denoted by $L[f(t)] = F(s)$ as usual.

Now, operating the L on both sides of the equations (2,1) (2,3) and (2,5), we obtain

$$D \frac{\partial^2 Y}{\partial x^2} = sY - \phi_0(x) \quad \cdots\cdots (2,6)$$

where $Y(x, s) = L[C(x, t)] \equiv \int_0^\infty e^{-st} C(x, t)\, dt \quad \cdots\cdots (2,7)$

$Y(x, s)$ satisfies the folowing conditions according to (2,3) and (2,5)

$$Y(0, s) = 0 \quad \cdots\cdots (2,8)$$

$$\lim_{x\to\infty} Y(x, s) = \frac{C_0}{s} \quad \cdots\cdots (2,9)$$

Here we have assumed that the order of two operations L and $\lim$ can be changed freely.

From (2,6) and (2,8), $Y(x, s)$ is readily found as

$$Y(x, s) = A(s)\left(e^{\sqrt{\frac{s}{D}}x} - e^{-\sqrt{\frac{s}{D}}x}\right) - \frac{1}{2\sqrt{sD}} \int_0^x \left\{e^{\sqrt{\frac{s}{D}}(x-\xi)} - e^{-\sqrt{\frac{s}{D}}(x-\xi)}\right\} \phi_0(\xi)\, d\xi \quad \cdots\cdots (2,10)$$

where $A(s)$ is the constant of intergration, and should be determined so as to satisfy the equation (2,9). If one chooses so that $A(s)$ takes the form

$$A(s) = \frac{1}{2\sqrt{sD}} \int_0^\infty e^{-\sqrt{\frac{s}{D}}\xi} \phi_0(\xi)\, d\xi$$

then one can see after slight elementary calculation that $Y(x, s)$ has all the required properties, including (2,9).

Inserting this value of $A(s)$ in the $Y(x, s)$, and operating the inverse operator L^{-1} on both sides, we get the required formula for $C(x, t)$ as follows

$$C(x, t) = \frac{1}{2\sqrt{\pi Dt}} \left\{ \int_x^\infty \phi_0(\xi)\, e^{-\frac{(\xi-x)^2}{4Dt}} d\xi - \int_0^\infty \phi_0(\xi)\, e^{-\frac{(x+\xi)^2}{4Dt}} d\xi + \int_0^x \phi_0(\xi)\, e^{-\frac{(x-\xi)^2}{4Dt}} d\xi \right\} \quad \cdots\cdots (2,11)$$

or

$$C(x,t)=\frac{1}{\sqrt{\pi}}\left\{\int_0^\infty \phi_0(x+2\sqrt{Dt}\,\xi)\,e^{-\xi^2}\,d\xi-\int_{\frac{x}{2\sqrt{Dt}}}^\infty \phi_0(2\sqrt{Dt}\,\xi-x)\,e^{-\xi^2}\,d\xi\right.$$
$$\left.+\int_0^{\frac{x}{2\sqrt{Dt}}} \phi_0(x-2\sqrt{Dt}\,\xi)\,e^{-\xi^2}\,d\xi\right\} \quad \cdots\cdots (2,12)$$

Here we used the well known inverse transformation

$$L^{-1}\left[\frac{1}{\sqrt{s}}e^{-k\sqrt{s}}\right]=\frac{1}{\sqrt{\pi t}}e^{-\frac{k^2}{4t}}$$

and assumed the changeability of the order of two operations L^{-1} and $\int^\infty d\xi$.

That $C(x,t)$ given above satisfies the original equation together with the conditions required, is readily seen by direct insertion of this in the corresponding equations.

The flux J is given by

$$J=-\frac{1}{4\sqrt{\pi D t^3}}\left\{\int_x^\infty(\xi-x)\,\phi_0(\xi)\,e^{-\frac{(\xi-x)^2}{4Dt}}\,d\xi\right.$$
$$\left.+\int_0^\infty(x+\xi)\,\phi_0(\xi)\,e^{-\frac{(x+\xi)^2}{4Dt}}\,d\xi-\int_0^x(x-\xi)\,\phi_0(\xi)\,e^{-\frac{(x-\xi)^2}{4Dt}}\,d\xi\right\} \quad \cdots\cdots (2,13)$$

or

$$J=-\sqrt{\frac{D}{\pi t}}\left\{\int_0^\infty \xi\phi_0(2\sqrt{Dt}\,\xi+x)\,e^{-\xi^2}\,d\xi\right.$$
$$\left.+\int_{\frac{x}{2\sqrt{Dt}}}^\infty \xi\phi_0(2\sqrt{Dt}\,\xi-x)\,e^{-\xi^2}\,d\xi-\int_0^{\frac{x}{2\sqrt{Dt}}} \xi\phi_0(x-2\sqrt{Dt}\,\xi)\,e^{-\xi^2}\,d\xi\right\} \quad \cdots\cdots (2,14)$$

The flux at the surface $(x=0)$ is denoted by J_{surf} and is given by

$$J_{surf}=-2\sqrt{\frac{D}{\pi t}}\int_0^\infty \xi e^{-\xi^2}\,\phi_0(2\sqrt{Dt}\,\xi)\,d\xi \quad \cdots\cdots (2,14')$$

In the special case when the initial distribution of "solute" can be considered to be uniform and equal to C_0, then we can naturally replace $\phi_0(x)$ by constant C_0, and the results will be

$$C(x,t)=C_0E(\lambda) \quad \cdots\cdots (2,15)$$

$$\lambda=\frac{x}{2\sqrt{Dt}}$$

where $E(\lambda)=\frac{2}{\sqrt{\pi}}\int_0^\lambda e^{-\xi^2}\,d\xi$,

$$J=-C_0\sqrt{\frac{D}{\pi t}}\,e^{-\lambda^2} \quad \cdots\cdots (2,16)$$

and $J_{surf}=-C_0\sqrt{\frac{D}{\pi t}}$ $\cdots\cdots (2,17)$

The total amount of the solute substance Q, which flows out through the unit area of the

surface $x = 0$ into the negative side of x in the interval $0 < t < T$, will be immediately obtained by integration, and is given by

$$Q = -\int_0^T J_{surf}\, dt \quad \cdots\cdots (2,18)$$

For the case when $\phi_0(x) = C_0$, Q becomes simply

$$Q = 2C_0\sqrt{\frac{Dt}{\pi}} \quad \cdots\cdots (2,19)$$

3) Time dependent surface concentration.

Next we will treat the more general case, in which the surface concentration $C(0, t)$ varies arbitrarily with time. In this case we have to use the new initial condition

$$C(0, t) = \psi(t) \quad \cdots\cdots (3, 1)$$

in place of (2, 3), where $\psi(t)$ is some known function.
Mathematical treatment is almost the same as before, and therefore, it is convenient to distinguish the quantities appearing in this article from the corresponding one in the preceding article by adding the suffix 1. Then the Laplace transform $Y_1(x, s)$ of new $C_1(x, t)$ becomes

$$Y_1(x, s) = Y(x, s) + \Psi(s)\, e^{-\sqrt{\frac{s}{D}}x} \quad \cdots\cdots (3, 2)$$

where $\Psi(s)$ is the Laplace transform of $\psi(t)$,
and from this it follows that

$$C_1(x, t) = C(x, t) + L^{-1}\left[\Psi(s)\, e^{-\sqrt{\frac{s}{D}}x}\right]$$

Now from the convolution theorem of Laplace transformation, and from the formula

$$L\left[\frac{x}{2\sqrt{\pi D t^3}}\, e^{-\frac{x^2}{4Dt}}\right] = e^{-\sqrt{\frac{s}{D}}x}$$

it follows that

$$C_1(x, t) = C(x, t) + \frac{x}{2\sqrt{\pi D}}\int_0^t \frac{\psi(t-\tau)}{\sqrt{\tau^3}}\, e^{-\frac{x^2}{4D\tau}}\, d\tau \quad \cdots\cdots (3, 3)$$

$$= C(x, t) + \frac{2}{\sqrt{\pi}}\int_{\frac{x}{2\sqrt{Dt}}}^{\infty} \psi\left(t - \frac{x^2}{4D\xi^2}\right) e^{-\xi^2}\, d\xi \quad \cdots\cdots (3, 4)$$

$C(x, t)$ in the right hand side of both equations is already given in the equations (2, 11) or (2, 12). The flux at the surface is given by

$$J_{1surf} = -\frac{2\sqrt{D}}{\sqrt{\pi t}}\int_0^\infty \xi e^{-\xi^2}\phi_0(2\sqrt{Dt}\,\xi)\, d\xi + \sqrt{\frac{D}{\pi t}}\,\psi(0)$$

$$+ \lim_{x\to 0}\frac{x}{\sqrt{\pi}}\int_{\frac{x}{2\sqrt{Dt}}}^{\infty} \psi'\left(t - \frac{x^2}{4D\xi^2}\right)\frac{1}{\xi^2}\, e^{-\xi^2} d\xi \quad \cdots\cdots (3, 5)$$

The third term of (3,5) must be treated very carefully, because as the lower limit of integral tends to zero, the factor $\frac{1}{\xi^2}$ tends to infinity.

But if one put $t - \frac{x^2}{4D\xi^2} = \eta$

in the integral, and write η again ξ, then the intergral becomes

$$\sqrt{\frac{D}{\pi}} \int_0^t \frac{\psi'(\xi)}{\sqrt{t-\xi}} e^{-\frac{x^2}{4D(t-\xi)}} d\xi$$

which tends to

$$\sqrt{\frac{D}{\pi}} \int_0^t \frac{\psi'(\xi)}{\sqrt{t-\xi}} d\xi \qquad \text{as } x \to 0$$

and therefore the surface flux becomes

$$J_{1surf} = 2\sqrt{\frac{D}{\pi t}} \int_0^\infty \xi e^{-\xi^2} \phi_0(2\sqrt{Dt}\,\xi)\, d\xi + \sqrt{\frac{D}{\pi t}} \psi(0) + \sqrt{\frac{D}{\pi}} \int_0^t \frac{\psi'(\xi)}{\sqrt{t-\xi}} d\xi \quad \cdots\cdots (3,\ 6)$$

In the special case where $\phi_0(x) = C_0$, (3,6) becomes

$$J_{1.surf} = (\psi(0) - C_0)\sqrt{\frac{D}{\pi t}} + \sqrt{\frac{D}{\pi}} \int_0^t \frac{\psi'(\xi)}{\sqrt{t-\xi}} d\xi \quad \cdots\cdots (3,\ 7)$$

4) Problems of washing.

The equation (3,7) of the preceding article will provide an interesting example of application in a problem of washing the substance with water. There are several different ways or systems to make the washing, and of these two are considered to be distinctive, and we call them provisionally the "continuous" and "batch" systems, respectively.
In the former system, continuously running fresh water washes the boundary surface and removes the emerging solute substance as soon as it comes out, whence, in this system $C(0,t)$ is considered to be always zero, and the results of former sections will be immediately applicable. On the contrary, in the latter system the water does not change continuously, but stays for definite time intervals in one tank, then flows to the next and so on. The water in the tank is effectively stirred so that the solute concentration becomes constant everywhere in the tank. But, of course, this concentration gradually increases with time, and consequently, the dissolving efficiency of the water becomes rather worse than in the former system.

To make the comparison of the two different systems clearer, we assume first that in the latter case there is only one tank, and the water remains sufficiently long time in it; and secondly, we assume that the initial C is constant C_0. If the volume of this tank is denoted by V, and the surface area by S, then evidently the next relation holds good.

$$-S\int_0^T J_{1surf}(t)\, dt = Q = V\psi(T) \quad \cdots\cdots (4,\ 1)$$

Inserting the J_{1surf} given in (3,7), (4,1) we obtain the equations.

$$2(\psi(0) - C_0)\sqrt{\frac{DT}{\pi}} + \sqrt{\frac{D}{\pi}}\int_0^T dt\int_0^t \frac{\psi'(\xi)}{\sqrt{t-\xi}}\,d\xi = -\frac{V}{S}\psi(T)$$

Differentiating both sides by T, we obtain the equation

$$(\psi(0) - C_0)\sqrt{\frac{D}{\pi T}} + \sqrt{\frac{D}{\pi}}\int_0^T \frac{\psi'(\xi)}{\sqrt{T-\xi}}\,d\xi = -\frac{V}{S}\psi'(T) \quad \cdots\cdots (4,\ 2)$$

which is an integral equation of Volterra type for unknown function ψ'. Replace T by t again and denote the Laplace transforms of $\psi'(t)$ and $\psi(t)$ by $\chi(s)$ and $\Psi(s)$, then,

$$\chi(s) = s\Psi(s) - \psi(0)$$

Operate L on both sides of (4,2) and we obtain

$$(\psi(0) - C_0)\sqrt{\frac{D}{s}} + \sqrt{\frac{D}{s}}\chi(s) = -\frac{V}{S}\chi(s)$$

which is merely an algebraic equation for the $\chi(s)$ and also for the $\Psi(s)$. $\Psi(s)$ is given by

$$\frac{A}{s(a+\sqrt{s})} + \frac{\psi(0)}{s}$$

where

$$a = \frac{S}{V}\sqrt{D} \text{ and } A = \frac{S}{V}\sqrt{D}\,(C_0 - \psi(0))$$

Using the well known formula

$$L^{-1}\left[\frac{1}{s(a+\sqrt{s})}\right] = \frac{1}{a}\left\{1 - \frac{2}{\sqrt{\pi}}e^{a^2t}\int_{a\sqrt{t}}^{\infty} e^{-\xi^2}\,d\xi\right\}$$

we odtain $\psi(t)$ and $\psi'(t)$ together with J_{1surf} as foollows

$$\left.\begin{aligned}\psi(t) &= \frac{A}{a}\left\{1 - \frac{2}{\sqrt{\pi}}e^{a^2t}\int_{a\sqrt{t}}^{\infty} e^{-\xi^2}\,d\xi\right\} + \psi(0)\\ \psi'(t) &= \frac{a^2C_0}{\sqrt{\pi}}\left\{a\sqrt{t} - 2e^{a^2t}\int_{a\sqrt{t}}^{\infty} e^{-\xi^2}\,d\xi\right\}.\end{aligned}\right\} \quad \cdots\cdots (4,\ 3)$$

$$J_{1.surf} = -C_0\sqrt{\frac{D}{\pi t}} + 2C_0a\sqrt{\frac{D}{\pi}}e^{a^2t}\int_{a\sqrt{t}}^{\infty} e^{-\xi^2}\,d\xi \quad \cdots\cdots (4,\ 4)$$

All these formulae are the required results. If we put $\psi(0) = 0$, the total amount of solute dissolved in the water in the interval $0 \leqq t \leqq T$ will be given as

$$Q = -S\int_0^T J_{1.surf}(t)\,dt = V\psi(T) \quad \cdots\cdots (4,\ 5)$$

To make the comparison easier it is convenient to adopt the following scheme of calculation together with new definitions and notations.

i) Zero suffix refers to "continuous system", and no suffix refers to "batch system".

ii) $\kappa = Q/Q_0 \qquad 1-\eta = J/J_0 \qquad \mu = \frac{S}{V}\sqrt{Dt}$ ..... (4, 6)

$$\Phi(\mu) = \frac{2}{\sqrt{\pi}}\int_0^{\mu} e^{-\xi^2}\,d\xi \qquad \Phi'(\mu) = \frac{2}{\sqrt{\pi}}\,e^{-\mu^2}$$ ..... (4, 7)

iii)
$$\left.\begin{aligned} \eta(\mu) &= 2\mu\,\frac{1-\Phi(\mu)}{\Phi'(\mu)} \\ Q(\mu) &= C_0V\left\{1-\frac{2}{\sqrt{\pi}}\,\frac{1-\Phi(\mu)}{\Phi'(\mu)}\right\} \\ \kappa(\mu) &= \frac{1}{\mu}\left\{\frac{\sqrt{\pi}}{2}-\frac{1-\Phi(\mu)}{\Phi'(\mu)}\right\}. \\ J_0(\mu) &= -\frac{C_0DS}{\sqrt{\pi}}\,\frac{1}{\mu} \end{aligned}\right\}$$ ..... (4, 8)

The numerical values of each function are shown in the Table 1 for the argument μ. Note that μ increases with $\sqrt{t}$. The Figures 1 and 2 show the graph of these functions.

Table 1

μ	t/V^2 SD	$\Phi(\mu)$	$\frac{1-\Phi(\mu)}{\Phi'(\mu)}$	$\frac{J_0(t)}{\sqrt{\pi}}\frac{1}{C\ SD}{V}$	$\frac{J(t)}{\sqrt{\pi}}\frac{1}{C\ SD}{V}$	$\eta(\mu)$	$1-\eta(\mu)$	$\frac{Q_0(t)}{C\ V}$	$\frac{Q(t)}{C\ V}$	$\kappa(\mu)$
0.0	0.00	0.0000	0.8862	∞	∞	0.0000	1.0000	0.0000	0.0000	1.0000
1	0.01	0.1125	7944	10.0000	8.4110	1589	8411	1128	1036	9180
2	0.04	0.2227	7170	5.0000	3.5660	2868	7132	2257	1909	8460
3	0.09	0.3286	6510	3.3333	2.0310	3906	6094	3385	2654	7840
4	0.16	0.4284	5945	2.5000	1.3110	4756	5244	4514	3292	7293
5	0.25	0.5205	5456	2.0000	0.9088	5456	4544	5642	3843	6812
6	0.36	0.6039	5032	1.6667	6603	6038	3962	6770	4322	6383
7	0.49	0.6778	4661	1.4286	4964	6525	3475	7899	4741	6001
8	0.64	0.7421	4334	1.2500	3833	6934	3066	9047	5110	5660
9	0.81	0.7969	4046	1.1111	3019	7283	2717	1.0156	5434	5351
1.0	1.00	0.8427	3789	1.0000	2422	7578	2422	1.1284	5724	5073
1.1	1.21	0.8802	3560	0.9091	1971	7832	2168	1.2412	5983	4820
1.2	1.44	0.9103	3356	8333	1622	8054	1946	1.3541	6213	4589
1.3	1.69	0.9340	3170	7692	1352	8242	1758	1.4669	6423	4378
1.4	1.96	0.9523	3002	7143	1139	8406	1594	1.5798	6613	4186
1.5	2.25	0.9661	2851	6667	0965	8553	1447	1.6926	6783	4007
1.6	2.56	0.9764	2717	6250	0816	8694	1306	1.8054	6934	3841
1.7	2.89	0.9838	2584	5882	0714	8786	1214	1.9183	7084	3693
1.8	3.24	0.9891	2468	5556	0619	8885	1115	2.0311	7215	3552
1.9	3.61	0.9928	2360	5263	0543	8968	1032	2.1440	7337	3422
2.0	4.00	0.9953	2266	5000	0468	9064	0936	2.2568	7443	3298
2.1	4.41	0.9970	2172	4762	0418	9122	0878	2.3696	7549	3186
2.2	4.84	0.9981	2083	4545	0380	9165	0835	2.4825	7650	3081
2.3	5.29	0.9989	2012	4348	0324	9255	0745	2.5953	7730	2978
2.4	5.76	0.9993	1946	4167	0275	9341	0659	2.7082	7804	2879
2.5	6.25	0.9996	1873	4000	0254	9365	0635	2.8210	7887	2796
2.6	6.76	0.9998	1814	3846	0218	9433	0567	2.9338	7953	2711
2.7	7.29	0.9999	1766	3704	0172	9536	0464	3.0469	8007	2628
2.8	7.84	0.9999	1711	3571	0149	9582	0418	3.1595	8069	2554

Note. suffix o refers to continuous system
no suffix refers to batch system.
$\Phi(\mu)$ = Gauß's error function.

Fig. 1.

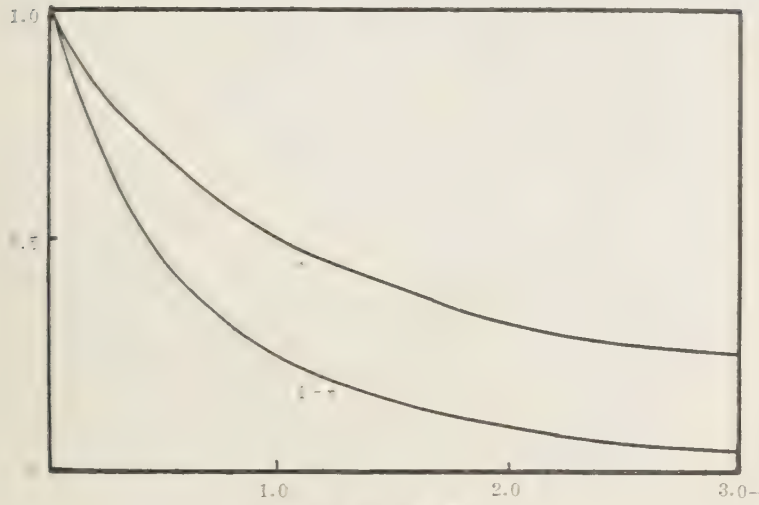

5. **Application for the counter-flow system.**

The preceding equations provide a sample of interesting applications also for the case of washing by the counter-flow system. In this system, n equal tanks are placed in series as shown in the Figure 1. The substances which contain the solute in it self solid, liquid or a mixture of both come into the n-th tank first, and then pass to the $(n-1)$-th tank, then $(n-2)$-th tank and so on, the interval of staying in each tank being equal to τ. Concentrations of the solute substance (which is to be washed out) are denoted by C_r when it enters into the r-th tank, and C_{r-1} when it leaves the r-th and passes to the $(r-1)$-th. The fresh water comes from the opposite side and first enters into the first tank, passes to the second and so on, and finally leaves the n-th tank, reserving in each tank an amount of solute substances. The concentration of the solute in the water in the r-th tank is denoted by C_r when it enters into the r-th tank, and C_{r-1} when it leaves. Moreover we denote by C_1 the concentration of the solute when it is taken out finally from the first tank, and by C_0 the concentration of the liquor when it is taken out from the last tank. In these circumstances if the assumptions made in the preceding chapters are valid it can be confirmed easily that the following equations will be valid in this case,

$$\frac{Q_r}{V} = C_{r-1} - C_r = C_r - C_{r+1} \qquad (5,\ 1)$$

Fig. 2.

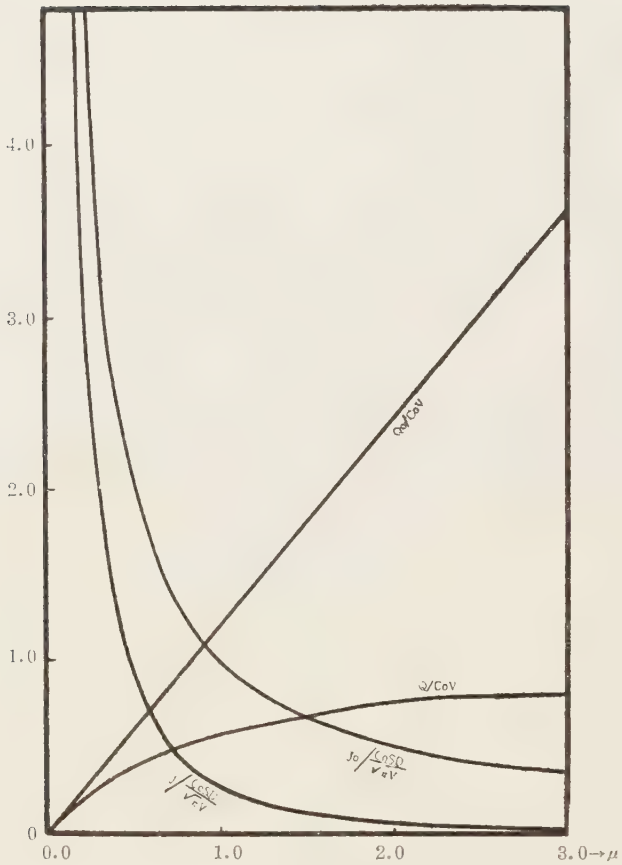

$$\frac{Q_0}{C_0V}=\frac{2}{\sqrt{\pi}}\mu, \qquad \frac{Q}{C_0V}=1-\frac{2}{\sqrt{\pi}}e^{\mu^2}\int_\mu^\infty e^{-\xi^2}d\xi$$

$$\frac{J_0}{\sqrt{C_0SD}/\sqrt{\pi V}}=\frac{1}{\mu} \qquad \frac{J}{\sqrt{C_0SD}/\sqrt{\pi V}}=\frac{1}{\mu}-2e^{\mu^2}\int_\mu^\infty e^{-\xi^2}d\xi.$$

Fig. 3

1. 2. r. n.

where Q is the amount of solute substance passed into the water in the r-th tank. Now, we use the Q from (4,8) for Q_r in (5,1), replacing simply C_0 by $C_r - C_r'$ and get

$$\left.\begin{aligned} &\frac{Q_r}{V} = (C_r - C_r')\,F(\mu) \\ &F(\mu) = 1 - \frac{2}{\sqrt{\pi}}\,\frac{1-\Phi(\mu)}{\Phi'(\mu)} \\ &\mu = \frac{S}{V}\sqrt{D\tau} \end{aligned}\right\} \quad \cdots\cdots (5,\ 2)$$

where τ is time interval of staying of the solute and the water in the r-th tank, and is considered to be constant. Consequently, μ and $F(\mu)$ are considered to be equal for all the tanks.

(5,2) will be rewritten in the forms

$$\left.\begin{aligned} &(C_1 - C_1')\,F = C_2' - C_1' = C_1 - C_0 \\ &(C_2 - C_2')\,F = C_3' - C_2' = C_2 - C_1 \\ &\cdots\cdots\cdots\cdots \\ &(C_n - C_n')\,F = C_f' - C_n' = C_n - C_{n-1} \end{aligned}\right\} \quad \cdots\cdots (5,\ 3)$$

from which we can get easily

$$\left.\begin{aligned} &C_n = \frac{C_n}{1+nG(\mu)} + \frac{nG(\mu)C_1'}{1+nG(\mu)} \\ &C_f' = \frac{nG(\mu)C_n}{1+nG(\mu)} + \frac{C_1'}{1+nG(\mu)} = C_1' + C_n - C_0 \\ &Q_r = V\frac{G(\mu)}{1+nG(\mu)}(C_n - C_1') \quad (r = 1.2 \cdots\cdots n) \end{aligned}\right\} \quad \cdots\cdots (5,\ 4)$$

where

$$G(\mu) \equiv \frac{F(\mu)}{1-F(\mu)} = \frac{1-\frac{2}{\sqrt{\pi}}\frac{1-\Phi(\mu)}{\Phi'(\mu)}}{\frac{2}{\sqrt{\pi}}\frac{1-\Phi(\mu)}{\Phi'(\mu)}} \quad \cdots\cdots (5,\ 5)$$

Some conclusions from these results are, ……

i) In almost all the practical cases, while C_n and C_1' are supposed to be known primarily, C_0 must take a value determined from other external condition. In this case, we should determine μ, and the number of tanks, n, from the equation

$$\frac{1}{n}\left(\frac{C_n - C_0}{C_0 - C_1'}\right) = G(\mu) \quad \cdots\cdots (5,\ 6)$$

The table for this purpose is added at the end of this article (Table. 2)

ii) C_f' will be determined from C_1', C_n and C_0 only. If $C_1' = 0$ as in the usual case, this is simply the difference of the concentrations of the solute at the end and the beginning of the washing.

iii) Amounts of the solute extracted in each tank are all equal, and hence, if we want to make the washing as perfect as possible, we must increase the number of tanks n, or

increase the parametre μ, which is proportional to $\sqrt{\tau}$

iv) Total time necessary for the washing may be found as constant times $n\mu^2$. The following numerical example shows how this total time changes with n.

Numerical example.

$C_n = 35\%$		$C_0 \cdot 1\%$	$C_1 = 0$
n	$G(\mu)$	μ	$n\mu^2$
7	4.86	3.3	76
8	4.25	2.9	67
9	3.78	2.6	59
10	3.40	2.3	53
11	3.09	2.1	49
12	2.83	1.9	45
13	2.62	1.8	43
14	2.43	1.7	41
15	2.27	1.6	39
16	2.13	1.5	37
17	2.00	1.4	35

Table. 2

μ	G (μ)	μ	G (μ)	μ	G (μ)
0.0	0.000				
1	0.116	1.1	1.489	2.1	3.080
2	0.236	1.2	1.641	2.2	3.255
3	0.361	1.3	1.796	2.3	3.405
4	0.491	1.4	1.953	2.4	3.554
5	0.624	1.5	2.109	2.5	3.732
6	0.761	1.6	2.262	2.6	3.885
7	0.902	1.7	2.429	2.7	4.018
8	1.045	1.8	2.591	2.8	4.179
9	1.190	1.9	2.755		
1.0	1.339	2.0	2.911		

μ	G (μ)	μ	G (μ)	μ	G (μ)	μ	G (μ)
3.0	4.587						
3.2	4.927	4.2	6.645	5.2	8.381	6.2	10.129
3.4	5.268	4.4	6.991	5.4	8.730	6.4	10.479
3.6	5.611	4.6	7.338	5.6	9.082	6.6	10.830
3.8	5.955	4.8	7.685	5.8	9.429	6.8	11.180
4.0	6.299	5.0	8.033	6.0	9.779	7.0	11.531
						7.2	11.883
						7.4	12.234

Asymptotic form of function G (μ) for large value of μ is obviously $\sqrt{\pi}\ \mu - 1$.

Acknowledgement

I wish to express my sincere thanks to Mr. Kamiya and Mr. Kurobe of Shin Nippon Chisso Co. for their kind helps and discussions on the subjects.

DISTRIBUTION OF HYDROGEN AND HELIUM IN THE INTERIOR OF THE STAR

Keisuke KAMINISI

(Received April 30, 1957)

Abstract

The distribution of H and He in the star is investigated on the assumption that the stellar structure is given by the polytropic gas sphere of index $n=3$. The present result suggests that in the deep interior of the star the chemical elements are well mixed even if there exists no appreciable convection current.

1. Introduction

It is an important problem for the theory of stellar structure and stellar evolution to determine the distribution of chemical element in the interior of the star[1]. At present it is considered that if a star possesses no appreciable mixing current in its interior, the hydrogen is in the envelope and the helium in the core because of the strong gravitational sorting of chemical elements. In the deep interior of a star, however, the gravitational field is rather weak and the temperature is considerably high. Therefore, in the central region of a star the chemical elements may be well mixed without no appreciable convection current. In the present work we shall investigate the effects of gravitational sorting and thermal mixing of hydrogen and helium.

2. Estimation of the mol-fraction of hydrogen

We shall consider the system which consists of hydrogen and helium. Let n_H, n_{He} and n_e be the number of protons, helium nuclei and electrons per unit volume; V and φ be the radial gravitational and electrical field potentials; e and m_H be the charge and mass of proton; m_e be the mass of electron. In the interior of usual main-sequence stars all the hydrogen and helium are considered to be thermally ionized and the pressure is satisfactorily given by the perfect gas law. Hence the equation of hydrostatic equilibrium is:

$$\nabla\{(n_H+n_{He}+n_e)kT\}=(n_Hm_H+4n_{He}m_H+n_em_e)\nabla V$$
$$+(n_H+2n_{He}-n_e)e\nabla\varphi \qquad (1),$$

where k is Boltzmann constant and T temperature.

As Eq. (1) holds for all n_s we get the following Eqs.:

$$\nabla(n_HkT)=n_H(m_H\nabla V+e\nabla\varphi) \qquad (1a)$$

$$\nabla(n_{He}kT)=n_{He}(4m_H\nabla V+2e\nabla\varphi) \qquad (1b)$$

$$\nabla(n_ekT)=n_e(m_e\nabla V-e\nabla\varphi) \qquad (1c).$$

Poisson's Eqs. are

$$\nabla^2 V = -4\pi[(n_H + 4n_{He})m_H + n_e m_e]G \quad \cdots\cdots (2a)$$

$$\nabla^2 \varphi = -4\pi(n_H + 2n_{He} - n_e)e \quad \cdots\cdots (2b).$$

Since the electric field arises from the gravitational sorting of electrons and nuclei, $-e\nabla\varphi$ is nearly equal, in magnitude, to $m_s \nabla V$ everywhere in the interior of the star. As, therefore, $-e\nabla^2\varphi$ is approximately equal to $m_s \nabla^2 V$, from Eqs. (2a) and (2b) we get the following relation

$$\left| \frac{n_H + 2n_{He} - n_e}{n_H + 4n_{He}} \right| \fallingdotseq \frac{Gm_H^2}{e^2} = 8 \times 10^{-37}$$

which is a negligible quantity. In other words there exists no appreciable excess charges within unit volume in the stellar interior, i. e.

$$n_H + 2n_{He} - n_e = 0 \quad \cdots\cdots (3).$$

From Eqs. (1a), (1b), (1c) and (3) we have

$$(m_H n_H + 8m_H n_{He} - n_e m_e)\nabla V + (n_H + 4n_{He} + n_e)e\nabla\varphi = 0$$

Since we may neglect the value of m_e/m_H as compared to unity, we obtain

$$cE = -\frac{n_H + 8n_{He}}{2n_H + 6n_{He}} m_H g \quad \cdots\cdots (4)$$

by using Eq. (3) again, where $E \equiv -\nabla\varphi$ and $g \equiv -\nabla V$.

Now let x_H be the mol-fraction of hydrogen, i. e.

$$x_H = \frac{n_H}{n_H + n_{He}} \quad \cdots\cdots (5).$$

We then get

$$\frac{dx_H}{dr} = \frac{5}{2}\frac{m_H g}{kT} \frac{x_H(1-x_H)(2-x_H)}{3-2x_H} \quad \cdots\cdots (6),$$

by making use of Eqs. (1a), (1b) and (4). Next we can, from Eq. (2a), get the following expression

$$g = G\frac{M_r}{r^2} \quad \cdots\cdots (7),$$

where M_r is the mass contained within the sphere of radius r.

We can determine x_H by Eqs. (1), (6) and (7), combining the equation of energy transfer, the equation of energy production and the equation of mass conservation. Such a legitimate procedure is, however, very complex and tedious. In oder roughly to estimate the distribution of hydrogen and helium we may satisfactorily employ in Eq. (6) the well-known values of T and M_r in polytropic gas sphere with index $n = 3$, for the structure of stellar model in radiative equilibrium is appproximately given by the structure of polytropic gas sphere with index $n = 3$ (Eddington model). In the polytrope the desired expressions for physical quantities are as follow[2]

$$\left.\begin{aligned} M_r &= -4\pi\left[\frac{(n+1)K}{4\pi G}\right]^{3/2}\rho_c^{\frac{3-n}{2n}}\xi^2\frac{d\theta}{d\xi}, \\ r &= \left[\frac{(n+1)K}{4\pi G}\rho_c^{\frac{1-n}{n}}\right]^{1/2}\xi, \\ T &= \frac{K_0 m_H}{k}\rho_c^{\frac{1}{n}}\theta, \end{aligned}\right\} \quad \cdots\cdots (8)$$

where central density ρ_c and K is the constant throughout a star, whereas the Emden function θ and mean molecular weight μ depend on the new independent variable ξ. In our system the expression for μ is as follows

$$\mu = \frac{n_H + 4n_{He}}{2n_H + 3n_{He}} = \frac{4-3x_H}{3-x_H} \quad \cdots\cdots (9).$$

By using Eqs. (6), (7), (8) and (9), we get

$$\frac{(3-2x_H)(4-3x_H)}{x_H(1-x_H)(2-x_H)(3-x_H)}\,dx_H = -\frac{5}{2}(n+1)\,d\log\theta \quad \cdots\cdots (10).$$

We can easily integrate this differential equation and get the following relation in the case of $n=3$:

$$\frac{1}{4}\log(3-x_H) + \frac{1}{20}\log(1-x_H) - \frac{1}{5}\log x_H - \frac{1}{10}\log(2-x_H) = \log\theta + C \quad \cdots\cdots (11),$$

where C is the integral constant.

Let us now study the problem in three cases; the three central values of $x_H = 0.1$,

Table

x_H	θ	ξ	$\frac{100r}{R}$	θ	ξ	$\frac{100r}{R}$	θ	ξ	$\frac{100r}{R}$
0.1	1.000 00	0.00	0.00						
0.12	0.962 46	0.486	7.04						
0.15	0.917 93	0.725	10.5						
0.2	0.862 53	0.970	14.1						
0.3	0.787 39	1.26	18.3						
0.4	0.735 17	1.44	20.9						
0.5	0.694 38	1.59	23.0	1.000 00	0.000	0.00			
0.55	0.676 56	1.65	23.9	0.974 34	0.402	5.83			
0.6	0.659 90	1.71	24.8	0.950 35	0.554	8.03			
0.7	0.628 69	1.82	26.4	0.905 41	0.782	11.3			
0.8	0.597 98	1.94	28.1	0.861 17	0.978	14.2	1.000 00	0.000	0.00
0.85	0.581 47	2.00	29.0	0.837 39	1.07	15.5	0.972 39	0.414	6.00
0.9	0.562 51	2.08	30.1	0.810 10	1.18	17.0	0.940 69	0.608	8.81
0.94	0.542 98	2.16	31.3	0.781 96	1.28	18.5	0.908 02	0.770	11.2
0.96	0.529 56	2.21	32.1	0.762 65	1.35	19.5	0.885 59	0.873	12.7
0.98	0.509 15	2.30	33.3	0.733 25	1.45	21.0	0.851 46	1.02	14.7
0.99	0.490 69	2.38	34.4	0.706 66	1.55	22.4	0.820 58	1.14	16.5

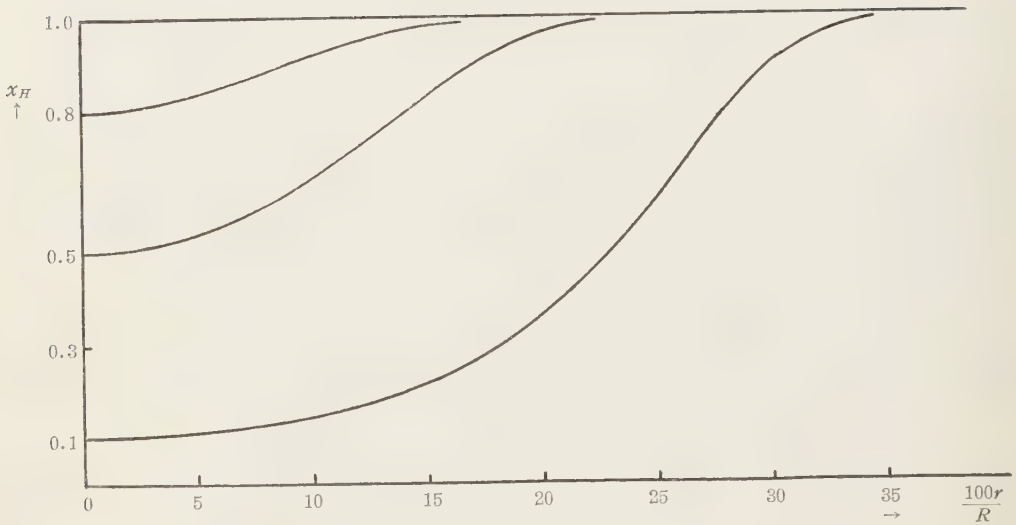

R denotes the radius and r the distance from the centre of the star

0.5 and 0.8 (at $\xi=0$; $\theta=1$). In these cases the values of C are as follow

$$C_{0.1}=0.285\ 44,\quad C_{0.5}=0.127\ 03 \text{ and } C_{0.8}=0.062\ 12.$$

In each case we can get the value of θ for the given x_H from Eq. (11) and determine the value of ξ for the above obtained value of θ from the available table. These results are tabulated in the table and illustrated in the figure.

3. Conclusions

From the figure we see that within the sphere of radius 0.1 R hydrogen and helium are well mixed, and the less the hydrogen content is, the more spacious the well mixing region. Thus we can conclude that although the gravitational sorting of chemical elements is rather conspicuous in the outer region of the star, *in the deep interior* (within the sphere of radius 0.1 R~0.2 R) of the main-sequance star (whose internal structure is approximately given by the Eddington model) *the chemical elements are well mixed even though there exists no appreciable convection current.*

The author wishes to express his thanks to the professors of the Department of Physics, Kumamoto University, for their constant encouragement.

References

1. For example : F. Hoyle and M. Schwarzschild : Ap. J., Suppl. 2, No. 13. '55
2. For example : A. S. Eddington : The Internal Constitution of the Stars.

THE CAGE MODEL BY NON-SPHERICAL INTERACTION POTENTIAL

Taturo NAGATA

(Received Apr. 28, 1957)

1. Introduction

In treating the liquid state, there are some methods. The methods employed by various authors can usually be classified as belonging to one of three general categories;

1) The development as a power series of activity.

2) The method of integral equations.

3) The cell method or free volume method.

The cell method is what is most frequently used to find approximate equations of state. It is originally more intuitive than formal in its derivation. The method can be regarded as a formal use of the principle that a real system at equilibrium always adjusts its distribution to give the minimum value of the appropriate thermodynamic potential.

The cell method of computation has been the one which has been the most fruitful in giving relatively simple numerical values for the equation of state over a wide range of densities and temperatures. It would seem as though this method is capable of considerable improvement although it is to be feared that introducing improvements will greatly increase the complications of the numerical computation.

We have extented the theory by adopting the familiar method of usual cage model by Lennard-Jones and Devonshire.

We suppose that one molecule exists into a cell and interacts between the nearest neighbour molecules. Now, as we suppose non-spherical molecule, the interaction potential is non-spherical, too. And as we suppose that the field in the cell is non-spherical, treatment of equation is troublesome very much.

Now, we stand for intermolecular potential by $\phi(r)$, at distance r between two molecules. Interaction potential energy acted from the nearest neighbour molecules, when all the molecules exist in the rest sites, in the following;

$$u(0) = \sum_{i=1}^{z} \phi(a_i), \qquad (1)$$

where z is the number of the nearest neighbour sites, and a_i is the distance between the rest sites. But in liquid state, each molecule moves freely around within the cell. Then if the molecule translates by r from the rest site, the interaction potential energy is the following;

$$u(r) = \sum_{i} \phi(r_i), \qquad (2)$$

where r_i represents the distance between the nearest neighbour molecules.

The interaction potential energy, measured from the rest potential energy, is

$$u(r)-u(0)=\sum_{i=1}^{z}\phi(r_i)-\sum_{i=1}^{z}\phi(a_i). \quad \cdots\cdots (3)$$

This potential energy is calculated as follows. First we make the centre molecule translate at a distance r into various direction, and we calculate the mean potential between the nearest neighbour molecules.

$$\bar{\phi}(r)=\iint_{\Omega}\phi(r)d\Omega \Big/ \iint_{\Omega}d\Omega, \quad \cdots\cdots (4)$$

where Ω is the whole configurational space.

Next, let distance between the nearest neighbour sites be a constant, a, then equ.(3) becomes

$$u(r)-u(0)=z\,\overline{\phi(r)}-z\phi(a). \quad \cdots\cdots (5)$$

Used this pot., free volume becomes

$$v_f=e\int_0^{\frac{a}{2}} e^{-\{u(r)-u(0)\}/kT}\,dr. \quad \cdots\cdots (6)$$

Moreover, when each molecule exists at each rest site, let total pot. energy denote $-N\chi_0$, where N is the total number of molecules in our system and;

$$-\chi_0=-\frac{1}{2}z\phi(a), \quad \cdots\cdots (7)$$

whereas, if we take count of interaction between the second nearest neighbour molecules, an error diminishes still more.

The partition function of system is, in using these equations,

$$Z=\left(\frac{2\pi mkT}{h^2}\right)^{\frac{3N}{2}}\cdot[j(T)]^N\cdot e^{\frac{\chi_0}{kT}}\cdot v_f^N, \quad \cdots\cdots (8)$$

where $j(T)$ is partion function of the degree of inner freedom of each molecule.

Helmholtz's free energy is

$$F=-NkT\ln\left(\frac{2\pi mkT}{h^2}\right)^{\frac{3}{2}}-NkT\ln j(T)-kT+\frac{Nz}{2}\phi(a)-NkT\ln v_f. \quad \cdots\cdots (9)$$

Pressure is

$$p=-\left(\frac{\partial F}{\partial v}\right)_T=\frac{kT}{v}\left[1-\frac{z}{2kT}\frac{\partial\phi(a)}{\partial v}+\left(\frac{v}{v_f}\frac{\partial v_f}{\partial v}-1\right)\right]. \quad \cdots\cdots (10)$$

2. Mean potential energy between two molecules at distance r.

Hence, we find that cage model is depended on the different estimations of equ. (4), mean pot. energy. Equ. (4) may be written down in following formula,

$$\bar{\phi}(r_{12})=\iint\phi(r_{12})F(r_1,\varphi_1,\theta_1)F(r_2,\varphi_2,\theta_2)dv_1dv_2 \Big/ \iint F(r_1,\varphi_1,\theta_1)F(r_2,\varphi_2,\theta_2)dv_1dv_2 \quad \cdots (11)$$

where r_{12} denotes the distance between two molecules,

(r, φ, θ) denotes the polar coordinate; (its origin is the point of rest sites of each molecule),

$\phi(r_{12})$ denotes the intermolecular pot. energy between two molecules at distance r_{12},

F denotes any function restricted its direction and distance of translation.

In the case of L-J. and D.,

$$\phi(r_{12}) = \phi_0 \left\{ \left(\frac{r_0}{r_{12}} \right)^{12} - 2 \left(\frac{r_0}{r_{12}} \right)^{6} \right\},$$

$$F(r_1, \phi_1, \theta_1) = \delta(r_1 - r),$$

$$F(r_2, \phi_2, \theta_2) = \delta(r_2),$$

where ϕ_0 denotes the minimum value of intermolecular potential and r_0 is the value of the distance r at which this minimum occurs.

In our case, we do not suppose that molecules can move in any direction freely, with same probability, but we suppose that they can move easily in one direction and uneasily in another direction. Namely, this assumption may shows it is non-spherical cell, but not spherical; or, we may think, the field, acted from surrounding cell to the cell, is non-spherical. The pot. energy, used by us, is alike one of Rowlinson and Sutton who correct the L-J. and D' s pot..

That correction is derived from oriantation, caused by non-spherical molecules and non-spherical pot. energy between two molecules. But, if we take the mean over all direction, this value of orientation becomes only a constant value, so the numerical correction, in the coefficient of the L-J. and D' s pot. answers the purpose.

Now, we suppose, molecule is spheroid, hence the potential is given by following formula;

$$\phi(r_1) = \frac{1}{\pi} \int_0^{\pi} \phi(r, \varphi) d\varphi,$$

where $\phi(r_{12}, \varphi) = \phi_0 \left\{ \left(\frac{r_0}{r_{12}\sqrt{1+\delta \sin^2\varphi}} \right)^{12} - 2 \left(\frac{r_0}{r_{12}\sqrt{1+\delta \sin^2\varphi}} \right)^{6} \right\},$

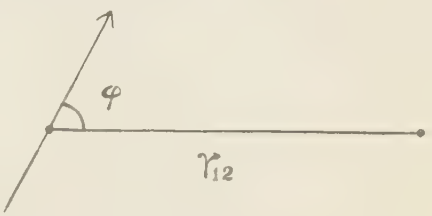

Fig. 1

φ is the angle between major axis of molecule and line connected with two molecules.

δ is defined by three major axis $a, a(1+\delta), a(1+\delta)$.

In order to estimate $\phi(r_{12})$, we expand $\phi(r_{12}, \varphi)$ in series of $\delta \sin^2\varphi$.

$$\phi(r_{12}, \varphi) = \phi_0 \left\{ \left(\frac{r_0}{r_{12}} \right)^{12} \sum_{n=0}^{\infty} a_n \delta^n \sin^{2n}\varphi - 2 \left(\frac{r_0}{r_{12}} \right)^{6} \sum_{n=0}^{\infty} b_n \delta^n \sin^{2n}\varphi \right\}.$$

Then, $\phi(r_{12})$ is given by

$$\phi(r_{12})=\phi_0\left\{\left(\frac{r_0}{r_{12}}\right)^{12}A_6-2\left(\frac{r_0}{r_{12}}\right)^{6}A_3\right\}, \quad \cdots\cdots (12)$$

where

$$A_\mu=\sum_{n=0}^{\infty}(-1)^n\frac{(\mu)_n}{n!}\frac{(2n-1)!!}{(2n)!!}\delta_n,$$

$$(2n-1)!!=1\cdot3\cdot5\cdots\cdots(2n-1),$$

$$(2n)!!=2\cdot4\cdot6\cdots\cdots(2n),$$

$$(\mu)_n=\mu(\mu+1)\cdots\cdots(\mu+n-1)=\frac{\Gamma(\mu+n)}{\Gamma(\mu)},$$

$\Gamma(m)=(m-1)!$ is the Γ function.

3. Calculation of the meam pot. $\overline{\phi(r_{12})}$.

In our model,

$$\overline{\phi(r_{12})}=\frac{\int\cdots\int\phi(r_{12})F_1\prod_{1,2}r_i^2\sin\theta_i d\theta_i d\varphi_i d\Theta_i d\Phi_i}{\int\cdots\int F_1\prod r_i^2\sin\theta_i d\theta_i d\varphi_i d\Theta_i d\Phi_i}. \quad \cdots\cdots (13)$$

Here, if we let the angles of polar coordinate of the major axis of the cell, measured out of the x, y, z-axis, denete (Φ, Θ), and let the angles of polar coordinate of the molecule, measured out of the major axis of the cell (r, φ, θ). Where

$$\phi(r_{12})=\phi_0\left\{A_6\left(\frac{r_0}{r_{12}}\right)^{12}-2A_3\left(\frac{r_0}{r_{12}}\right)^{6}\right\},$$

$$F_1=\exp\cdot-Ar^2\{a_{11}\sin^2\eta\cos^2(\Theta+\xi)+a_{22}\sin^2\eta\sin^2(\Theta+\xi)+a_{33}\cos^2\eta$$
$$+2a_{12}\sin^2\eta\sin(\Theta+\xi)\cos(\Theta+\xi)+2a_{23}\sin\eta\cos\eta\sin(\Theta+\xi)$$
$$+2a_{31}\sin\eta\cos(\Theta+\xi)\},$$

$$a_{11}=a\cos^2\Theta\sin^2\Phi+b\sin\Theta^2+c\cos^2\Theta\cos^2\Phi,$$

$$a_{22}=a\sin^2\Theta\sin^2\Phi+b\cos^2\Theta+c\sin^2\Theta\cos^2\Phi,$$

$$a_{33}=a\cos^2\Phi+c\sin^2\Phi.$$

$$a_{12}=a\sin\Theta\cos\Theta\sin^2\Phi-b\sin\Theta\cos\Theta+c\sin\Theta\cos\Theta\cos^2\Phi,$$

$$a_{23}=a\sin\Theta\sin\Phi\cos\Phi-c\sin\Theta\sin\Phi\cos\Phi,$$

$$a_{31}=a\cos\Theta\sin\Phi\mathrm{sco}\Phi-c\cos\Theta\sin\Phi\cos\Phi,$$

$$r_{12}^2=a^2+r^2-2ar\cos\chi,$$

$$\cos\chi=\sin\eta\sin(\Theta+\xi).$$

$$\cos\eta=\cos\Phi\cos\varphi+\sin\Phi\sin\varphi\cos\left(\frac{\pi}{2}-\theta\right),$$

$$\cos\xi=\frac{\cos\varphi-\cos\eta\cos\Phi}{\sin\eta\sin\Phi}$$

(We shall show the way of derivation of these equations in App. 1.)

We see that it may be impossible to perform the computation of these equations directly.

We perform this computation by the following approximation.

$$\overline{\phi(r_{12})} = \frac{1}{3}\{\overline{\phi_x(r_{12})} + \overline{\phi_y(r_{12})} + \overline{\phi_z(r_{12})}\}, \quad \cdots\cdots\cdots\cdots (14)$$

where $\bar{\phi}_x$, $\bar{\phi}_y$ and $\bar{\phi}_z$ represent the mean pot. energy when the rotational axis lies in the direction of x, y and z axis respectively. Such an approximetion is the way used frequently. The computation becomes very simple.

$$F_x = F_y = F_z = e^{-\gamma r^2(1+\Delta \sin^2\alpha)},$$

where α denotes the angle measured from the rotational axis.

When the rotational axis lies in the x or z axis, the equation replaced x with z sets the same result.

$$r_{12}^2 = a^2 + r^2 - 2ar\sin\alpha\sin\beta.$$

In the y axis lies,

$$r_{12}^2 = a^2 + r^2 - 2ar\cos\alpha,$$

where α and β are shown in Figs. 3 and 4.

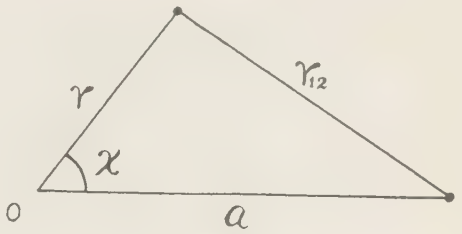

Fig. 2

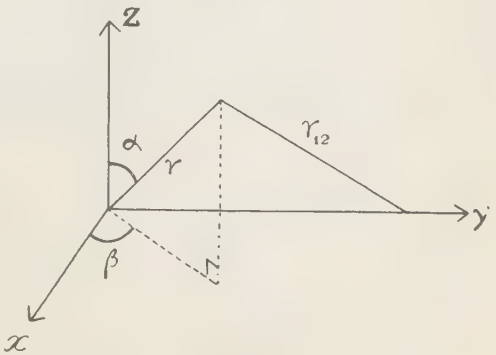

Fig. 3

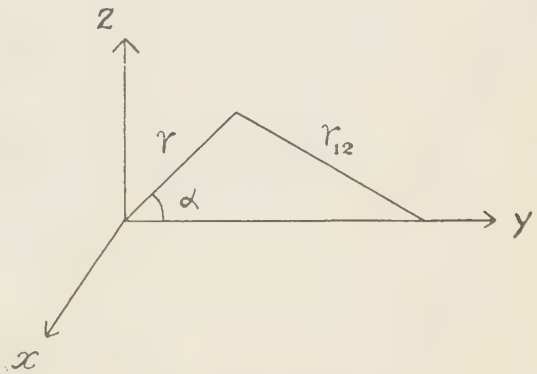

Fig. 4

4. Expansion of r_{12}^{-n} in series

As we need the computation of r_{12}^{-12} and r_{12}^{-6} in $\phi(r_{12})$, we show its expansion.

$$r_{12}^2 = a^2 - 2ar\cos\chi + r^2 = a^2\left\{1 - 2\left(\frac{r}{a}\right)\cos\chi + \left(\frac{r}{a}\right)^2\right\},$$

$$A_6\left(\frac{r_0}{r_{12}}\right)^{12}-2A_3\left(\frac{r_0}{r_{12}}\right)^6$$

$$=A_6\left(\frac{r_0}{a}\right)^{12}\sum_{n=0}^{\infty}C_n^6(t)\left(\frac{r}{a}\right)^n-2A_3\left(\frac{r_0}{a}\right)^6\sum_{n=0}^{\infty}C_n^3(t)\left(\frac{r}{a}\right)^n,$$

wehre $t=\cos\chi$. and $C_n^\nu(t)$ is the Gegenbauer's function. (See App. 2)

$$C_n^\nu(t)=\frac{\Gamma(n+2\nu)}{n!\,\Gamma(2\nu)}\cdot{}_2F_1\left(n+2\nu,-n;\nu+\frac{1}{2};\frac{1-t}{2}\right),$$

where $\Gamma(x)$ is the Γ-function, $(\alpha)_k=\alpha(\alpha+1)\cdots\cdots(\alpha+k-1)=\Gamma(\alpha+k)/\Gamma(\alpha)$, and ${}_2F_1\left(n+2\nu,-n;\nu+\frac{1}{2};\frac{1-t}{2}\right)$ is the hyper-geometric function.

(Especially, $C_n^{\frac{1}{2}}(t)$ becomes the Legendre function.) From this formula, we can introduce its expansion easily.

$$A_6\left(\frac{r_0}{r_{12}}\right)^{12}-2A_3\left(\frac{r_0}{r_{12}}\right)^6$$

$$=A_6\left(\frac{r_0}{a}\right)^{12}\left\{1+12t\left(\frac{r}{a}\right)+6(-1+14t^2)\left(\frac{r}{a}\right)^2+28(-3t+16t^3)\left(\frac{r}{a}\right)^3+\cdots\cdots\right\}$$

$$-2A_3\left(\frac{r_0}{a}\right)^6\left\{1+6t\left(\frac{r}{a}\right)+3(-1+8t^2)\left(\frac{r}{a}\right)^2+8(-3t+10t^3)\left(\frac{r}{a}\right)^3+\cdots\cdots\right\}.$$

5. Free energy and equation of state

Using the above equations, we get

$$\phi(\overline{r_{12}})=\phi_0\left[\left\{A_6\left(\frac{r_0}{a}\right)^{12}-2A_3\left(\frac{r_0}{a}\right)^6\right\}+2\pi\left\{A_6\left(\frac{r_0}{a}\right)^{12}-2A_3\left(\frac{r_0}{a}\right)^6\right\}\frac{B}{D}\right.$$

$$\left.+8\left\{7A_6\left(\frac{r_0}{a}\right)^{12}-4A_3\left(\frac{r_0}{a}\right)^6\right\}\frac{C}{D}-3\left\{A_6\left(\frac{r_0}{a}\right)^{12}-A_3\left(\frac{r_0}{a}\right)^6\right\}\frac{\left(\frac{r}{a}\right)^2}{D}+\cdots\cdots\right],$$

where

$$B=\sum_{n=1}^{\infty}(-1)^{n-1}\frac{(2n+1)!!}{(2n+2)!!}\frac{(\gamma\triangle)^{n-1}}{(n-1)!}\left(\frac{r}{a}\right)^{2n-1},$$

$$C=\left(\frac{r}{a}\right)B,$$

$$D=\sum_{n=1}^{\infty}(-1)^{n-1}\frac{(2n-1)!!}{(2n)!!}\frac{(\gamma\triangle)^{n-1}}{(n-1)!}\left(\frac{r}{a}\right)^{2n-2}.$$

Put this into equ. (5) and $y=\frac{r^2}{a_0}$, so free volume v_f is

$$v_f=\rho v\int_0^{\frac{1}{4}}y^{\frac{1}{2}}\,e^{-\{u(y)-u(0)\}/kT}\,dy,$$

where

$$u(y)-u(0)=z\phi_0\left[2\pi\left\{A_6\left(\frac{v_0}{v}\right)^4-A_3\left(\frac{v_0}{v}\right)^2\right\}\frac{B'}{D'}+8\left\{7A_6\left(\frac{v_0}{v}\right)^4-4A_3\left(\frac{v_0}{v}\right)^2\right\}\frac{C'}{D'}-3\left\{A_6\left(\frac{v_0}{v}\right)^4-A_3\left(\frac{v_0}{v}\right)^2\right\}\frac{y}{D}+\cdots\cdots\right],$$

B and C, D replaced by $y=\frac{r^2}{a^2}$ denote B' and C', D', respectively.

Then, Helmholtz's free energy is

$$\frac{F}{N}=-kT\ln\left(\frac{2\pi mkT}{h^2}\right)^{\frac{3}{2}}-kT\ln j(T)-kT+\frac{1}{2}z\phi_0\left\{A_6\left(\frac{v_0}{v}\right)^4-2.4A_3\left(\frac{v_0}{v}\right)^2\right\}-kT\ln v_f.$$

And the equation of state is

$$p=-\left(\frac{\partial F}{\partial v}\right)_T=z\phi_0\left\{2A_6\left(\frac{v_0}{v}\right)^4-2.4A_3\left(\frac{v_0}{v}\right)^2\right\}\frac{1}{v}+kT\frac{\partial}{\partial v}\ln v_f$$

$$=\frac{kT}{v}\left[1+\frac{2z\phi_0}{kT}\left\{A_6\left(\frac{v_0}{v}\right)^4-1.2A_3\left(\frac{v_0}{v}\right)^2\right\}+\frac{z\phi_0}{kT}\left[4\pi\left\{2A_6\left(\frac{v_0}{v}\right)^4-A_3\left(\frac{v_0}{v}\right)^2\right\}\left(\frac{B}{D}\right)\right.\right.$$

$$\left.\left.+32\left\{7A_6\left(\frac{v_0}{v}\right)^4-2A_3\left(\frac{v_0}{v}\right)^2\right\}\left(\frac{C}{D}\right)-6\left\{2A_6\left(\frac{v_0}{v}\right)^4-A_3\left(\frac{v_0}{v}\right)^2\right\}\left(\frac{y}{D}\right)+\cdots\cdots\right]\right],$$

where

$$\left(\frac{\overline{B}}{D}\right)=\int_0^{\frac{1}{4}}y^{\frac{1}{2}}\frac{B}{D}e^{-\{u(y)-u(0)\}/kT}dy\Big/\int_0^{\frac{1}{4}}y^{\frac{1}{2}}e^{-\{u(y)-u(0)\}/kT}dy,$$

$$\left(\frac{\overline{C}}{D}\right)=\int_0^{\frac{1}{4}}y^{\frac{1}{2}}\frac{C}{D}e^{-\{u(y)-u(0)\}/kT}dy\Big/\int_0^{\frac{1}{4}}y^{\frac{1}{2}}e^{-\{u(y)-u(0)\}/kT}dy,$$

$$\left(\frac{\overline{y}}{D}\right)=\int_0^{\frac{1}{4}}y^{\frac{1}{2}}\frac{y}{D}e^{-\{u(y)-u(0)\}/kT}dy\Big/\int_0^{\frac{1}{4}}y^{\frac{1}{2}}e^{-\{u(y)-u(0)\}/kT}dy.$$

When $\triangle$ is small, if we neglect the 2nd and higher term than 2, Helmholtz's free energy and the equation of state become

$$\frac{F}{N}-\frac{F_0}{N}=\cdots\left[\frac{3}{2}z\phi\left\{\frac{1}{2}\left(\frac{v_0}{v}\right)^4-2.4\left(\frac{v_0}{v}\right)^2\right\}\right],$$

$$p-p_0=\cdots\left[\frac{2z\phi}{vkT}\left\{\left(\frac{v_0}{v}\right)^4-2.4\left(\frac{v_0}{v}\right)^2\right\}\right],$$

where F_0 and p_0 show the values of the L-J. and D., respectively.

The author wishes to express his sincere thanks to the member of Busseiron Group of Kumamoto University, especially Mr. K. Kaminishi, for their useful discussions given to this work.

References

Lennard-Jones, J. E, & Devonshire, A. F, Proc. Roy. Soc. A. 163 (1837) 53.
165 (1938) 1.
Rowlinson, J. S. & Sutton, J. R, Proc Roy. Soc. A. 229 (1955) 271.
Oomori & Ono. Chemical Physics. (Kyoritu Press) p. 385. (in Japanese)
Harasima. Theory of Liquid State. (Iwanami Press) p. 40. (in Japanese)

Appendices

[App. 1]

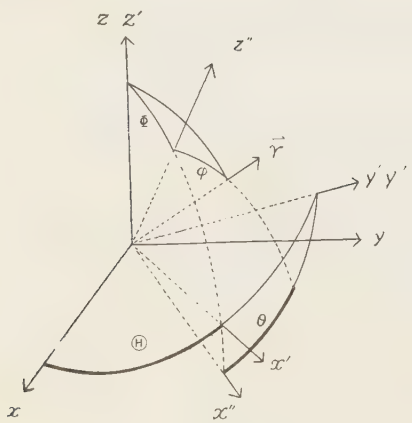

Fig. A1

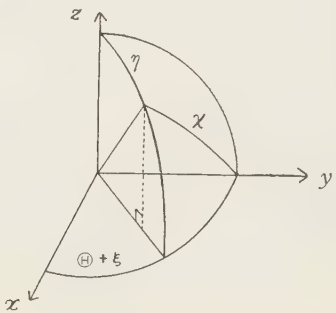

Fig. A2

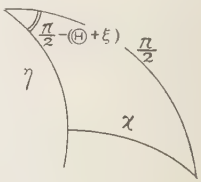

Fig. A3

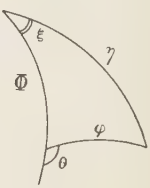

Fig. A4

By the theorems of spherical trigonometry,

$$\cos\eta = \cos\Phi\cos\varphi + \sin\Phi\sin\varphi\cos\left(\frac{\pi}{2}-\theta\right),$$

and

$$\cos\xi = \frac{\cos\varphi - \cos\eta\cos\Phi}{\sin\eta\sin\Phi}.$$

Then $\dot{r}(x, y, z)$ in cartesian coord. is $\dot{r}(r, \eta, \Theta+\xi)$ in polar coord..

By the translations of axis of coordinate (rotation), first by rotating around z-axis by angle Θ,

$$\begin{cases} x' = x\cos\Theta + y\sin\Theta, \\ y' = -x\sin\Theta + y\cos\Theta, \\ z' = z, \end{cases}$$

next by rotating around y'-axis by angle Φ,

$$\begin{cases} x'' = z'\cos\Phi + x'\sin\Phi, \\ y'' = y', \\ z'' = -z'\sin\Phi + x'\cos\Phi. \end{cases}$$

Then,

$$\begin{cases} x'' = x\cos\Theta\sin\Phi + y\sin\Theta\sin\Phi + z\cos\Phi, \\ y'' = -x\sin\Theta + y\cos\Theta, \\ z'' = x\cos\Theta\cos\Phi + y\sin\Theta\cos\Phi - z\sin\Phi. \end{cases}$$

Hence,

$$\begin{aligned} ax''^2 + by''^2 + cz''^2 &= (a\cos^2\Theta\sin^2\Phi + b\sin^2\Theta + c\cos^2\Theta\cos^2\Phi)x^2 \\ &\quad + (a\sin^2\Theta\sin^2\Phi + b\cos^2\Theta + c\sin^2\Theta\cos^2\Phi)y^2 \\ &\quad + (a\cos^2\Phi + c\sin^2\Phi)z^2 \\ &\quad + 2(a\sin\Theta\cos\Theta\sin^2\Phi - b\sin\Theta\cos\Theta + c\sin\Theta\cos\Theta\cos^2\Phi)xy \\ &\quad + 2(a\sin\Theta\sin\Phi\cos\Phi - c\sin\Theta\sin\Phi\cos\Phi)yz \\ &\quad + 2(a\cos\Theta\sin\Phi\cos\Phi - c\cos\Theta\sin\Phi\cos\Phi)zx. \end{aligned}$$

By the theorems of spherical trigonometry,

$$\cos\chi = \sin\eta\sin(\Theta + \xi).$$

[App. 2]

The Gegenbauer's function, $C_n^\nu(t)$, is defined by

$$(1-2\alpha t+\alpha^2)^{-\nu} = \sum_{n=0}^{\infty} C_n^\nu(t)\alpha^n.$$

$C_n^\nu(t)$ is combimed with the hyper-geometrycal function ${}_2F_1$ as follow,

$$C_n^\nu(t) = \frac{\Gamma(n+2\nu)}{n!\Gamma(2\nu)} \cdot {}_2F_1\left(n+2\nu, -n; \nu+\frac{1}{2}; \frac{1-t}{2}\right),$$

where ${}_2F_1$ is given by

$${}_2F_1\left(n+2\nu, -n; \nu+\frac{1}{2}; \frac{1-t}{2}\right) = \sum_{n=0}^{\infty} \frac{(n+2\nu)_k(-n)_k}{\left(\nu+\frac{1}{2}\right)_k} \cdot \frac{1}{k!}\left(\frac{1-t}{2}\right)^k.$$

Table of $C_n^\nu(t)$

$$\begin{aligned} C_0^6 &= 1 & C_0^3 &= 1 \\ C_1^6 &= 12t & C_1^3 &= 6t \\ C_2^6 &= 6(-1+14t^2) & C_2^3 &= 3(-1+8t^2) \\ C_3^6 &= 28(-3t+16t^3) & C_3^3 &= 8(-3t+10t^3) \\ C_4^6 &= 21(1-32t^2+96t^4) & C_4^3 &= 6(1-20t^2+40t^4) \\ C_5^6 &= 336(t-12t^3+24t^5) & C_5^3 &= 18(5t-40t^3+56t^5) \end{aligned}$$

THE PRECIPITATION IN THE ASO CRATER BASIN AND ITS EFFECT TO THE WATER-LEVEL OF THE SHIRAKAWA (PART 1)

THE PRECIPITATION IN ASO VALLEY AND THE WATER-LEVEL AT UCHINOMAKI

Tosisato MUROTA

(Received April 30, 1957)

Abstract

This is a study on the relation between the precipitation and the water-level at Uchinomaki which stands by the Kurokawa (a branch of the Shirakawa), as a part of a study on the flood-prediction of the Shirakawa. Introducing an idea which the writer calls "equi-run-off time line", he proposes a method of the flood-prediction that may be applicable to some sort of rivers.

1. The Drainage-basin of the Shirakawa

The Kurokawa is running inside the Aso-valley which lies in the north side of Aso central cones, having catchment area about *195 km²*, and the upper part of the Shirakawa is running inside the Nango-valley which lies in the south side of Aso central cones, having catchment area about *165 km²*. These two rivers join at Toshita which is situated at the west border of Aso crater atrio, and flows through Tateno-ravine of Aso old crater wall and flows into Shimabara-bay running through the Plain of Kumamoto from east to west[1].

2. Observed Data of Precipitation and Water-level at Uchinomaki

In the previous paper the writer reported about the diurnal variation of the water-level on no-rainy days, comparing and examining the records of water-level at the two spots: Uchinomaki and Matoishi both stand by the Kurokawa[2].

In the present paper, as a part of a study on the flood-prediction of the Shirakawa, the writer will study about the relation between the precipitation and the change of water-level at Uchinomaki. The records of water-level at Uchinomaki (see Table 1) tell us that when precipitation amounts to about *3~5 mm* the water-level begins to rise, and viewed from the flood phenomenal standpoint it is proper to study the case that daily amount of precipitation is more than *50 mm*. For comparison and contrast we will treat not only the case where daily amount of precipitation is more than *50 mm*, but also the case daily amount is less than *50 mm*. The data of hourly precipitation W *mm/hour* and the water-level H *cm* at every hour at Uchinomaki, which we will make use of for our discussion, are as given in Table 1 (at the end of this paper).

3. Time of the Highest Water-level

From the data in Table 1, we first obtain the following values:

the begining time and the end time of continuous precipitation (every hourly amount $\geqq$ *1 mm/hour*), the duration of the continuous precipitation t_r hours, the total amount of the continuous precipitation W *mm*, its hourly mean W/t_r *mm/hour*, the maximum hourly precipitation during t_r hours W_m *mm/hour*, its time t'_m, the time when water-level begins to rise t^h, the water-levl at t^h H *cm*, the highest water-levl H' *cm*, its time t'^h, the amount of the rise of water-level $(H'-H)$ *cm*, time-lag $(t'-t_m)$ hours (from the time of the maximum hourly precipitation to the time of the highest water-level), the amount of the rise of water-level per hour $\frac{H'-H}{t'-t}\ \frac{cm}{hour}$, the same per unit precipitation $\frac{H'-H}{W}\ \frac{cm}{mm}$, three hours precipitation before the maximum hourly precipitation $(W)_{-3}$ *mm* and the same after the maximum hourly precipitation $(W)_{+3}$ *mm*. And then the results are classified into two classes for $W \geqq 40$ *mm* or $W_m \geqq 15$ *mm* and for not so. (see Fig. 1)

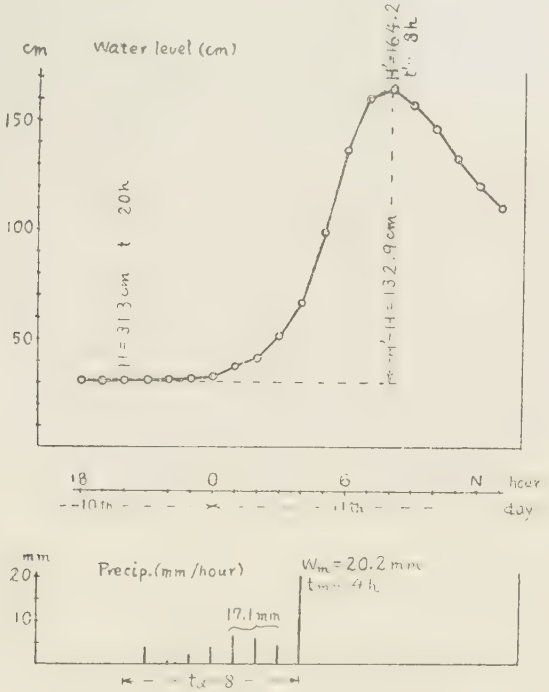

Fig. 1. Water-level and Precipitation on Jan. 10~11, 1947

The former is given in Table 2.1 and the latter in Table 2.2.

Table 2.1. ($W \geqq 40mm$ or $W_m \geqq 15mm$)

Year	Month Day	Hour from-to	t_d	W	$\frac{W}{t_d}$	W_m	t_m	H	t	H'	t'	$H'-H$	$t'-t_m$	$\frac{H'-H}{t'-t}$	$\frac{H'-H}{W}$	W_{-3}	W_{-6}
		h h					h		h		h						
1944	2.12	10~24	14	53.3	3.8	9.0	18	31.4	10	141.0	23	109.6	5	8.4		17.2	7.1
	4. 7	6~19	13	83.9	6.5	15.6	17	27.8	9	237.4	20	209.6	3	19.1	2.5	25.0	9.2
	5. 9	12~21	9	94.8	10.5	32.6	20	28.7	12	388.0	24	359.3	4	29.9	3.8	33.0	19.0
	5.10	7~13	6	72.0	12.0	32.2	10	340.7	9	394.0	14	53.3	4	10.7	0.7	12.4	27.4
	5.10~11	22~ 5	7	57.6	8.2	20.4	24	373.8	24	406.0	8	32.2	8	4.0	0.6	11.0	20.4
	6. 4	3~18	15	107.9	7.2	38.2	7	135.4	4	350.0	11	214.6	4	30.7		23.5	17.6
	7.21	5~17	12	48.0	4.0	13.6	14	104.4	5	249.2	20	144.8	6	9.7	3.0	8.2	13.7
	8.8~9	14~ 3	13	78.8	6.1	20.7	21	72.3	14	326.0	1	253.7	4	23.1		11.5	14.5
1946	2.24~25	14~23	9	40.9	4.5	12.7	19	18.9	14	104.7	1	85.8	6	7.8	2.1	14.1	9.8
	3.18~19	16~ 1	9	41.6	4.6	18.5	19	58.4	18	190.3	2	131.9	7	16.5	3.2	4.9	8.5
	4. 4	0~ 8	8	53.0	6.6	11.2	4	17.1	0	166.8	9	149.7	5	16.6	2.8	21.7	17.6
	4. 5	14~22	8	57.0	7.1	12.0	18	18.7	14	230.6	23	211.9	5	26.5	3.7	15.2	22.0
	4.24	14~21	7	75.8	10.8	34.4	19	49.1	15	323.0	23	273.9	4	34.2	3.6	23.6	16.3
	5.12	9~23	14	160.9	11.5	22.0	20	36.0	10	420.0	23	384.0	3	29.5	2.4	65.0	12.0
1947	1.10~11	20~ 4	8	48.1	6.0	20.2	4	31.3	20	164.2	8	132.9	4	11.1	2.8	17.1	0.0
	4.1~2	21~ 1	4	36.2	9.1	19.1	22	42.8	21	104.6	3	61.8	5	10.3	1.7	0.0	17.1
	5.2~3	7~ 1	18	50.7	2.8	7.3	21	49.4	7	156.0	3	106.6	6	5.3	2.1	12.4	7.1
	5.24~25	17~10	17	45.0	2.6	5.0	2	48.2	17	141.8	11	93.6	9	5.2	2.1	6.1	9.0
	6.23~24	20~11	15	164.8	11.0	22.9	6	59.5	21	430.0	12	370.5	6	24.7	2.2		
	6.24~25	14~23	9	65.7	7.3	17.0	16	422.0	14	449.5	24	27.5	7	2.8	0.4	7.0	30.8
	6.27	3~13	10	46.1	4.6	8.7	10	120.1	3	211.2	14	91.1	4	8.3	2.0	23.0	10.3
	6.28	6~16	10	51.1	5.1	7.8	13			134.0	18		5			16.9	10.8
	7. 9	4~16	12	47.5	4.0	12.3	14	12.0	4	194.3	19	182.3	5	12.2	3.8	2.9	9.1
	7.16	13~14	1	15.4	15.4	15.4	14	23.0	13	151.7	18	128.7	4	25.7	8.4	0.0	1.2
	7.18	12~18	6	35.4	5.9	20.6	14	33.8	13	161.6	18	127.8	4	25.6	3.6	6.7	6.9
	7.19	6~13	7	47.1	6.7	16.6	10			217.2	15		5			13.4	17.1
	8.18	16~17	1	18.6	18.6	18.6	17	37.0	16	54.5	21	17.5	4			0.0	0.0
1948	3.13~14	7 11 (13th)(14th)	28	62.2	2.2			39.7	7 (13th)	109.5	11 (14th)	69.8		2.5	1.1		
	6.13~14	14~16 (13th)(14th)	26	103.6	4.0	11.4	14 (14th)	34.0	14 (13th)	150.3	20 (14th)	116.3	6	3.9	1.1	22.0	11.7
	7. 3	13~20	7	83.3	11.9	56.2	17	124.8	13	353.4	22	228.6	5	25.2	2.7	15.5	11.6
	7. 8	0~ 8	8	46.9	5.9	16.0	5	49.8	3	90.5	9	40.7	4	6.8	0.9	19.2	7.7
	7. 8	11~17	6	44.6	7.4	20.2	13	61.3	11	289.2	18	227.9	5	32.6	5.1	8.5	13.7
	7.16	19~20	1	15.7	15.7	15.7	20	128.4	19	146.3	23~24	17.9	3~4	4.5	1.1	0.3	0.4
	7.22	10~15	5	24.5	4.9	15.0	11	108.7	10	176.3	18	67.6	7	8.5	2.8	0.2	5.8
	8. 5	17~19	2	20.4	10.2	19.1	19	74.3	17	124.0	22	49.7	3	9.9	2.4	1.3	0.0
	8.25~26	16~12	20	69.7	3.5	14.2	7	55.0	16	159.6	12	104.6	5	5.2	1.5	19.7	9.2
	8.27~28	14~ 7	17	93.4	5.5	19.8	23	72.5	14	165.0	5	92.5	6	6.2			
	9.23	16~18	2	22.0	11.0	20.1	17	64.4	16	129.0	21	64.6	4	12.9	2.9	0.0	1.9
	9.26	19~20	1	16.7	16.7	16.7	20	56.0	19	112.4	24	56.4	4	11.3	3.4	0.8	0.1
	12 .6	5~16	11	40.7	3.7	7.3	14	31.7	5	92.2	18	60.5	4	4.7	1.5	18.5	3.3
	12.20~21	15~ 3	12	42.1	3.5	7.0	2	39.4	15	112.2	6	72.8	4	4.9	1.7	15.8	4.4
1949	3.10	10~16	6	50.0	8.3	19.5	14	40.0	10	201.7	18	161.7	4	20.2	3.2	20.3	10.2
	4.26	11~24	13	78.5	6.0	12.0	15	41.0	11	191.4	22	150.4	7	13.7		15.5	30.1
	5.19~20	14~ 6	16	127.2	8.0	18.4	1	53.8	14	283.2	9	229.4	8	12.1	1.8	28.9	20.0
	5.22~23	18~16	22	126.2	5.7	14.6	6	59.0	19	292.5	13	233.5	7	13.0		18.7	12.1
	5.27~28	23~ 9	10	46.2	4.6	8.8	6	61.6	23	177.0	12	115.4	6	8.9	2.5	10.6	16.8
	6.6~7	21~15	18	64.0	3.6	10.8	14	55.9	21	174.5	18	118.6	4	5·6	1.9	8.6	8.0
	6.15~16	22~11	13	70.9	5.5	12.0	8	53.3	22	237.2	11	183.9	3	14.1	2.6	27.4	11.5
	6.18~19	9~11 (18th)(19th)	26	151.8	5.8	10.9	8 (19th)	73.3	9 (18th)	350.6	12 (19th)	277.3	4	10.3	1.8	19.8	15.0
	8. 1	16~20	4	32.3	8.1	19.5	17	106.3	16	168.5	21	62.2	4	12.4	1.9	0.0	12.8
	8.13	13~15	2	38.2	19.1	23.7	14	129.1	13	173.3	18~19	44.2	3~4	8.8	1.2	0.0	14.5
	10. 5	6~20	14	65.0	4.6	8.0	14	181.7	7	284.2	20	102.5	6	7.9	1.6	17.7	12.6
	11. 4	3~19	16	68.9	4.3	10.0	14	108.8	3	189.8	20	81.0	6	4.8	1.2	22.0	9.7

Table 2.2. ($W < 40mm$, $W_m < 15mm$)

Year	Month Day	Hour from-to	t_d	W	$\frac{W}{t_d}$	W_m	t_m	H	t	H'	t'	$H'-H$	$t'-t_m$	$\frac{H'-H}{t'-t}$	$\frac{H-H}{W}$
		h h					h		h		h				
1945	12.21~22	23~ 4	5	8.4	1.7	2.6	3			43.8	9		6		
"	12.22	11~22	11	38.0	3.5	5.4	17	39.1	13	144.0	24	104.9	7	9.5	2.8
1946	2. 5~ 6	14~ 3	13	28.9	2.2	4.2	15	12.9	14	71.2	8	58.3	17	3.2	2.0
	2.28	12~21	9	17.0	1.9	2.9	17	16.4	13	56.0	24	39.6	7	3.6	2.3
	3. 2	6~22	16	32.2	2.0	4.0	19	14.0	7	76.3	23	62.3	4	3.9	1.9
	3. 6	5~10	5	13.4	2.7	4.2	8	14.0	6	45.0	14	31.0	6	3.9	2.3
	3.10	9~13	4	28.7	7.2	9.6	12	19.0	9	56.5	19	37.5	7	3.8	1.3
	3.14					1.5	19	19.2	19	40.4	3		8		
	3.18	3~ 8	5	20.0	4.0	8.9	7	29.7	3	118.0	11	88.3	4	11.0	4.
	3.23	7~12	5	23.3	4.7	7.7	11	36.8	7	94.3	14	57.5	3	8.2	2.5
	3.28~29	18~ 1	7	29.5	4.2	8.4	22	16.7	18	108.4	3	91.7	5	10.2	3.1
1947	1.17	14~18	4	16.7	4.2	7.0	17	30.6	14	44.9	20	14.3	3	2.4	0.9
	1.24	8~12	4	9.2	2.3	3.0	11			42.8	20		9		
	2.14	1~14	13	32.0	2.5	5.9	13	43.6	1	67.6	20	24.0	7	1.3	0.8
	4.20~21	21~ 1	4	11.6	2.9	4.9	23	51.3	21	61.5	6	10.2	7	1.1	0.9
	4.27~28	17~ 1	8	28.3	3.5	5.0	24	51.1	17	81.9	6	30.8	6	2.4	1.1
	6. 6~ 7	21~23	2	10.9	5.5	9.9	23	55.6	21	63.8	11	8.2	12	0.6	0.8
	6.10	0~ 9	9	32.0	3.6	8.0	9	52.1	0	133.9	15	81.8	6	5.5	2.6
	6.14~15	17~ 8	15	30.0	2.0	3.9	21	52.3	17	128.2	14	75.9	17	3.6	2.5
	6.30	17~22	5	39.5	7.9	13.8	20			240.5	24		4		
	8.19	14~15	1	7.7	7.7	7.7	15	33.4	14	40.0	22	6.6	7	0.8	0.9
	8.24	14~16	2	19.8	9.9	13.1	15	32.3	13	97.5	18	65.2	3	13.0	3.3
	9. 2	11~14	3	12.2	4.1	8.8	14	35.2	11	58.8	18	23.6	4	3.4	1.9
	9. 9	5~ 8	3	14.0	4.7	10.2	6	32.0	5	44.2	10	12.2	4	2.4	0.9
	9.11	18~20	2	12.6	6.3	10.2	19	38.1	18	50.0	24	11.9	5	2.0	0.9
	9.28~29	19~22	3	18.3	6.1	14.6	20	31.2	19	47.0	2	15.8	6	3.3	0.9
	10.27	13~17	4	12.9	3.2	6.2	15	26.7	13	32.0	20	5.3	5	0.8	0.4
	11.29	11~17	6	27.4	4.6	12.0	16	41.0	11	65.2	22	24.2	6	2.2	0.9
	12. 1	14~19	5	29.0	5.8	9.6	16	36.8	14	73.2	22	36.4	6	4.6	1.3
	12.27~28	17~ 3	10	32.5	3.3	6.4	21	42.0	17	104.4	4	62.4	7	5.7	1.9
1948	7.19~20	15~22	7	32.7	4.7	11.5	22	99.9	15	146.6	1	46.7	3	4.7	1.4
	9. 2	2~ 4	2	12.8	6.4	9.6	4	63.8	2	72.3	14	8.5	10	0.8	0.7
	9.10	14~17	3	17.5	5.8	11.1	15	58.4	14	63.8	20	5.4	5	0.9	0.3
	9.11	2~ 7	5	10.8	2.2	3.2	6	60.9	3	71.4	12	10.5	6	1.2	1.0
	9.11~12	17~23	6	19.1	3.2	6.2	20	65.3	18	89.6	1	24.3	5	3.5	1.3
	9.20	17~20	3	8.9	3.0	5.4	19	56.3	17	61.3	23	5.3	4	0.9	0.6
	9.23	5~12	7	16.8	2.4	7.6	8	35.7	5	64.0	14	8.3	6	0.9	0.5
	10. 9~10	22~ 3	5	25.7	5.1	8.3	24	51.0	22	94.3	6	43.3	6	5.4	1.7
	10.29~30	14~22	8	32.5	4.1	6.7	18	50.7	14	93.0	1	42.3	7	3.8	1.3
	11. 3	12~18	6	10.5	1.8	6.3	14	43.0	12	53.0	22	10.0	8	1.0	1.0
	12.24	9~13	4	22.8	5.7	11.8	12	40.2	9	84.5	17	44.3	5	5.5	1.
	12.25					4.4	6			60.2	13		7		

Year	Month Day	Hour from-to	t_d	W	$\frac{W}{t_d}$	W_m	t_m	H	t	H'	t'	$H'-H$	$t'-t_m$	$\frac{H'-H}{t'-t}$	$\frac{H'-H}{W}$
1948	12.25~26	h 18~22 h	4	17.0	4.3	7.0	h 21	57.0	h 19	92.8	h 1	35.8	4	6.0	2.1
	12.26~27					2.5	23 (26th)			68.1	9 (27th)		10		
1949	1.30	1~ 7	6	23.2	3.9	9.0	3	46.3	1	70.6	9	24.3	6	3.0	1.0
	2. 1	10~16	6	21.0	3.5	12.6	12	40.2	10	67.3	17	27.1	5	3.9	1.3
	2.11	16~20	4	20.2	5.1	7.2	18	44.9	16	68.7	24	23.8	6	3.0	1.2
	2.22	9~15	6	17.2	2.9	5.4	13	45.3	10	65.8	19	20.5	6	2.3	1.2
	2.23	2~ 8	6	12.9	2.2	3.5	5	60.0	3	83.7	13	23.7	8	2.4	1.8
	2.24~25	21~ 5	8	21.1	2.6	5.4	3	41.3	22	85.0	9	43.7	6	4.0	2.1
	3. 5	2~ 9	7	38.5	5.5	12.4	7	3.91	2	120.5	11	81.4	4	9.0	2.1
	3.13~14	20~ 2	6	34.3	5.7	12.5	23	41.3	21	145.8	2	104.5	3	20.9	3.0
	3.14~15	13~ 9	20	37.7	1.9	3.3	20	83.1	14	119.0	9	35.9	13	1.9	1.0
	3.17~18	19~23	4	12.2	3.1	5.0	20	58.0	20	74.7	3 (18th)	16.7	7	2.4	1.4
	4.23	3~15	12	21.9	1.8	5.1	8	44.0	3	61.2	19	17.2	11	1.1	0.8
	4.30	13~23	10	34.0	3.4	7.0	20	46.3	13	126.5	24	80.2	4	7.3	2.4
	5. 6	0~ 6	6	19.7	3.3	6.0	3	43.5	1	76.9	13	33.4	10	2.8	1.7
	5.12	5~18	13	34.9	2.7	10.0	18	44.0	5	96.1	22	52.1	4	3.1	1.5
	8.12~13	19~23	4	27.2	6.8	14.9	23	112.0	19	143.8	3	31.8	4	4.0	1.2
	8.22	4~11	7	34.2	4.9	8.3	8	135.1	5	170.6	11	35.5	3	5.9	1.0
	8.25	18~21	3	30.6	10.2	12.8	21	130.5	18	164.4	24	33.9	3	5.7	1.1
	8.27	16~21	5	14.2	2.8	5.0	19	134.7	17	151.7	24	17.0	5	2.4	1.2
	10. 3~ 4	17~ 1	8	15.0	1.9	3.5	21	130.0	17	143.7	2	13.7	5	1.5	0.9
	10. 4	10~21	11	30.6	2.8	7.4	16	132.5	11	202.0	23	69.5	7	5.8	2.3
	11. 8	10~20	10	27.2	2.7	5.0	16	116.0	10	148.3	23	32.3	7	2.5	1.2
	11.12	2~ 9	7	19.3	2.8	7.4	9	118.4	2	149.0	14	30.6	5	2.6	1.6
	12.10~11	15~24	9	1.65	1.8	4.0	22	106.5	15	117.9	5 (11th)	11.4	7	0.8	0.7
	12.20~21	14~23	9	32.6	3.6	7.4	15	109.3	14	165.0	1	55.7	10	5.1	1.7
	12.24	1~ 6	5	24.1	4.8	9.2	4	112.5	1	148.1	9	35.6	5	4.3	1.5
	12.30	12~19	7	16.8	1.0	5.7	15	112.9	12	132.8	21	19.9	6	2.2	1.2

Table 3 gives the frequency of $t'-t_m$ in Table 2.1 for two cases, viz., $W_m<15$ *mm/hour* and $W_m\geqq 15$ *mm/hour*, and also their total.

The frequency of $t'-t_m$ for $W_m\geqq 15$ is maximum when $t'-t_m$ is equal to four, it means

Table 3. Frequency of $t'-t_m$ for Table 2.1.

	$t'-t_m$ (hour)	3	4	5	6	7	8	9
Frequency	$W_m<15$	1	5	6	7	2	0	1
	$W_m\geqq 15$	3	16	4	2	2	3	
	total	4	21	10	9	4	3	1
	$(W)_{-3}>(W)_{+3}$	3		1	1		1	
	$(W)_{-3}<(W)_{+3}$			3		2	2	

that in the case of heavy rain ($\geqq 15$ *mm/hour*) the highest water-level appears mostly 4 hours after the time of heavy hourly rain. In regard to precipitation $\geqq 15$ *mm/hour* frequency of the case $(W_{-3}) > (W)_{+3}$ and $(W)_{-3} < (W)_{+3}$ is also given in Table 3, and we can recognize such a tendency that $t' - t_m \geqq 4$ according as $(W)_{-3} \geqq (W)_{+3}$.
In other words, as it should be, it is that the highest water-level appears early when the rainfall before the maximum hourly rainfall is much amount, and the highest water-level appears lately when the rainfall after the maximum hourly rainfall is much amount. Table 4 gives the frequency of $t' - t_m$ in Table 2.2. From this Table, we can see that the value of $t - t_m$ increases according as W_m decreases, in other words, the highest water-level appears later following the amount of the mauimum hourly rainfall becomes smaller.

Table 4. Frequency of $t' - t_m$ for Table 2.2.

	$t - t_m$ (hour)	3	4	5	6	7	8	9	10	11	12	13	17
Frequency	$W_m < 5$		1	1	3	4	2	1	1			1	2
	$5 \leqq W_m < 10$	3	5	6	10	9	1		3	1	1		
	$10 \leqq W_m < 15$	4	5	4	2								
	total	7	11	11	15	13	3	1	4	1	1	1	2

In general the precipitation in the catchment basin of a river may be divided into three parts, viz., run-off, seepage and evaporation, among which the first two, viz., the run-off and the seepage chiefly effect on the change of water-level of the river. But in the case of heavy rain, the run-off has great effect on the water-level of the river, in comparison with the seepage, consequently the rise of the river appears early, on the contrary the effect of the run-off decreases as the intensity of rain decreases and the rise of the river appears lately. This way of thinking will explain readily the fact previously described about the time of the highst water-level at Uchinomaki.

Now, to see the effect of the amount of rain on the waterlevel at Uchinomaki, the mean values of t_d, W, W/t_d, W_m and $(H' - H)/W$ in Table 2.1 and 2.2 are calculated respectively and given in Table 5. From this Table it is seen that, on an average, continuous rain during 8 hours results the rise of water-level at the rate of about *2 cm* per *1 mm* of precipitation.

Table 5.

t_d	W	$\frac{W}{t_d}$	W_m	$H' - H$	$\frac{H' - H}{W}$
8.0	38.6	5.4	11.6	76.4	1.9

Table 6.

	t_d	W	$\frac{W}{t_d}$	W_m	$H' - H$	$\frac{H' - H}{W}$
$W < 40$ $W_m < 15$	6.9	24.1	4.0	7.7	36.5	1.5
$W > 40$ $W_m < 15$	14.4	61.7	4.4	10.7	127.7	2.2
$W_m \geqq 15$	6.7	59.0	9.8	22.0	141.8	2.4

Next, classifying them according to the amount of rain, the mean values as shown in Table 6 are obtained. Using the results in Table 5 or 6, we can roughly estimate the amount of the rise of water-level due to precipitation.

4. Precipitation Effect and Coefficient of Precipitation Effect

The change of water-level of a river due to the run-off depends on various factors, among which the main factors are as followings:
(1) the configuration of the basin, (2) the nature of soil in the basin, (3) the state of the river, (4) amount of rain and its hourly distribution, (5) water-level of the river when it begins to rain, (6) the seasons, (7) the states of growth of plants in the basin and etc. But it is impossible to consider simultaneously the above-described factors.

For the present case treating the water-level at Uchinomaki, we study as follows. First, we consider the relation between the amount of precipitation and the change of the water-level at Uchinomaki in such a case as it rained heavily only one hour (precipitation $\geqq$*15 mm/hour*). For instanse, the amount of rain for $16^h\sim17^h$, 23rd, Sep-tember 1948 was *20.1 mm/hour* (see Fig. 2) and its data is given in Table 7:

where H_0 (*cm*): water-level at 17^h,

H_n (*cm*): water-level at $(17+n)^h$.

Table 7. Data on September 23~24, 1948

Time (h)	t_{-1} 16	t_0 17	t_1 18	t_2 19	t_3 20	t_4 21	t_5 22	t_6 23	t_7 0	t_8 1	t_9 2
H_n	H_{-1} 64.4	H_0 67.2	H_1 73.0	H_2 94.0	H_3 116.0	H_4 129.0	H_5 122.5	H_6 110.5	H_7 108.0	H_8 102.8	H_9 100.0
H_n-H_{n-1}		2.8	5.8	21.0	22.0	13.0	−6.5	−12.0	−2.5	−5.2	−2.8
$\frac{H_n-H_{n-1}}{H_4-H_{-1}}\times100$		4	9	33	34	20	−10	−19	−4	−8	−4

$H_4-H_{-1}=64.6$

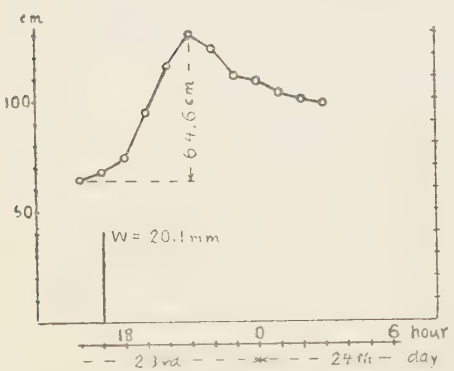

Fig. 2. Water-level and Precipitation on Sep. 23~24, 1948

In this example, the highest water-level is that at 21^h, i. e., $H_4=129$ (*cm*). Hourly rise of water-level H_n-H_{n-1} and its percentage to the total amount of rise of water-leve $H_4-H_{-1}=64.6$ (*cm*) are also given in Table 7. Similar calcuiation was performed for the similar cases where it rained heavily only one hour, namely, *18.6 mm* $16^h\sim17^h$ 18th Aug. 1947, *19.1 mm* $18^h\sim19^h$ 5th Aug. 1948 and *16.7 mm* $19^h\sim20^h$ 26th Sep. 1948. Using the result for the above four cases, the mean value of $\frac{H_n-H_{n-1}}{H_4-H_{-1}}\times100$ and the value $\sum_{N=0}^{N} H_n-H_{n-1}$ for $N=0, 1, 2, \cdots\cdots, 9, 10$ were calculated and are given in Table 8, and the latter is represented graphically in Fig. 3.

Table 8. Mean Value of $\frac{H_n-H_{n-1}}{H_1-H_{-1}}\times 100$ and $\sum \frac{H_n-H_{n-1}}{H_1-H_{-1}}\cdot 100$

Time (h)	t_{-1}	t_0	t_1	t_2	t_3	t_4	t_5	t_6	t_7	t_8	t_9	t_{10}
$\frac{H_n-H_{n-1}}{H_1-H_{-1}}\times 100$		10	12	22	36	20	−12	−16	−9	−6	−5	−2
$\sum \frac{H_n-H_{n-1}}{H_1-H_{-1}}\times 100$		10	22	44	80	100	88	72	63	57	52	50

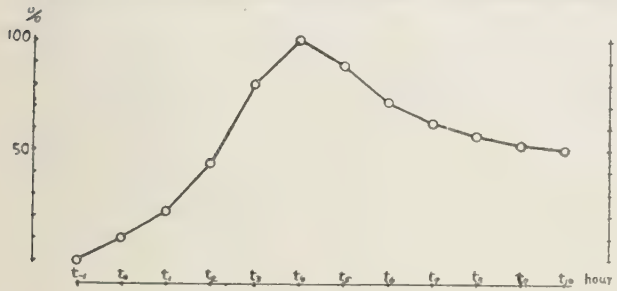

Fig. 3.

Let W_n: hourly rainfall at t_n^h (from t_{n-1}^h to t_n^h)

H_n: water-level at t_n^h,

then, if it rained heavily only one hour, $(\triangle H')_n=H_{n+4}-H_{n-1}$ should depend on W_n. So we may assume the following relation:

$$(\triangle H')_n=H_{n+4}-H_{n-1}=\alpha W_n \cdots (1)$$

where α unknown function.

Next, we consider such a case as we have continuous rain during several hours, and let the time, the precipitation and the water-level be as follows:

Time (h)	t_{-8}	t_{-7}	t_{-6}	t_{-5}	t_{-4}	t_{-3}	t_{-2}	t_{-1}	t_0	t_1	t_2	t_3	t_4
Precip.	W_{-8}	W_{-7}	W_{-6}	W_{-5}	W_{-4}	W_{-3}	W_{-2}	W_{-1}	W_0	W_1	W_2	W_3	W_4
Water-level	H_{-8}	H_{-7}	H_{-6}	H_{-5}	H_{-4}	H_{-3}	H_{-2}	H_{-1}	H_0	H_1	H_2	H_3	H_4

Assuming that the % in Table 8 can be applied to each amount of rainfall W_{-3} *1 mm hour* and taking the water-level H_0 at t_0^h as the base-level, we attempt to calculate the water-level H_1 at t_1^h. Then we have to sum up the % with respect to each rainfall during 4 hours from t_0^h to t_4^h as shown in Table 9, and the result and its ratio ($\times 10^{-2}$) are given in the last two columns in Table 9, neglecting small value ± 0.1 among the just-described ratio, we calculated the rise of water-level H_1-H_0 due to 10 hourly rainfalls W_{-5}, W_{-4}, W_{-3}, W_{-2}, W_{-1}, W_0, W_1, W_2 and W_3 by the equation (1) and the result is as follows:

$$H_1-H_0=\alpha(-0.2W_{-5}-0.4W_{-4}-0.4W_{-3}-0.2W_{-2}+0.3W_{-1}+0.7W_0+0.9W_1+0.8W_2+0.4W_3+0.2W_4) \cdots (2)$$

We will call the brackets term in the right side of the expression (2) "precipitation effect for t_4^h and denote it by "W_e". Then we obtain

$$H_1-H_0=\alpha W_e \cdots (3)$$

hence

$$\alpha=\frac{H_1-H_0}{W_e}=\frac{\triangle H}{W_e} \cdots (4)$$

We call α "coefficient of precipitation effect".

For an instance, the calculated value of W_e and α for the data on 3rd July, 1948 is given in Table 10. As the expression (1) and the ratio in the last column in Table 9 have been, in the first place, obtained from the case of precipitation ≥ 15 *mm hour*, there should be somewhat error in the calculation of W_e and α, because of including the case of precipitation <15 *mm/hour*.

Table 9.

Time / Precip	t_{-8}	t_{-7}	t_{-6}	t_{-5}	t_{-4}	t_{-3}	t_{-2}	t_{-1}	t_0	t_1	t_2	t_3	t_4	total	ditto ratio
W_{-8}	10	12	22	36	20	−12	−16	− 9	− 6	− 5	− 2			− 7	−0.1
W_{-7}		10	12	22	36	20	−12	−16	− 9	− 6	− 5	− 2		−13	−0.1
W_{-6}			10	12	22	36	20	−12	−16	− 9	− 6	− 5	− 2	−22	−0.2
W_{-5}				10	12	22	36	20	−12	−16	− 9	− 6	− 5	−36	−0.4
W_{-4}					10	12	22	36	20	−12	−16	− 9	− 6	−43	−0.4
W_{-3}						10	12	22	36	20	−12	−16	− 9	−17	−0.2
W_{-2}							10	12	22	36	20	−12	−16	28	0.3
W_{-1}								10	12	22	36	20	−12	66	0.7
W_0									10	12	22	36	20	90	0.9
W_1										10	12	22	36	80	0.8
W_2											10	12	22	44	0.4
W_3												10	12	22	0.2
W_4													10	10	0.1
water-level	H_{-8}	H_{-7}	H_{-6}	H_{-5}	H_{-4}	H_{-3}	H_{-2}	H_{-1}	H_0	H_1	H_2	H_3	H_4		

Table 10.

W_e and α for the data on 3rd July, 1948

Time (hour)	W (mm/hour)															
14	12.7	2.5	5.1	10.2	11.4	8.9	3.8	−2.5	−5.1	−5.1	−2.5					
15	2.1		0.4	0.8	1.7	1.9	1.5	0.6	−0.4	−0.8	−0.8	−0.4				
16	0.0															
17	56.2				11.2	22.5	45.0	50.6	39.3	16.9	−11.2	−22.5	−22.5	−11.2		
18	2.4					0.5	1.0	1.9	2.2	1.7	0.7	−0.5	−1.0	−1.0	−0.5	
19	4.0						0.8	1.6	3.2	3.6	2.8	1.2	−0.8	−1.6	−1.6	−0.8
20	5.2							1.0	2.1	4.2	4.7	3.6	1.6	−1.0	−2.1	−2.1	−1.0
W_e for t hour		2.5	5.5	11.0	24.3	33.8	52.1	53.2	41.3	20.5	−6.3	−18.6	····· W_e			
		15	16	17	18	19	20	21	22	23	24	1	····· hour			
water level (H)				234.3	248.2	303.0	343.7	350.2	353.4	353.5	346.8	332.2				
$H_t - H_{t-4}$								115.9	105.2	50.5	3.1	−18.0				
α								2.2	2.5	2.5	−0.5					

In order to check the validity of the expression (4), we will make a trial as follows. There are shown three examples of calculation of W_e in Table 11. In the first example, W_e and $H_t - H_{t-4}$ have the same sign, in this case if we leave the magnitude out of consideration, then we can foresee whether the water-level H_4 rises or falls compared with the water-level H_0. On the contrary, in the second example, although W_e becomes negative $H_t - H_{t-4}$ remains positive, and in the third example while W_e is positive $H_t - H_{t-4}$ becomes negative. In the last two cases, the foreseeing whether H_4 rises or falls compared with H_0 should fail. We denote the first case by $(W_e)_0$, the second case by $(W_e)_{-\varepsilon}$

Table 11.

April 24~25, 1946

Time (h)	W mm/hour	W_e	H_t	H_t-H_{t-4}	
15	1.5				
16	1.1				
17	12.1		51.3		
18	10.4		64.0		
19	**34.4**		109.0		
20	14.9		193.0		
21	1.4	36.6	284.0	232.7	
22		51.4	320.0	256.0	
23		53.6	323.0	214.0	
24	1.6	38.3	311.0	118.0	
1	3.1	14.7	292.2	8.2	
2		−10.0	289.3	−30.7	$(W_e)_0$

January 10~11, 1947

Time (h)	W mm/hour	W_e	H_t	H_t-H_{t-4}	
21	4.1				
22					
23	2.5				
24	3.7				
1	6.7				
2	5.6				
3	4.8				
4	**20.2**		67.6		
5			100.0		
6			137.4		
7		23.9	161.4		
8		19.5	164.2	96.6	
9		9.7	157.0	57.0	
10		−0.5	146.0	8.6	
11		−9.4	133.0	−28.4	$(W_e)_{-1}$

July 19, 1947

Time (h)	W mm/hour	W_e	H_t	H_t-H_{t-1}	
7	2.2				
8					
9	10.7		100.0		
10	**16.6**		110.2		
11	4.8		139.3		
12	9.5		179.8		
13	2.8	27.4	201.8	101.8	
14		30.2	213.9	103.7	
15		26.9	217.2	77.9	
16		16.2	203.8	24.0	
17		2.6	192.9	− 8.9	
18		−7.0	183.1	−30.8	$(W_e)_{+1}$

where the suffix $-t$ means that H_t-H_{t-4} remains positive during t hours after W_e has become negative, and the third case by $(W_e)_{+t}$ where H_t-H_{t-4} becomes negative t hours before W_e becomes negative. For continuous precipitation, including maximum hourly rainfall $\geqq 15$ *mm/hour*, the values of W_e and H_t-H_{t-4} were calculated in the same way as shown in Table 11, and the frequency of $(W_e)_0$, $(W_e)_{-t}$ and $(W_e)_{+t}$ is presented in Table 12.

Table 12

(W_e)	$(W_e)_{-2}$	$(W_e)_{-1}$	$(W_e)_0$	$(W_e)_{+1}$	$(W_e)_{+2}$	$(W_e)_{+3}$
Frequency	*1*	*9*	*10*	*6*	*1*	*1*

In the observed data, as the water-level is recorded at every hour, the time of true highest level may be differed from the tabulated time, and the expression for calculating W_e, which should hold for precipitation $\cdot 15$ *mm hour*, is applied to precipitation $\cdot 15$ *mm hour*. Therefore, in a rough estimation, both cases $(W_e)_{-1}$ and $(W_e)_{+1}$ should be

thought of as the case $(W_e)_0$, consequently whether H_1 rises or falls compared with H_0 may be determined by the sign of W_e.
This fact tells us that the expression

$$H_1 - H_0 = \alpha W_e$$

is approximately right.

5. Equi-run-off Time Line

We consider such a case as the upper stream basin of a river at P section being small, the precipitation in this basin can be considered uniform (see Fig. 4). We assume that when we have heavy hourly rainfall (W *mm/hour*) from t_{-1}^h to t_0^h in the just-descrived basin, the water-level and quantity of flow at P are as follows.

Time (h)	t_{-1}	t_0	t_1	t_2	t_n .....
Water-level	H_{-1}	H_0	H_1	H_2	H_n .....
Quantity of flow	Q_{-1}	Q_0	Q_1	Q_2	Q_n .....
Precip.		W	O	O	O .....

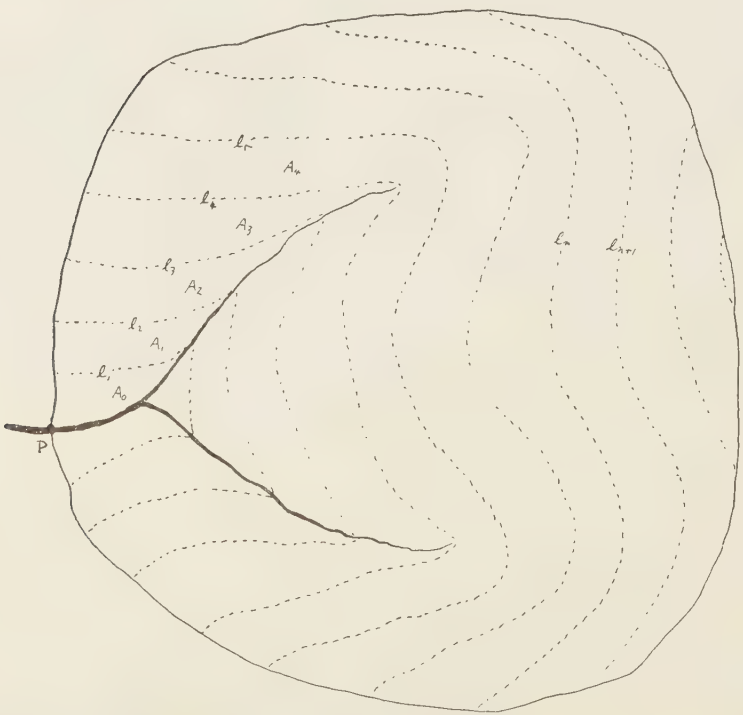

Fig. 4. Catchment Area and Equi-run-off Time Line

Then, we imagine such lines $l_1, l_2, l_3, \cdots\cdots, l_n, \cdots\cdots$ in the basin as the rainfall on the line l_n takes n hours to reach the section P (see Fig. 4). We will call l line "equi-run-off time line". Next, we name the area bounded by l_1 and the periphery of the basin "A_1", the area bounded by l_1, l_2 and the periphery "A_2" and so on. As we are considering heavy uniform rain, assuming f (coefficient of run-off) to be uniform and neglecting seepage and etc., we obtain the following expression.

$$\left.\begin{array}{l} Q_0 = kfA_0W + Q_{-1} \\ Q_1 = kfA_1W + Q_{-1} \\ \cdots\cdots\cdots\cdots\cdots\cdots \\ Q_n = kfA_nW + Q_{-1} \\ \cdots\cdots\cdots\cdots\cdots\cdots \end{array}\right\} \quad \cdots\cdots\cdots\cdots\cdots\cdots (5)$$

where k is constant.

If $A_0 < A_1 < A_2 \cdots\cdots\cdots < A_i$ then $Q_0 < Q_1 < Q_2 \cdots\cdots\cdots < Q_i$

and if $A_i > A_{i+1} > A_{i+2} \cdots\cdots\cdots$ then $Q_i > Q_{i+1} > Q_{i+2} \cdots\cdots\cdots$

in this case the discharge Q_i at t_i^h is maximum.
From the expression (5) we obtain

$$\left.\begin{array}{l} Q_j - Q_0 = kf(A_j - A_0)W, \\ Q_j - Q_{j-4} = kf(A_j - A_{j-4})W \end{array}\right\} \quad \cdots\cdots\cdots\cdots\cdots\cdots (6)$$

If there are sufficient data of precipitation W and discharge Q for the case in which we had uniform heavy rain only one hour, we can determine kfA. Then using the value of kfA, we may foresee the discharge at P. In the just-descrived discussion, if we put $i = 4$ it will be applicable to the study on the water-level at Uchinomaki.

Next, we consider such a case as we have continuous rain during several hours and put as follows.

Time (h)	t_{-7}	t_{-6}	t_{-5}	t_{-4}	t_{-3}	t_{-2}	t_{-1}	t_0	t_1	t_2	t_3	t_4
Amount of rain $\left(\frac{mm}{hour}\right)$	W_{-7}	W_{-6}	W_{-5}	W_{-4}	W_{-3}	W_{-2}	W_{-1}	W_0	W_1	W_2	W_3	W_4
Waterlevel	H_{-7}	H_{-6}	H_{-5}	H_{-4}	H_{-3}	H_{-2}	H_{-1}	H_0	H_1	H_2	H_3	H_4
Discharge	Q_{-7}	Q_{-6}	Q_{-5}	Q_{-4}	Q_{-3}	Q_{-2}	Q_{-1}	Q_0	Q_1	Q_2	Q_3	Q_4

Assuming that the maximum hourly rainfall is W_i mm/hour at t^h, we obtain the following relation from the expression (6):

$\cdots\cdots\cdots\cdots\cdots\cdots\cdots\cdots\cdots\cdots\cdots\cdots$

part of $Q_4 - Q_0$ due to $W_{-7} = kf(A_{11} - A_7)W_{-7}$

the same $W_{-6} = kf(A_{10} - A_6)W_{-6}$

$\cdots\cdots\cdots\cdots\cdots\cdots\cdots\cdots\cdots\cdots\cdots\cdots$

$\cdots\cdots\cdots\cdots\cdots\cdots$ $W_{-1} = kf(A_5 - A_1)W_{-1}$

$\cdots\cdots\cdots\cdots\cdots\cdots$ $W_0 = kf(A_4 - A_0)W_0$

$\cdots\cdots\cdots\cdots\cdots\cdots$ $W_1 = kf\,A_3W_1$

$\cdots\cdots\cdots\cdots\cdots\cdots\cdots\cdots\cdots\cdots\cdots\cdots$

$\cdots\cdots\cdots\cdots\cdots\cdots$ $W_4 = kf\,A_0W_4$

We sum up the above values and obtain,

$$\triangle Q=Q_4-Q_0=kf\{\cdots\cdots+(A_{11}-A_7)W_{-7}+(A_{10}-A_6)W_{-6}+\cdots\cdots+(A_4-A_0)W_0+A_3W_1+A_2W_2+A_1W_3+A_0W_4\} \quad (7)$$

6. Expression for Coefficient of Rain-effect

If we apply the previous article to our study at Uchinomaki it will be,

$$A_0<A_1<A_2<A_3<A_4>A_5>A_6>\cdots\cdots>A_9>A_{10}>A_{11}\cdots\cdots$$

As the observed data of Q is poor, it is difficult to determine kfA strictly. But, using our estimation of Q, if we assume roughly,

$$A_0:A_1:A_2:A_3:A_4:A_5:A_6:A_7:A_8:A_9:A_{10}=1:2:4:8:10:9:7:6:6:5:5$$

and neglect A_0W_4, $(A_{11}-A_7)W_{-7}$, $\cdots\cdots$, as it should be small, then from the epuation (7) we obtain

$$\triangle Q=k'f(-0.2W_{-6}-0.4W_{-5}-0.4W_{-4}-0.2W_{-3}+0.3W_{-2}+0.7W_{-1}+0.9W_0+0.8W_1+0.4W_2+0.2W_3)$$

$$\therefore \quad \triangle Q=k'fW_e \quad (8)$$

In a case of heavy rain, the value of coefficient of run-off will increase in accordance with the increase of amount of rain and approaches to unity, therefor we may put

$$f=d+gW_e \quad (9)$$

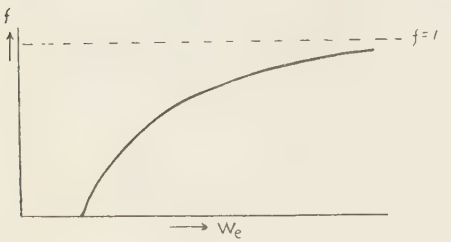

where W_e not small, and $\lim_{W_e\to\infty} f=1$, and d, g constant.

Next, if we assume the quantity of flow of the Kurokawa at Uchinomaki as follows:

$$Q=a+bH+cH^2$$

where H is water-level

then
$$\begin{aligned}\triangle Q&=Q_4-Q_0\\&=a+bH_1+cH_1^2-(a+bH_0+cH_0^2)\\&=a+b(H_0+\triangle H)+c(H_0+\triangle H)^2-(a+bH_0+cH_0^2)\end{aligned}$$

$$\therefore \quad \triangle Q=\triangle H(b+c\cdot\triangle H+2cH_0) \quad (10)$$

From the equations (8), (9) and (10) we obtain

$$k'(d+gW_e)W_e=\triangle H(b+c\cdot\triangle H+2cH_0)$$

putting $\quad b+c\cdot\triangle H=B, \quad 2c=C$

we obtain, $\quad k'(d+gW_e)W_e=\triangle H(B+CH_0)$

$$\therefore \quad \frac{\triangle H}{W_e}=\frac{k'(d+gW_e)}{B+CH_0}=\frac{k'd(1+\frac{g}{d}W_e)}{B(1+\frac{C}{B}H_0)}$$

$$\therefore \quad \frac{\triangle H}{W_e} = \frac{k'd}{B}\left(1+\frac{g}{d}W_e\right)\left(1+\frac{C}{B}H_0\right)^{-1}$$

if $\quad 1 > \frac{g}{d}W_e$ and $1 > \frac{C}{B}H_0$

then $\quad \frac{\triangle H}{W_e} \fallingdotseq \frac{k'd}{B}\left(1+\frac{g}{d}W_e\right)\left(1-\frac{C}{B}H_0\right)$

$$\therefore \frac{k'd}{B}\left(1+\frac{g}{d}W_e-\frac{C}{B}H_0\right)$$

from this we obtain the following expression

$$\alpha = \frac{\triangle H}{W_e} = p+qW_e-rH_0 \quad \cdots\cdots (11)$$

7. Calculation of α and W_e

The similar calculation to that shown in Table 10, is carried out in cases in which the hourly precipitation was larger than *15 mm hour*, and the results are given in Table *13*, and also diagram, showing the relation between α and H_0, is given in Fig. 5. From this diagram it is seen that (1) in the case $H < 190$, points being at random, correlation between α and H_0 can not be recognizsd, (2) in the case $H_0 = 190$ the value of α decreases as H_0 increases. This fact may be readily explained as follows: the mean water-level at Uchinomaki being about *50 cm*, the water-level *190 cm* should appear as a result of a great deal of rain.

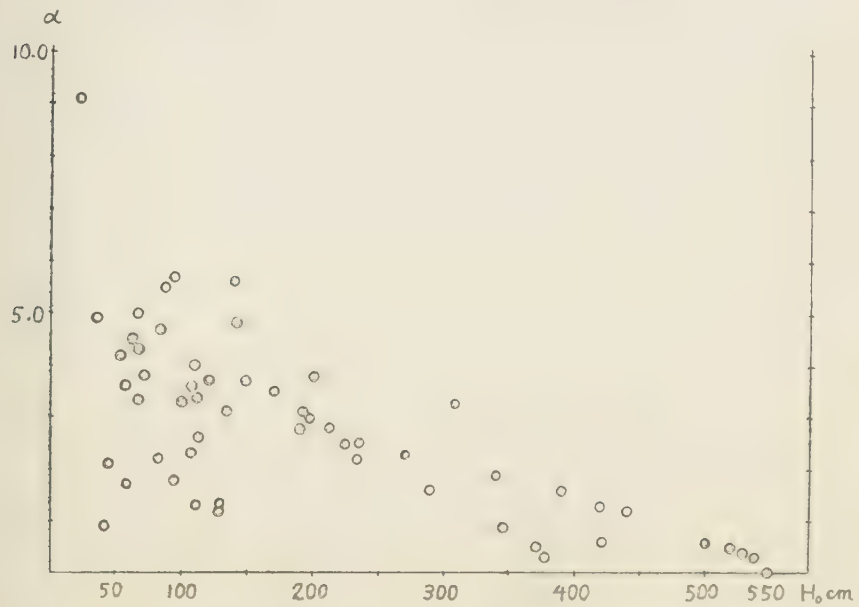

Fig. 5. $\alpha - H_0$ Diagram

Table 13

Year	Month	Day	Hour	W_0	W_e	H_0	H_4	H_4-H_0	α	$\frac{W_e}{W_0}$	$W_{-1}+W_0+W_1$	$\frac{W_e}{W_{-1}+W_0+W_1}$
1944	4	7	17	15.6	18.7	141.5	230.4	88.9	4.8	1.2	33.9	0.6
	5	9	20	32.6	51.8	94.9	388.0	293.1	5.7	1.6	65.0	0.8
	5	10	10	32.2	54.9	346.4	394.0	47.6	0.9	1.7	62.1	0.9
			11	18.5	48.0	379.0	393.6	14.6	0.3	2.5	56.0	0.9
	5	11	0	20.4	31.0	373.8	389.7	15.9	0.5	1.5	33.0	0.9
	6	4	7	38.2	53.9	149.1	350.0	200.9	3.7	1.4	57.9	0.9
	7	22	0	17.1	21.1	237.6	290.0	52.4	2.5	1.2	22.9	0.9
	8	8	21	20.7	33.0	140.0	326.0	186.0	5.6	1.6	39.9	0.8
1946	3	18	19	18.5	25.7	63.0	178.0	115.0	4.5	1.4	29.9	0.9
	4	24	19	34.4	53.6	109.0	323.0	214.0	4.0	1.6	59.7	0.9
			20	14.9	38.3	193.0	311.0	118.0	3.1	2.6	50.7	0.8
1947	1	11	4	20.2	19.5	67.6	164.2	96.6	5.0	1.0	25.0	0.8
	4	1	22	19.1	27.4	45.8	102.0	56.2	2.1	1.4	28.1	1.0
	6	24	1	15.4	37.8	67.4	229.4	162.0	4.3	2.5	35.9	1.1
			2	19.4	47.7	84.6	308.4	223.8	4.7	2.5	51.6	0.9
			3	16.8	54.3	120.0	318.3	198.3	3.7	3.2	55.8	1.0
			4	19.6	52.0	197.8	356.0	158.2	3.0	2.6	50.3	1.0
			6	22.9	31.9	308.4	412.5	104.1	3.3	1.4	47.6	0.7
			16	17.0	29.4	421.7	440.4	18.7	0.6	1.7	34.5	0.9
	7	16	14	15.4	13.9	25.7	151.7	126.0	9.1	0.9	15.4	0.9
	7	18	14	20.6	25.4	38.4	161.6	123.2	4.9	1.2	27.3	0.9
	7	19	10	16.6	30.2	110.2	213.9	103.7	3.4	1.8	32.1	0.9
	8	18	17	18.6	16.7	40.1	54.5	14.4	0.9	0.9	18.6	0.9
1948	7	3	17	56.2	53.2	234.3	350.2	115.9	2.2	0.9	58.6	0.9
	7	8	5	16.0	19.2	58.6	90.5	31.9	1.7	1.2	24.0	0.8
			13	20.2	31.6	87.8	262.4	174.6	5.5	1.6	38.4	0.8
	7	16	20	15.7	13.5	130.2	146.3	16.1	1.2	0.9	15.7	0.9
	7	22	11	15.0	16.6	112.8	156.0	43.2	2.6	1.1	17.9	0.9
	8	5	19	19.1	18.1	82.0	121.1	39.1	2.2	0.9	20.4	0.9
	8	27	22	17.6	34.5	94.4	155.7	61.3	1.8	2.0	39.2	0.9
			23	19.8	34.0	111.3	157.0	45.7	1.3	1.7	42.0	0.8
	9	23	17	20.1	18.9	67.2	129.0	61.8	3.3	0.9	22.0	0.9
	9	26	20	16.7	15.0	57.8	112.4	54.6	3.6	0.9	16.7	0.9
1949	3	10	14	19.5	34.8	54.9	201.7	146.8	4.2	1.8	42.4	0.8
	5	19	21	15.1	33.9	100.0	212.7	112.7	3.3	2.2	41.4	0.8
			22	15.2	31.3	133.2	229.5	96.3	3.1	2.1	37.1	0.8
	5	20	1	18.4	17.7	212.7	262.1	49.4	2.8	1.0	30.4	0.6
	5	22	21	17.1	39.0	71.8	219.4	147.6	3.8	2.3	43.2	0.9
			22	16.0	31.6	107.3	220.5	113.2	3.6	2.0	35.5	0.9
	8	1	17	19.5	26.2	107.7	168.5	60.8	2.3	1.3	29.5	0.9
	8	13	14	23.7	32.9	130.2	173.3	43.1	1.3	1.4	38.2	0.9
1953	6	25	15	21.3	23.1	170	250	80	3.5	1.1	36.1	0.6
	6	26	11	24.2	58.5	200	420	220	3.8	2.4	55.0	1.1
			12	22.0	73.9	270	440	170	2.3	3.4	72.4	1.0
			13	26.2	82.7	340	500	160	1.9	3.2	70.9	1.2
			14	22.7	83.7	390	520	130	1.6	3.7	78.7	1.1
			15	29.8	84.9	420	530	110	1.3	2.9	97.7	0.9
			16	45.2	82.7	440	540	100	1.2	1.8	100.5	0.8
			17	25.5	78.9	500	550	50	0.6	3.1	98.0	0.8
			18	27.3	75.3	520	560	40	0.5	2.8	95.1	0.8
			19	42.3	66.8	530	560	30	0.4	1.6	96.8	0.7
			20	26.7	57.3	540	560	20	0.3	2.1	92.7	0.6
			21	23.7	44.1	550	550	0	0.0	1.9	78.5	0.6
			22	28.1	29.1	560	530					
			23	16.7	12.7	560	520					
1954	6	25	22	16.7	46.3	190	320	130	2.8	2.8	48.3	1.0
	6	26	0	24.2	48.9	225	345	120	2.5	2.0	70.7	0.7
			1	24.7	34.3	290	345	55	1.6	1.4	51.3	0.7

Hence, in order that water-level rises over *190 cm.* it must rain continuously after a long or heavy rain. In such a case, the evaporation may be neglected, and the plants and everything on the ground and under-ground are saturated with water, therefore the most part of rain will flow as run-off into rivers. Consequently the distribution of α should be in order for $H_0 \geqq 190$ *cm.*

Next, for to see the relation between α and W_e, classifying the value of α in three classes about H_0, viz., $190 \leqq H_0 < 310$, $310 \leqq H_0 < 400$ and $400 \leqq H_0$, α–W_e diagram is given in Fig. 6.

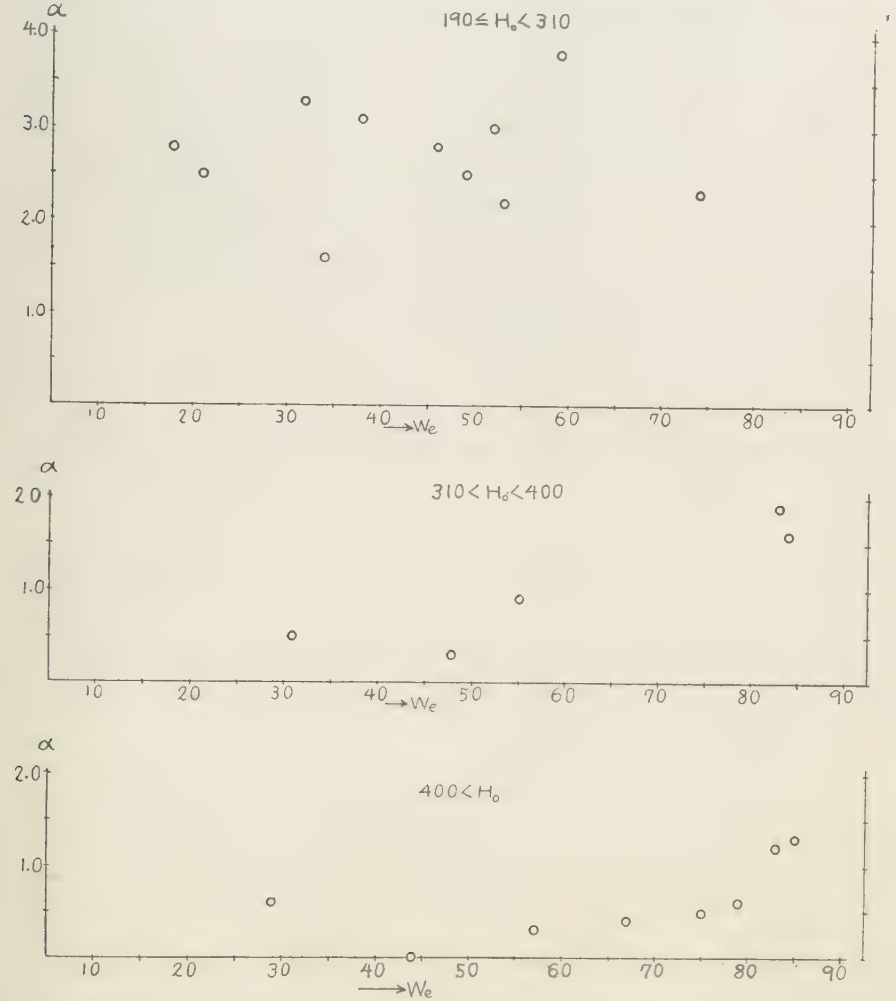

Fig. 6. $\alpha - W_e$ Diagram

From this diagram, it is seen that α increases as W_e increases. Above-mentioned facts tell us that for the case $190 \leqq H_0$ the expression

$$\alpha = p + qW_e - rH_0$$

will be satisfied by the observed data at Uchinomaki.

Using the values of α, W_e and H_0 in Table 13, the value of p, q and r was determined by the means of least square, the result is as following:

$$\alpha_1 = 4.257 + 0.008W_e - 0.0088H_0 \quad (190 \leqq H_0) \quad \cdots\cdots (12)$$

The values of α_1 calculated by this expression and that in Table 13, both are given in Table 14 and graphicly represented in Fig. 7. The irregularity for $300 < H_0 < 400$ in the diagram shows that at such a water-level the flood begins to take place and the quantity of surface-detention irregularly increases.

When H_0 increases more and overs *400 cm*, the increase of surface-detention becomes comparatively uniform and the flood in the true meaning takes place.

Classifying the base-level H_0 into two classes, viz., $190 \leqq H_0 < 400$ and $400 < H_0$, we obtain expression for α as follows:

$$\left.\begin{aligned} \alpha_2 &= 5.069 + 0.008W_e - 0.0119H_0 \\ &\quad (190 \leqq H_0 < 400) \end{aligned}\right\}$$
$$\left.\begin{aligned} \alpha_3 &= 2.942 + 0.0114W_e - 0.0063H_0 \\ &\quad (400 < H_0) \end{aligned}\right\} \quad \cdots\cdots (13)$$

Table 14

W_e	H_0	α	α_1	α_2	α_3
46	190	2.8	3.0	3.2	
38	193	3.1	2.9	3.1	
52	198	3.0	3.0	3.1	
59	200	3.8	3.0	3.2	
18	213	2.8	2.5	2.7	
49	225	2.5	2.7	2.8	
53	234	2.2	2.6	2.7	
21	238	2.5	2.4	2.4	
74	270	2.3	2.5	2.5	
34	290	1.6	2.0	1.9	
32	308	3.3	1.8	1.7	
83	340	1.9	2.0	1.7	
55	346	0.9	1.7	1.4	
31	374	0.5	1.2	0.9	
48	379	0.3	1.3	0.9	
84	390	1.6	1.5	1.1	
85	420	1.3	1.3		1.3
29	422	0.6	0.8		0.6
83	440	1.2	1.1		1.1
79	500	0.6	0.5		0.7
75	520	0.5	0.3		0.5
67	530	0.4	0.2		0.4
57	540	0.3	0.0		0.2
44	550	0.0	−0.2		0.0

α_1 $4.257 + 0.008W_e - 0.0088H_0$
$\alpha_2 = 5.069 + 0.008W_e - 0.0119H_0$
α_3 $2.942 + 0.0114W_e - 0.0063H_0$

The calculated values of α_2 and α_3 are also given in Table 14 and illustrated in Fig. 8, and the values of α are also shown in Fig. 8. Using the expression (12) or (13) we can determine α, then from the expression

$$H_4 = H_0 + \alpha W_e$$

we can calculate H_4. It means that we can calculate the water-level H_4 at t_4^h taking the water-level H_0 at t_0^h as base-level. But to calculate the value W_e it is necessary to know the values of W_1, W_2 and W_3 which are quantity of three hourly rainfalls after t_0^h. Therefore from the standpoint of the flood-prediction, the above-described method is not suitable. To remove this difficulty, the following method will be of use. The last two columns in Table 13 give the amount of three hours rainfall $W_{-1}+W_0+W_1$ and the value $W_e/(W_{-1}+W_0+W_1)$. The values of $W_e/(W_{-1}+W_0+W_1)$ lie in the range $0.6 \sim 1.2$, and its mean value is *0.83*. Therefore we obtain as an approximate expression,

$$W_e = 0.8(W_{-1}+W_0+W_1) \sim 0.9(W_{-1}+W_0+W_1)$$

Especially in such a case where the rainfall before W_e is comparatively great, we have

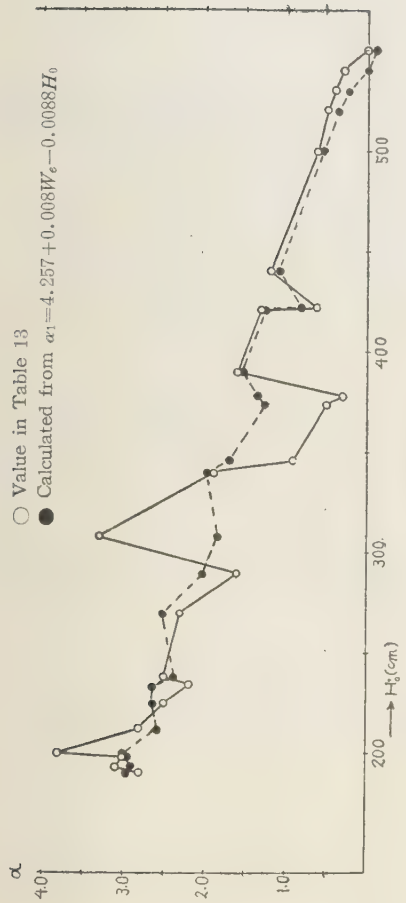
○ Value in Table 13
● Calculated from $\alpha_1=4.257+0.008W_e-0.0088H_0$
α
4.0
3.0
2.0
1.0
200
300
400
500
H_0(cm)

Fig. 7.

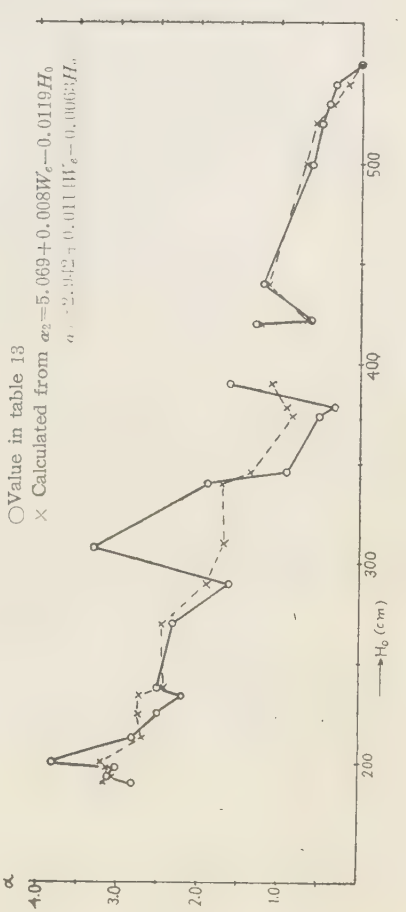
○Value in table 13
× Calculated from $\alpha_2=5.069+0.008W_e-0.0119H_0$
α
4.0
3.0
2.0
1.0
200
300
400
500
H_0 (cm)

Fig. 8.

to use

$$W_e=0.6(W_{-1}+W_0+W_1)\sim 0.7(W_{-1}+W_0+W_1)$$

and if we expect to have a great quantity of rain after W_1 we have to use

$$W_e=1.0(W_{-1}+W_0+W_1)\sim 1.2(W_{-1}+W_0+W_1)$$

Lastly we have to consider such a case as $H_0<190$ and $W\geqq 15$ *mm/hour*. As we have mentioned, the distribution of α is at random, therefore we treat α in an average. Then we obtain the mean value of α from the data in Table 13 as follows:

Range of base-level H_0	$0\sim 50$	$50\sim 100$	$100\sim 190$
α (*mean*)	4.3	3.9	3.2

8. Summary

The main points are summarised as follows.

(1) The water-level of the Kurokawa at Uchinomaki rises, on an average, at the rate of about *2 cm* per *1 mm* precipitation.

(2) The water-level at Uchinomaki mostly attains a maximun 4 hours after heavy houry rainfall.

(3) If it rains heavily from t^h_{-1} to t^h_0 among continuous rain and the water-level at t^h_0 is H_0, then the water-level H_1 at t^h_1 (4 hours after t^h_0) can be calculated from the expression,

$$H_1 = H_0 + \alpha W_e$$

where W_e is quantity which the writer calls "precipitation effect" and α "coefficient of precipitation effect".

(4) Imagining lines, which the writer calls "equi-run-off time line" in the drainage basin of a river, he attempted to propose a method to foresee the water-level and quantity of flow.

This method may be available for the study of some sort of rivers.

(5) Applying the method just-described to the study on the water-level at Uchinomaki, the writer obtained the expression for α as follows,

$$\alpha = p + qW_e - rH_0$$

And using the observed data of precipitation and water-level at Uchinomaki, he also obtained the same form of the expression for α.

(6) Numerical vale of p, q and r in the expression for α was determined by the means of least square as follows,

$$\alpha=4.257+0.008W_e-0.0088H_0 \quad (190\leqq H_0)$$

and etc……

(8) For the purpose of flood-prediction at Uchinomaki, the following expression for W_e is available for practical use.

$$W_e = C\,(W_{-1} + W_0 + W_1)$$

where the value of C ranges $0.6 \sim 1.2$ in accordance with amount of rain and its hourly distribution.

References

1. Murota : Kumamoto J. Sci. A Vol. 1 No.4 (1954), 43
2. Murota : The same Vol.1 No. 2 (1953), 62—106

Table 1. Observed Data of Precipitation and Water-level at Uchinomaki

1944

Month	Feb.				Apr.				May								June			July				
Day	12		13	14	7		8	9	9		10		11		12	13	4		5	21		22		23
W H / Time	W	H	H	H	W	H	H	H	W	H	W	H	W	H	H	H	W	H	H	W	H	W	H	H
0																								
1			137.7	33.7			184.0	41.7					5.6	376.7	254.0	169.5			269.0	1.2	136.5	5.8	247.0	161.0
2			130.4	32.7			170.2	41.2					9.6	380.9					258.8	2.5	122.0	2.0	260.0	154.3
3			121.8	31.4			157.5	40.0					5.2	384.8					249.2	2.0	112.7	3.1	277.0	148.3
4			112.4	31.4			144.4	39.2					6.4	389.7			5.9	135.4	240.5	2.4	106.3	10.0	290.0	143.0
5			105.6	30.5			130.6	38.3				372.5	3.4	395.7			10.7	135.4	231.7	0.6	104.4	7.7	297.0	137.0
6			85.0		0.8		118.9	37.5				359.1	0.8	400.7	224.5	169.0	8.9	141.0	223.0	4.6	104.8		308.0	129.4
7			78.0		2.4		109.0	37.9				347.5	0.9	404.5			38.2	149.1	215.4	2.1	110.3	2.5	314.0	128.3
8			71.7		2.1		101.6	37.6			1.0	341.5	0.2	406.0			10.8	180.2	203.9	1.6	112.5	6.3	320.0	122.8
9		31.2	63.4		0.2	27.8	91.3	36.3			11.4	340.7		406.0			4.7	229.0	184.1	2.5	143.5	3.0	319.0	111.0
10		31.4	59.0		3.7	28.1	83.8	36.3		28.9	32.2	346.4		404.6			2.1	327.5	165.3	1.7	153.0	1.1	318.0	103.4
11	1.4	33.4	56.6		9.6	32.8	77.0	35.1		28.9	18.5	379.0		402.8			2.1	350.0	157.4	3.6	156.0		317.0	98.3
12	2.9	33.4	53.2		6.3	41.2	72.7	34.2		28.7	5.3	389.6		400.0	197.1	164.6	9.6	349.1	150.8	0.7	160.5		316.0	95.0
13	3.5	34.3	49.6		9.8	56.0	68.0	35.7	1.4	31.7	3.6	389.7		397.6			5.2	343.2	137.6	3.9	169.0	3.4	312.3	92.8
14	5.2	36.3	47.4		11.0	82.5	64.5	35.1	1.7	32.6	0.2	394.0		395.1			0.1	341.7	131.2	13.6	182.1		302.0	86.4
15	4.4	39.0	47.2		2.6	108.0	59.7	35.2	1.8	32.1		397.6		392.3				341.2	129.3	0.6	200.0		287.0	84.0
16	4.6	44.6	46.8		11.4	121.8	56.2	35.1	5.8	35.7		393.0		387.2			5.2	332.7	127.0	11.5	220.5		271.5	80.5
17	8.2	54.5	44.0		15.6	141.5	52.5	34.4	9.7	39.0		391.7					2.8	324.5	124.6	1.6	228.5		253.0	79.8
18	9.0	76.5	42.2		6.9	187.0	48.2	33.4	9.9	46.3		389.6			188.9	160.1	3.6	318.5	123.4	0.5	239.0		236.0	77.7
19	2.9	106.0	40.8		2.3	227.0	47.7	33.3	13.3	66.0	2.0	386.9					0.8	316.0	124.1		248.0		222.6	77.7
20	2.0	128.0	37.3		0.2	237.1	46.5	33.6	32.6	94.9		384.2					0.4	314.6	124.3	1.1	249.2		204.8	78.2
21	2.2	138.1	36.1			250.1	45.6	33.2	19.0	160.1	1.0	381.1						311.9	124.6	2.7	236.5		193.5	76.6
22	4.4	139.6	35.1			240.1	43.4	32.6		257.0		378.3						304.0	125.7	1.7	255.0		184.5	77.3
23	1.0	141.0	33.8			211.2	42.4	32.1		317.0	1.0	376.1						294.8	122.8	0.1	241.3		176.5	77.0
24	1.6	141.0	34.2			196.7	42.1	31.9		328.0	20.2	373.8		259.8	140.0	178.0		279.8	122.3	17.1	237.6		170.0	73.4

1944					1945				1946																	
Month	Aug.						Dec.			Feb.								Mar.								
Day	8		9		21		22		23	5		6		7	24		25	28		1		2		3		4
	W	H	W	H	W	H	W	H	H	W	H	H	W	H	W	H	H	W	H	W	H	H	W	H	W	H	H
0																											
1			3.6	326.0			1.6	25.7	141.5			2.4	39.3	20.7			104.7			1.6	56.0		15.1	1.0	71.2	18.1
2			[illegible]				1.0	[illegible]	[illegible]			2.3	17.8	19.8			100.7			0.8	[illegible]		[illegible]	2.5	[illegible]	17.3
3			[illegible]				[illegible]	[illegible]	[illegible]			1.1	56.7	18.0			95.7			0.1	55.8		14.6		66.2	17.4
4			0.7	300.2			2.2	28.5	115.2			0.7	60.6	18.2			88.0				55.0		14.6		65.2	16.5
5			2.1	293.7			0.8	30.0	106.0			0.3	64.1	17.0			75.6				52.7		14.2		62.8	16.5
6			0.6	286.2				34.7	97.1				65.2	16.1			65.4				50.0	0.9	14.0		59.4	16.5
7				277.3				38.8	89.9				68.0	15.8			57.0				46.6	2.3	14.0		55.8	
8		69.9		272.0				42.0	83.5				71.2	15.1			50.5				43.9	2.2	14.3		51.6	
9	0.4	68.2		268.3				43.8	76.0				70.1	14.2			44.8				40.7	2.4	15.6		47.6	
10	0.6	69.1						43.8	68.0		12.8		61.6	14.3		17.3	39.0		18.8		36.5	0.7	18.3		43.4	
11	1.4	69.5					0.2	42.2	63.9				56.2	14.3	0.1	17.7	35.0		17.7		34.8	0.8	21.2		40.0	
12	[illegible]	[illegible]					1.0	[illegible]	[illegible]				[illegible]	[illegible]	[illegible]	[illegible]	[illegible]	[illegible]	[illegible]		[illegible]	[illegible]	[illegible]		[illegible]	
13	0.4	71.3					3.1	39.1	57.2		12.8		50.0		0.6	18.2	29.0	1.9	16.4		30.0	1.0	27.1		36.0	
14	0.5	72.3					4.0	39.7	53.6	0.5	12.9		47.2		0.9	18.9	26.0	2.6	16.5		27.8	1.8	29.5		32.3	
15	6.7	73.5					5.2	45.4	50.0	4.2	13.1		42.1		1.9	19.8	23.0	1.7	17.9		25.3	2.4	32.9		30.2	
16	[illegible]	[illegible]					[illegible]	[illegible]	[illegible]	[illegible]	[illegible]		[illegible]		[illegible]	[illegible]	[illegible]	[illegible]	[illegible]		[illegible]	[illegible]	[illegible]		[illegible]	
17	[illegible]	[illegible]					[illegible]	[illegible]	[illegible]	[illegible]	[illegible]		[illegible]		[illegible]	[illegible]	[illegible]	[illegible]	[illegible]		[illegible]	[illegible]	[illegible]		[illegible]	
18	[illegible]	[illegible]					[illegible]	[illegible]	[illegible]	[illegible]	[illegible]		[illegible]		[illegible]	[illegible]	[illegible]	[illegible]	[illegible]		[illegible]	[illegible]	[illegible]		[illegible]	
19	1.1	110.0					3.2	108.5	39.7	2.0	18.1		31.0		12.7	38.0	14.2	1.8	39.6		18.4	4.0	57.2		23.0	
20	10.2	117.2					4.5	123.5	37.0	0.2	21.1		28.9		3.8	58.0	14.1	1.6	45.5		17.2	1.9	65.4		22.3	
21	20.7	140.0			23.7		3.5	134.2	34.2	2.7	24.0		26.8		2.4	80.0		1.0	50.0		16.3	1.8	72.6		21.2	
22	9.0	241.0			23.7		1.4	140.3	33.1	1.9	28.7		24.6		3.6	93.5		0.5	53.6		16.2	1.8	75.8		20.0	
23	3.9	280.0			0.8	23.7	0.9	143.2	31.6	2.0	34.0		23.3		2.4	100.0		0.5	55.4		15.5	0.6	76.3		19.4	
24	[illegible]	[illegible]			[illegible]	[illegible]	[illegible]	[illegible]	[illegible]	[illegible]	[illegible]		[illegible]		[illegible]	[illegible]	[illegible]	[illegible]	[illegible]		[illegible]	[illegible]	[illegible]		18.9	14.2

1 9 4 6

Month	Mar.																							
Day	6		7	10		11	14		15		17		18		19		20	22		23		24	28		29	
Hour	W	H	H	W	H	H	W	H	W	H	W	H	W	H	W	H	H	W	H	W	H	H	W	H	W	H
0																										
1			24.0	1.5	14.2	38.6			0.9	38.7			1.3	28.7	1.0	186.8	47.7			0.8	16.6	43.3			1.7	87.0
2			23.5	0.2	14.3	35.6			0.5	40.3				29.0	0.2	190.3	45.0			2.4	19.0	41.1			0.5	100.6
3			22.7	0.2	15.0	32.6			0.6	40.4				29.7	0.2	189.0	43.2			1.4	23.3	38.3			0.4	108.4
4			22.1	0.1	16.5	29.8			0.4	40.3			1.4	30.6	0.1	176.0	42.0			0.1	28.1	37.0				107.0
5	0.3		21.1	0.1	18.4	26.1			0.4	39.5			0.4	30.8	0.1	162.5	39.4			0.1	33.2	34.2				95.2
6	1.5	14.0	20.4	0.2	19.1	23.7			0.3	37.2			6.6	34.4	0.2	151.0	36.5			0.1	36.2	32.4				87.0
7	2.3	14.0	19.9	0.1	19.7	20.6			0.1	35.7			8.9	40.7	1.0	141.7	35.7			0.1	36.8	31.4				78.0
8	4.2	15.2	19.4	0.1	19.7	18.0			0.6	34.4			2.7	52.0	0.3	135.0	33.9			1.4	37.1	30.2				70.7
9	4.1	18.4	18.7		19.0	17.0				33.0			0.1	87.5	0.3	129.1	33.0			6.9	38.4	28.7				64.4
10	1.3	28.3	17.9	3.2	19.4	15.8				31.0				117.4	0.2	120.7	31.9			5.6	44.3	26.9				55.2
11	0.3	36.2	17.0	8.6	21.2	15.7								118.0	0.1	114.0	30.8			7.7	57.0	26.0				50.5
12	0.5	42.6	16.5	9.6	22.6					28.5				108.0	0.1	108.0	29.9			1.7	79.5	23.9				46.5
13	0.1	44.8	16.1	7.3	25.2									96.0		102.7	29.5			0.4	90.0	22.6				42.4
14		45.0	15.5		32.2	15.0								85.0	1.1	96.0	27.4			0.2	94.3	22.0				38.0
15		43.8	15.6		42.0			18.4						75.0	0.1	90.0	26.3			0.1	93.5	20.2				33.5
16		42.0	15.2		47.3		0.2	18.5						67.0	0.1	85.0	25.0				87.6	19.0	0.1			30.4
17		39.5	15.0		53.0		0.7	18.5				29.0	1.0	62.3		80.3	24.9				81.0	18.5	0.1			27.5
18		36.6	14.9		56.0		1.3	18.6		22.5		29.1	3.9	58.4		74.8	24.1			0.2	73.1	16.7	0.1	16.7		24.8
19		34.4			56.5		1.5	19.2			0.7	29.1	18.5	63.0		70.1	23.4				67.0	16.0	1.6	16.7		22.4
20		31.8			55.4		0.8	21.3			1.0		7.5	90.0	0.3	66.1	22.5			0.4	62.0	15.5	3.7	17.7		20.6
21		30.3			52.5		0.4	24.6			0.3		0.6	132.0		62.4	21.6				57.5	15.3	2.5	20.7		19.2
22		28.4			48.0		0.5	27.8			0.1	27.4	0.4	161.0	0.1	57.5	21.5	0.6	15.2		55.0	15.1	8.4	27.7		18.0
23		26.2			45.2		1.0	31.6				27.4	6.5	178.0		53.6	21.0	0.6	15.0		50.6	15.1	5.4	40.0		17.2
24		25.0	14.7		41.8		0.7	35.9		18.2	0.8	27.6	1.7	179.4	0.1	51.0	21.6	1.0	15.3		47.0	15.1	6.2	53.0		16.6

1946 1947

Month	Apr.												May								Jan.			
Date	4		5		6		7	24		25		30	1		2		3	12		13	10		11	
	W	H	W	H	W	H	H	W	H	W	H	W H	W	H	W	H	H	W	H	H	W	H	W	H
0		17.1																						
1		18.2		21.2		214.0	38.9		48.9	3.1	292.2		2.1	25.4	18.0	239.0	144.0			415.4			6.7	36.2
2		20.9		29.0	0.2	207.0	44.2		46.3	3.0	289.3		1.3	26.4	11.4	250.0	131.5			415.2			5.6	41.5
3	8.2	24.6		26.3	0.3	191.5	41.4		45.8	2.2	287.0		2.3	27.6	8.6	263.0	118.4			416.0			4.8	50.7
4	11.2	35.0		25.2	0.4	179.0	40.0		45.6	1.8	283.3		0.8	29.1	0.4	276.5	110.0			415.9			20.2	67.6
5	7.6	56.0		24.4	0.6	167.8	38.2	0.5	45.2	0.6	279.8		3.7	30.5	2.6	288.0	101.2			414.2				100.0
6	9.5	98.0		22.7	0.7	158.0	37.7	2.9	45.2	0.6	276.3		2.1	31.8	6.2	295.8	94.1			411.2				137.4
7	0.5	120.0		22.4	0.4	149.5	36.7	3.0	44.7	0.2	270.4		1.8	34.2	2.3	301.4	86.0			408.0				161.4
8	2.5	162.0		21.3		140.5	35.8	3.3	45.3		265.0		0.8	35.7	0.8	305.1	80.0	1.6		404.2				164.2
9	0.3	166.8		20.5		130.1	33.9	0.9	48.3		259.0		0.1	36.8	0.8	307.3	72.2	0.7		400.5				157.0
10		[illegible]		[illegible]		118.2	33.6	0.3	53.2		254.0		3.5	38.1	0.2	308.5	63.0	1.3	36.0	398.1				156.0
11		140.0		19.6		110.0	32.2	0.2	53.3				6.5	38.8	1.2	307.8	57.0	3.6	36.3	390.3				133.0
12		123.5		18.9		102.0	31.4	1.7	53.4				7.7	41.7	3.8	307.0	51.2	5.4	36.2	385.7				121.0
13		110.0		18.8		95.0	30.8	0.4	52.3				7.6	47.6	0.3	304.2	46.8	5.0	50.0	380.2				111.0
14		[illegible]		[illegible]		[illegible]			[illegible]				3.1	58.2		301.0	43.0	8.6	75.0	384.8				102.8
15		87.2	1.6	18.8		82.5	28.4	1.5	49.1				0.4	69.4	1.5	297.6	39.0	22.0	107.0					95.2
16		78.0	3.6	21.6		77.4	28.7	1.1	49.0				2.7	76.0	0.2	294.2	33.0	13.0	228.0					89.8
17		70.3	10.0	34.0		72.0	27.9	12.1	51.3				0.3	80.6	0.1	280.0	31.1	27.0	270.0					85.2
18		63.5	12.0	85.0		67.0	27.0	10.4	64.0				10.0	81.4	0.1	274.4	26.9	19.0	300.0			31.3		79.7
19		56.5	5.4	138.0		63.0	25.4	34.4	109.0				15.9	82.2		264.5	25.7	19.0	350.0			31.3		74.3
20		51.0	8.8	172.0		60.1	24.0	14.9	193.0				9.9	95.5		258.2	23.3	22.0	400.0			31.3		69.4
21		[illegible]	[illegible]	[illegible]		[illegible]		[illegible]	[illegible]			0.6	[illegible]	[illegible]		[illegible]	[illegible]					[illegible]		[illegible]
22		[illegible]	[illegible]	[illegible]		[illegible]			[illegible]			1.6	[illegible]	[illegible]		[illegible]	[illegible]					[illegible]		[illegible]
23		[illegible]	[illegible]	[illegible]		[illegible]		[illegible]	[illegible]			1.3	[illegible]	[illegible]		[illegible]	[illegible]					[illegible]		[illegible]
24		[illegible]	[illegible]	[illegible]		[illegible]		[illegible]	[illegible]			1.1	[illegible]	[illegible]		[illegible]	[illegible]					[illegible]		[illegible]

1947

Month	Jan.									Feb.			Apr.												
Day	12	17		18	23		24		25	14		15	1		2		3	20		21		27		28		29
H.W. Time	H	W	H	H	W	H	W	H	H	W	H	H	W	H	W	H	H	W	H	W	H	W	H	W	H	H
0										0.6	43.5															
1	52.0			40.0			0.4	35.4	40.6	0.1	43.6	59.8			1.4	79.6	47.8			3.9	53.0				4.1	61.1	54.0
2	50.4			39.0			0.4		40.2	2.6	44.2	57.4				102.0	46.0			0.5	53.7				0.3	66.2	53.5
3	48.7			38.7			0.3		39.4	1.8	44.6	55.2				104.6	45.6				56.0				0.1	72.7	53.1
4	46.6			37.9			0.4	35.4	38.7	1.8	45.0	53.7				104.0	43.4				58.9				0.1	77.9	52.5
5	45.6			37.2			0.4		38.0	2.6	45.3	50.0				100.0	42.4				61.0				0.8	81.3	52.0
6	44.8			36.2			0.3	35.3	38.0	1.8	45.4	49.0				94.8	42.4				61.5				0.4	81.9	51.5
7	44.2			35.8			0.3	35.8	37.9	2.0	46.1	48.0				89.6					61.5				0.4	81.9	50.6
8	44.4			35.2			0.8		37.6	3.2	48.2	47.2				83.4					61.5				0.3	81.3	50.0
9	40.7			34.6			1.5	35.8	37.5	1.2	51.6	46.4				79.2					59.3				0.1	80.3	49.5
10	39.5		30.5	34.0		34.0	2.2	36.0	37.4	0.8	53.5	46.2				74.6	42.2				57.5		50.0	0.1	78.6	48.2
11	38.9	0.1	30.5	33.3	2.1		3.0	36.8		1.7	57.4	46.1				71.2					56.7				0.3	77.5	48.1
12	38.3	0.5	30.6	33.1	1.9	34.3	2.5	37.0		4.4	60.0	45.9				68.1					55.0					76.3	48.0
13	37.7		30.8	32.7	1.6		0.1	37.3		5.9	61.4	45.9				65.3					54.3		50.1			75.8	48.0
14	37.6		30.6	32.4	1.4			37.8		2.2	61.3	45.7				62.9					53.6		50.6			75.0	48.0
15	37.6	3.0	31.2	32.5	1.0	34.4		39.1	36.6		61.2	45.5		38.2		60.6			50.3		52.6		50.7			73.5	
16	37.2	5.7	33.8	31.8	1.3	34.5		40.2			62.4					58.5					51.8		51.0			72.5	
17	36.2	7.0	36.9	31.3	1.0	34.8		41.8			64.7			38.3		57.2			50.9		50.8	0.3	51.1			71.0	
18	35.2	1.0	40.8	31.3	0.4	34.9		42.1			66.9					56.6			51.3		50.2	3.1	51.8			69.4	
19	35.0		43.6		0.5			42.5			67.5			39.3		54.1			51.3		50.0	3.3	52.2			67.4	
20			44.9		0.4			42.8			67.6			41.0		53.1			51.3		49.5	2.0	52.6			64.8	
21			44.6		0.2			42.8			67.3			42.8		52.1		0.5	51.3			1.2	53.1			62.9	
22			43.5		0.2			42.3			66.5		19.1	45.8		51.5		1.8	5.21			4.8	54.2			60.3	
23			42.9		0.2	34.9		42.0			63.8		9.0	51.0		50.7		4.9	5.32			4.8	55.2			58.4	
24	34.5		41.8	31.1	0.2	35.2		41.0			61.8		6.7	66.7		48.8		1.0	5.32		49.5	5.0	56.9			56.0	

Month	May													June															
	2		3		4	21		25		26		27	6		7	10		11	14		15		16	23		24	
	W	H	W	H	H	W	H	W	H	W	H	H	W	H	H	W	H	H	W	H	W	H	H	W	H	W	H		
0																0.6	52.1													
1			3.0	151.	69.0			2.1	71.8	2.2	83.6	59.3			57.8	4.8	52.7	97.5			0.7	84.2	98.0			15.4	67.4			
2			0.9	155.6	68.4			5.0	80.6	2.4	83.1	59.0			59.6	1.8	53.4	95.2			0.9	87.2	96.4			19.4	84.6			
3			0.1	156.0	68.0			3.6	87.1	3.2	83.6	58.3			60.0	3.3	53.4	93.6			1.6	88.8	94.2			16.8	120.0			
4				156.4	67.6			2.4	97.8	0.8	85.3	57.7			60.5	2.5	54.1	91.8			2.2	92.0	92.8			19.6	197.8			
5		49.2	0.1	149.0	67.0			2.7	106.5	0.3	87.6	57.5			60.5	0.4	57.2	90.2			1.8	94.0	90.8			13.9	229.4			
6		49.2		143.7	66.7			3.8	115.0		88.6	57.2			60.5	7.1	61.4	89.0			1.3	96.3	88.8			22.9	308.4			
7		49.4		138.8	66.2			0.8	123.5		88.5	57.1			61.0	2.2	67.6	87.0			2.7	98.6	86.5			10.8	318.3			
8	1.0	49.7		133.4	66.1			0.6	128.6		87.8	57.1			61.2	1.9	78.0	85.3			2.6	103.3	82.6			9.2	356.0			
9	1.8	49.8		127.7	65.8			2.5	130.9		87.0	56.9			61.3	8.0	88.7	82.2			0.8	109.8				5.2	400.0			
10	1.6	50.0		121.6			5.0	2.2	130.8		86.4	55.7			63.4	0.1	100.0	82.2		70.4		115.1				11.1	412.5			
11	2.1	50.0		113.8					131.8		86.6	55.0			63.8		118.0				0.1	118.0				6.8	422.1			
12	2.3	50.2		108.0			46.7		141.3		85.4	55.0			63.8		128.7					119.6				0.7	430.0			
13	2.2	51.0		103.2					139.8		83.3	55.0			63.5		131.6				0.1	121.4				0.2	419.2			
14	1.9	50.5		98.6			47.4		136.3		81.2	54.5			63.3		132.0			71.3	0.1	128.2	50.0			0.5	422.0			
15	3.5	61.8		94.0			47.7		132.0		78.8	54.0			62.7		133.9			51.6	0.2	126.9	50.0			6.5	421.9			
16	0.8	68.2		90.1			47.7		124.4		76.6	53.5			62.3		131.6			51.8	0.5	123.6				17.0	421.7			
17	2.7	77.7		86.6			48.2		121.7		75.4	53.0			61.9		122.6			57.3	0.8	120.1				11.0	424.4			
18	3.0	88.0		82.2		1.4	48.3		116.6		74.0	52.7			60.6		113.0		1.5	62.7	1.0	116.0			55.0	8.0	428.8			
19	4.1	98.8		80.2		3.9			108.0		73.4	52.3			60.0		113.3		2.8	68.3	1.4	111.9	50.4	1.5	61.1	11.8	434.2			
20	4.3	108.4		78.4		4.3	78.6		97.2		73.3	52.2			59.1		110.1		1.4	75.0	0.4	107.1		0.1	60.4	2.8	430.4			
21	4.8	118.4		77.1		4.8			92.3		73.6	51.6			58.0		107.0		3.2	61.3	0.1	106.2		1.5	59.8		425.0			
22	4.8	128.4		76.1		5.1	78.5		88.6		73.2	51.2	1.0	56.7	57.6		106.6		2.3	65.5	0.3	106.1		11.1	59.5	8.1	438.1			
23	4.5	138.4		75.4		5.3	78.9	0.5	87.0		81.8	51.0	0.1	54.4	57.6		101.2		1.5	72.6		101.3		0.2	61.6	1.5	439.6			
24	4.3	148.4		75.1		4.8	78.5	0.1	87.4		80.7	49.8		57.1	57.6				3.0	79.5		100.0	46.1	1.1	62.0	0.4	439.5			

1 9 4 7

Month	June												July															
Day	25		26		27		28		29		30		1		2	9		10	16		17		18		19		20
h.	W	H	W	H	W	H	W	H	W	H	W	H	W	H	H	W	H	H	W	H	H	W	H	H	H	H
0																												
1	0.7	448.7		152.3	0.2	119.4	2.1	85.0	0.6	94.0		28.4	1.1	229.0	41.2			140.0			109.7				0.2	136.0	123.2
2	0.5	446.4		150.0	0.2	120.9	1.1	82.0	0.6	89.0		25.3	6.4	217.0	40.6			138.0			105.0				0.1	130.8	123.7
3	0.8	443.5			0.3	120.1	1.6	80.5	0.2	85.8	0.5	22.0	1.3	206.6	40.1			132.5			96.0					125.6	125.3
4	0.7	440.3		146.8	1.0	120.1	0.8	78.2	0.2	82.8	1.2	20.3	0.5	196.9	39.8		12.0	119.1			89.3					121.0	120.0
5	0.7	437.3		147.1	1.6	122.0	0.3	76.8		80.0	0.8	20.1		185.6	38.3	4.1	14.5	115.8			82.7					116.5	122.7
6		433.8		142.6	1.5	123.9	0.1	74.1		77.0	1.3	21.2	0.1	173.5	41.2	1.6	21.2	109.0			76.5					112.9	108.1
7		430.0		143.0	9.0	126.3	2.6	70.0		72.5	5.9	25.7		162.7	39.2	9.0	25.0	94.7			70.8				2.2	111.4	109.8
8		426.2		139.2	5.9	135.1	5.9	66.0		56.0		33.6		150.8	39.1	4.5	37.0	91.8			65.6				0.5	104.8	100.7
9		421.3		135.0	8.1	135.1	7.1	65.6		51.0		45.0		139.5	39.3	0.2		83.5			59.1				10.7	100.0	83.6
10				133.1	8.7	135.1	3.9	70.5		46.8	4.3	53.0		114.5	40.8	0.5	84.5	71.5			54.8		35.0	16.6	16.6	110.2	72.3
11				130.2	4.0	150.0	7.5	82.7		41.1	3.8	61.6		102.6	42.1		93.5	65.5			52.5				4.8	139.3	68.3
12				127.1	3.3	192.6	5.5	92.9		38.2	4.6	73.8		98.8	41.5		105.8	60.0		22.8	49.0		34.2		9.5	179.8	63.8
13				126.1	3.0	209.0	7.8	102.3		32.1	2.6	145.0		82.8	40.0	2.9	110.0	51.8		23.0	44.0	6.7	33.8		2.8	201.8	61.2
14		321.3		124.7	0.3	211.2	3.8	111.0		28.7	3.1	207.5		74.4	38.1	12.3	116.5	45.7	15.1	25.1	40.0	20.6	38.1		0.6	213.9	65.1
15				126.1		204.5	3.8	122.2		25.5		230.6		65.7	38.7	6.8	137.8	31.7		45.3	40.0	0.4	35.6		0.1	217.2	53.3
16				123.0		197.0	3.2	129.2		24.8		224.4		61.8		2.3	164.7	28.8	0.6	88.3	36.7	4.8	16.2		0.1	203.8	58.9
17				122.3		177.8	0.2	133.8		22.0		210.1		63.0			179.4	26.8	0.6	141.8	35.9	1.7	138.0		0.1	192.9	
18				122.1		158.8		134.0		23.8	7.1	192.5		57.1			192.0	26.5	1.8	151.7	35.8	1.2	161.9		0.2	183.1	
19		193.1		121.2		145.3		130.1		22.0	1.2	188.0		58.8			194.3	26.8	1.3	133.5	32.0	0.1	159.7		0.1	171.7	
20				119.7		131.3	0.1	123.3		21.7	13.8	185.0		58.5	34.5		182.5	24.2	1.7	125.5	31.1	0.2	160.5		0.3	168.5	
21				119.7		122.7	0.6	117.1		22.1	11.1	205.8		46.5			164.7	23.0	1.0	126.0	24.0	0.2	158.2		0.2	153.2	
22			0.7	119.3		114.0	0.1	110.0		24.1	6.0	230.2		43.5			150.0	27.8	0.1	126.3	32.2		157.1			146.7	
23			0.6	119.4		106.8	0.3	103.0		25.5	0.7	230.1		41.8			141.8	29.5	0.1	123.7	29.3	0.3	152.8			134.4	
24		139.0	0.1	118.4	2.0	89.5	0.7	98.7		28.1	0.2	240.5		41.6			139.3	27.0		117.4	28.5	1.0	141.6			129.7	

1 9 4 7

Month	Aug.										Sep.										Oct.				Nov.				Dec.			
	18		19		24		25		2		3		9		11		12		28		29		27		28		29		30		1		2	
	W	H	W	H	W	H	H	W	H	H	W	H	W	H	W	H	H	W	H	W	H	W	H	H	W	H	H	W	H	H	W	H
0																																
1			47.0			63.5			43.9								49.5				1.3	45.9			30.8			62.0				67.4
2			46.0			60.5			43.1								47.0				0.1	47.0			30.3			57.4				64.3
3			45.4			58.3			42.9								45.2					47.0			30.6			54.8				61.6
4			44.6			55.4			42.8								43.3				0.3	45.3			30.6			53.0				59.4
5			43.0			55.4			43.8		0.4	32.0					42.7				0.3	43.3			30.3			50.0				
6			41.9			53.0			43.8		10.2	33.0					42.2				0.7	42.2			30.2			49.0				56.5
7			42.3			50.0			43.3		1.6	34.0				0.1	40.7				0.6	41.9			29.2			48.0				
8			41.8			50.0			43.0		2.2	36.4				5.6	40.3				0.1	40.7			29.0			45.2				
9			39.5			46.8			39.6		0.2	39.1				9.5	42.6				0.2	40.6			27.0			45.8				
10			31.2			[illegible]			[illegible]			38.6		44.2		3.8	[illegible]					39.7			27.3	0.6	40.5	45.8				
11			32.5			49.0			35.2					44.1		1.4	50.0					39.2				0.2	41.0	41.2				
12			35.3			49.5	1.		35.5					42.8			43.8					38.1				1.6	41.1	41.4	0.3	36.1	44.3	
13			34.5		32.3	45.8	2.0		35.9					41.6			81.2					37.5		26.7		2.0	40.9	44.0		36.8		
14			33.4	0.7	33.9	44.4	8.8		38.4					40.2			78.2		28.7			36.8	2.0	27.1		1.9	39.3	45.1		36.8		
15	[illegible]		[illegible]		[illegible]				[illegible]					40.2			71.9	0.1	28.0			34.3	6.2	28.2		5.9	30.9	42.8	5.4	38.9		
16	[illegible]		37.0		[illegible]				33.6					39.6			69.0	5.	28.5			32.3	3.7	29.0		12.0	41.8	41.0	9.6	39.1		
17	[illegible]		[illegible]		0.				37.0					37.8		38.2	65.9		30.2			31.2	1.0	29.7		4.0	44.5	50.9	7.0	42.1		
18	[illegible]		[illegible]		[illegible]				[illegible]					36.7	0.1	38.1	65.1	0.1	29.8			30.6	0.1	30.1		0.7	41.4	40.7	4.6	48.2		
19		44.0		39.0	0.4	91.8			57.9					36.8	10.2	39.3	63.8		31.2			29.8		31.7			50.0	40.9	2.4	55.8		
20		47.5		39.2		89.0			56.0					37.0	2.4	40.2	63.8	14.6	32.0			29.4		32.0			56.1	41.2	0.7	63.9		
21		54.5		39.3		81.7			52.9					37.8		41.8	60.0	1.2	35.4			29.3		31.7			61.8	41.6		70.0		
22		53.2		40.0		73.2			50.0					39.1		47.0	56.3	2.5	38.6					31.7			65.2	40.6		73.2		
23		50.8		40.0		68.5			48.6					38.4		49.5		0.2	42.0					31.5			65.2	40.6		73.0		
24		[illegible]		39.0		[illegible]			45.1					35.9		60.0		0.8	44.0			29.0		31.3			64.2	40.3		71.0	38.1	

1947 1948

Month	Dec.													Mar.					June						July					
D.	7		8		9		10		27		28		29	13		14		15	13		14		15	3		4		5	
h m / Tide	W	H	W	H	W	H	W	H	W	H	W	H	H	W	H	W	H	H	W	H	W	H	H	W	H	W	H	W	H	H
0																														
1			0.6	41.5			3.4	50.7			1.6	94.0	55.3			1.9	68.0	100.2			0.6	63.9	107.6			0.1	232.2	96.1		
2			0.1	42.0			1.4	52.8			1.6	96.3	55.2			3.1	72.3	98.3			6.8	62.6	100.3				313.0	86.7		
3				44.2			2.2	56.8			1.4	103.6	54.2			2.6	77.5	94.1			3.6	63.9	98.7				300.0	82.6		
4				44.7			0.3	61.3			0.1	104.4	51.3			0.4	86.5	77.4			2.4	64.3	96.7				290.0	79.4		
5				44.7				69.8			0.8	101.1	47.7			0.4	94.0	75.0				64.6	81.0				271.6	77.3		
6				45.2			0.1	71.2			2.2		48.7	39.3		2.0	99.0	74.5				64.6	68.0				261.3	73.2		
7				45.1			0.1	71.1			2.8		46.9	39.7		1.7	103.5				9.0	64.6	61.3				251.0	72.3		
8				45.8			0.1	70.1			1.2	98.2	45.0	1.0	40.1	1.9	106.0				4.2	64.6	50.2				231.5	70.7		
9								68.5			0.4	96.6	44.5	2.9	40.7	0.7	107.7				0.8	64.6	47.6				215.8	70.5		
10				41.3		37.6	2.0	65.6			0.3	95.0	42.3	2.0	41.7	1.7	108.5				4.0	68.2	46.1		120.7		195.5	70.5		
11				41.1				64.3				93.8		2.4	51.1	1.0	109.5				5.8	74.3	37.2		123.2		188.0	70.2		
12				41.3		38.6		63.9				90.7		8.3	51.2	0.2	109.5			35.4	6.6	87.0	35.5		128.1		185.0			
13				40.8				64.1	1.2			86.7		5.0	51.3	0.5	109.5			36.0	9.6	96.4	35.3		124.8		167.8			
14				40.8				64.0	1.0			81.5		0.8	51.4		109.5		0.6	34.0	11.4	97.7	34.0	12.7	124.6		162.5			
15				40.2		38.0		63.5	0.8			82.1	40.0	0.6	51.5	0.9	109.5		1.7	38.6	6.8	98.4	25.0	2.1	143.5		153.0			
16				39.9	2.7	38.0		62.0	0.8			79.4		6.8	52.4	2.1	109.5		0.1	36.0	4.2	99.2	23.6	0.7	152.0		141.1			
17				38.6	1.1	38.6		61.4	0.9	42.6		74.8		1.5	53.4	3.3	106.0		1.6	34.9	0.7	100.3	29.1	56.2	234.3		132.8			
18				39.0	5.6	40.2		58.9	3.0	42.3		71.0		3.0	54.6	1.1	104.0		3.0	36.5	0.2	106.0	27.5	2.4	248.2		125.0			
19		34.9		38.9	0.4	42.1		57.9	5.5	45.2		69.7		1.9	54.6		104.0		2.8	38.8		150.0	24.0	4.0	303.0		121.0			
20	3.0	35.3				43.3		55.5	3.8	52.6		67.8		3.0	54.7		104.7		4.5	46.6		150.3	22.0	5.2	343.7		120.8			
21	2.8	36.2			0.1	45.1		55.0	6.4	81.7		60.8		1.8	55.0		106.3		3.9	52.5		149.0	17.0	0.5	350.2		118.0			
22	1.0	36.6			0.2	46.6		53.5	3.8	91.1		56.8		1.4	55.6		106.3		3.5	55.5		131.1	20.0	0.4	353.4		111.7			
23	0.8	37.2			3.1	48.0		51.0	3.4	96.3		54.5		1.0	57.0		104.8		1.7	60.0		123.1	19.0	0.1	353.3		106.2			
24	0.7	39.7		37.3	1.9	49.0		50.0	2.0	97.5		54.6	37.0	1.1	65.0		102.2		5.0	60.0		115.0	18.4		346.8		102.0			

Month	July																				Aug.				
	8		9		16		17		18	19	20		21		22		23		24		4		5		6
	W	H	W	H	W	H	W	H	H	W	H	W	H	W	H	W	H	W	H		W	H	W	H	H
0																									
1	4.0		5.5	249.5			0.2	144.8	119.0		110.6		146.6		118.2		111.6	0.1	159.0	122.5		70.3		82.5	108.6
2	10.4		0.8	236.6				144.2				0.6	146.0		117.2	0.4	112.5	0.2	153.5	122.0			0.2	83.4	105.0
3	3.6	49.8	0.3	224.5			0.1	145.4					143.0		116.9	1.8	112.1	0.7	149.5	120.7			0.1	83.3	102.6
4	5.2	50.0	0.2	218.8				146.0					140.4		116.6		113.2	4.4	147.5	120.1				84.0	101.2
5	16.0	58.6	0.1	214.4			0.4	144.0					139.1		116.0	0.2	112.6	1.7	147.5	119.3				82.9	101.0
6	2.8	53.5	0.2	210.1			0.1	143.1	116.8		111.0		137.2		115.1	0.1	112.3	0.6	148.6	118.5		71.7		81.2	100.0
7	2.9	89.7	0.1	203.0				140.0					134.9		115.2	0.1	111.4		149.8	118.8				81.1	98.7
8	2.0	90.0	0.3	199.0				138.6					133.5		110.1	0.1	111.1		149.2	118.4				80.1	97.0
9	0.9	90.5	1.9	188.2				137.4					131.3		109.7	0.1	108.8	0.3	149.0	118.8				79.7	94.7
10	2.5	89.1	0.3	185.3				136.7					129.8		107.4		108.7		148.4	118.2				79.0	94.3
11	0.8	91.5		180.5				136.5					128.8		106.2	15.0	112.8		145.6	118.2				76.4	93.7
12	0.8	91.5		177.3				135.1	111.5		106.1		127.8		105.0	2.5	122.0		143.6	117.6		71.5		75.6	91.1
13	20.2	87.8		171.7				134.4			105.0		125.9	1.7	104.3	1.2	130.0		140.0	116.5				76.0	83.0
14	1.5	91.0						131.2			102.2	0.1	124.2	1.9	103.6	1.7	138.6		136.4	115.6				74.8	82.1
15	1.2	90.5				135.2		131.1			99.4		122.9	0.8	104.6	3.7	156.0		130.8	115.2				74.4	82.3
16		90.1			1.4	135.0		128.2	3.6	100.8	0.1	121.9		106.2		160.3		125.5	114.0				73.1	81.2
17	0.8	87.5				132.6		126.2	5.6	100.6		120.8	3.3	109.6		174.6		126.6	112.6				73.6	81.1
18	3.1	289.2			0.1	131.5		126.7	110.2	2.3	102.6		119.9	1.2	108.6	0.1	156.5		124.1	110.2		70.0	1.3	75.1	80.0
19	1.5	277.0			0.1	128.5		127.0		11.0	112.0		119.4		106.8		175.5		123.6	109.8		70.3	19.1	82.0	79.9
20	1.8	277.0				127.5		127.0		0.1	128.7	0.3	119.1	0.1	107.5		173.6		122.5	108.5		69.2		83.5	79.5
21	2.7	277.7				137.3		124.8		0.7	134.4		118.4	0.5	108.0	1.1	171.7		124.5	108.1	0.3	71.2		104.4	80.6
22	5.3	270.2				144.3		122.0		11.5	140.0	0.1	119.4	0.1	109.1		168.8		124.0	109.6	1.6	73.0		123.6	82.5
23	3.8	267.7			0.4	146.3		120.8		0.1	145.0		119.0	0.2	109.2	0.3	166.1		124.2	106.8	3.8	78.0		121.1	83.0
24	2.8	254.0				146.3		116.6	115.0		145.5		118.3	1.4	110.3		162.7		123.6	106.5		80.9		116.0	83.6

1 9 4 8

Month	Aug.											Sep.															
Day	25		26		27		28		29		30	2		3	10		11		12		13	20		21		22	23	
W.H Time	W	H	W	H	W	H	W	H	W	H	H	W	H	H	W	H	W	H	W	H	H	W	H	W	H	H	W	H
0																												
1		57.8	0.8	67.6	0.1	110.7	2.1	149.0	0.1	101.6	77.8		63.8	66.5				62.9	0.1	89.6	83.7		55.5	0.6	59.6	58.9		56.6
2			5.5	67.8		108.6	6.4	155.7	0.1	99.2		0.1	63.8	65.6			0.3	61.2	1.6	89.3	81.0			1.0	60.0			56.0
3			1.2	68.2		100.5	7.2	157.0	0.1	98.9		3.2	64.5	65.6			2.0	60.9	0.1	87.0	78.7				60.4		0.6	56.2
4			7.7	70.0		98.1	6.6	164.0		98.2		9.6	65.8	64.7			0.8	61.3	0.2	84.0	77.6				60.2		0.6	56.5
5			8.4	76.0		96.0	1.2	165.0		97.6		0.3	65.8	63.9			1.6	62.1		83.4	76.4			1.7	60.4		0.2	55.7
6		55.4	3.6	85.0		91.3	1.3	160.7	0.1	96.1	75.0	1.0	65.7	64.0		58.8	3.2	62.3	4.7	82.1	76.0		56.0		60.0	57.6	1.9	56.7
7			14.2	97.0		88.0	2.2	155.0	0.1	91.5		0.1	65.8				3.2	63.0	0.3	81.3	75.1				59.4		3.3	57.7
8			2.5	110.5		87.2	0.1	147.0		91.9			66.5				0.9	65.0	0.2	82.8	74.5				61.4		7.6	59.0
9			5.3	128.3		85.0		140.0		90.0			65.0				0.1	68.0	1.0	84.7	74.5			0.5	62.3		0.6	59.7
10		53.7	1.4	148.0		80.5	0.8	132.6		89.4			66.0				0.7	70.7	1.3	87.5	72.6			1.4	64.6		0.9	60.0
11		53.0	1.9	157.4		77.0		126.0		88.4			65.8				0.3	71.2	0.7	87.5	71.9				62.3		1.2	61.0
12		52.2	1.0	159.6		74.2	0.1	121.2		87.3	73.2		65.2	67.6		57.3		71.1	3.1	87.6	71.5		55.1		62.6		1.3	62.1
13		53.1	0.1	159.0		74.1	0.2	116.0		86.3			66.0			58.5		70.5	4.1	86.4	71.0		55.5		62.7	58.0	0.1	63.5
14		54.1		159.0		72.3	1.8	113.9		85.2			72.3			58.4	0.5	70.0	6.8	84.6	70.9	0.1	55.8		61.9			61.0
15		54.1	2.1	146.1	6.1	73.5	0.4	112.3		83.1			72.3		11.1	60.1		68.2	9.6	85.8	70.6	0.2	54.9		62.0			63.3
16		55.0	1.6	141.4	6.9	74.4	0.3	111.2		82.2			71.9		5.4	60.5		66.8	0.1	90.0		0.9	55.6		63.6			64.4
17	1.0	56.2	6.5	136.4	0.2	76.5	0.7	109.8		81.8			71.2		1.0	60.5	0.1	65.9		102.1		0.9	56.3		62.8		20.1	67.2
18	0.5	56.3	0.7	133.0	2.7	79.3	0.1	108.3		82.3	71.5		70.0	65.1	0.1	61.7	2.0	65.3		100.4	70.2	1.1	56.3		62.5	57.2	1.9	73.0
19	1.7	57.0		129.6	0.4	81.0		107.8		81.0			69.0			63.5	5.4	66.3		98.3		5.4	57.4		62.8			94.0
20	4.2	57.6		125.2	6.3	84.4		107.3		80.8			67.2			63.8	6.2	68.6		96.0		2.4	58.7		61.8			116.0
21	6.6	59.1	1.2	122.6	1.8	88.0	0.7	107.0		80.6			67.3			63.0	3.0	72.0		94.7	70.2		59.6		60.6			129.0
22	1.6	60.4	4.0	120.9	17.6	94.4		106.3		81.8			67.6			62.3	0.4	77.7		92.0			60.0		60.1			122.5
23	0.3	63.2	1.5	118.0	19.8	111.3		102.3		79.6			67.1			62.2	2.1	82.6		89.9			61.3		59.7			110.5
24	0.3	66.3	0.5	111.1	4.6	130.0	0.1	102.1		78.6	70.2		66.8	66.0		63.7	0.3	88.0		84.8	68.8		61.2		58.6	57.3	0.4	108.0

1948

Month	Sep.					Oct.										Nov.							Dec.					
Day	24		25	26		27	28	9		10		11	29		30	3	4		24		25		6	7	8	20	
	W	H	H	W	H	H	H	W	H	W	H	H	W	H	H	W	H	H	W	H	W	H	W	H	H	H	W	H
0																												
1		102.8	58.6		55.0	100.0	58.6			7.0	55.7	57.6		48.6	93.0		42.6	50.5		40.0	1.2	58.0		31.7	72.1	37.9		39.9
2		100.0				90.0				5.6	61.0				91.8		49.6				0.1	59.3		31.9	69.2			
3	1.6	98.0				83.5				2.1	71.0				91.0		48.2					59.7		31.3	61.0			
4		94.5				81.2				0.2	85.0				89.0		49.2					60.1	0.8	31.4	54.7			
5		92.8				78.0					91.6				86.0		49.2					60.1	0.4	31.7	52.4			
6		89.0	58.2		52.7	75.5	58.3				84.3	58.0		48.1	83.5		41.5	47.9		41.5		59.1	1.8	32.5	49.5	36.7		41.0
7		89.0				73.1					92.0				80.6		47.1			41.1		58.3	2.1	33.2	49.8			
8		87.2				71.1					89.8				78.0		45.6		3.5	42.0		57.2	1.1	34.4	48.9			
9		89.0				69.0					86.7				75.4		44.6		2.7	42.7		57.7	3.1	37.0	47.0			
10		88.0				68.1					83.0				72.1		41.9	45.3	1.5	43.6		55.0	3.5	37.9	46.2			
11		87.2				66.0					78.0				69.3		42.2	45.4	0.9	44.4		48.8	7.2	38.5	43.2			
12		87.0	1.6		57.0	67.5	56.3				77.8	55.7		50.5	67.0	0.9	43.0	46.2	0.6	45.1		47.6	5.7	42.2	39.5	34.5		39.0
13		87.0				68.1					82.6		0.2	50.8	65.2	1.1	44.3		2.3	45.0		48.0	5.6	46.9	39.8			39.5
14		84.5				61.5					80.2		0.4	50.7	58.8	6.3	45.0		1.8	47.5		51.5	7.3	56.1	40.5			39.5
15		71.0			57.1	63.0					67.8		2.6	50.9	47.8	1.5	46.1		1.9	49.0		43.0	1.4	68.9	39.4		0.5	39.4
16		69.1			58.0	63.0					66.5		3.0	51.1	59.1	0.1	46.9		1.6	49.2		42.0	1.9	79.0	39.3		1.1	39.7
17		68.7			56.8	62.0					64.9		2.6	53.0	49.2	0.2	48.0		0.4	50.3		41.0		88.8	39.2		2.1	40.2
18		67.0	0.8		58.0	61.8	56.0				63.7	55.1	6.1	55.0	49.2	1.3	49.9	45.6	0.4	52.7		39.5		92.2	39.2	39.5	3.1	40.5
19		60.9			56.0	61.4					62.1		3.2	57.2	47.8	0.1	50.8		0.3	54.0		37.8		90.8	39.0		4.3	41.7
20		61.2		16.7	57.8	61.0					60.5		4.1	61.0	44.0		51.7		0.1	55.8		39.2		87.8	38.8		1.8	43.2
21		62.3		0.1	62.4	60.3					60.2		5.3	66.0	43.1		51.6		0.9	56.3		38.0		86.0	38.7		0.3	44.6
22		60.6			72.0	60.5			51.0		59.5		4.0	74.0	43.5		53.0		2.4	56.6		38.8		80.6	38.4		2.5	46.9
23		59.0			101.0	59.9		2.7	51.1		59.5		0.8	80.4	41.3		52.4		0.6	56.7		38.6		77.7	37.3		4.9	50.4
24		58.5	1.6		112.1	59.0	61.2	8.3	53.3		59.1	51.8		83.0	43.6		51.6	45.2	0.6	57.0		38.6		74.9	38.2	37.2	1.0	52.5

	1948												1949															
Month	Dec.												Jan.			Feb.												
	21		22	23		24		25		26		27	30		31	1		2		11		12		13	22		23		24	
	W	H	H	W	H	W	H	W	H	W	H	W	H	W	H	H	W	H	H	W	H	W	H	H	W	H	W	H	W	H
0																														
1																														
2	7.0	68.4	53.1		37.0			0.2	64.0		90.4		58.0	6.4	46.6	51.3			58.8			1.3	67.8					0.4	60.3		45.6
3	3.8	81.5	50.4	1.0	36.0				61.0		89.3	1.3	58.6	9.0	48.3	50.7			58.4			0.9	66.8					2.4	60.0		44.6
4	0.3	98.0	50.4	2.5	38.6				54.2		85.4	1.3	59.4	5.7	50.0	50.5			57.0			1.1	67.5					2.5	60.2		44.6
5	0.3	109.9	44.0	0.8	39.2			1.8	52.4		80.8	0.4	62.7		53.2	49.5			54.9			0.5	66.1					3.5	61.6		42.6
6	0.5	112.2	41.0	2.4	41.2		36.2	4.4	53.0		78.5		62.5		58.3	49.9			58.1			0.5	66.3	57.5		44.9		1.2	65.3		41.3
7	0.1	111.3	40.2	0.8	40.2		35.3		53.1		75.0		65.1	2.1	63.5	49.8			44.1				66.4			45.4		1.1	69.8		40.5
8	0.6	112.4	42.4	0.4	43.0		38.6		56.2		71.0		66.7		67.8	49.7			42.1				67.1			46.3		2.2	74.3		38.4
9	0.3	107.2	41.2	1.0	45.1	0.4	40.2	0.8	56.4		70.2		68.1		70.6	49.1			41.0				66.3		0.5	45.6	0.2	78.3		38.0
10	1.0	100.6	41.4	0.8	46.3	3.0	42.1	0.2	58.6		69.2		67.8		69.5	44.6		40.2	41.8		41.0		66.9		2.5	45.3		80.3		37.0
11	2.3	97.7	42.1		49.5	2.5	41.3	0.7	59.4		69.0		66.4		68.5		3.2	41.0	43.3		41.7		65.0		3.0	45.0		82.0		38.6
12		95.4	40.0		51.2	11.8	44.0	0.3	59.4		68.0		61.8		67.1		12.6	43.3	44.3		43.0		64.5		2.6	46.2		82.5		37.9
13		93.5	40.2	0.1	51.8	5.5	51.3	1.1	60.2		63.0		62.0		65.5		1.0	49.0		0.8	44.0		65.9		5.4	45.7		83.7		34.7
14		90.0	41.0		49.5	0.4	65.0	0.1	60.2		60.8		61.2		64.4		0.4	56.7		0.2	44.0		63.1		2.7	48.7		82.9		34.7
15		89.5	39.7	0.8	51.0		76.0		59.8		63.2		60.7		63.2		1.4	63.0			44.4		62.1		1.0	54.2		81.3		37.2
16		88.5	40.2	0.9	49.5		83.5		58.0		62.8		60.5		62.3		2.4	65.0		0.8	44.9	1.0	61.4			60.0		78.6		38.2
17		85.6	40.0	0.1	49.9		84.5		58.1		61.9		60.0		61.9			67.3		4.4	45.6		60.6		0.2	63.1		77.1		38.5
18		82.4	39.0	0.1	51.2		83.2		57.1		59.3		59.4		61.0			67.3	43.9	7.2	48.5		59.7		0.3	65.1		75.6	0.5	38.4
19		80.5	39.7		52.5		81.0	2.6	57.0		59.2		58.0		59.9			65.9		7.0	51.2	0.6	57.5			65.8		73.3		35.9
20		77.0	40.0		52.4	0.5	77.9	3.6	58.6		58.4		56.4		57.9			63.4		1.6	54.6		56.8			65.4		70.7		35.9
21		72.5	39.0		52.9	0.2	74.8	7.0	61.7		57.9		52.4		56.0			64.8		0.8	58.3	0.4	56.6			64.6		68.2	0.5	
22		71.4	39.5		47.0	0.9	70.4	3.8	71.0		57.2		54.9		55.1			65.2		0.6	62.8		58.2		0.2	63.3		65.5	2.0	41.3
23		56.0	39.3		42.4	0.2	65.8	0.5	80.8	2.5	50.7		55.5		55.1			63.0			68.0		58.9			62.1		66.3	3.0	43.5
24		49.4	38.7		41.6	0.4	65.6	0.5	88.5	1.5	55.2		52.3		53.2			52.5	43.1		68.7		59.9		0.6	61.6		65.0	5.0	44.2

1 9 4 9

Month	Feb.			Mar.																Apr.						
Day	25		26	5		6	10		11	12	13		14		15		16	17		18	3		4	23		24	25
	W	H	H	W	H	H	W	W	H	H	W	H	W	H	W	H	H	W	H	H	W	H	H	W	H	H	H
0																											
1																											
2																											
3																											
4																											
5	1.5	78.2	57.9	5.2	41.0	49.6			139.1	49.8				121.7	2.7	103.6	77.1			69.4		50.8		1.0	46.1	53.3	
6																											
7		83.8	57.2	12.4	50.5	45.5			128.8	44.5				108.2	1.6	114.0	76.8			64.6		52.3		3.3	47.2	50.2	
8		84.8	53.3	5.4	66.8	45.7			122.0					102.3	1.1	118.0	76.4			66.7		53.1		5.1	48.9	49.6	
9		85.0	53.3	1.2	84.5	49.7		40.0	118.3					100.5	1.2	119.0	75.5		55.1	65.0		53.5		1.2	40.6	49.3	
10																											
11																											
12																											
13																											
14																											
15																											
16																											
17																											
18																											
19																											
20		60.9	45.2		77.5	1.1	186.7	69.0				42.0	3.3	95.1		94.7	57.4	5.0	58.0	57.2		56.6			60.6	42.8	
21																											
22																											
23																											
24																											
25																											

Month	Apr.							May																		
Day	26		27		28	30		1	2	6		7	12		13	14	19		20		21	22		23		24
W.-H. / Time	W	H	W	H	H	W	H	H	H	W	H	H	W	H	H	H	W	H	W	H	H	W	H	W	H	H
0																										
1		36.3	0.4	171.6	62.5			123.3	61.4	5.0	43.5	65.2		42.9	90.3	51.7		59.0	18.4	212.7	138.2			3.2	219.4	174.3
2			0.3	161.7				120.0		1.4	46.6	63.3		43.9	88.0	51.0			5.1	229.5	130.3			9.6	220.5	173.7
3			0.3	154.6				116.4		6.0	48.9	60.1		44.3	86.6	50.3			7.4	241.7	118.3			4.3	222.5	171.3
4			0.4	146.6				113.1		3.0	52.3	59.7		45.2	85.5	50.0			7.5	254.7	116.2			7.3	234.0	172.6
5				141.5				104.7		2.5	56.7	59.0		44.0	83.9				6.0	262.1	118.3			7.1	249.5	160.0
6		38.0	0.4	135.7	59.5		42.7	102.5	60.1	1.8	62.1	59.0	2.0	44.0	82.1			59.4	3.0	270.5	112.5			14.6	266.0	148.7
7				130.8				101.8			67.2	56.7	1.2	44.5	81.1				0.2	279.3	102.0			3.1	275.7	151.9
8				127.6				102.9			70.8	57.4		46.0						283.0	99.0			3.8	280.8	139.0
9				130.3				100.5			73.7	59.8	1.0	47.3	79.5					283.2	98.6			5.2	284.0	128.5
10			0.5	131.5				97.8			75.5	58.2	1.0	48.1	77.0					279.5	96.5			0.6	286.8	125.7
11	0.3	41.0		126.7				96.7			76.5	55.5	1.0	49.5	73.9					272.1	95.3			5.4	290.0	105.5
12	4.8	41.5		121.5	50.3		45.5	94.5	52.5		76.4	55.1		49.9	72.9			55.2		264.5				2.3	288.7	106.0
13	2.2	42.4		117.8			46.3	92.0			76.9		4.0	49.7	68.3			55.4		254.4	89.8			0.6	292.5	107.7
14	8.5	44.1		107.7		1.8	47.4	88.1			76.5		2.3	51.3	64.1		0.2	53.8		244.9	86.2			1.3	288.6	106.8
15	12.0	48.0		103.9		6.1	49.7	84.9			75.9		3.0	54.0	65.2		1.4	55.9		209.8	75.4			1.0	280.7	
16	11.6	54.7		102.4			51.7	82.0			70.2		3.4	56.8	63.1		1.1	55.9		194.0	80.2			1.4	268.7	
17	9.6	72.8		94.7		4.4	56.5	77.3			70.0		6.0	61.9	60.0		4.0	55.7		180.5	84.0				254.1	
18	8.9	105.0		92.0	44.1	4.0	64.1	76.4	49.5		68.8	53.7	10.0	67.9	59.0		13.8	58.3		168.2	81.9		59.5		240.0	
19	10.0	136.3		75.0		5.6	78.6	75.6			71.0			76.3	57.1		4.4	64.3		158.0	87.0	7.0	59.0		228.8	
20	5.5	165.0		63.6		7.0	96.2	75.0			70.7			84.7	53.4		11.1	75.8		154.9	86.5	10.1	63.1		218.0	
21	0.8	186.1		63.9		3.1	109.3	65.7			69.0			90.9	53.0		15.1	100.0		149.3	87.6	17.1	71.8		205.0	
22	1.7	191.4		58.7		0.4	119.5	58.7			67.9			96.1	54.5		15.2	133.2		145.2	85.4	16.0	107.3		195.5	
23	1.8	187.7		60.6		1.6	126.2	58.5			64.1			94.9	53.0		6.8	164.0		141.8	71.6	2.4	156.0		190.1	
24	1.1	179.7		62.8	41.0		126.5	61.8	45.5		64.9	51.1		91.0	54.2		6.9	186.7		137.1	71.1	2.8	212.0		188.1	

Month	May						June																Aug.		
Date	27		28		29	30	6		7		8	9	15		16		17	18		19		20	1		2
Hour	W	H	W	H	H	H	W	H	W	H	H	H	W	H	W	H	H	W	H	W	H	H	W	H	H
0																									
1			2.5	61.1	103.1	66.7			3.6	56.0	124.1	78.2		57.8	5.5	64.0	116.4		69.6	8.9	301.2	281.5			153.7
2			5.6	63.9	100.3	73.1			9.5	59.7	123.3				2.4	71.5	105.0		70.3	8.0	307.8	277.5			149.3
3			4.0	68.1	90.5	73.6			6.8	67.8	114.0				5.6	78.7	99.3		71.4	5.8	311.3	273.5			145.8
4			3.2	73.5	92.8	72.0			2.4	80.0	110.3				2.5	89.0	105.1		71.9	6.8	312.1	268.8			142.0
5			3.4	80.5	88.7	74.0			2.7	88.0	109.9				4.6	102.7	104.5		72.0	5.4	314.2	264.4			137.9
6			8.8	89.5	88.5	74.2			2.3	95.1	107.5	76.7		58.5	9.7	127.0	97.6		71.8	8.4	318.0	259.3			134.0
7			4.3	104.2	87.7	74.3			2.5	103.7	103.9				9.1	166.0	93.8		72.1	6.0	323.7	251.4			132.5
8			6.6	120.3	80.7	74.7			1.0	115.9	101.5				12.0	203.0	90.3		73.1	10.9	331.0	239.0			130.8
9			5.9	142.3	78.7	75.5			1.4	111.0	101.2				7.1	222.1	88.7	0.2	73.3	4.0	339.0	228.5			129.1
10				168.2	73.7	76.0			1.0	116.1	97.2				3.2	232.3	86.7	1.2	73.9	7.0	344.8	222.1			126.9
11				175.6	72.5	74.7			3.2	112.7	93.9				1.2	237.2	84.4	3.7	76.0	4.0	349.7	214.8			125.3
12				177.0	74.0	73.8			0.9	111.2	92.7	74.8		58.7		235.6	81.3	3.6	74.5		350.6	208.0			123.0
13				171.6	72.5	75.2			4.5	416.5	90.3					226.8	80.6	1.8	81.9		349.2	201.0			121.1
14				160.8	70.8	75.2			10.8	122.8	87.0					217.0	79.0	3.4	90.0		345.7	195.5			119.8
15				152.5	71.5	74.1			7.4	140.0	80.1					206.5	76.3	5.1	99.7		341.0	190.0		106.3	118.5
16				140.0	69.6	75.0			0.3	163.7	80.1					195.7	76.4	5.1	136.3		336.1	185.9		106.3	117.5
17				133.5	68.7	74.8			0.3	172.1	79.4					185.7	74.5	6.2	162.7		328.7	181.8	19.5	107.7	118.2
18				125.8	70.7	72.2			0.3	174.5	79.5	71.8				166.6	74.5	5.2			322.5	178.7	10.0	123.1	118.1
19				121.5	71.7	71.2	52.1	0.3	169.8	70.8				55.8		154.0	73.9	5.6	203.9		313.3	177.1		155.5	117.9
20		61.1		115.7	70.8	62.9	53.4		159.3	79.0				56.1		139.0	73.2	7.6	228.1		307.3	176.8	2.8	167.7	117.4
21	0.5	59.3		113.0	69.5	69.1	55.9		149.7	78.4				52.4		126.9	72.1	6.1	250.7		301.8	177.8		168.5	117.7
22		61.1		107.1	67.9	66.7	2.0	55.8	142.7	76.8				53.3		122.0	71.8	8.0	271.0		294.7			166.0	118.7
23	0.2	61.6		106.5	69.4	67.0	0.6	54.9	136.5	76.2			2.4	54.8		119.6	71.2	7.0	282.0		290.0			162.0	119.0
24	2.0	62.8		105.1	70.5	65.3	1.4	55.0	131.8	77.7	68.4	5.6		57.3		118.9	70.3	7.0	290.7		286.1			159.0	119.5

1 9 4 9

Month Aug.

Day	3	12		13		14	15		16		17		18		19	20	21	22		23		24	25	
W, H / Time	H	W	H	W	H	H	W	H	W	H	W	H	W	H	H	H	H	W	H	W	H	H	W	H
0																								
1	119.0			0.2	136.2	140.0			1.0	247.0	5.7	265.9		315.5	220.0	166.7	142.8		137.2		149.5			134.8
2					142.0	137.1				260.2	3.6	268.3	1.6	315.7	216.2			0.2	136.8		149.9	139.2		
3					143.8	134.0			0.5	264.2	3.8	271.1	12.0	310.7	214.5			0.1	136.3		148.2			
4					143.1	132.4			0.8	261.8	3.0	272.7	7.6	310.7	213.5			0.3	136.0		147.9			
5					142.1	131.5			1.8	255.9	5.0	274.9	0.5	313.5	211.2			3.2	135.1		146.7			
6	116.3				141.7	130.1			0.3	252.0	11.0	276.2	1.0	313.1	212.1	158.8	141.9	2.8	135.9	1.5	148.3	137.5		133.1
7					141.0	128.3			0.3	248.7	6.4	281.2		311.0	210.3			7.6	140.0	5.2	153.9			
8					140.0	126.5			0.2	243.7	11.7	290.0	0.3	307.0	206.6			8.3	144.9		156.7			
9					136.7	125.3			1.2	240.0	7.7	298.0		300.9	202.1			5.5	150.0	5.4	156.3			
10					133.9	124.3			0.6	236.0	9.8	306.0		293.7	198.0			3.2	161.5		155.7			
11					131.4	123.5			2.9	233.6	12.4	316.8		280.1	195.5			3.6	170.6		154.3			
12	113.6				130.5	122.7		126.4	1.3	233.2	1.4	324.4		273.7	192.8	151.3	140.7		169.6		155.3			132.6
13					129.1	121.8	1.5	126.0	3.9	233.9	1.7	327.5		268.3	189.0				169.6		153.5			
14				23.7	130.2	121.2	0.3	127.5	2.6	236.0	7.5	326.8		263.9	185.8				167.6		150.9			
15			110.5	14.5	149.3	122.2		129.1	2.5	238.3	1.1	323.1		260.4	184.5				162.3		148.5			
16			111.2		166.3		2.4	133.4	6.9	241.5		319.0		257.8	181.8				158.2		146.7			
17		1.0	111.6		173.3		5.6	142.5	3.9	246.3		313.0		254.9	177.6				156.3		144.9			
18	113.8		111.6		173.3		8.9	158.1	4.4	249.7	0.2	306.8		250.5	175.9	149.3	138.3		153.0		144.3	138.3		130.5
19			112.0		168.3		4.4	190.1	5.4	252.3	3.8	299.7		246.8	173.5				152.3		143.2		6.3	134.1
20		5.9	112.8		161.7		0.9	229.4	2.7	255.5	2.3	299.8		242.2	172.7				150.3		142.4		11.5	141.3
21		0.6	113.0		155.0		0.5	244.3	2.4	247.7	9.0	292.8		236.3	171.0				149.3		141.6		12.8	148.1
22		6.0	114.0		149.7		0.6	238.0	6.8	248.5	5.0	294.3		230.3	169.5				148.5		141.0			150.3
23		14.9	117.6		145.6		1.6	245.1	6.0	249.6	4.4	301.0		227.6	168.8				149.0		140.0			154.9
24		0.9	125.7		142.3			243.7	4.4	262.5		308.0		224.3	167.6	140.1	137.5		148.9			135.4		164.4

Month	Aug.									Oct.									Nov.				
	26		27		28	29	30	3		4		5		6	7	8	4		5	6	7	8	
	W	H	W	H	H	H	H	W	H	W	H	W	H	H	H	H	W	H	H	H	H	W	H
0																							
1		153.8		149.3	151.6	134.9	129.5		134.9	1.0	141.4	1.2	198.0	271.8	175.2	146.0		109.0		121.1	117.9		116.5
2		149.3		147.0	151.1					0.4	143.7	0.6	195.2	268.1	172.7			109.0					
3		152.3		147.8	150.3						143.3	1.0	193.6	264.0	169.4			108.0					
4		158.8		144.5	148.9						142.8	0.2	190.7	260.3	167.6		1.5	108.8					
5		156.8		144.7	147.1						143.1	0.5	187.6	256.1	165.2		1.7	109.0					
6		156.2		146.3	146.0	135.1	128.7		132.2		139.5	0.9	184.5	249.8	163.2	130.1	2.0	109.2		119.7	117.6		116.1
7		158.9		141.0	144.0						138.2	2.1	181.7	245.5	160.5		1.4	109.7				0.1	116.1
8		153.2		140.0	142.1						135.7	1.8	182.0	243.3	157.1		3.4	110.6				0.4	116.0
9		153.3		138.1	140.8						134.9	3.2	183.4	240.0	156.6		3.6	111.2				0.3	116.1
10		152.4		138.1	142.3					0.8	133.8	6.6	185.6	237.5	155.2		5.0	112.8	131.6			0.8	116.0
11	1.6	152.6		136.3	140.3					2.1	132.5	8.5	198.6	236.0	154.5		8.5	113.3	130.2			1.6	116.2
12	1.9	153.4		136.4	141.1	134.1	127.1		130.3	1.0	132.7	3.4	217.3	232.1	152.1	137.6	6.8	118.9	128.1	118.6	117.1	2.7	116.4
13		153.3		136.7	136.4					4.0	134.0	5.8	230.1	227.5	151.4		6.7	126.0	127.4			1.7	116.8
14		150.6		136.3	135.4					1.0	136.7	8.0	240.7	222.3	152.0		10.0	138.2	126.5			3.4	117.3
15		152.7	0.7	136.1	134.5					3.0	139.5	6.8	255.8	218.1	150.8		7.2	152.0	125.5			2.0	118.1
16	0.2	152.5		135.7	133.2				129.5	7.1	146.3	3.9	272.7	211.5	150.5		2.5	165.8	124.1			5.0	119.1
17	1.1	153.9	1.0	135.1	132.7			0.4	130.0	5.1	157.0	1.9	281.5	205.3	151.2			145.1	123.8			3.0	120.2
18	1.5	154.1	0.5	134.1	133.6	130.1	128.1	1.5	129.9	3.0	172.1	1.0	282.9	201.2	150.1	136.1	5.0	181.2	123.2	118.6	116.5	3.0	123.1
19	1.2	153.1	1.0	134.1	134.8			1.0	130.1	2.3	182.3	1.5	283.1	195.5	149.6		3.6	184.2	122.8			2.7	130.0
20	1.0	153.1	1.0	141.1	135.6			2.6	130.1	0.8	190.2	1.5	284.2	190.0	148.5			189.8	122.1			1.1	137.1
21	1.5	153.6	1.8	146.0				3.5	131.8	1.6	197.0	1.9	283.8	188.5	148.1			187.1	122.0				143.3
22		148.1	1.8	149.0				2.4	134.4		200.6		283.0	185.3	148.1			182.8	121.7			0.4	147.4
23		148.5	0.8	150.8				1.6	138.2		202.0		280.5	181.9	148.0			177.7	121.8			0.4	148.3
24		149.3	0.1	151.7		129.3	126.3	1.3	140.9	1.2	201.4		276.7	178.0	147.1	134.5			121.5	118.1	116.6	3.5	147.5

1 9 4 9

Month	Nov.						Dec.																
Day	9		10	12		13	10		11	12	20		21		22	24		25	26		27		28
h	W	H	H	W	H	H	W	H	H	H	W	H	W	H	H	W	H	H	W	H	W	H	H
0																							
1	1.0	145.2	123.0	0.8	118.5	124.8		106.8	112.9	109.6		104.6		165.0	118.6		112.5	118.7		113.7	2.8	114.8	117.9
2	3.0	142.6		0.6	118.4	124.1			114.3				4.6	164.0	118.2	2.2	113.2	118.1			4.0	115.5	117.7
3	0.8	144.0		1.1	118.6	123.6			115.8				3.9	162.5	118.0	2.0	113.3	117.7			3.5	116.8	117.4
4	1.0	145.5			118.7	123.0			117.0				2.4	166.6	117.2	9.2	114.3	117.4			0.8	119.6	117.3
5	0.5	148.8		0.9	118.9	122.6			117.9			104.6		173.1	117.3	8.0	115.8	117.2			4.0	123.0	116.9
6		151.4	122.1	1.0	119.1	122.6		106.7	117.8	109.2	0.4	104.9	0.8	173.7	116.6	2.7	120.2	116.9		113.0	2.2	126.2	116.3
7		150.5		3.5	119.8	122.7			117.3		0.6	105.1		172.2			133.9	116.6			3.0	128.4	115.6
8		148.2		5.4	120.8	122.6			116.3		0.6	105.2		167.0			144.4	116.3				130.1	115.1
9		144.0		7.4	122.5	122.5			115.7		1.0	105.5		161.7			148.1	116.0				131.3	114.9
10		141.0		0.4	125.6	122.1			114.9		2.0	106.0		156.6			146.3	115.3				131.7	114.8
11		138.5			135.9	121.9			114.2		0.8	106.8		149.3			144.6	114.8				132.0	114.8
12		135.4	120.6		144.2	121.9		106.8	113.9	109.0	0.2	107.7		143.9	115.6		140.5	114.6		112.6		131.0	115.1
13		133.3			148.2				113.4		0.2	108.8		140.4			137.0	114.9				130.2	
14		131.6			149.0				113.1		0.2	109.3		137.0			134.1	114.8				128.7	
15		129.8			146.6			106.5	112.8		7.4	110.3		134.0			131.2	114.7				126.5	
16		128.1			143.7		1.5	106.7	112.6		4.7	110.8		131.6			128.4	114.8				124.9	
17		127.3			140.0		1.0	106.9	112.2		2.3	113.2		129.0			126.5	114.7				123.7	
18		126.7	120.0		136.9		2.0	107.9	111.7	109.1	1.8	117.0		126.5	114.8		124.7	114.6		113.5		122.7	115.8
19		126.1			133.7		2.0	107.5	111.4		1.8	124.0		124.8			122.8	114.6				121.8	
20		125.4			131.0		0.5	108.1	110.9		1.5	130.4		123.2			121.8	114.4		113.9		121.1	
21		125.1			128.7		0.9	108.6	110.4		3.1	134.3		121.8			121.1	114.3		113.9		120.4	
22		124.5			127.5		4.0	109.3	110.3		6.4	139.0		120.7			120.3	114.3		113.8		119.6	
23		123.9			126.4		3.4	110.5	110.2		3.6	146.2		120.0			120.0	114.2	1.6	114.1		118.9	
24		123.3	119.2		125.4		1.2	111.8	109.9	108.5	0.8	158.6		119.3	114.1		119.4	113.9	2.3	114.3		118.3	114.8

	1949		1953						1954			
Month	Dec.		June						June			
Day	30		25		26		27		25		26	
W.H / Time	W	H	W	H	W	H	W	H	W	H	W	H
0												
1		113.5				205	1.8	550			24.7	290
2						200	2.2	530			2.4	320
3						190	1.7	520			2.1	335
4					5.4			500			6.7	345
5					2.9	180	1.1	490			7.1	345
6		113.0			1.6	170	1.4	480			10.4	335
7					1.4	160	1.5	470				320
8			2.3		1.4	160	3.4	460				
9			10.2			150	14.3	450				
10			9.1	20	8.8	160	13.1	450	1.2			
11		112.9	11.1	30	24.2	200	3.9	430	1.6			
12	0.9	112.9	11.6	50	22.0	270	7.0	430				
13	1.0	113.0	6.0	130	26.2	340	7.3	420				
14	0.7	113.1	3.3	150	22.7	390	5.4	420				
15	5.7	113.7	21.3	170	29.8	420	2.2	410	4.4			
16	4.8	114.6	11.5	200	45.2	440	8.5	410	3.3			
17	1.4	116.4	6.1	220	25.5	500	9.3	400	13.0			
18	2.2	120.6	2.7	240	27.3	520	1.9	390	5.5			
19	1.0	127.0		250	42.3	530		380	15.1			
20		131.0	7.6	280	26.7	540			12.0	125		
21		132.8	3.8	260	23.7	550			10.3			
22		132.1	4.3	240	28.1	560			16.7	190		
23		131.2		220	16.7	560			21.3			
24		129.4		210	10.0	560			24.2	225		

ON THE CATALYTIC ACTIVITY AND FIBRILLAR STRUCTURES OF EJECTA OF VOLCANO ASO

Daisei YAMAMOTO and Syozo TANOUYE*

In an attempt to learn more of the detailed structure of clay minerals, Sudo and his associates showed by electronmicrograph of Imaichi-clay etc that the interesting ball like structure from which fibrious crystals jut out is formed by the alteration of volcanic materials[1].

These rounded grains are sometimes called as Sudo-ball.

The present author is concerned with the discovery of those fibrillar crystals in the electronmicrograph of ejecta gathered close by the mouth of the crater of Mt. Aso.

In the course of one of the author's (D. Yamamoto) chemical studies of those ejecta in recent years, it became evidant that those ejecta contained several catalytic properties such as benzidine colouration, cracking ability upon paraffins etc[2][3][4].

The idea occured that there may be some possibility of finding fibrious structures in these ejecta.

The actual electronmicrograph of the ejecta was taken by S. Tanouye and as expected, several fibrillar structures were revealed in those photographs.

In A (Fig. 1), in addition to feather and comb like forms a woolly mass is shown. (A potion of A is enlarged in B)

In C, the woolly like mass structure which shows some inner texture can be observed and in D a ball shape formation is shown.

Perhaps, these minerals which have fibrillar structures correspond to the transition stage of alteration of volcanic glass fragments.

Concerning the formation of these materials, attention must be paid to the fact that an acidic water pool often forms in the bottom of the crater especially in the dormant period of the volcano.

When the volcano erupts anew, those hydrothermally altered fragments at the bottom of the crater are ejected around the mouth of the crater.

The author's opinion is that these clay minerals may have been formed in the crater itself by the action of fumaroles, condensed water and magma-heat.

Details will be dealt with in another publication.

References

1) T. Sudo, Science Reports of the TOKYO KYOIKU DAIGAKU Section C No. 43 P. 39~55 (1956)
2) D. Yamamoto, J. Chem. Soc. Japan 76, 1242 (1955)
3) D. Yamamoto, Ibid 77, 750 (1956)
4) D. Yamamoto, Ibid 78, 160 (1957)

* Electronmicroscope Chamber, Faculty of Medicine.
Kumamoto University.

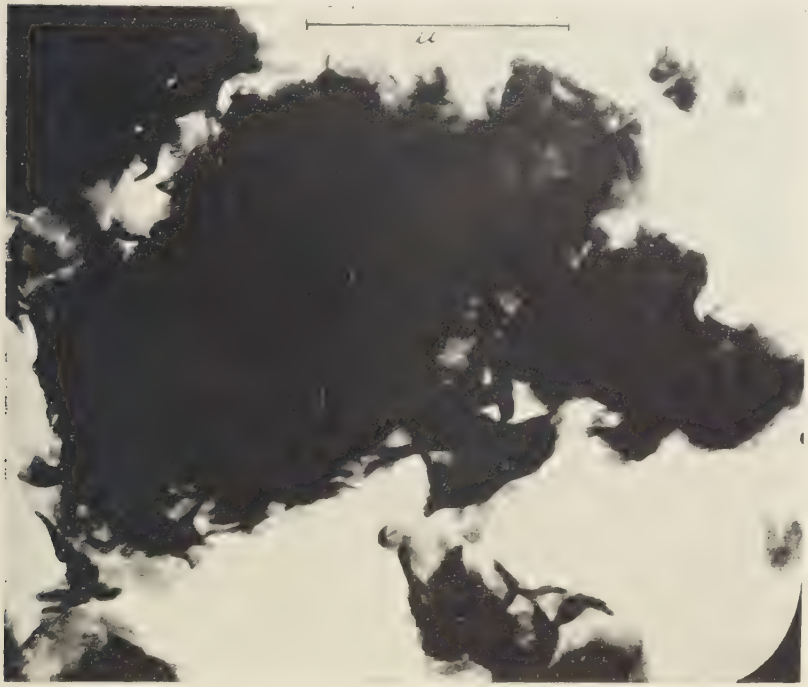

(A)

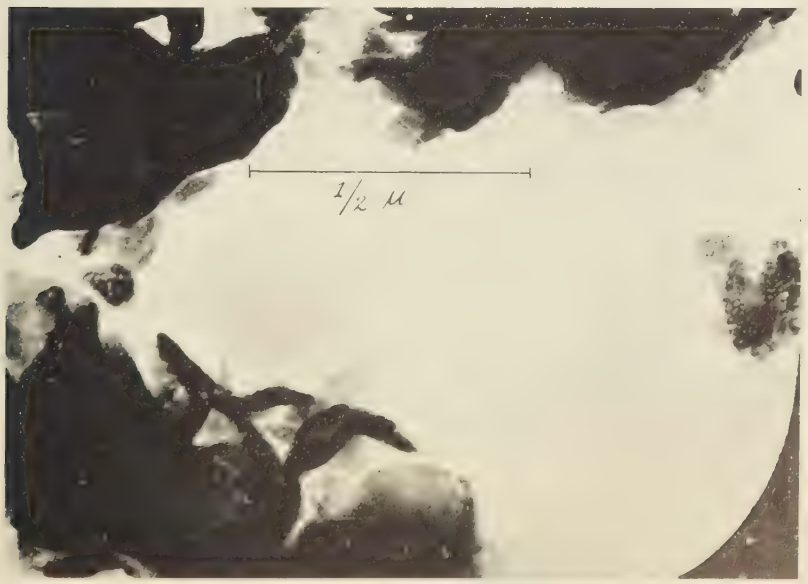

(B)

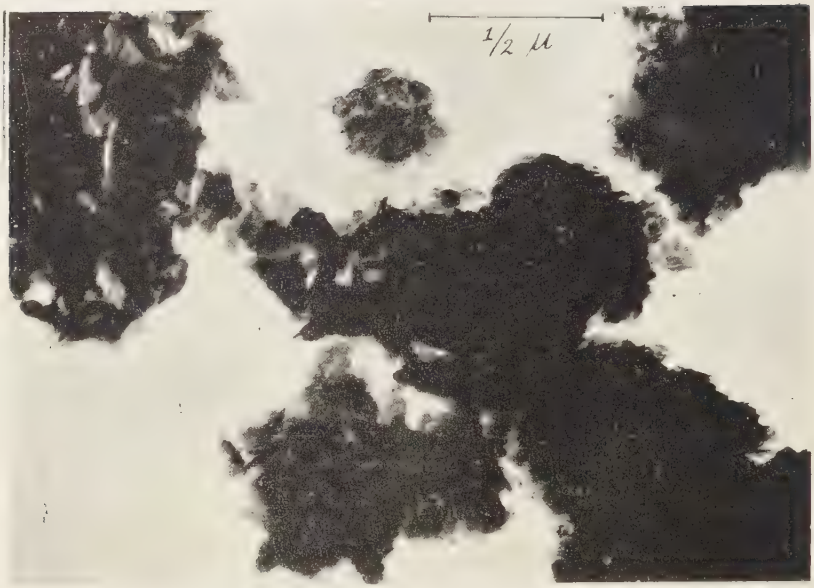

(C)

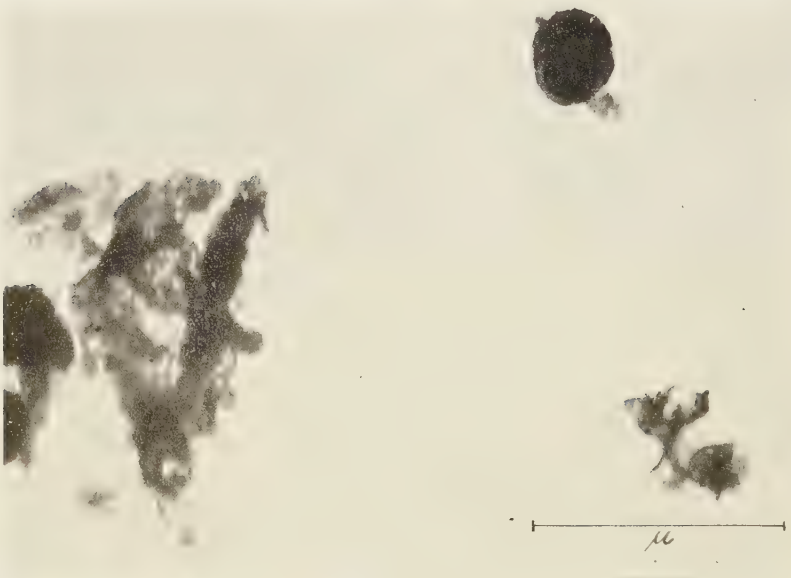

(D)

Fig. 1 Electronmicrograph of the ejecta of Volcano Aso

PAPER CHROMATOGRAPHY OF INORGANIC IONS BY USING ORGANIC ANALYTICAL REAGENTS. IV.

Precipitation Chromatography of Cations with 8-Quinolinol. (Part 3)

Hideo NAGAI

(Received March 25, 1957)

On the filter paper impregnated with 8-quinolinol (oxine), some metal ions were chromatographically precipitated in the form of their oxinates[1)2)]. In the case, the precipitation chromatography, which was obtained by adequately reducing the dissolving power of the developing solvents, was superior in the separation of cations to the usual soluble form chromatography[1)]. And, moreover, when the development was executed in the proper *p*H range, the separation of the metal ions became more clearly defind. In the experiments, mentioned above, 2% acetic acid saturated with *n*-butanol showed the best results[2)].

In this paper, the author intended to improve the steps of the operation of precipitation chromatography by reconsidering the details of the operation which had been done, so as to be able to confirm the foundation of this analytical technique and to look foreward to the wider application of the separation of the metal ions.

A. Impregnation of Filter Paper

The filter paper, impregnated with oxine through the procedure of dipping the paper in to alcoholic solution of the oxine and then drying off at the room temperature, is not sufficiently uniform enough for our purpose. This failure would be caused by the poor reproducibility of the very fine details of the drying conditions. So, the sizes of the oxine crystals and their distribution on the filter paper would be different in each procedure. These irregularities were confirmed by the observation of these modified paper under a microscope. It is so tedious and difficult to equalize the each drying condition to almost the same degree that the other easier procedure would be worth being researched. The following procedure utilizing the comparatively low melting point of oxine (75C) would be recommended: at first, the filter paper was treated as usual procedure, and when the paper was almost dried (somewhat still moist), then the paper was dried up in an electrical drier at 130~140C for some minutes to apparently complete dryness. In the last heating step, the oxine crystals were melted and impregnated in the filter paper. The papers, treated above, were sufficiently uniform both in the observation under a microscope and the chemical properties to the metal ions. The decomposition of the oxine through this heating process was scarcely observed.

B. Application of Sample

When appling the sample on the modified paper, the aqueous sample solution was spotted at the center of the filter paper with a micropipette, and then allowed to the

development. But if the quantities of the cations in the sample was in some degree large, lot of metal oxinates precipitated at the center of the filter paper, distubed the permeation of the remaining cations in the aqueous solution towards the circumference. Thereby, the regularity of the zonal precipitation of the oxinates (the order of the degree of insolubility) was also disturbed. And if the quantities of the cation in the sample were still more large, then, the applied sample solution remained on the filter paper for a long time before thoroughly absorbed.

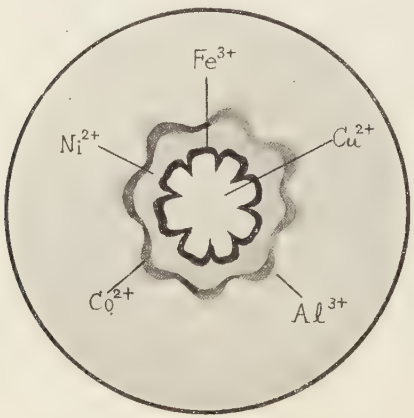

Figure 1A

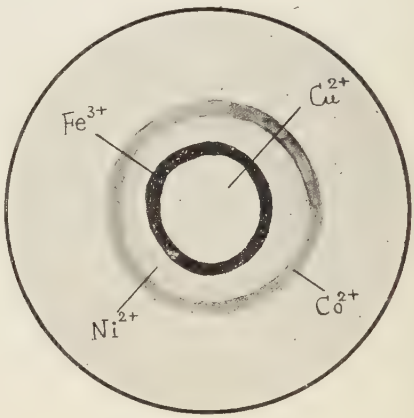

Figure 1B

The cause of the disturbance of the regularity of precipitation was more clearly found out by observing the figures of the developed chromatograms. In the precipitation chromatogram, obtained by the procedure which was previously reported[1-3], the irregular peak-and-valley was observed as shown in Figure 1A. In this figure, peak-and-valley of Fe^{3+} zone was the most clearly outlined and that of the outer zones of cations seems to be governed solely by the peak-and-vally of Fe^{3+} zone. Moreover, at the peaks of thd Fe^{3+} zone, the outer cation zones were narrow and at the valleys of the Fe^{3+} zone, the outer cation zones were wide. And in the most outer zone of Al^{3+}, the width of the valley portions was so narrow that the most quantity of Al^{3+} was found at the peak portions which were the counterparts of the Fe^{3+} valleys. These phenomena would be explained as follows. The cations precipitated at the outer portion of the Fe^{3+} zone were strongly resisted at the Fe^{3+} precipitation layer when they were permeating through the Fe^{3+} layer, and they had to push their way through the layer: the valleys of the Fe^{3+} zone were the portions comparatively low resisted and peaks were the portions highly resisted. So, the greater parts of the outer cations would pass through the portions of the valleys of the Fe^{3+} zone. Accordingly, to obtain the clear circular pattern on the chromatogram, it would be necessary to smooth out and reduce the resistance to the permeation of cations through the Fe^{3+} zone. The saturation of the sample solution with *n*-butanol, which showed the excellent properties as the developing solvent[1], was suitable for this purpose. After the application of thus treated sample solution to the filter paper impregnated with oxine,

the development was executed as usual. The precipitation chromatogram given by the procedure mentioned above had far less peak-and-valley in each cation zone, and was very nearly concentric circular (Figure 1B). The developing solvents of Figure 1A and 1B were both 2% acetic acid saturated with *n*-butanol.

C. Developing Solvent

At the choice of the developing solvent the combination of the following two factors were considered.

1) Dissolving power of the solvent for the metal oxinates[1].

2) PH value of the solvent which control the stability of the precipitation of oxinates[2].

But, sometimes, we might be able to satisfy these factors with one organic acid. Lactic acid was an example for this kind of developing solvent but the results of the development were poor in reproducibility (this might be owing to the complex reaction of some sorts of hydrogen bonds such as lactide bond, etc.). However, the separate control of the two factors (dissolving power and *p*H value) according to the demand, would be able to expect the better result of the development. From this point of view, acetic acid-*n*-butanol combination is a widely applicable developing solvent. In this combination, the *p*H value of 2% acetic acid saturated with *n*-butanol[3], which gave the excellent result for the separation of Cu^{2+}, Fe^{3+}, Ni^{2+} and Co^{2+} was 2.6, and lower than *p*H 2.8[3] which is the value for the incipient precipitation of Ni^{2+} and Co^{2+} oxinates. Therefore, continuing the development after the complete precipitation of the oxinates, the precipitation began to dissolve from the outer portion. Then, ceasing the development when the most outside zone (Co^{2+} zone) was completely dissolving away and treating with ammonia gas[2], the very clearly separated chromatogram (Figure 2) was obtained. This redissolving process was a new factor of separation of the zones in the precipitation chromatography. And 1% acetic acid saturated with *n*-butanol was more suitable for this purpose.

Acetic acid—*n*-butanol combination, described above, had one undesirable property. *n*-Butanol in the solvent was used always in the state of saturation. *n*-Butanol decreases the solubility in water with the increase of the temperature, near the room temperature. And the content of *n*-butanol in the solvent was the most powerful factor of controling solubility to the metal oxinates, at the same *p*H of the solvent. Thereby, the deficiency of dissolving power of the solvent in summer is expected. In fact, at above 20°C in the solvent temperature, the chromatogram obtained by that solvent combination was unsatisfactory in the separation of the zones of cations and quite undesirable for the solvent of the new process of

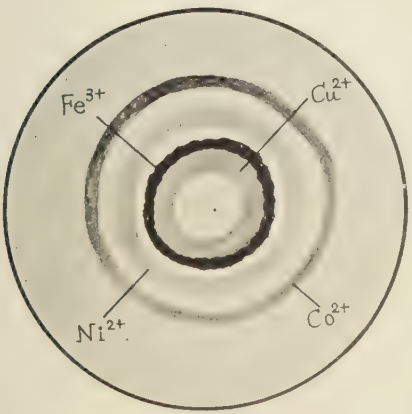

Figure 2

redissolution. If we atempt to increase the dissolving power with the increase of the content of acetic acid, the descent of *p*H of the solvent will make the developing solvent unsuitable. Accordingly, addition of *n*-butyric acid, which was a way of maintaining *p*H at the proper range and of increasing the dissolving power of the solvent to the metal oxinates, gave the suitable result. The following developing solvent gave the satisfactory results in the experiments to 33°C, the highest temperature of the solvent in the last summer in our laboratory:

n-butyric acid : 2% acetic acid: *n*-butanol : H_2O=1 : 20 : 4 : 40 (in volume).

Conclusion

The precipitation chromatographic procedure on oxine-impregnated filter paper, was reconsidered, and, by improving the following steps, the chromatogram was obtained with a more reproducible and clean separated.

1. The method of impregnation of oxine, which had usually been used, was followed by the heating process utilizing the comparatively low melting point of oxine, to modify the filter paper with oxine in the melted state.
2. Before applying the sample on the modified paper, the sample solution was saturated with *n*-butanol.
3. When *p*H of the developing solvent was lower than the *p*H value of incipient precipitation of the metal oxinates, the once precipitated zone were redissolved by the prolonged development. Utilizing this phenomenon, the appearance of zones was improved more clearly.
4. In summer, acetic acid—*n*-butanol combination was deficient in solubility to the metal oxinates. This defect was improved by the addition of *n*-butyric acid.

The contents of this paper have mainly been published in J. Chem. Soc. Japan, Pure Chem. Sect., ***77***, 1794 (1956).

Literature Cited

(1) H. Nagai, Kumamoto Journal of Science Series A. Vol. 2, No. 3, 304 (1955).
(2) H. Nagai, Ibid., No. 4, 81 (1957).
(3) F. J. Welcher, "Organic Analytical Reagents" (1947).

PAPER CHROMATOGRAPHY OF INORGANIC IONS BY USING ORGANIC ANALYTICAL REAGENTS. V.

Precipitation Chromatography of Cations with 8-Quinolinol. (Part 4)

Hideo NAGAI

(Received March 25, 1957)

On the oxine-impregnated filter paper, the four kinds of cations–Cu^{2+}, Fe^{3+}, Ni^{2+} and Co^{2+}—were separated in the concentric circular precipitation[1),2),3)]. In this paper, the author intended to investigate the mechanism of separation of cations. And, following the results of the investigation, the separation of the five kinds of cations, the four cations mentioned above and Zn^{2+}, was studied.

Mechanism of Separation of Cations

As the factor of the separation of metal ions in precipitation chromatography, the solubilities of metal oxinates in the developing solvent alone, had hitherto been considered. The experiments were executed taking the following points into consideration: as indicated by the solubility product rule, the cations in the sample solution were precipitated in the concentric circular zones. But the measurements of the solubility products of the hardly soluble salts were difficult and, moreover, the values obtained were often said to be inaccurate[4),5)]. Therefore, it is desirable to devise the experimental plan on the basis of the more accurate and easily measurable physico-chemical constants other than solubility product. From this point of view, the concept of Irving *et al.*, the order of the stability of the metal complex salts[6)], seems to be a convenient one for this purpose. The digest of their concepts is as follows. The formation of an inner complex represented by the equation

$$M^{n+} + nHR \rightleftarrows MR_n + nH^+$$

involves essentially a competition between (hydrated) protons and metal cations for the anion of the reagent forming the complex: the more stable the complex, the lower the *p*H at which it can persist, and *vice verse*. On the basis of this concept, the precipitation chromatography with oxine may be explained using following rules.

(a) The order of precipitation of the hardly soluble complexes is the same as that of the values of the stability constants of them.

(b) The order of extraction of metal complexes for a constant excess of reagent in a constant *p*H is the same as that of the stability constants of them.

(c) When the value of stability constant of a complex is not obtained, the *p*H for 50% precipitation 50% extraction, or incipient precipitation may be used as a measure of relative stability of the complex. (In this connection Merritt has also reported the approximate values of *p*H at incipient procipitation of various oxinates of transition

metals as a measure of the stabilty of the chelates[7].)

At the execution of the chromatography, the two factors (a) and (b) are counteract each other. In the case of the oxinate chromatography, the precipitation chromatography, in which the factor (a) prevailed over (b), was, as a rule, superior in the separation of cations to the usual soluble form chromatography, in which (b) prevailed over (a)[1]. Accordingly from the rule (a) the stability constant may be used instead of the solubility product, which has been used for a measure of the order of precipitation in the chromatography. Considering (b), the amount of organic solvent added in the developing solvent would be retained in the minimum range, sufficient for the smooth development. However, in the practical development, the substances to be developed were desirable to be in as complete a soluble form as possible. And, moreover, the precipitation appeared was more suitable to become sediment slowly step by step than did at once with a rush. Thereby, the amount of the organic solvent added in the practical developing solvent was comparatively larger than the amount expected from the factor (b) alone.

If the chromatograph was developed in such a state as described above, the dissolving power of the solvent to the oxinates would influence in some degree upon the development. So, it would be doubtful to decide that the order of precipitation of the oxinates was first and principally governed by the stability constants, but so far as the four foregoing cations were concerned, the order of precipitation was the same in the development with water as with the various kinds of organic solvents[1),2),3)]. Therefore, it would be reasonable to consider that the development with these organic solvents would be the one of the following cases.

(1) The differences of the stabilities among the metal oxinates are much larger than those of solubilities.

(2) The order of the stabilities of metal oxinates is the same as the order of insolubilities.

When the solubilities of the metal oxinates in the developing solvent are large, (2) contradicts against the rule (b), which has been described in this paper. The dissolving power of the solvents in this study was not so large as in the case of (b) that the situation would differ from (b). But, in spite of that possible difference, the dissolving power of the solvent used is fairly large, so that the factor (1) would possibly be prevailing over (2). Thereby, the experimental plan may be deviced on the principal consideration of the stability of oxinates and then the solubility of them may be taken up supplementally. This general principle was supported by the results of the development of many cations (Cu^{2+}, Fe^{3+}, Ni^{2+}, Co^{2+}, Pb^{2+}, Cd^{2+}, Mn^{2+}, Mg^{2+} and Ca^{2+}*). But in the separation of the oxinates of the same stabilities, it would be necessary to consider the solubility principally. As an example of these cases, the separation among the five cations (Zn^{2+} in addition to the four cations which had been treated) was undertaken.

Table 1

Metal Ion	Log K[8)]	Metal Ion	Log K[8)]
Cu^{2+}	29.0	Co^{2+}	20.8
Ni^{2+}	22.0	Zn^{2+}	20.8

* In these cations, the preceding four cations have been treated and the remainings will be treated in the next report.

The stability constants of the metal oxinates which are necessary in this study, are shown in Table I. The stability constants of Fe^{3+} oxinate could not be found out, so the discussion concerning this cation would be taken up later in this paper. But the stability constant of Zn^{2+} oxinate is not situated between Cu^{2+} and Ni^{2+}, so that the position of Zn^{2+} oxinate in the precipitation chromatogram is supposed to be well out of place of Fe^{3+}. Accordingly, the discussion concerning the Zn^{2+} oxinate in the chromatograph would not be disturbed by the neglect of Fe^{3+} oxinate.

The stability constants of Co^{2+} oxinate and Zn^{2+} oxinate are equal, so the difficulty of their separation would be expected. In their separation, as it has been pointed out, the difference of their solubilities should be utilized. So the choice of the organic solvents and their amount added to the developing solvent would be the important factors.

Experiment and Discussion

As the sample of Zn^{2+}, $Zn(NO_3)_2 \cdot 6H_2O$ was used and dissolved in water about 10 mg/ml, as the other cations were treated. The aqueous solution, containing the five cations (Cu^{2+}, Fe^{3+}, Ni^{2+}, Co^{2+} and Zn^{2+}) in it, was applied to the filter paper modified with oxine, and developed with 2% acetic acid saturated with *n*-butanol. In the chromatogram obtained, Co^{2+} and Zn^{2+} were not visually separated, as expected before. But when the sample

Tablce II[8]

Metal ion	PH at which precipitation begins	Range through which precipitation is complete	Order of precipitation
Cu^{2+}	2.2	5.3~14.6	1
Fe^{3+}	2.4	2.8~11.2	2
Ni^{2+}	2.8	4.3~14.6	3
Co^{2+}	2.8	4.2~11.6	4
Zn^{2+}	2.8	4.6~13.4	5

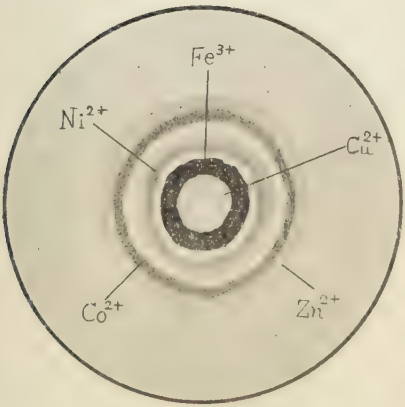

Figure 1

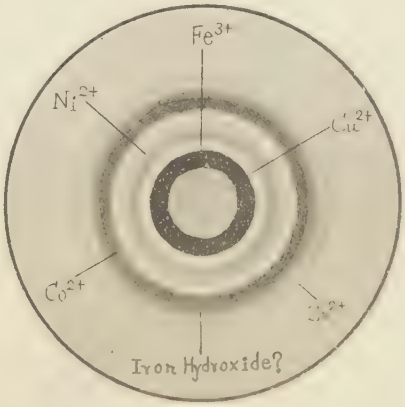

Figure 2

solution was used with the saturation of *n*-butanol[8], Co^{2+} and Zn^{2+} were able to be discerned in the chromatogram, after the development. Next, the redissolving process, which had been reported[3] in the separation of Ni^{2+} and Co^{2+}, was applied with a good result of almost complete separation of Co^{2+} and Zn^{2+} zones. This is clearly seen in Figure 1. In the experiment described above, 1% acetic acid saturated with *n*-butanol was also more favorably adopted than 2% acetic acid as reported[8] and the addition of *n*-butyric acid was suitable in summer[8]. At the separation of Co^{2+} and Zn^{2+} oxinates, the solubilities of them have to be principally considered, as described above.

In the column of "Range through which precipitation is complete" in Table II, Zn^{2+} oxinate appeared to be slightly more soluble than Co^{2+} oxinate, in the weak acidic range. This explains that the Zn^{2+} zone was situated at the outside of the Co^{2+} zone, and that both of the cation zones were more clearly separable with the operation of redissolution[3]. The amount of *n*-butanol added to the developing solvent seriously influenced the separation of them, as expected. Fe^{3+} in this precipitation chromatography, which has been retained, is now to be discussed here. Applying the concept of Irving *et al.*[6),7)], it is quite natural that Fe^{3+} oxinate was situated between Cu^{2+} and Ni^{2+}, because, in the Table II, *p*H of incipient precipitation of Fe^{3+} is found between Cu^{2+} and Ni^{2+}. But in the chromatogram of the five cations which has been treated in this paper, a faint gray colored zone was often found between Co^{2+} and Zn^{2+} as illustrated in Figure 2. And the appearance of this zone closely related to the treatment of Fe^{3+} sample: when Fe^{3+} was used rapidly after a careful refinement, the gray zone was hardly found, but with a duration of time, the zone grew large and clear. And this phenomenon was prevailing in summer and depressive in winter. Observing this zone under a microscope, the black crystals which were quite the same figured as found in the Fe^{3+} zone (the second layer from the center) were scattered roughly. When *p*H of the sample solution was lowered, the zone was somewhat suppressed, but this lowering of *p*H was limited by the capability of existence of oxinates. Considering the various phenomena described above, the gray zone would be able to be decided as Fe^{3+} oxinate. The split of Fe^{3+} zone might be caused by the change of Fe^{3+} into two or more kinds of substances with the duration of time, or by the tautomerical change of two substances[10]. But the former would be more possible because the aging effect of Fe^{3+} was found before the reaction with oxine. And considering the influence of *p*H, the split of Fe^{3+} zone must be closely related with the growth of iron hydroxide which is caused by the hydrolysis of a part of Fe^{3+} in the sample solution. The gray zone had appeared in the chromatogram before the addition of Zn^{2+} to the other four cations, but the author had failed to find it because of the faint color and the utmost outsided situation.

Conclusion

1. The order of precipitation of cations in the precipitation chromatography is explained principally by the stabilities of complexes, and then, supplementally by the solubilities of them.
2. The five kinds of cation–Cu^{2+}, Fe^{3+}, Ni^{2+}, Co^{2+} and Zn^{2+}–were separated satisfactoryly with the procedure which had been reported.
3. The faint gray zone which was often found between Co^{2+} and Zn^{2+} is considered to be

caused by iron hydroxide.

The contents of this paper have mainly been published in J. Chem. Soc. Japan, Pure Chem. Sect. ***78***, 285 (1957).

Literature Cited

(1) H. Nagai, Kumamoto Journal of Science Series A, Vol. 2, No.3, 304 (1955).
(2) H. Nagai, Ibid., No.4, 81 (1957).
(3) H. Nagai, Part 3 in this volume.
(4) T. Sasaki, "The Kagaku Zikken Koza (The Lecture of Chemical Experiments)", ***12***, 464 (1956).
(5) Z. Matsuura, Anal. Chem. Japan, ***5***, 411 (1956).
(6) H. Irving, R.J.P. Williams, Nature, ***162***, 746 (1948).
(7) Merritt, Record Chem. Progress (Kresge-Hooker Sci. Lib.), ***10***, 59 (1949).
(8) A. E. Marthell, M. Calvin, "Chemistry of the Metal Chelate Compounds" (1953).
(9) F. J. Welcher, "Organic Analytical Reagents" (1947).
(10) F. Feigl, "Chemistry of Specific, Selective and Sensitive Reactions" (1949).

PAPER CHROMATOGRAPHY OF INORGANIC IONS BY USING ORGANIC ANALYTICAL REAGENTS. VI.

Precipitation Chromatography of Cations with 8-Quinolinol. (Part 5)

Hideo NAGAI

(Received March 30, 1957)

On the filter paper impregnated with oxine, the five kinds of metal ions-Cu^{2+}, Fe^{3+}, Ni^{2+}, Co^{2+} and Zn^{2+}-were separated in concentric zonal precipitation. The order of precipitation was principally governed by the stability constant and supplementarily governed by the solubility of oxinates[1]. Applying these principles, the separation of the ten kinds of cations-Cu^{2+}, Fe^{3+}, Ni^{2+}, Co^{2+}, Zn^{2+}, Pb^{2+}, Cd^{2+}, Mn^{2+}, Ca^{2+} and Mg^{2+}-was studied in this paper.

Experiment (Part 1)

The author has reported about the order of precipitation of the insoluble complex: the order of precipitation agree with the order of stability constant, and if the numerical value of the stability constant could not be obtained, the relative order of stability was the order of the descending *p*H of incipient precipitation[1]. According to this concept, the experimental plan was established. In Table I, the numerical values of the *p*H at which precipitation begins and the range through which precipitation is complete with oxine are tabulated.

The sample to be chromatographed was prepared from the nitrates of the cations: they were dissolved in the separate glass bottles about 10mg/ml ion-conc. in each cation, and before the use of the sample solutions they were mixed together with the equal volume.

The mixed sample solution was saturated with *n*-butanol, applied on the filter paper modified with oxine and allowed to be chromatographed[3]. The apparatus used [4], the procedure of development[1] and the treatment of chromatogram with ammonia gas[5] were the same as reported before. Cu^{2+}, Fe^{3+}, Ni^{2+}, Co^{2+} and Zn^{2+} (hereafter these cations are called the cations of A group in this paper) were precipitated as the order described here with oxine[1]. The sample to be chromatographed in this study was prepared as follows.

One of the cations below Cd^{2+} in the

Table I[2]

Metal ion	PH at which precipitation begins	Range through which precipitation is complete
Cu^{2+}	2.2	5.3~14.6
Fe^{3+}	2.4	2.8~11.2
Ni^{2+}	2.8	4.3~14.6
Co^{2+}	2.8	4.2~11.6
Zn^{2+}	2.8	4.6~13.4
Cd^{2+}	4.0	5.4~14.6
Mn^{2+}	4.3	5.9~10.0
Pb^{2+}	4.8	8.4~12.3
Ca^{2+}	6.1	9.2~13.0
Mg^{2+}	6.7	9.4~12.7

Table I was added to the cations of A group one by one from the bottom of the Table I. The solutions containing six kinds of cations, made just mentioned above, were allowed to be chromatographed. When the first sample solution containing Mg^{2+} and the cations of A group was chromatographed, the result was as follows. When treated with ammonia gas the yellow ring zone of oxine was discolored[5] and the light yellow zone of Mg^{2+} appeared just outside the discolored oxine zone. The color of this zone was somewhat faint in day light but the strong greenish blue fluorescence was observed under the ultraviolet light (Figure 1A).

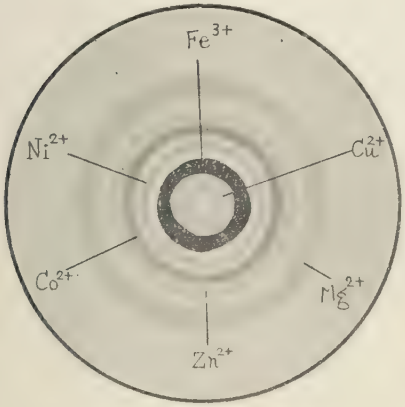

Figure 1A

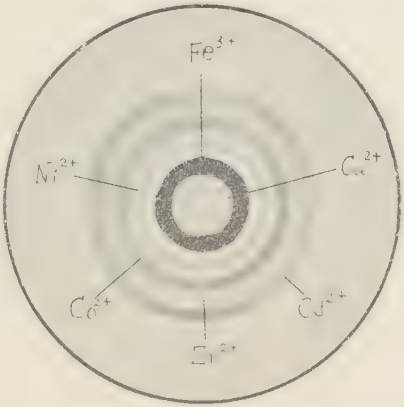

Figure 1B

In the case of the sample containing Ca^{2+} and the cations of A group, the result of development was almost the same as the first sample but the fluorescence of the Ca^{2+} zone was greenish yellow.

In the case of the sample containing Pb^{2+} and the cations of A group, the result of development was quite the same as the sample of the cations of A group alone. So the position of Pb^{2+} zone could not be located. But observing the chromatogram under the ultraviolet light, Pb^{2+} seemed to precipitate in the Zn^{2+} zone. Certifying this finding, the following experiment was undertaken. The sample containing Cu^{2+}, Fe^{3+}, Ni^{2+}, Co^{2+} and Pb^{2+} was chromatographed. The result was quite the same as the sample of the cations of A group, so Zn^{2+} and Pb^{2+} acted quite equally in these chromatography. But observing these two chromatograms in the ultraviolet light, Pb^{2+} zone was somewhat blueish yellow and Zn^{2+} zone was plain yellow.

In the case of the sample containing Mn^{2+} and the cations of A group, a yellow zone appeared near the front line of the development (somewhat inner portion of Mg^{2+} or Ca^{2+} zone). And the yellow Mn^{2+} zone became brownish after a weak or two. This is perhaps owing to the production of MnO_2.

In the case of the sample containing Cd^{2+} and the cations of A group, the light greenish yellow Cd^{2+} oxinate was precipitated just outside the position of Zn^{2+}, as shown in Figure 1B. The separation between Zn^{2+} and Cd^{2+} was not perfect, but it was easy to discern them. Moreover, the Cd^{2+} zone became brownish after a few days.

Discussion

The *p*H value of incipient precipitation of the cations below Cd^{2+} in Table I were so distinctly higher than that of the cations of A group that the separation of these newly treated cations from the cations of A group was naturally expected to be easy. The expectation was almost realized except the case of Pb^{2+}. In the case of Pb^{2+}, it was precipitated apparently inside the zone of Mn^{2+} and somewhat inner than the zone of Cd^{2+}. The *p*H value of incipient precipitation of Mn^{2+} was a little lower than that of Pb^{2+}, and the value of Cd^{2+} was far lower than that of Pb^{2+}. These phenomena might be expained as follows. Comparing the existing data of stability constants of these three cations with many other complexing agents, it is found that almost all Pb^{2+} comlexes were more stable than Mn^{2+} or Cd^{2+} complexes. So in the case of oxinates, it may be natural to consider that the actual value of stability constant of Pb^{2+} oxinate is larger than that of Mn^{2+} or Cd^{2+} oxinate. This finding differs from the concept of Irving *et al*[6]., but the cations illustrated in their theory was limited almost to the transition metals, so some irregularities might be permitted in the case of nontransition metals. Among the published data of stability constants of Pb^{2+} and Zn^{2+} complexes, the regular tendency of stability could not be found between the two cations. So it is impossible to presume the order of stability of these two cations. But their relative stabilities might be determined as follows.

At first, the sample containing the cations of A group was chromatographed. And as soon as the precipitation of Co^{2+} zone was almost finished, the development was stopped, then Co^{2+} and Zn^{2+} were scarcely separated. This phenomenon had previously been expected because the stability constants of the oxinates of these two cations were equal.

On the other hand, the sample containing Cu^{2+}, Fe^{3+}, Ni^{2+}, Co^{2+} and Pb^{2+} was treated as the same procedure as the cation of A group, mentioned above, then, Co^{2+} and Pb^{2+} were separated fairly well.

Considering the two experiments mentioned above, it may be said that the relative stability of Zn oxinate is greater than that of Pb.

However, the sample containing Pb^{2+} and the cations of A group was unable to be separated completely with the one development: Zn^{2+} mixed with Co^{2+} (in the shorter development) or Zn^{2+} mixed with Pb^{2+} (in the prolonged development).
The next question is that Pb^{2+} would be coprecipitated with Zn^{2+} oxinate. This question was examined as follows.

The sample containing Pb^{2+} and the cations of A group was chromatographed, and as soon as the precipitation of Co^{2+} zone almost finished, the development was stopped. The obtained chromatogram was examined under the ultraviolet light after ammonia gas treatment[5], then, at the utmost outer zone of the chromatogram, the fluorescence seemed to be Pb^{2+} oxinate alone. Thereby, it may be said that such a remarkable amount of Zn^{2+} oxinate did not exist in the zone that Pb^{2+} would not coprecipitate remarkably with Zn^{2+} oxinate.

Among the five newly treated cations, Pb^{2+} presented a few troublesome problems, as mentioned above, but the other four cations acted as expected from the stability or *p*H of incipient precipitation.

Experiment (Part 2)

On the basis of the experiments and discussions described above, the combinations of cations, which contained as many cations as possible and would be able to separate them sufficiently, were Cu^{2+}, Fe^{3+}, Ni^{2+}, Co^{2+}, Cd^{2+} (or Zn^{2+}, or Pb^{2+}), Mn^{2+} and Mg^{2+}. The result of development of these cations is shown in Figure 2A. If it is permitted to mix slightly in some parts of the chromatogram, the combination of the following eight cations may be adopted: Cu^{2+}, Fe^{3+}, Ni^{2+}, Co^{2+}, Zn^{2+}, Cd^{2+}, Mn^{2+} and Mg^{2+} (or Ca^{2+}). The result of the development of these cations is shown in Figure 2B.

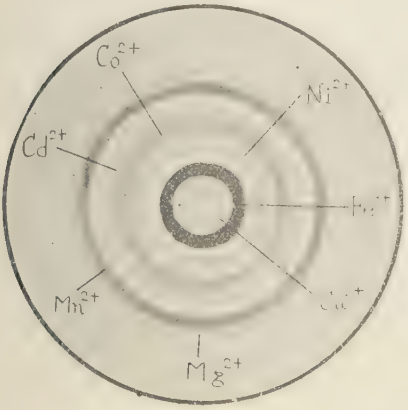

Figure 2A

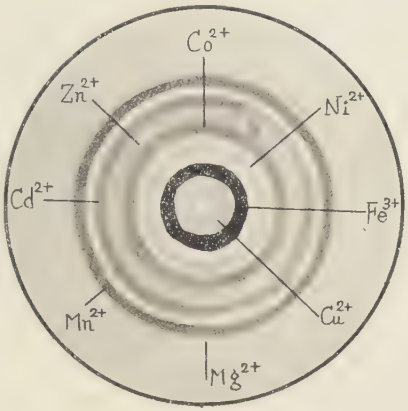

Figure 2B

Conclusion

1. When the sample containing the cations of A group (Cu^{2+}, Fe^{3+}, Ni^{2+}, Co^{2+}, Zn^{2+}) and one of the following three cations Mg^{2+}, Ca^{2+} or Mn^{2+} was chromatographed, the newly added cation migrated very near to the front line as shown in Figure 1A.
2. When the sample containing the cations of A grop and Cd^{2+} was chromatographed, Cd^{2+} precipitated just outside the Zn^{2+} zone, but the separation between the two cations was not sufficient (Figure 1B).
3. When the sample containing the cations of A group and Pb^{2+} was chromatographed, Zn^{2+} mixed with either Co^{2+} (in the shorter development) or Pb^{2+} (in the prolonged development). And the complete separation of these six cations with the one development could not be achieved.
4. The combination of cations which contained as many cations as possible in a clean separated state, was Cu^{2+}, Fe^{3+}, Ni^{2+}, Co^{2+}, Cd^{2+} (or Zn^{2+}, or Pb^{2+}), Mn^{2+} and Mg^{2+} (or Ca^{2+}) (Figure 2A). If it is permitted to mix slightly some parts of the chromatogram, the combination of the following eight cations may be adopted: Cu^{2+}, Fe^{3+}, Ni^{2+}, Co^{2+}, Zn^{2+}, Cd^{2+}, Mn^{2+} and Mg^{2+} (or Ca^{2+}) (Figure 2B).

The contents of this paper will mainly be published in J. Chem. Soc Japan, Pure Chem. Sect.

Literature Cited

(1) H. Nagai, Report V (Part 4) in this volume.
(2) F. J. Welcher, "Organic Analytical Reagents" (1947).
(3) H. Nagai, Report IV (Part 3) in this volume.
(4) H. Nagai, Kumamoto Journal of Science, Series A, Vol. 2, No. 3, 304 (1955).
(5) H. Nagai, *Ibid.*, No. 4, 81 (1957).
(6) H. Irving, R. J. P. Williams, Nature, ***162***, 746 (1948).

PAPER CHROMATOGRAPHY OF INORGANIC IONS BY USING ORGANIC ANALYTICAL REAGENTS. VII.

Precipitation Chromatography of Cations with 8-Quinolinol. (Part 6)

Hideo NAGAI

(Received March 30, 1957)

On the filter paper impregnated with oxine, a number of cations have been separated as their oxinates in the concentric zonal precipitations. In this paper, some possibilities of quantitative analysis of cations using this precipitation chromatographic technique were researched. The experiment was executed to find if the width or the area of the cation zone had any relation with the quantity of the cation or not.

Among the zones of the cations, Fe^{3+} zone was taken up. Because this zone was most clear and discrete. 2% acetic acid saturated with *n*-butanol was adopted as the developing solvent which had been most widely used as that of the precipitation chromatography with oxine[1]. Using this developing solvent, the well cared development made it possible to determine the quantity of Fe^{3+} by the width or the area of the zone with fairly good accuracy. Moreover, Cu^{2+} which precipitated at the center of the filter paper and just inside the portion of Fe^{3+} zone, was also semiquantitatively determined by the area of its zone, though not so accurate as the case of Fe^{3+}.

Experimental

The experiment was excuted as reported before[1),2),3),4),5)]. But some details of the experiment were determined as follows.

1. The width of the untreated filter paper tab which was inserted at the center of the modified filter paper[1)], was determined as 1mm, 2mm, and 3mm.
2. Cations treated in this paper were Cu^{2+} and Fe^{3+}. Each of the nitrates of these cations was separately dissolved in a glass bottle containing 20mg/ml ion-conc. of the cation. Using these solutions, the following four series of sample were made.
   a) At first 1 ml of the Fe^{3+} solution, mentioned above, was poured into five test tubes. Then 1 ml of Cu^{2+} solution, mentioned above, was poured into the first test tube, 2 ml into the second one, 3 ml into the third, 5 ml into the fourth, 7 ml to the fifth. Finally, all the contents of the five test tubes were diluted equally to 10 ml with distiled water.
   b) 2 ml of the Fe^{3+} solution was poured into the five test tubes and the other procedure was quite the same as the case of a).
   c) 3 ml of the Fe^{3+} solution was poured into the five test tubes and the other procedure was quite the same as the case of a).
   d) 5 ml of the Fe^{3+} solution was employed and the other procedure was quite the same as the case of a).
   But in the fourth test tube, the contents of it reached to 10 ml when the Cu^{2+} solution was added. So the fifth was not prepared.

3. The small Petri dish which was used as the vessel of the developing solvent, was 6.3 cm in diameter and 1.55 cm in height. The volume of the developing solvent in the vessel was 5 ml.
4. As the developing solvent, 2% acetic acid saturated with *n*-butanol was used as described above. The temperature change of this solvent so influenced seriouly upon the reproducibility of the experiment that the following cautions were needed.
   a) The temperature of the solvent was kept unchanged (observing with the thermometer of 1° division) at least 5 hours before use.
   b) The temperature of the solvent in the experiment was also kept unchanged in the same way.
   c) The temperature in which the experiment was executed was 9°~12°C.
5. The impregnation of filter paper with oxine was operated as reported before[3]. For about two months after the treatment, the paper was stored in a closed vessel and the midst portion of the pack of the paper (for example, in 100 sheets of paper which had been treated at the same time, 60 sheets of the paper were taken) was used for the quantitative purpose.
6. The sample solution for the experiment was saturated with *n*-butanol[3], and then 5μl of the solution was applied to the modified paper with a micropipette. The development was followed immediately after the application of the sample to the paper.

Table I

Width of Tab	Cu^{2+} (γ/5μl) : Fe^{3+} (γ/5μl)	a_1 (mm)	a_2 (mm)	b_1 (mm)	b_2 (mm)	$W_1=\frac{a_2-a_1}{2}$ (mm)	$W_2=\frac{b_2-b_1}{2}$ (mm)	$\frac{W_1+W_2}{2}$ (mm)	$A_1=\frac{\pi}{4}a_1b_1$ (mm^2)	$A_2=\frac{\pi}{4}a_2b_2$ (mm^2)	A_2-A_1 (mm^2)
1 mm	10 : 10	10.6	12.6	10.4	12.6	1.00	1.10	1.05	86.6	124.8	38.2
	20 : 10	13.1	15.3	12.9	14.9	1.10	1.00	1.05	132.7	179.0	46.3
	30 : 10	13.7	15.9	13.6	15.6	1.10	1.00	1.05	146.3	194.8	48.5
	50 : 10	18.6	20.6	18.2	20.0	1.00	0.90	0.95	265.9	323.5	57.6
	70 : 10	21.6	23.6	20.8	22.6	1.00	0.90	0.95	352.8	418.5	65.7
2 mm	10 : 10	11.0	13.8	9.6	11.8	1.40	1.10	1.25	82.8	127.9	45.1
	20 : 10	14.0	16.4	12.1	14.7	1.20	1.30	1.25	133.0	189.5	56.5
	30 : 10	15.2	17.6	15.2	17.4	1.20	1.10	1.15	181.2	240.5	59.3
	50 : 10	20.9	22.7	17.6	19.6	0.90	1.00	0.95	289.0	349.5	60.5
	70 : 10	21.8	23.4	18.6	20.2	0.80	0.80	0.80	318.2	371.0	52.8
3 mm	10 : 10	9.3	11.9	8.9	11.1	1.30	1.10	1.20	65.0	103.8	38.8
	20 : 10	14.5	16.9	11.1	13.7	1.20	1.30	1.25	126.4	182.0	55.6
	30 : 10	16.9	19.5	14.1	16.1	1.30	1.00	1.15	187.0	246.8	59.8
	50 : 10	22.9	24.9	17.6	19.6	1.00	1.00	1.00	316.5	383.0	66.5
	70 : 10	23.4	25.8	19.0	20.8	1.20	0.90	1.05	349.2	421.0	71.8
1 mm	10 : 20	11.1	15.7	10.2	14.2	2.30	2.00	2.15	89.0	175.0	86.0
	20 : 20	12.3	16.9	12.0	16.8	2.30	2.40	2.35	116.0	223.0	107.0
	30 : 20	13.6	18.8	12.0	17.0	2.60	2.50	2.55	128.1	251.0	122.9
	50 : 20	19.5	23.5	16.4	20.0	2.00	1.80	1.90	251.2	369.0	117.8
	70 : 20	21.2	24.4	20.6	24.0	1.60	1.70	1.65	343.0	460.0	117.0

Width of Tab	Cu^{2+} ($\gamma/5\mu l$) : Fe^{3+} ($\gamma/5\mu l$)	a_1 (mm)	a_2 (mm)	b_1 (mm)	b_2 (mm)	$W_1 = \frac{a_2-a_1}{2}$ (mm)	$W_2 = \frac{b_2-b_1}{2}$ (mm)	$\frac{W_1+W_2}{2}$ (mm)	$A = \frac{\pi}{4} a b$ (mm²)	$A = \frac{\pi}{4} a_1 b_1$ (mm²)	$A_2 - A$ (mm²)
2 mm	10 : 20	11.0	16.0	10.1	14.3	2.50	2.10	2.30	87.3	179.6	92.3
	20 : 20	14.8	19.8	12.8	17.0	2.50	2.10	2.30	148.8	264.1	115.3
	30 : 20	15.7	20.7	14.1	18.1	2.50	2.00	2.25	174.0	294.0	120.0
	50 : 20	19.8	24.0	16.9	20.3	2.10	1.70	1.90	262.9	382.5	119.6
	70 : 20	22.1	25.1	21.1	24.1	1.50	1.50	1.50	366.0	475.0	109.0
3 mm	10 : 20	14.8	20.4	11.0	15.8	2.80	2.40	2.60	127.9	253.1	125.2
	20 : 20	15.0	20.0	12.4	17.0	2.50	2.30	2.40	146.0	267.0	121.0
	30 : 20	21.2	25.6	13.2	17.2	2.20	2.00	2.10	219.9	345.9	126.0
	50 : 20	21.4	25.2	15.8	19.0	1.90	1.60	1.75	265.5	376.0	110.5
	70 : 20	27.2	30.6	18.2	21.4	1.70	1.60	1.65	388.7	514.0	125.3
1 mm	10 : 30	14.1	20.5	14.0	19.8	3.20	2.90	3.05	155.0	319.0	164.0
	20 : 30	13.2	19.2	13.4	19.0	3.00	2.80	2.90	139.0	286.5	147.5
	30 : 30	15.4	21.2	13.9	19.7	2.90	2.90	2.90	168.0	328.0	160.0
	50 : 30	19.8	25.6	19.0	24.0	2.90	2.50	2.70	295.5	482.0	186.5
	70 : 30	24.0	29.2	21.5	25.9	2.60	2.20	2.40	405.0	594.0	189.0
2 mm	10 : 30	15.0	21.6	13.2	19.4	3.30	3.10	3.20	155.4	329.0	173.6
	20 : 30	14.4	21.2	12.8	18.0	3.40	2.60	3.00	144.8	300.0	155.2
	30 : 30	17.8	23.8	16.0	21.6	3.00	2.80	2.90	223.7	404.0	180.3
	50 : 30	22.0	27.0	19.0	24.0	2.50	2.50	2.50	328.0	509.0	181.0
	70 : 30	23.0	27.2	20.0	24.4	2.10	2.20	2.15	361.2	521.0	159.8
3 mm	10 : 30	16.6	23.2	11.6	17.0	3.30	2.70	3.00	151.2	309.7	158.5
	20 : 30	14.7	20.9	12.2	17.8	3.10	2.80	2.95	140.9	292.0	151.1
	30 : 30	19.0	25.6	15.4	21.0	3.30	2.80	3.05	229.8	422.0	192.2
	50 : 30	26.6	31.6	17.0	22.6	2.50	2.80	2.65	355.0	561.0	206.0
	70 : 30	29.6	34.6	22.0	27.0	2.50	2.50	2.50	511.5	734.0	222.5
1 mm	20 : 50	14.5	24.3	14.0	23.8	4.90	4.90	4.90	159.5	454.0	294.5
	30 : 50	18.6	29.0	17.9	28.1	5.20	5.10	5.15	261.5	640.0	378.5
	50 : 50	23.6	34.6	21.5	30.9	5.50	4.70	5.10	398.1	840.0	441.9
2 mm	20 : 50	15.1	25.9	13.5	24.7	5.40	5.60	5.50	160.0	502.0	342.0
	30 : 50	13.4	24.2	18.0	28.8	5.40	5.40	5.40	189.5	547.0	357.5
	50 : 50	21.0	31.4	19.6	28.8	5.20	4.60	4.90	323.3	710.0	386.7
3 mm	20 : 50	16.8	28.6	13.8	23.8	5.90	5.00	5.45	182.0	535.0	353.0
	30 : 50	18.8	29.0	15.2	26.2	5.10	5.50	5.30	224.2	597.0	372.8
	50 : 50	35.0	43.8	19.8	28.0	4.40	4.10	4.25	544.0	964.0	420.0

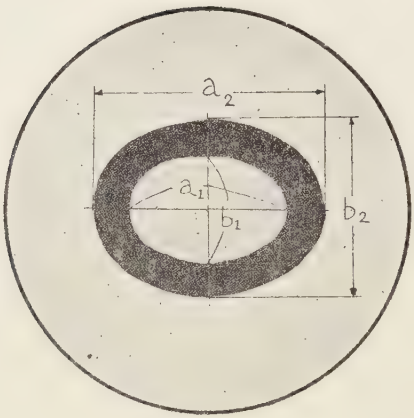

Figure 1

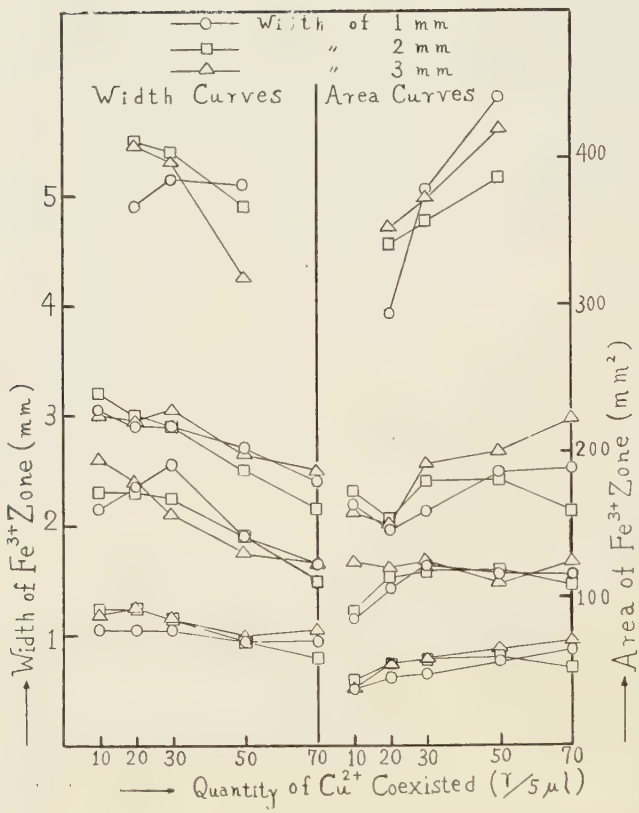

Figure. 2

Result of Experiment and Discussion

The chromatogram obtained after the development was as follows: Cu^{2+} situated at the center of the paper and just outside of the Cu^{2+} zone came the Fe^{3+} zone as reported before[1),2),3),4),5)]. The shape of the chromatogram was almost elliptic. So the figure was presumed to be a complete ellipse and from the measurement of the both axes, the width and area of the zones were determined, as shown in Figure 1 and Table I.

Figure 2 shows the relation between the width or the area of the Fe^{3+} zone and the quantity of Cu^{2+} coexisted. In this Figure the left half portion is the width—quantity of Cu^{2+} coexited curves and the right one is the area—quantity of Cu^{2+} coexisted curves. In each portion, the four groups of curves may be descernible (each group is composed of three curves). These groups correspond with $10\gamma/5\mu l$, $20\gamma/5\mu l$, $30\gamma/5\mu l$ and $50\gamma/5\mu l$ of Fe^{3+} from the bottom.

The variation of the width of the tab seems to give no definite influence upon both width and area of the Fe^{3+} zones. The reason of the defect of the value of $50\gamma/5\mu l$ Fe^{3+} coexisted with 10γ, $5\mu l$ Cu^{2+} was imperfect and indistinct in the separation between the two zones of Cu^{2+} and Fe^{3+}. The points corresponding with $50\gamma/5\mu l$ Fe^{3+} fractuate somewhat distinctly, so the limit of the quantity of Fe^{3+} determined with this method would be near this quantity.

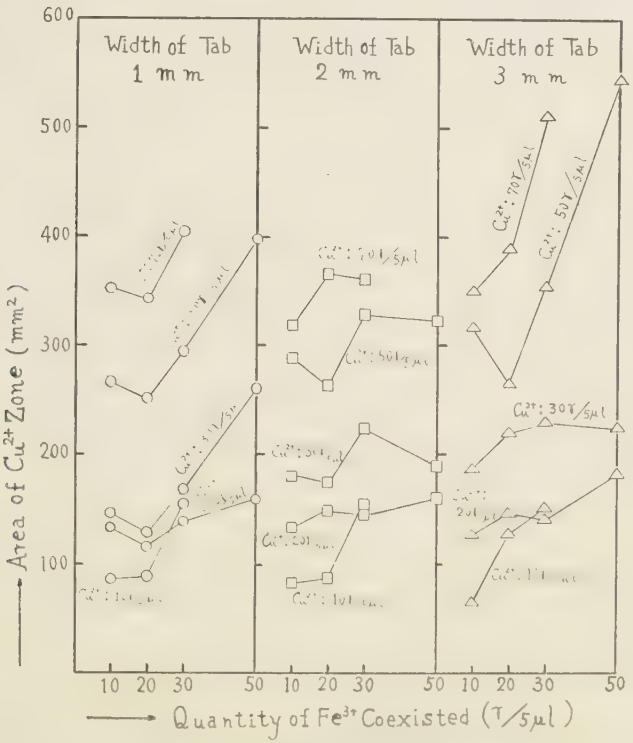

Figure. 3

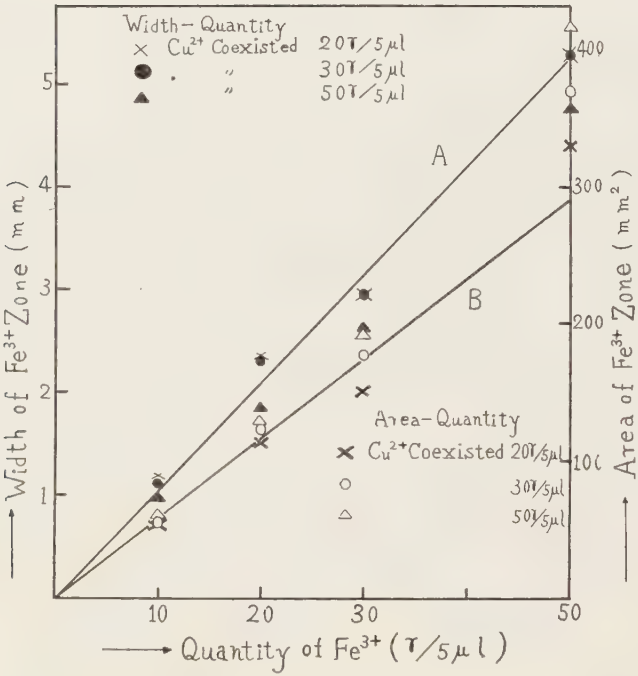

Figure. 4

The quantity of Cu^{2+}, $70\gamma/5\mu l$ would also be the limit of coexistence.

Thus, the quantity of Cu^{2+} should be roughly determined and, if possible, the adoption of the area of Cu^{2+} zone in this chromatogram would be desirable for this purpose. Figure 3 is drawn by the value of Table I as the same way as Figure 2 and shows the relation betwen the area of the zone and the quantity of Fe^{3+} coexisted. This relation would be able to be utilized as the rough determination of Cu^{2+} quantity.

Figure 4 is drawn to obtain the more difinite judgment for the determination of the quantity of Fe^{3+}. In Figure 2, the variation of the width of the tab gives no definite influence upon the width or the area of the zone, so the mean value of the three points, corresponding with the three kinds of different width tab for the same quantity of Fe^{3+}, is taken for that quantity of Fe^{3+}.

In Figure 4, the points corresponding with the width of the zones situates not so far from the line A, but in the case of the area the points corresponding with $50\gamma/5\mu l$ Fe^{3+} were far apart from the line B, though the other points situate more nearly alone the line than the case of width.

Conclusion

1. The quantity of Fe^{3+} would be possibly determined with sufficient accuracy by the width or the area of the zone in the precipitation chromatogram with oxine, in the case of the

coexistence of Cu^{2+}. Moreover, the qantity of Cu^{2+} would also be able to be determined roughly by the area of the zone.

2. Using the width of the zone, the wider range measurement of the quantity of Fe^{3+} would be possible and the calculation becomes easier than the case of the area of the zone.
3. Using the area of the zone, the less influence of the coexisted Cu^{2+} upon the measurement of the qantity of Fe^{3+} would be expected than the case of the width of the zone.

The contents of this paper will mainly be published in J. Chem. Soc. Japan, Pure Chem. Sect.

Literature Cited

(1) H. Nagai, Kumamoto Journal of Science, Series A, Vol. 2, No. 3, 304 (1955).
(2) H. Nagai, Ibid., Vol. 2, No. 4, 81(1957).
(3) H. Nagai, Ibid., Report IV. (Part 3) in this volume.
(4) H. Nagai, Ibid., Repert V. (Part 4) in this volume.
(5) H. Nagai, Ibid., Report VI. (Part 5) in this volume.

A NOTE ON COORDINATED SPACES

Mituo INABA

(Received Nov. 30, 1957)

1. *Preliminary.* Preparing the previous paper [1][(1)], we were interested in some properties of coordinated spaces, that is, especially in relations between the coordinatedness and the existence of basis of linear convex topological spaces and in those between the coordinatedness of a linear convex topological space and that of its dual space. In the case of Banach spaces, one of the former relations is well-known ([2], pp. 110–111) and one of the latter is partially solved by Karlin [3]. In the present paper we shall generalize these relations to the case of linear convex topological spaces and moreover afford a more general positive answer to one of the three unsolved problems proposed by Karlin ([3], p. 984): "If the dual space E′ has a basis does that imply that the space E has a basis ?"

Here by a sequence space we mean an abstract linear space, whose each point x is represented uniquely, or more precisely one to one, by an infinite sequence of real or complex numbers $\{x_1, x_2, \cdots\cdots, x_n, \cdots\cdots\}$, or simply denoted by $\{x_n\}$, such that each mapping $x_n(x)$: $x \to x_n$ $(n=1,2,\cdots\cdots)$ is linear, and by a coordinated space a sequence space topologized locally convex, such that each mapping $x_n(x)$: $x \to x_n$ $(n=1,2,\cdots\cdots)$ is continuous. For each point x, the point which is constructed by equating to zero the coordinates with indices greater than n is denoted by $x^{(n)}$. A coordinated space is called to have the property "Abschnittkonvergenz", or simply (AK) [4], if for every point x of the space, the sequence $\{x^{(n)}\}$ converges to x as n tends to ∞.

2. *Coordinatedness and Basis.* Coordinated spaces have not always a basis, as it is seen in the space (m) and (c).

Theorem 1. Let E be a linear convex topological space. If E is coordinated and has the property (AK), then E has a basis.

Proof. For $i=1,2,\cdots\cdots, n, \cdots\cdots$, let e^i be a point represented by the sequence $\{\delta_{in}; n=1,2,\cdots\cdots\}$, where δ_{in}'s are Kroncker's deltas. For each point x of E represented by the sequence $\{x_n\}$, $x^{(n)}$ can be expressed in the following form:

$$x^{(n)} = \sum_{i=1}^{n} x_i e^i.$$

Since the property (AK) implies $x^{(n)} \to x$ as $n \to \infty$, x can be expressed in the form:

$$x = \sum_{i=1}^{\infty} x_i e^i. \qquad (1)$$

The uniqueness of the representation by coordinates implies that of the representation (1), and therefore the set of points $\{e^1, e^2, \cdots\cdots, e^n, \cdots\cdots\}$ is a basis of the space E, which

(1) Numbers in brackets refer to the bibliography at the end of the paper.

proves the theorem.

The converse of this theorem can be given in the form of the following

Theorem 2. If E is an F-space (i. e. a complete, metrizable, linear, convex topological space) and has a basis, then E is a coordinated space with the property (AK).

Proof. Let $\{e^n\}$ be the basis, and then for each x of E we have

$$x=\sum_{i=1}^{\infty} x_i e^i,$$

$\{x_i\}$ being uniquely, or more precisely one to one, determined, or

$$\sum_{i=1}^{n} x_i e^i \to x \quad \text{as} \quad n\to\infty.$$

We consider a sequence space $\tilde{E}$, consisting of the sequences $\tilde{x}$:

$$\tilde{x}=\{x_1, x_2, \cdots\cdots, x_n, \cdots\cdots\}.$$

Thus we have a mapping Φ of E onto $\tilde{E}$, i. e. $\Phi: x\to\tilde{x}$. This mapping Φ is linear and one-to-one.

Let the topology of the space E be defined by a family of semi-norms:

$$p_\lambda(x)=\|x\|_\lambda \qquad (\lambda\in\Lambda)$$

Since $\sum_{i=1}^{\infty} x_i e^i$ is convergent, $\|\sum_{i=1}^{n} x_i e^i\|_\lambda$ is bounded for each λ and we define semi-norms $\|\tilde{x}\|_\lambda$ of the space $\tilde{E}$ as follows:

$$\|\tilde{x}\|_\lambda=\sup_{1\leqq n<\infty}\|\sum_{i=1}^{n} x_i e^i\|_\lambda.$$

The space $\tilde{E}$ thus semi-normed is an F-space.

The inverse mapping $x=\Phi^{-1}(\tilde{x})$ of the mapping Φ is linear, one-to-one and continuous. In fact, by the definition of $\|\tilde{x}\|_\lambda$, we have

$$\|x\|_\lambda=\|\Phi^{-1}(\tilde{x})\|_\lambda\leqq\|\tilde{x}\|_\lambda,$$

([5] II, § 5, p. 100, Prop. 9). Thus the mapping Φ^{-1} of the F-space $\tilde{E}$ onto the F-space E is bicontinuous ([2], p. 41, The. 5, or [5] Chap. I, § 3, p. 36, Cor. 1), and therefore Φ is an isomorphism.

The functional $\tilde{x}'$ defined on $\tilde{E}$, such that $<\tilde{x}, \tilde{x}'>=x_i$ where $\tilde{x}=\{x_n\}$, is evidently linear, and also continuous. In fact, for each $\lambda\in\Lambda$, $\|x_i e^i\|_\lambda\leqq 2\|\tilde{x}\|_\lambda$, or $|x_i|\leqq 2\|\tilde{x}\|_\lambda/\|e^i\|_\lambda$ for semi-norms $\|\ \|_\lambda$, such that $\|e^i\|_\lambda>0$. Hence the space $\tilde{E}$ is coordinated, and so is the space E, since the mapping $x_n(x): x\to x_n$ is continuous as composed mapping of two continuous ones

$$x \to \tilde{x} \quad \text{and} \quad \tilde{x} \to x_n .$$

The property (AK) is obvious. Thus the proof is completed.

We can conclude the equivalence of the coordinatedness with the property (AK) and the existence of basis for F-spaces.

3. Coordinatedness of a space E and that of its dual space E'.

Theorem 3. If E is coordinated with the property (AK), then its dual space E' is also coordinated with the property $*$-weak-(AK) (that is, (AK) for the topology $\sigma(E', E)$).

Proof. For each point x of E represented by the sequence $\{x_n\}$, we denote $x_n e^n$ by $x_{(n)}$, where each e^i is a point represented by the sequence $\{\delta_{in}\}$ as before, and $x_{(n)} = x_{(n)}(x)$, where $x_{(n)}$ on the right-hand side is the mapping: $x \to x_{(n)}$. The space $E_{(n)}$ of the points $x_{(n)}$ is a subspace of E isomorphic to R^1 or C, the space of real or complex nwmbers.

The dual space E' is a sequence space. In fact, for every point $x' \in E'$, since the continuous linear functional $x'_{(n)}$ defined by

$$\langle x, x'_{(n)} \rangle = \langle x_{(n)}(x), x' \rangle = \langle x_{(n)}, x' \rangle$$

can be considered as a linear continuous functional defined on the 1-dimensional linear subspace $E_{(n)}$, we may put

$$x'_{(n)} = x'_n e'^{(n)}.$$

Hence x' can be represented by the sequence $\{x'_n\}$. This representation is unique, because if, for all n, $x'_n = 0$, then $x'_{(n)} = 0$ for all n, which implies that for all n and for every $x \in E$, $\langle x, x'_{(n)} \rangle = 0$, or $\langle x_{(n)}, x' \rangle = 0$, or furthermore $\langle x^{(n)}, x' \rangle = 0$, and from the property (AK) and the continuity of the functional x, it follows that, for every point $x \in E$, $\langle x, x' \rangle = 0$, which proves that $x' = 0$.

Each mapping $x'_n(x')$: $x' \to x'_n$ is continuous. In fact, a fundamental system of neighbourhoods of the origin in the dual space E' consists of the polars of the bounded subsets of E, *i. e.* of the subsets $\{x'; |\langle x, x' \rangle| \leqq 1, x \in B\}$ where B is a bounded subset of E, and a fundamental system of neighbourhoods of the origin in the space $E'_{(n)}$ of the points $x'_{(n)}$ consists of the polars of the bounded subsets of the subspace $E_{(n)}$. Bounded subsets in the space $E_{(n)}$ is also bounded in the space E. Thus the mapping $x'_{(n)}(x')$: $x' \to x'_{(n)}$, accordingly $x'_n(x')$: $x' \to x'_n$ is continuous.

The representation $\{x'_n\}$ is $*$-weak-(AK). In fact, since

$$\langle x, x'^{(n)} \rangle = \langle x, \sum_{i=1}^{n} x'_{(i)} \rangle = \sum_{i=1}^{n} \langle x, x'_{(i)} \rangle$$

$$= \sum_{i=1}^{n} \langle x_{(i)}, x' \rangle = \langle \sum_{i=1}^{n} x_{(i)}, x' \rangle = \langle x^{(n)}, x' \rangle,$$

the property (AK) for the space E implies that, for all $x \in E$, $\langle x, x'^{(n)}\rangle = \langle x^{(n)}, x'\rangle$ converges to $\langle x, x'\rangle$ as n tends to ∞, and therefore $x'^{(n)}$ converges $*$-weakly to x'. The theorem is proved.

The converse of this theorem is given for F-spaces by the following

Theorem 4. Let E be an F-space. If the dual space E' is coordinated with the property $*$-weak-(AK), then the space E itself is also coordinated with the property (AK).

Proof. For each point x' of E' represented by the sequence $\{x'_n\}$, we denote the sequence $\{\delta_{in}x'_n;\ i=1, 2, \cdots\cdots\}$ by $x'_{(n)}$ and $\{\delta_{in};\ i=1, 2, \cdots\cdots\}$ by $e'^{(n)}$, and then we have $x'_{(n)} = x'_n e'^{(n)}$. For each point x of E, we have

$$\langle x, x'_{(n)}\rangle = x'_n \langle x, e'^{(n)}\rangle.$$

Here if we put $\langle x, e'^{(n)}\rangle = x_n$, then we have $\langle x, x'_{(n)}\rangle = x_n x'_n$. Therefore the point x is represented by $\{x_n\}$.

This representation $\{x_n\}$ is linear and unique. The linearity is evident. If, for all n, $x_n = 0$, *i. e.* $\langle x, e'^{(n)}\rangle = 0$, hence $\langle x, x'_{(n)}\rangle = 0$, then $\langle x, x'^{(n)}\rangle = 0$. The property $*$-weak (AK) implies that, for every $x' \in E'$, $\langle x, x'\rangle = 0$, and therefore $x = 0$. Thus the uniqueness of the representation is verified.

The mapping $x_n(x)$: $x \to x_n$ is continuous. Since $x_n = \langle x, e'^{(n)}\rangle$ is a continuous functional of x, the mapping is continuous.

The property $*$-weak-(AK) implies that for every $x \in E$ and every $x' \in E'$, since

$$\langle x, x'\rangle = \lim_{n\to\infty} \langle x, x'^{(n)}\rangle = \lim_{n\to\infty} \sum_{i=1}^{n} \langle x, x'_{(i)}\rangle$$

$$= \lim_{n\to\infty} \sum_{i=1}^{n} x'_i \langle x, e'^{(i)}\rangle = \lim_{n\to\infty} \sum_{i=1}^{n} x_i x'_i,$$

the series $\sum_{n=1}^{\infty} x_n x'_n$ is convergent, and also that $\langle e^m, e'^{(n)}\rangle = \delta_{mn}$, where $e^{(m)} = \{\delta_{mn}; n = 1, 2, \cdots\cdots\}$.

The representation has the property weak-(AK). In fact, for each $x' \in E'$ we have

$$\langle x^{(n)}, x'\rangle = \sum_{i=1}^{n} \langle x_i e^{(i)}, x'\rangle = \sum_{i=1}^{n} x_i \langle e^{(i)}, x'\rangle$$

$$= \sum_{i=1}^{n} x_i \sum_{m=1}^{\infty} \delta_{mi} x'_m = \sum_{i=1}^{n} x_i x'_i,$$

and since $\sum_{i=1}^{n} x_i x'_i$ is convergent to $\langle x, x'\rangle$, $\langle x^{(n)}, x'\rangle$ converges to $\langle x, x'\rangle$ as n tends to ∞ for each $x' \in E'$, and hence $x^{(n)}$ converge to x weakly as n tends to ∞.

Thus the completion of the proof will be reduced to the following

Lemma. If E is a coordinated F-space and its dual space E' is a sequence space, then the property weak-(AK) implies the property (strong-) (AK) (that is, the property (AK) is equivalent for both the weak topology and the original one).

Proof. Now let E_1 denote the closed linear subspace generated by the countable

set $\{e^1, e^2, \cdots\cdots, e^n, \cdots\cdots\}$ of points of the basis of E.

We first show that $E_1 = E$. If we suppose the contrary, then there exists such a point x^0 of E, as does not belong to E_1, hence by virtue of Hahn-Banach theorem, there exists a linear continuous functional x' defined on E, such that

$$<x^0, x'> = 1 \quad \text{and} \quad <x, x'> = 0 \quad \text{for each } x \in E_1.$$

Hence we have $<e^n, x'> = 0$ or $\sum_{i=1}^{\infty} \delta_{in} x'_i = x'_n = 0$ for each n, accordingly $x' = 0$, which contradicts to the propepeety $<x^0, x'> = 1$.

In order to prove that each point $x \in E_1$ or E satisfies the condition (AK), *i. e.* the point

$$x^{(n)} = \sum_{j=1}^{n} x_{(j)} = \sum_{j=1}^{n} x_j e^j = \sum_{j=1}^{n} <x, e'^{(j)}> e^j$$

converges (strongly) to the point x as n tends to ∞, we must previously prove that the countable subset $\{\sum_{i=1}^{n} x_i e^i;\ n = 1, 2, \cdots\cdots\}$ is bounded. Since $\sum_{i=1}^{\infty} x_i x'_i$ is convergent, the countable set of numbers $\{\sum_{i=1}^{n} x_i x'_i;\ n = 1, 2, \cdots\cdots\}$ is bounded, and let $\sup_{1 \leq n < \infty} |\sum_{i=1}^{n} x_i x'_i|$ be denoted by (x, x'). Let U be an arbitrary weak neighbourhood of the origin in the space E, *i. e.* $U = \{x; |<x, x'_k>| \leqq 1,\ k = 1, 2, \cdots\cdots, l\}$, and $\max_{1 \leq k \leq l} [(x, x'^k)]$ be denoted by M_x. Then we have $|<\sum_{i=1}^{n} x_i e^i, x'^k>| \leqq (x, x'^k) \leqq M_x$, and hence $\sum_{i=1}^{n} x_i e^i \in M_x U$ for $n = 1, 2, \cdots\cdots$. This shows that the contable set $\{\sum_{i=1}^{n} x_i e^i;\ n = 1, 2, \cdots\cdots\}$ is weakly bounded, and accordingly (strongly) bounded.

Putting $s_n(x) = \sum_{i=1}^{n} x_i e^i$, a sequence of linear countinuous applications $s_n(x)$ on E into itself: $x \to \sum_{i=1}^{\infty} x_i e^i$ is defined. Secondly we must prove that the set of applications $\{s_n;\ n = 1, 2, \cdots\cdots\}$ is equicontinuous. A neighbourhood of the origin in the space $\mathfrak{L}(E, E)$, with the topology of simple convergence, of all linear continuous applications on E into itself is defined by the set of linear continuous applications $u(x)$ such that $u(M) \subset V$, where M is a finite subset of E and V a neighbourhood of the origin in E, and is denoted by $T(M, V)$. For each pair of a finite subset M and a neighbourhood V of the origin in E, since the subset $\{s_n(M);\ n = 1, 2, \cdots\cdots\} = \bigcup_{x \in M} \{s_n(x);\ n = 1, 2, \cdots\cdots\}$ is bounded as a finite sum of bounded subsets, there exists a positive number λ such that

$$s_n(M) \subset \lambda V,$$

and accordingly

$$\{s_n;\ n = 1, 2, \cdots\cdots\} \subset \lambda T(M, V).$$

Thus the set of applications $\{s_n : n = 1, 2, \cdots\cdots\}$ is bounded in the space $\mathfrak{L}(E, E)$ with

the topology of simple convergence, and accordingly equicontinuous ([6] Chap. IV, § 3, p. 27, Th. 2).

We have now to prove that $s_n(x)$ converges to x as n tends to ∞. In case $x = \sum_{i=1}^{m} x_i e^i$, the proof is evident, since $s_n(x) = \sum_{i=1}^{m \leqq n} x_i e^i$ converges to $\sum_{i=1}^{m} x_i e^i = x$. In case the point x is a limit point of the sequence of points $\{x^m;\ m = 1, 2, \cdots\cdots\}$, where $x^m = \sum_{i=1}^{m} x_i^m e^i$, we proceed as follows. Because of the equicontinuity of the set of applications $\{s_n:\ n = 1, 2, \cdots\cdots\}$, for an arbitrary neighbourhood V of the origin there exists a neighbourhood U of the origin (independent of n), such that $s_n(U) \subset V$ for $n = 1, 2, \cdots\cdots$. $V' = U \frown V$ being a neighbourhood of the origin, there exists a positive integer m_0, such that

$$x^{m_0} - x \in V' = U \frown V \subset V,$$

and accordingly

$$s_n(x^{m_0} - x) = s_n(x^{m_0}) - s_n(x) \in V.$$

From the first case, it follows that there exists a positive integer n_0 (depending on m_0), such that $n \geqq n_0$ implies the relation:

$$s_n(x^{m_0}) - x^{m_0} \in V.$$

These three relations implies that

$$s_n(x) - x \in 3V \qquad \text{for } n \geqq n_0,$$

which proves that $s_n(x)$ converges x as n tends to ∞. Thus the proof of the lemma is completed.

Remark to the lemma. In the case of the dual space E', the result of the lemma does not hold, that is, the property *-weak-(AK) does not always imply the property strong-(AK), as is seen in an example: $E = (l)$, the space of the absolutely convergent sequences and its dual space $E' = (m)$, the space of the bounded sequences.

References

1. M. Inaba, Differential Equations in Coordinated Spaces, Kumamoto Journal, Series A, Vol. 2, pp. 233-243, (1955).
2. S. Banach, Théorie des Opérations Linéaires, Warszawa, 1932.
3. S. Karlin, Duke Mathematical Journal, Vol. 15, pp. 971-985, (1948).
4. K. Zellar. FK-Räume in der Functionen Theorie I, Math. Zeitschr. Bd. 38, pp. 228-305, (1953).
5. N. Bourbaki, Espaces vectoriels topologiques, Chap. I et II (Actual, Scient. et Ind. 1189).
6. N. Bourbaki, Espaces vectoriels topologiques, Chap. III, IV et V (Actual. Scient. et Ind. 1229)

THE INVESTIGATION OF "SARA-ISI" BY THE X-RAY AND THE MICROSCOPE (Report 3)

Tadashi OKAHATA

1. Abstract

With Sara-isi, the structure of the core and the mantle part was examined by the microscope and was ascertained that there is a definite difference between them, not only in the structure but also in the origin of their formation.

Next, to investigate the growth mechanism of the mantle part, X-ray was applied to the specimen of this part, but he could not come to the decisive conclusion till now.

2. Introduction

"Sara-isi" means "Stone shaped like a dish" in Japanese, and they are gathered on the Mt. Aso. Hitherto, it is said that Sara-isi is a kind of volcanic bombs, and has been produced as follows, viz. at the time when the volcano Aso were erupting, the volcanic bombs which were thrown out high into the air fell down with cooling and collided to the ground, then by the reaction they were transformed into the Sara-isi.

But, the writer have been convinced himself by his own studies of Sara-isi, that the opinion concerning to the origin of it is not true. They have been produced secondarily by the adhesion and coagulation of the volcanic ashes upon the outside surface of the volcanic bombs and such likes lying on the ground. Hence, the Sara-isi consists of the core part and the mantle part which surround the former. The one is the volcanic bomb or such like, and the other is the metamorphic part of the ashes, since they differ in formation considerably. The very mantle part is the characteristic one of the Sara-isi. He is going to research the mechanism of the growth of them. This paper reports the results of the microscopic observation and the experiment by the X-ray.

3. Microscopic examination

The specimen A. which was cut from a Sara-isi by the xz-plane, was examined under the microscope. The core part was coated with the coagulated part of 0.5~3 mm in thickness, and there was definite difference between them.

(a). The core part of the specimen A.

In the core part were seen some pretty crystals of plagioclase and its size were about 2 mm. Some of them showed the polysynthetic twins. Those plagioclase lied here and there in the amorphous ground mass of the core part, but the quartz was seen nowhere. The magnetite was very few in this part, on the other hand, a large number of them was seen in the coagulated or mantle part.

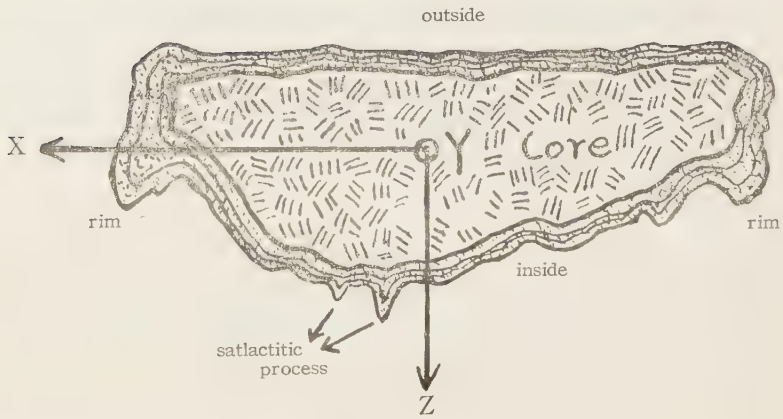

Fig. 1 Model section of Sara-isi.

(b). The mantle part of the specimen A.

In the mantle part, there were seen the reddish brown stripes piled one over another running round the core, and there were the following mineral crystals or fragments in the amorphous ground mass of this part.

Plagioclase: They showed the idiomorphic crystals or the fragment forms of 0.05~0.1 mm size and among them the polysynthetic twins were seen.

Augite. (probably common augite): They were roundish crystals of 0.1~0.2 mm size, and their extinction angle were 40° under the polarizing microscope.

Magnetite: They showed the irregular forms of 0.05~0.1 mm size and their numbers were very large compared with the one in the core part.

With the other specimen B. which was cut from the other Sara-isi by the xz-plane, was observed as before. There was a definite difference between the core and the mantle part as same as the case of the specimen A.

(a'). The core part of the specimen B.

In this case, the core part showed a porous structure which were formed of almost equal spherical or ellipsoidal holes of 0.2~0.3 mm in diametre. It seemed that these holes are the marks of the emission of gases which were leaved by the volcanic bomb when it was cooling.

In the glassy ground mass of the structure, following minerals were distributed in the form of phenocryst.

Plagioclase: The idiomorphic crystals of 0.5~2 mm size, and some of them showed the polysynthetic twins.

Hypersthene: The idiomorphic or often roundish crystals 0.5~1.5 mm size, and had notable pleochroism and right extinction angle.

Common Augite: The idiomorphic or roundish crystals 0.5~0.8 mm size. extinction angle 40°, and they were far smaller than the quantity of hypersthene.

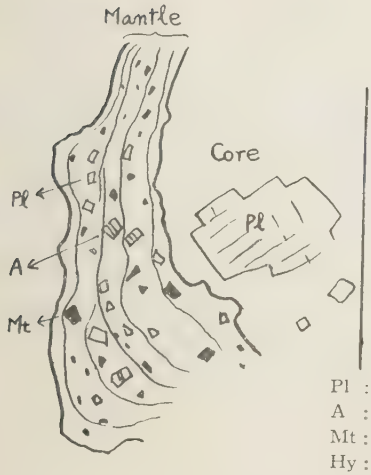

Fig. 2 Specimen A.

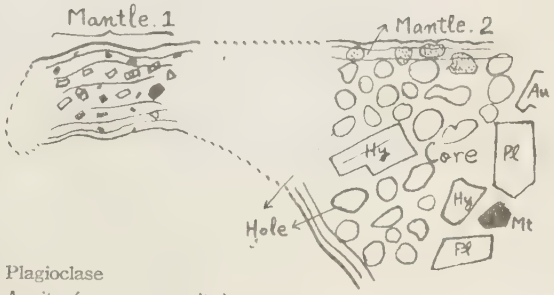

Fig. 3 Specimen B.

Pl : Plagioclase
A : Augite (common augite)
Mt : Magnetite
Hy : Hypersthene

Magnetite: Square or polygon forms, 0.3~1.0 mm size.

(b'). The mantle part of the specimen B.

The mantle part showed the same structure as the case of the specimen A. There distributed the very little fragments of plagioclase, augite, and magnetite. They were agglutinated by some amorphous substance, i. e. groud mass.

It was observed that, some of the holes lying close by the mantle part were filled up by this same amorphous substance. (Fig. 3) This fact illustrate that, to filling up the holes by the amorphous substance was done gradually, in the span of a long time.

The results of the microscopic examination with the specimen C, D, E, F, ····· etc. are all alike to the above mentioned, and then there are no great difference among the structure of the mantle part of every specimen.

He recognized a material difference between the core and the mantle part of the Sara-isi, as following.

i. Both part differed distinctly the kind of mineral elements and their crystal size.
ii. The core part had been subjected to the action of vitrification but the mantle part has not a vestiges of evidence for this assertion.
iii. In the mantle part, the reddish brown stripes piled one over another, run round the core, but no such structure was seen in the core part.

4. Investigation by the X-ray

When the writer was gathering the Sara-isi on the Mt. Aso, chanced upon a piece of a beer bottle which adhered with the substance just the same appearance as the one of mantle part of Sara-isi. This adherent substance was taken off, and the X-ray powder

photograph was taken with it. This powder photograph coinsided with the one from the mantle part.

As above stated, together with the conclusion from the microscopic examination, the mantle part is never a direct or primary volcanic product, but he asserts that it is made of fine particles of volcanic ashes coagurated on the outside of the core substance e.g. volcanic bomb, rock fragment, piece of glass bottle and such like lying on the ground.

About the general distribution of the size of crystal grains in the mantle part had been reported (I). To investigate the growth mechanism of mantle part, more details of the grain size distribution was examined by the X-ray with the specimen, which was cut off, by the xz-plane, from the rim of a Sara-isi. (Fig. 4) X-ray beam was applied in y-direction upon the mantle part of this specimen, and about a hundred of Laue photographs were taken by turning the incident point of the beam in succession.

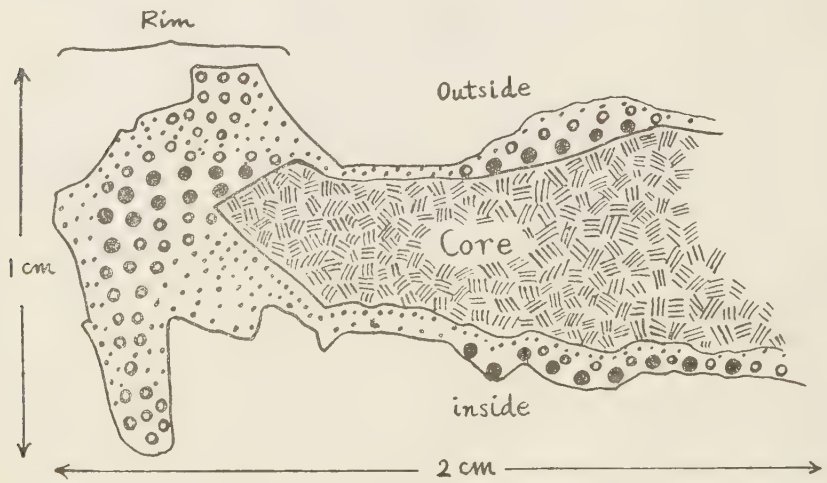

Fig. 4

Grain size distribution in the mantle part.

..... minute grains

oooooo medium sized grains

•••••• large grains

By this experimental procedure, following results as are shown by the Fig. 4 was obtained with this specimen. Roughly speaking, similer sized crystal grains formed associations mutualy at various place in the mantle part. The outside of Sara-isi are formed of the layer of minute crystal grains above the one of comparatively large grains, but the inside are formed of the latter above the former. In the rim, the accumulating state of these layers are so complicated that as if they show the complication of the growth mechanism of this part. The whole figure of this specimen may be related to the core's shape.

Above mentioned is the result examined by the X-ray with the sole specimen, hence

even if he could think moreover with this in various ways, but can not comes to any conclusion.

From the stalactitic process which existed on the surface of Saraisi were cut off two kinds of specimen, xz- and xy-cut. In these specimens are seen the annual rings like reddish brown stripes piled one over another running round the core part as was seen in the mantle part. Then he thought that the process might has been brought by way of the such process as of the stalactite growth. But, the results examined by the X-ray with the specimens were negative as following,

The Laue method was applied to the specimen. Hardly any Laue spots but the D. S-rings came out on the radiograph. Then, the xz-plane of the specimen of xz-cut was held perpendicular to the incident X-ray beam (y-direction), and rotated by a small angle around the x-axis, and the radiograph was taken. Next, in the same direction around the same axis, the specimen was rotated again by a small angle and radiographed, and so on. In this manner, they were taken by rotating the same specimen around the z-axis, too. Besides, with the specimen of xy-cut, the radiographs of same kind were taken and examined. But, after all, no radiographs showed the fibrous structure.

The writer wishes to express his thanks to Dr. M. Namba who gave kind advice to him.

Reference

(1). M. Namba; Mem. Col. Sci. Kyoto Imp. Uni. Vol. 19, No. 3, 1936.
(2). T. Okahata; Kumamoto J. of Sci. Vol. 1, No. 4, 1954.
(3). ditto, Series A. Vol. 2, No. 1, 1954.

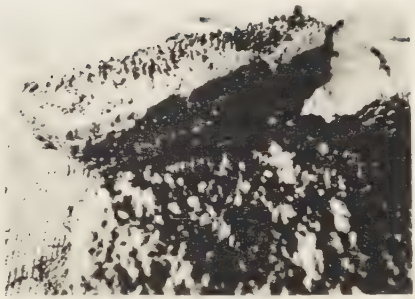

Fig. (a

Stalactitic processes on the surface of Sara-isi.

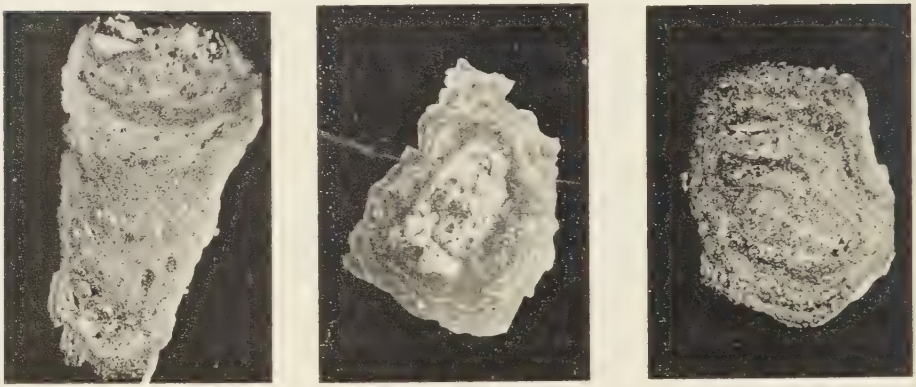

i) xz-cut ii) xy-cut iii) xy-cut

Fig. (b) Sction of the stalactitic process.

Fig. (c)

A part of section of Sara-isi.

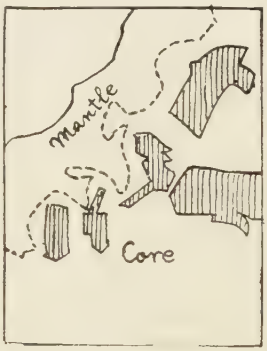

Boundary

Crystal

Fig. (d

A piece of glass adhering the substance same as the one of the mantle part.

SOME STUDIES ON VOLCANO ASO AND KUJU PART 14, ON VOLCANIC SOUNDING.

Munetoshi NAMBA & Yasuhiro SUGIMOTO

(Recived Sept. 1st, 1957)

Abstract

The writer explained a volcanic sounding and some phenomena acconpanied with it. Then he advocated "an edge tone generated by a piece of magma in the volcanic conduit tube" as one of its causes from a result of the analysis of the volcanic sounding records.

And then he knew that the sounding source is situated on a very upper part of the volcanic conduit tube.

Furthermore, present writer explained a feed cock noising as a similar case of a volcanic sounding. The sounding source is a distorted packing rubber which is suspended on the side wall of the surrounding of the hole of a water supply cock and an edge tone so-called the feed cock sound generated by the eddy current of the water.

§ 1. Volcanic Sounding or Noising.

At volcano Aso, before the explosion of a fumeroling volcanic crater, there often occurrs a sounding as a roar, and the sounding spreads over the crater. The sounding is said commonly a volcanic sounding or volcanic noising.

He explained more precisely about it:-

1) Just before a volcanic sounding, the fumeroling gas decreases suddenly its amounts and its speed. After a short time, it sounds as a lion roar and then the volcanic sounding begins its roll.

2) The atomosphere in the crater begins its resonance, the rim of the crater obviously is resonant and the volcanic ash and sand on the rim are often vibrating too. When it sounds powerfully, man can hear it at a distance of about ten kilometers.

3) A volcanic sounding is always changes its intensity, and so man commonly feels it as a beating.

4) The amount of effusing gas varies as the volcanic sounding varies. That is the effusion increases in its amount when the volcanic sounding becomes severe, and it decreases when the volcanic sounding becomes weak. Especiany man can sometimes scarcely talk about at the crater rim when the sounding increases its intensity.

5) The sounding, however, scarcely does not changes its tone, sometimes suddenly the sounding stops its activity and the gas stops its effusion. In this case the crater becomes to be a short quite stop. After a while an explosion occurres with a violent sound and spreads out the volcanic debris. When the explosion ceases, it becomes to be a steam effusion stage, and after a while gas decreases its amount and again a volcanic sounding begins its activity. In the Aso crater the volcanic sounding and explosion are

Fig. 1 A. 1955 July 19th. Aso First Crater (before explosion)

Fig. 1 B. 1955 July 25th. 12^{h} Aso First Crater.
white smoke, volcanic sounding.

Fig1. 1 C. 1955 July 25th. 16h 05m Aso First Crater Explosion (after scunding stops

Fig. 1 D. 1955 July 25th. 20^h 30^m Aso First crater (night view in Sounding).

often repeated.

When he goes down into the crater basin while it is in a sounding stage, it may be observed that the sounding source exsits in the conduit tube.

A tradition among Aso volcanic region "that man can safely go down into the crater while it is in a volcanic sounding stage, but can scarcely do while it ceases the sounding" is a matter of reasoning.

The followings are some of the states showing the relation of volcanic sounding and explosion of Aso volcano, and a recent explosion of volcano Sakura-jima which the writer observed on March 12, 1957.

§ 2. On a Feed cock Noising.

If the packing rubber becomes aged, there often happens a feed cock noising or water cap noising when man get slightly loosen a feed cock: It easily happens in summer (warm) season, but not easily in winter (cold) season and more easily does it after the water supply has failed. When man get loosen the feed cock more slightly, then the

noising becomes sever, but the noising stops when more loosen of the cock, the feed water (discharges) increases its amount and the out flow of water becomes smoothly.

Fig. 2. A Section of a Noising Feed Cock

Fig. 2. B.

distorted rubber packing (left)

normal rubber packing (right)

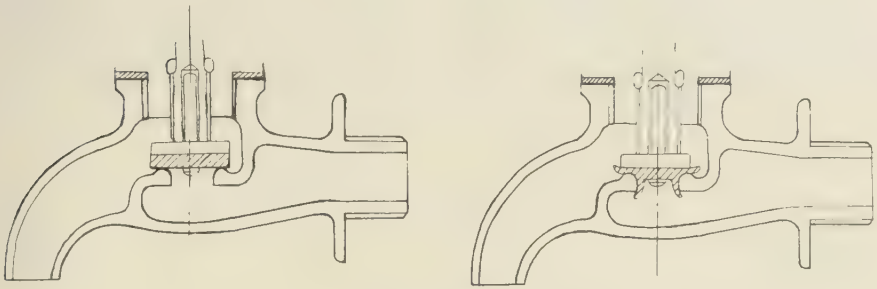

Fig. 2. C. Section of a Noising Cock
Left:-normal packing rubber.
Right:-distorted packing rubber.

Now when man can suitably adjusting, the feed cock noising becomes change to the sounding. Disjointing a noising feed cock man can find the crushing of the cock rubber. (Fig. 2).

Testing the noising cock, man can find that the brush up of the surrounding of the hole is not perfect and there exist abundant spinous processes around the hole.

Therefore the crushed cock rubber can easily be caught by the spinous processes. In the above state, if man get slightly loosen the feed cock, the water flows through the narrow path between the side wall and the crushed rubber, and then the suspended rubber acts as a reed in a water current. The reed in a water current vibrates by the eddy and a feed cock noising should be resulted at a state of resonant state. And then the water current becomes intermit caused by oscillation of the reed.

By more loosing of the cock, the feed water increases its amount and the noising becomes severe too. By getting more and more loosing the cock, the packing rubber should be disjointed from the spinous processes, and then the noising stops and the out flow of water becomes smoothly.

Now, the deformed packing rubber should often be recaught again by the spinous processes when the feed cock was closed. Then the feed cock should again be noised when man made the cock be loosing slightly.

The noising becomes to be sounding after man suitably adjusting the cock.

But if the water is cold, the noising does not occur because the deformed rubber does not be caught by the wall. If, however, the feed cock was heated by a gas burner, the packing rubber becomes deformable and then should be caught by the spinous processes on the wall and therefore the noising is able to occurs easily and it becomes to be a sounding by suitably adjusting the cock.

§ 3. Model experiment of a feed cock sounding.

This writer made an apparatus similar to a strained packing rubber which is suspended on the side wall as is indicated in Fig. 3.

Fig. 3 Model experiment of a Feed cock Noising.

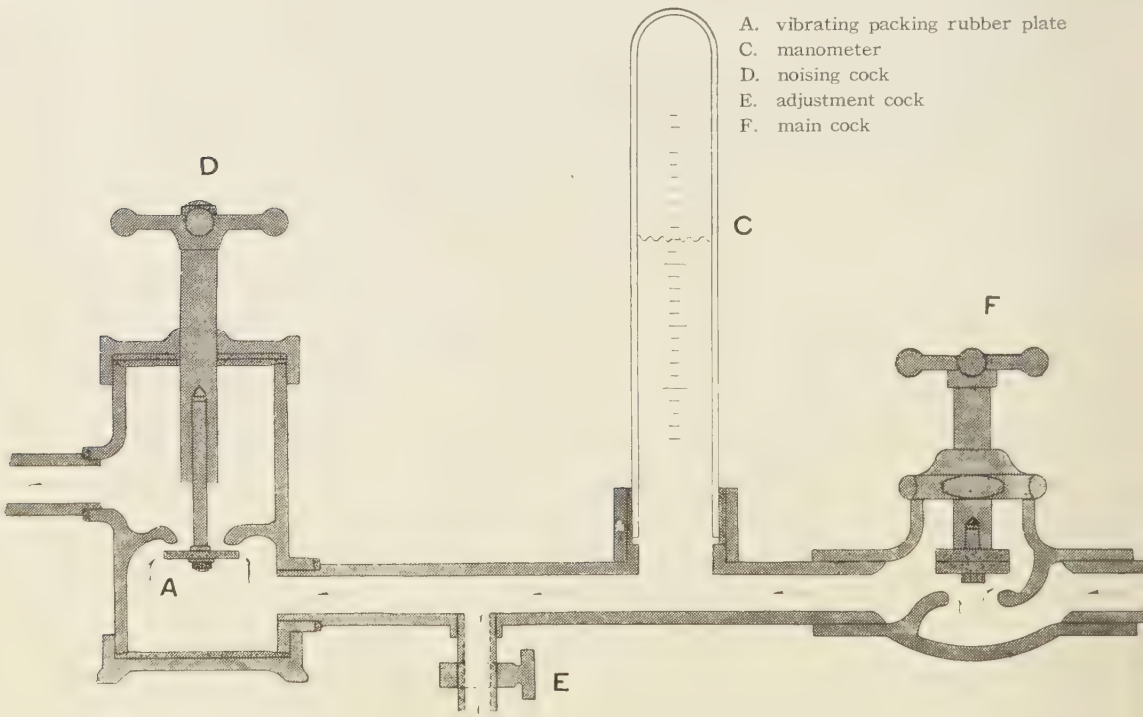

In the above apparatus, a soft rubber circular plate A is supported by a rod B. Then he made the water flow through a narrow space as is shown by an arrow indication.

The plate A in the water current originates a forced oscillation by the eddy after some adjusting, and at last it becomes to a state of a feed cock noising. In this case the feed cock and supply tube vibrates under a sever forced oscillation.

The intensity of noising (or sounding) depends only on the supply water pressure, because the force of eddy current depends on the supply water pressure. Water head in the manometer always changes as the water pressure always changes in a civil water supply.

Therefore in this case the feed cock noising varies its intensity, and so it seems as a beating. Of cause, the quantity and the velocity of the flow vary according to the water pressure.

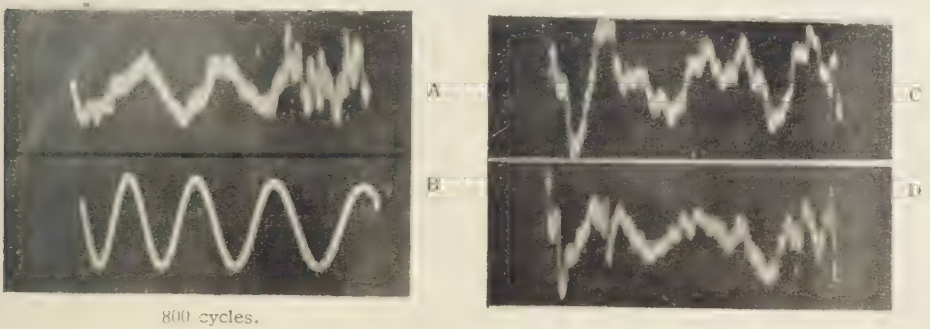

Fig. 4 Oscillographic records of Feed cock Sounding.
A. D. C. vibration of noising
B. 800 cycle (about)

To observe the above phenomena, an effectual apparatus was made as the following figure.

Adjusting the main cock F and regulating cock E and the feed cock D, there occurs a noising, and it becomes to a sounding when they are suitably adjusted.

Then the amplitude of the wave on the water surface in the manometer C becomes maximum at the resonant state, at last water-drops disperse over the surface. The intensity of sounding varies according to the water head in the manometer, but the tone (cycle) of noising (sounding) does not varies so much. By fitting a suitable resonance box on the supply tube, the noising increases its intensity.

The packing rubber was supported at its center, then the fundamental frequency N_1 becomes to

$$N_1 = 0.4745 \frac{h}{(a/2)^2} \sqrt{\frac{E}{\rho(1-\sigma}}$$

in which a : radius
h : thickness

σ : poison's ratio

E : young's modulus

ρ : density

Now in this experiment the N_1 of the packing rubber is calculated by taking into account of the following values,

$a = 0.883$ cm.

$h = 0.45$ cm.

$\rho = 0.96$

$E = 0.046 \times 10^{11}$

$\sigma = 0.4$

After the above calculation, the N_1 must be 12420, but is measured as frequency N_1 800 by an oscillogragh at the resonant state; therefore h must be 0.06 cm. for the oscillation of a circular plate.

The above results show that in this case the disc does not vibrate as a whole circular plate but only a part of it should be vibrated by the eddy current.

Eddy tone of the feed cock sounding should be occurs causing by vibration of a peace of packing rubber in the water current. In other word, when a rod with thickness h cm. of one end fixed and length l cm., the fundamental frequency N_1 must be

$$N_1 = \frac{k}{2\pi} \frac{m_1^2}{l^2} \sqrt{\frac{E}{\rho}}$$

where

$m_1 = 1.875$

$k = \sqrt{\frac{h^2}{12}}$

$E = 0.046 \times 10^{11}$

$\rho = 0.96$

$l = 0.883$ cm.

$h = 0.46$ cm.

After of all, N_1 is calculated as the following

$$N_1 = \frac{0.46}{\sqrt{12}} \cdot \frac{1}{2\pi} \frac{(1.875)^2}{(0.883)^2} \sqrt{\frac{0.046 \times 10^{11}}{0.96}} \fallingdotseq 800$$

The above result was observed through a transparent feed cock.

§ 4. A Consideration on the Cause of "Volcanic Sounding".

After some treatments of the feed cock noising, observations of some actual volcanic

soundings and the analysis of the sounding records, this writers reached to the following results on a cause of a volcanic sounding.

1) The volcanic sounding does not caused by any of Rijke's phenomena in the atmosphere of the crater.

2) Volcanic sounding occurs in the volcanic vent tube under the crater basin, and should be some of the edge tones as that caused by an American organ.

More precisely:

When the volcanic gas flows out with a great velocity through the narrow path in a volcanic vent tube, the eddy of volcanic gas flow make the magma reed vibrate, in this case, there occurs an edge tone by the forced oscillation. If its natural frequency resonantes to that of the crater air column, sever volcanic soundings are generated, and the crater rim should be vibrates too.

If the elastic data of the magma in the conduit tube were that of the rubber in the above model experiment, and a peace of magma of 10 cm. length vibrates in natural frequency of 800 cycle its thickness must be about 5 cm.

The writers studied the sounding records from the first crater of volcano Aso, and analysed them by a wave analyser. The analysis tells us that the most predominate frequency is 800 cycles.

The length of the open pipe is calculated by the following formula, in which the tempreture of the magma is about 1100—1200 °C.

$$l = \frac{v_0}{2 \cdot N_1} \sqrt{1 + \alpha t}$$

where

l :– length of open pipe (conduit tube)

v_0 :– sound velocity in air at 0 °C

α :– 1/273

t :– temperature of gas (magma)

N_1 :– frequency of volcanic sounding (800 cycle)

Thus, from the above values, he has obtained that the length is 0.50 meters.

From the above result, it may be supposed that the upper volcanic conduit tube is the volcanic sounding source. In other words, the sounding source of the first crater is produced by a peace of the magma inside of the very upper volcanic conduit tube following the crater basin. A peace of magma acts as a reed and the eddy tone occurs by the eddy of volcanic gas which is effused through the narrow path. A volcanic sounding occurs after the resonance with the eddy and the natural frequency of the reed, and more they resonante with the natural frequency of the atmospheric column in the rather may act as a resonance box.

The depth of the first crater is about 85 meters and the proper oscillation is about one cycle, thus it may be concidered that they has some probability of action as a resonance box.

As the quantity of volcanic gas effusion always varies according to the inner pre-

ssure of the volcanic gas reservoir and also varies the intensity of the eddy, the sounding may acts like a beating.

If the narrow path in the magma was closed by a pieace of magma, the gas effusion and noising must be ceased and the crater suddenly becomes to a quite stop. In this case

Fig. 5 Sakurajima Volcano. (Every Stage of the activity)

(1)
1957 Mar. 12 th 7h 30m before
(in Sounding; White smoke)

(2)
1957 Mar. 12th Just 7h 30m
(Stop Sounding and white smoking)

(3)
1957 Mar 12th 12h 25m
(Explosion, black smoking)

(4)
Explosion (12h 26m)

(5)
Slopits explosion (13h 00m)

if the volcanic gas pressure increased, the crater may explode, if the packing magma was safely dislocated, volcanic sounding may be regenerated.

He experienced of a volcanic sounding at volcano Sakurajima as well as Aso volcano. The following photo-records are some of them.

The writers express a thanks to Mr. Hichiro Watanabe (JOGK, NHK) who gave some encourages about the sounding records, and Prof. Nakatomi who co-operated on the analysis, and also Mr. G. Koyashiki for his studies on the model experiment of a feed cock noising.

References

1. As reports on the volcanic sounding by Volcano Aso are too much, the writers abridged them in this paper.
2. Natural frequency of a plate are originally calculated by Rayleigh:–sound, 1, Chap. X. Lamb:–Dynamical theory of sound, P. 152.

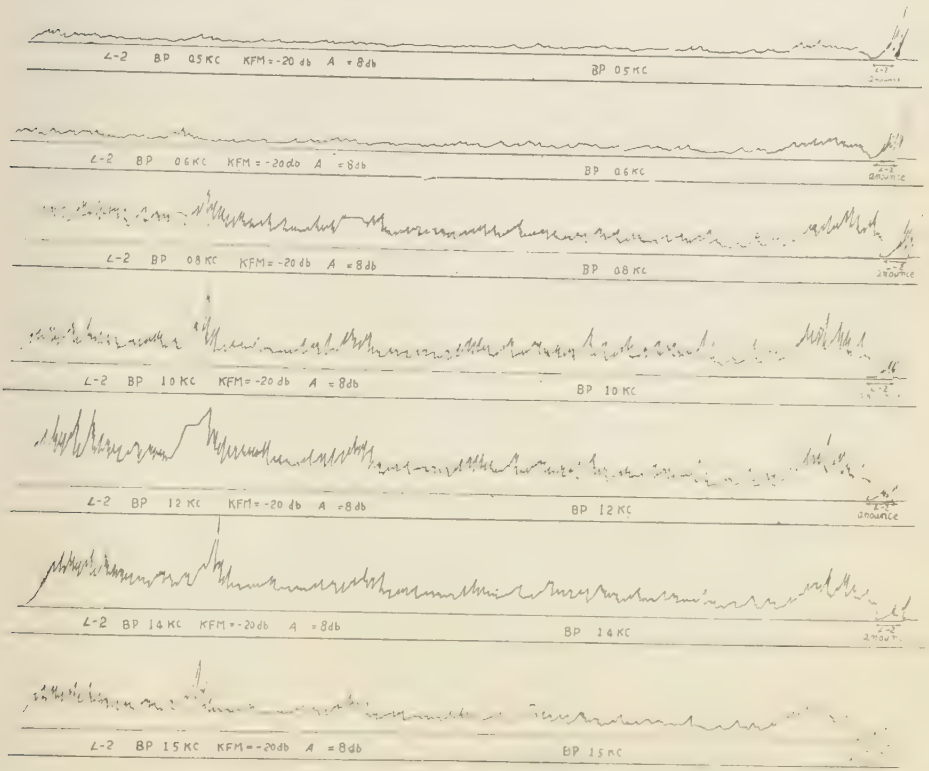

Fig. 6 Analysis of volcanic Sounding (Aso First crater 1955 July 25th)

RELATION BETWEEN A VIBRATION AND ITS GALVANOMETRIC REGISTRATION AND THEIR INITIAL STATES

Ryuzo ADACHI

(Received Dec. 11, 1957)

1. Introduction

On the registration of a vibration such as an earthquake or seismic prospecting e. t. c. by transducer and galvanometer, let $x(t)$, $\varphi(t)$ be the displacement of the vibration and the deflection of galvanometer respectively.

At first, I discussed a problem that to find one of $x(t)$, $\varphi(t)$ when the other is given arbitrarily, and obtained their accurate solutions.

Next, I get approximate formulas which express initial states of $x(t)$, $\varphi(t)$ and some remarks were given.

2. Fundamental Formulas

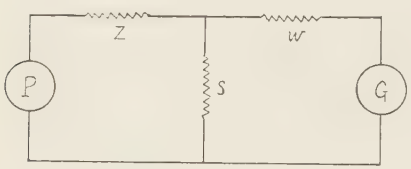

P : Transducer, G : Galvanometer
R_p=Electric resistance of transducer
R_g=Electric resistance of galvanometer
$r_0 = R_p + z$, $r_1 = R_g + w$
$R^2 = r_0 r_1 + r_1 s + s r_0$

Fig. 1

There are many way to connect a transducer and a galvanometer, and as an example, we take a connection shown in Fig. 1.

Let $x(t)$ be the displacement of earthground and $\theta(t)$, $\varphi(t)$ be the deflections of the pendulum of transducer and the mirrored coil of galvanometer at any time t. Next, V_p, V_g be the electromotive forces induced in the coil which settled to the pendulum of transducer and in the coil of galvanometer respectively, and put

$$V_p = g_0 \dot{\theta}, \quad V_g = g_1 \dot{\varphi} \qquad (1)$$

where g_0, g_1 are some constants.

Let the equations of motion of the pendulum of transducer and the coil of galvanometer be

$$\left.\begin{aligned} I_0 \ddot{\theta} + b_0 \dot{\theta} + k_0 \theta &= -LM\ddot{x} \\ I_1 \dot{\varphi} + b_1 \dot{\varphi} + k_1 \varphi &= 0 \end{aligned}\right\} \qquad (2)$$

respectively when the both circuits of coils are switched off, then it is well known result that the equations of motion are

$$\ddot{\theta} + 2\varepsilon_0 \dot{\theta} + n_0^2 \theta = -K\ddot{x} + E\dot{\varphi} \quad \cdots\cdots (3),$$

$$\ddot{\varphi} + 2\varepsilon_1 \dot{\varphi} + n_1^2 \varphi = F\dot{\theta} \quad \cdots\cdots (4),$$

when both circuits are switched on, where

$$\left.\begin{aligned} 2\varepsilon_0 &= \frac{1}{I_0}\left(b_0 + \frac{s+r_1}{R^2}\mathcal{G}_0^2\right), \quad n_0^2 = \frac{k_0}{I_0} \\ 2\varepsilon_1 &= \frac{1}{I_1}\left(b_1 + \frac{s+r_0}{R^2}\mathcal{G}_1^2\right), \quad n_1^2 = \frac{k_1}{I_1} \\ E &= \frac{s\mathcal{G}_0\mathcal{G}_1}{I_0 R^2}, \quad F = \frac{s\mathcal{G}_0\mathcal{G}_1}{I_1 R^2}, \quad K = \frac{LM}{I_0} \end{aligned}\right\} \quad \cdots\cdots (5)$$

As the initial condition we take

$$\theta_0 = 0, \quad \dot{\theta}_0 = -K\dot{x}_0, \quad \varphi_0 = 0, \quad \dot{\varphi}_0 = 0 \quad \cdots\cdots (6),$$

where θ_0 means $\theta(0)$ and so on.

In the following section, we consider the solutions of (3), (4) under the condition (6).

3. Solution of $\varphi(t)$ when $x(t)$ is given

Substituting (4) to (3) gives

$$\varphi^{(\mathrm{IV})} + a\dddot{\varphi} + b\ddot{\varphi} + c\dot{\varphi} + d\varphi = -KF\dddot{x} \quad \cdots\cdots (7),$$

where

$$\left.\begin{aligned} a &= 2(\varepsilon_0 + \varepsilon_1), & b &= n_0^2 + n_1^2 + 4\varepsilon_0\varepsilon_1 - EF \\ c &= 2(\varepsilon_0 n_1^2 + \varepsilon_1 n_0^2), & d &= n_0^2 n_1^2 \end{aligned}\right\} \quad \cdots\cdots (8)$$

Eq. (7) is linear with respect to $\varphi(t)$ and the coefficients are constant, and it can be solved by ordinary method, that is, let α_1, α_2, α_3, α_4 be the four roots of

$$y^4 + ay^3 + by^2 + cy + d = 0 \quad \cdots\cdots (9),$$

then the solution of Eq. (7) which satisfies (6) is

$$\varphi(t) = KF\left[\sum_{i=1}^{4} \frac{\dddot{x}_0 + \alpha_i \ddot{x}_0}{B_i} e^{\alpha_i t} - e^{\alpha_i t}\int e^{(\alpha_2-\alpha_i)t}dt \int e^{(\alpha_3-\alpha_i)t}dt \int e^{(\alpha_4-\alpha_i)t}dt \int e^{-\alpha_i t} x dt\right] \quad \cdots\cdots (10),$$

where

$$\left.\begin{aligned} B_1 &= (\alpha_1-\alpha_2)(\alpha_1-\alpha_3)(\alpha_1-\alpha_4), & B_2 &= (\alpha_2-\alpha_1)(\alpha_2-\alpha_3)(\alpha_2-\alpha_4) \\ B_3 &= (\alpha_3-\alpha_4)(\alpha_3-\alpha_1)(\alpha_3-\alpha_2), & B_4 &= (\alpha_4-\alpha_1)(\alpha_4-\alpha_2)(\alpha_4-\alpha_3) \end{aligned}\right\} \quad \cdots\cdots (11)$$

(10) can be transformed to following form

$$\varphi(t) = KF\sum_{i=1}^{4}\frac{\alpha_i^2}{B_i}e^{\alpha_i t}\left(x_0 - \alpha_i\int_0^t e^{-\alpha_i t}x\,dt\right) \quad \cdots\cdots (12).$$

The solution of $\theta(t)$ which satisfies (6) can be obtained by substituting (12) to (4) and is as follows

$$\theta(t) = K\left[\sum_{i=1}^{4}\frac{A_i}{B_i}e^{\alpha_i t}\left(x_0 - \alpha_i\int_0^t e^{-\alpha_i t}x\,dt\right) - x\right] \quad \cdots\cdots (13)$$

where

$$A_i = \alpha_i^3 + 2\varepsilon_1\alpha_i^2 + n_i^2\alpha_i, \quad i = 1, 2, 3, 4 \quad \cdots\cdots (14).$$

We can show that (12) and (13) satisfy (3) by substitution.

Here, if (9) has some imaginary roots the right hand side of (10), (12), (13) must be taken their real parts, and if (9) has some multiple roots suitable limit must be taken.

4. When $E = 0$

In most cases, g_1/g_0 is very small, hence in Eq. (3), E is very small as compared with $(s+r_1)\,g_0^2/I_0R^2$, and if we put to $E=0$, (9) becemes

$$(y^2 + 2\varepsilon_0 y + n_0^2)(y^2 + 2\varepsilon_1 y + n_1^2) = 0$$

and we can suppose that

α_1, α_2 are two roots of $y^2 + 2\varepsilon_0 y + n_0^2 = 0$

α_3, α_4 are two roots of $y^2 + 2\varepsilon_1 y + n_1^2 = 0$

and the computation of $\varphi(t)$ by above formulas can be simplified.

5. Approximate formula for $\varphi(t)$ when $|t|$ is small

In this case we can expand $\varphi(t)$ by a power series of t, that is

$$\varphi(t) = \varphi_0 + t\dot{\varphi}_0 + \frac{t^2}{2}\ddot{\varphi}_0 + \frac{t^3}{3!}\dddot{\varphi}_0 + \cdots\cdots$$

At first, by the condition (6), we have $\varphi_0 = \dot{\varphi}_0 = 0$. Next, from (12) or directly from (3), (4) we can find $\ddot{\varphi}_0$, $\dddot{\varphi}_0$, $\varphi_0^{(\mathrm{IV})}$, $\cdots\cdots$ and get

$$\varphi(t) = KF\left[-\frac{t^2}{2}\dot{x}_0 + \frac{t^3}{3!}\left\{-\ddot{x}_0 + 2(\varepsilon_0+\varepsilon_1)\dot{x}_0\right\}\right.$$
$$+ \frac{t^4}{4!}\left\{-\dddot{x}_0 + 2(\varepsilon_0+\varepsilon_1)\ddot{x}_0 + (n_0^2+n_1^2-4\varepsilon_0^2-4\varepsilon_0\varepsilon_1-4\varepsilon_1^2-EF)\dot{x}_0\right\}$$
$$\left. + \frac{t^5}{5!}\left\{-x_0^{(\mathrm{IV})} + 2(\varepsilon_0+\varepsilon_1)\dddot{x}_0 + (n_0^2+n_1^2-4\varepsilon_0^2-4\varepsilon_0\varepsilon_1-4\varepsilon_1^2-EF)\ddot{x}_0\right.\right.$$

$$+\left(8\varepsilon_0^3+8\varepsilon_0^2\varepsilon_1+8\varepsilon_0\varepsilon_1^2+8\varepsilon_1^3-2\varepsilon_0 n_1^2-2\varepsilon_1 n_0^2-4\varepsilon_0 n_0^2-4\varepsilon_1 n_1^2+4\overline{\varepsilon_0+\varepsilon_1}\,EF\right)\dot{x}_0\Big\}$$

$$+ \cdots\cdots\cdots\cdots$$

$$\cdots\cdots\cdots\cdots\Big] \cdots\cdots \quad (15).$$

In this formula, when $\dot{x}_0 \neq 0$, E appears in the coefficient of t^4 initially, and when $\dot{x}_0=0$, $\ddot{x}_0 \neq 0$, E appears in the coefficient of t^5 initially and so on. Therefore when $|t|$ is very small, $\varphi(t)$ is almost independent of E no matter whether $E=0$ or $E \neq 0$.

Next, we have

$$x(t) = x_0 + t\,\dot{x}_0 + \frac{t^2}{2}\ddot{x}_0 + \frac{t^3}{3!}\dddot{x}_0 + \cdots\cdots \quad (16)$$

therefore when $x_0 = 0$, from (15) and (16) we get

$$\varphi(t)/x(t) = O(t) \cdots\cdots \quad (17).$$

6. Solution for $x(t)$ when $\varphi(t)$ is given

We can obtain the solution of $x(t)$ by integrating Eqs. (3), (4) immediately. But in this case x_0, $\dot{x}_0$ are unknown, hence we take the conditions

$$x_0 = 0,\ \dot{x}_0 = 0,\ \theta_0 = 0,\ \dot{\theta}_0 = 0,\ \varphi_0 = 0,\ \dot{\varphi}_0 = 0 \cdots\cdots \quad (18)$$

instead of (6). This is always possible by taking the origin of t suitabily supposing that $x(t)$, $\theta(t)$, $\varphi(t)$ are well behaved functions of t, and integrating (3) and (4), we get

$$x(t) = \frac{-1}{KF}\left[\dot{\varphi}(t) + a\varphi(t) + b\int^t \varphi(t)\,dt + c\int^t\!\!\int^t \varphi(t)\,dt + d\int^t\!\!\int^t\!\!\int^t \varphi(t)\,dt\right] \cdots\cdots \quad (19),$$

this is required solution.

Next, when $|t|$ is small we get following formula

$$x(t) = \frac{-1}{KF}\left[\frac{t^2}{2}\dddot{\varphi}_0 + \frac{t^3}{3!}\left\{\varphi_0^{(\mathrm{IV})} + a\dddot{\varphi}_0\right\} + \frac{t^4}{4!}\left\{\varphi_0^{(\mathrm{V})} + a\varphi_0^{(\mathrm{IV})} + b\dddot{\varphi}_0\right\} + \cdots\cdots\right] \cdots \quad (20).$$

To find $x(t)$ from the record of a seismograph was tried already by several researchers, but there exists some difficulty concerning friction. While in the galvanometric registration, the record is drawn optically and there is no difficulty concerning friction.

7. When $E = 0$ and $\varepsilon_0 = n_0$, $\varepsilon_1 = n_1$

When $\varepsilon_0 = n_0$, $\varepsilon_1 = n_1$ by taking the values of s, w, z suitablly, that is when transducer and galvanometer are adjusted in the state of critical damping, we can put to

$\alpha_1 = \alpha_2 = -n_0$, $\alpha_3 = \alpha_4 = -n_1$, moreover we suppose that $E = 0$. Then the solution of $\varphi(t)$ is obtained by taking the limit of the right hand side of (10) or (12). Of course, in this case, (3), (4) become

$$\ddot{\theta} + 2n_0\dot{\theta} + n_0^2\theta = -K\ddot{x} \quad \cdots\cdots (3)'$$

$$\ddot{\varphi} + 2n_1\dot{\varphi} + n_1^2\varphi = F\dot{\theta} \quad \cdots\cdots (4)'$$

and solving these Eqs. under the condition (6), we get

$$\theta(t) = K\left[e^{-n_0 t}\left\{n_0^2\int_0^t e^{n_0 t}\, tx(t)dt + (2-n_0 t)n_0\int_0^t e^{n_0 t}\, x(t)dt + (1-n_0 t)x_0\right\} - x(t)\right] \quad \cdots\cdots (13)'$$

$$\varphi(t) = Fe^{-n_1 t}\left[(1-n_1 t)\int_0^t e^{n_1 t}\,\theta(t)dt + n_1\int_0^t e^{n_1 t}\, t\theta(t)dt\right] \quad \cdots\cdots (12)'.$$

These forms are rather convenient than the limitting forms of (10) or (12). From (15) we get

$$\varphi(t) = KF\left[-\frac{t^2}{2}\dot{x}_0 + \frac{t^3}{3!}\left\{-\ddot{x}_0 + 2(n_0+n_1)\dot{x}_0\right\} + \frac{t^4}{4!}\left\{-\dddot{x}_0 + 2(n_0+n_1)\ddot{x}_0 - (3n_0^2+4n_0n_1+3n_1^2)\dot{x}_0\right\} + \cdots\cdots\right] \quad \cdots\cdots (15)'$$

8. Concluding Words

On the seismology, several forms of $x(t)$ were supposed, e. g.

$x(t) = Ate^{-\alpha t}\sin\omega t$ ..... H. P. Berlage

$x(t) = A(\cos\omega t - 1)$ ..... T. Matuzawa

$x(t) = Ae^{-\alpha t^2}$ ..... T. Suzuki

and then the motion of seismometer was discussed. When the vibration starts from the state of rest in equilibrium, we can put to $x_0 = 0$, $\dot{x}_0 = 0$ and the formulas (12), (13) e. t. c. become more simple.

On the seismic prospecting, the initial kick time of $\varphi(t)$ is very important, and we should give attentions to the initial form of $\varphi(t)$ and the relation that $\varphi(t)/x(t) = O(t)$.

References

(1 F. w. Sohon : Introduction to Theoritical Seismology p. 84~91 (1932)
(2) T. Hagiwara : Jishinkei (Seismometer) p. 37~43 and p. 70~76 (1943)

A METHOD OF PROMOTING THE ULTIMATE VACUUM AND THE PUMPING SPEED OF VACUUM PUMPS

Shigeichi FUJITA

(Received, Dec, 10, 1957)

1. Introduction

The ultimate vacuum and the pumping speed of a vacuum pump are the principal qualities which characterize the faculty of the pump. Many studies on the two principal qualities of vacuum pump have been made until now.

There are various vacuum pumps which are composed on different principles, but it is desirable in many pumps that the ultimate pressure is as low as possible and the pumping speed is as large as possible. We want to state a method which can make the pumps to attain some higher ultimate vacuum and some higher speed of pumping, and this method is considered possible to be used for almost all vacuum pumps.

2. Ultimate Pressure and External Pressure

(i) Piston vacuum pump

The pump of this kind has been employed from old times and is still used now in special cases. The piston moves forward and backward in the cylinder, and the gas in a vessel which is to be evacuated is sucked in the cylinder by the backward motion of the piston, and the gas is compressed and exhausted by the forward motion of the piston. If the external pressure is p_a, the ultimate pressure p_0 is given by $p_0 = \frac{\triangle V}{V} p_a$, where V is the maximum volume of the space in the cylinder which is produced when the piston moves backward to the limit and $\triangle V$ is the minimum volume of the space in the cylinder which is produced when the piston moves forward to the limit. $\triangle V$ is said "dead volume", and it is desirable that $\triangle V$ is as small as possible.

(ii) Oil rotary pump

There are three principal types of this kind of vacuum pumps, Gaede type, Cenco type, and Kinney type. In each type of them, the pump is mainly consisted of a cylindrical stator and a cylindrical rotor placed eccentric in the space of the stator. There produced between stator and rotor the crescent-shaped space, and with the rotation of the rotor, the gas in the vessel is sucked in a part of the space, and the gas in the other part of the space is compressed and exhausted outward through the exhaust valve.

In the pump of this kind. pump oil is employed sufficiently and the oil reduces the friction between the stator and the rotor. More over, the oil fills up the dead volume so as it becomes approximately zero. Accordingly, if the oil contains no gas and the pressure of the oil vapor is extremely low, the ultimate pressure will become extremely

low. But in the actual case, the oil which has touched the external air contains air and it releases the air when it transfers to the low pressure side. The ultimate pressure is determined principally by the gas contained in the oil. Thus the actual ultimate pressure of the oil rotary pump is usually about 10^{-3}mmHg. The quantity of the gas contained in the oil depends upon the pressure of the gas touched to the oil, it becomes smaller when the pressure of the gas touched to the oil decreases. Accordingly, if the external pressure decreases the ultimate pressure becomes lower. Actually we can obtain usually about 10^{-4}mmHg as the ultimate pressure when we use the two oil rotary pumps, connected in series.

(iii) Diffusion pump[1]

In this pump, the gas molecules in the high vacuum side diffuses into the flow of the oil vapor and is conveyed by the flow from the high vacuum side to the auxiliary vacuum side. The ultimate pressure of the pump is affected by the back diffusion of the gas molecule from the auxiliary vacuum side to the high vacuum side, by the release of gas from the wall of the vessel, by the passage of gas through the wall of the vessel and by the thermal decomposition of the oil vapor. If the vacuum apparatus is constructed perfectly and there is no release of gas from the wall, no passage of gas through the wall and no thermal decomposition of the oil vapor, the ultimate pressure is determined by the back diffusion of the gas from the auxiliary vacuum side to the high vacuum side. In this case, the gas of the high vacuum side is conveyed by the flow of the oil vapor from the high vacuum to the auxiliary vacuum and returns partly by the back diffusion to the high vacuum. In the state of the ultimate vacuum, the number of the gas molecules conveyed per unit time by the flow of the oil vapor is equal to the number of gas molecules which diffuse backward per unit time. Now, if, at a point in the flow of oil vapor, apart x from the origin of the flow, the molecular density of the gas is $n(x)$, and the diffusion coefficient of the gas in the oil vapor is D, there is the following relation in the state of ultimate vacuum.

$$n(x)\,u = D\frac{dn(x)}{dx}, \qquad (2.1)$$

where u is the velocity of the flow of oil vapor.

If the length of the flow of oil vapor is L, there is the following ralation

$$n(L) = n(0)\,e^{\frac{uL}{D}}, \qquad (2.2)$$

where $n(0)$ and $n(L)$ are the molecular densities of gas at $x = 0$ and $x = L$. $n(0)$ is equal to the molecular density of gas at the ultimate vacuum, and $n(L)$ is equal to the molecular density of gas at the auxiliary vacuum. Therefore, if the pressure of gas at the ultimate vacuum is p_0, and the pressure of the auxiliary vacuum is p_L, the following relation holds.

$$p_0 = p_L e^{-\frac{uL}{D}} \qquad (2.3)$$

From this we see that the pressure p of the ultimate vacuum becomes lower according as the auxiliary pressure p_L decreases, the length of the oil vapor flow L becomes larger, the diffusion coefficient D becomes smaller.

(iv) Molecular pump[2]

Molecular pump is a high vacuum pump which operates without oil. This pump is used where the existence of oil is undesirable. In the interior of the cylindrical stator, a concentric cylindrical rotor rotates with a high speed. The stator and the rotor are very closely fitted, the clearance between them is very narrow, almost gas-tight. In a part of the stator a groove of some depth is cut. At a initial part of the groove, a suction tube is fitted and at a final part of the groove, a exhaust tube is fitted. With the rotation of the rotor, gas moves with the motion of the surface of the rotor from the place of the suction tube to the place of the exhaust tube.

If a vessel is connected to the suction tube of the pump and an auxiliary pump is connected to the exhaust tube and the pumps operate, the vessel is evacuated to a high vacuum. In the state of ultimate vacuum, between the pressure of the vessel p_0 and the pressure of the auxiliary vacuum p_a, there exist the following relations.
In the case of viscous flow,

$$p = p_a - \frac{6\eta u l}{h^2} \qquad (2.4)$$

where η is the coefficient of viscosity, u is the speed of the surface of the rotor, l is the length of the groove and h is the depth of it.
In the case of molecular flow,

$$p = p_a e^{-\frac{3u}{8h}\sqrt{\frac{\pi\mu}{2RT}}l} \qquad (2.5)$$

where μ is the molecular weight of the gas, T is the absolute temperature. Thus in both cases, the ultimate pressure p_0 becomes lower according as the auxiliary pressure p_a decreases.

In each of the pumps above mentioned, it is known that the ultimate pressure p_0 becomes lower according as the external pressure p_a decreases. In other pumps, not mentioned above, also, the ultimate pressure p_0 becomes in many cases lower according as the external pressure p_a decreases.

3. Pumping Speed and External Pressure

The pumping speed of a pump is measured by the volume of gas exhausted per unit time when the gas takes the pressure at the suction tube. When a vessel of volume V is evacuated by a pump of some kind, if the pressure p of the vessel accepts a small change dp in a small time dt, the quantity of gas exhausted is given by $-Vdp$. The pumping speed S is, therefore, given by

$$S = -\frac{V dp}{p dt} \quad \cdots\cdots (3.1)$$

If S is a constant, the pressure becomes lower and lower and attains O in a long time. But, in the actual cases some finite ultimate pressure exists, and therefore S can not be a constant, it becomes small gradually as the vacuum promotes, and becomes O at the ultimate state.

There is other definition of pumping speed which is given by

$$S' = -\frac{V dp}{(p-p_0)dt} \quad \cdots\cdots (3.2)$$

where p_0 is the ultimate pressure.
This pumping speed S' is constant in wide scope of pressure, and the value of the constant is peculiar to the pump. S and S' are said as "measured speed of pump" and "admittance" respectively. Between the two pumping speeds, there is the relation

$$S = S' \frac{p-p_0}{p} \quad \cdots\cdots (3.3)$$

(i) Pumping speed of piston pump and oil rotary pump

If the maximum volume of the chamber of the pump, in which gas of the vessel is sucked, is v, and the number of reciprocation or rotation per unit time is N, the volume of the exhausted gas per unit time is given by Nv. If the pressure of gas at the suction tube is p and the ultimate pressure is p_0, the quantity of gas exhausted per unit time is given by $Nv(p-p_0)$, and S and S' are given by

$$S = \frac{p-p_0}{p} Nv \quad \text{and} \quad S' = Nv \quad \cdots\cdots (3.4)$$

respectively.
S' is nearly constant in a wide scope of pressure, but S becomes smaller as the pressure decreases till it becomes O at the ultimate pressure.

(ii) Pumping speed of diffusion pump[1]

If the molecular density of gas at high vacuum side is ν, and the molecular density of gas in the oil vapor flow at $x = 0$ is $n'(0)$, the quantity of flow of gas per unit area per unit time is given by

$$q = \frac{\bar{v}}{4}\left\{\nu - n'(0)\right\} \quad \cdots\cdots (3.5)$$

where $\bar{v}$ is the mean velocity of molecules of the gas.
The pumping speed per unit area is given by

$$S = \frac{q}{\nu} = \frac{\bar{v}}{4}\left(1 - \frac{n'(0)}{\nu}\right). \quad \cdots\cdots (3.6)$$

Also there is a relation

$$q = un(x) - D\frac{dn(x)}{dx} \quad \cdots\cdots (3.7)$$

From this we get

$$n'(L) - \frac{q}{u} = \left\{n'(0) - \frac{q}{u}\right\} e^{\frac{uL}{D}} = \left\{n'(0) - \frac{q}{u}\right\} \frac{n(L)}{n(0)}, \quad \cdots\cdots (3.8)$$

where $n'(L)$ is the molecular density of gas at $x=L$, $n(L)$ and $n(0)$ are the molecular densities of the ultimate state at $x=L$ and $x=0$ respectively. Putting the relation $q = \nu S$ in (3.8), we get

$$S = \frac{\frac{\bar{v}}{4}\left\{1 - \frac{n'(L)}{n(L)}\frac{n(L)}{n(0)}\right\}}{1 + \frac{\bar{v}}{4u}\left\{1 - \frac{n(0)}{n(L)}\right\}}. \quad \cdots\cdots (3.9)$$

Initially $\frac{n'(L)}{n(L)}$ is equal to 1, but it becomes larger and larger as the vacuum promotes until it becomes equal to $\frac{n(L)}{n(0)}$ at the ultimate state where S becomes 0.

If p_L or $n(L)$ becomes small, $n'(L)$ becomes small and S increases.

(iii) Pumping speed of molecular pump

The quantity of gas exhausted per unit time by a molecular pump is given by

$$q = p\frac{u}{2}bh - \frac{4}{3}bh^2\sqrt{\frac{2RT}{\pi\mu}}\frac{dp}{dx} \quad \cdots\cdots (3.10)$$

where x is the distance measured from high vacuum side along the length of the groove and p is the pressure at x. If the pressure of the high vacuum side or the pressure at $x=0$, is p'_0, from (3.10) we get

$$p = \frac{q}{U} + \left(p'_0 - \frac{q}{U}\right) e^{\frac{3u}{4h}\sqrt{\frac{\pi\mu}{2RT}}x}, \quad U = \frac{u}{2}bh \quad \cdots\cdots (3.11)$$

Put the condition, $p=p_a$ at $x=l$, in (3.11), we get by the aid of (2.5)

$$\frac{q}{U}(p_a - p_0) = p_a(p'_0 - p_0), \quad \cdots\cdots (3.12)$$

$$S' = \frac{q}{p'_0 - p_0} = \frac{ubh}{2}\frac{p_a}{p_a - p_0}, \quad S = \frac{ubh}{2}\frac{p_a}{p_a - p_0}\frac{p'_0 - p_0}{p'_0}. \quad \cdots\cdots (3.13)$$

S' is independent of p_L, but S becomes small as p_L decreases. S and S' increases as p_L decreases.

Thus the pumping speeds of the pumps above mentioned increases by the exponential

pressure decreases.

4. A Method of Promoting the Ultimate Vacuum and the Pumping Speed

In every pumps above mentioned, the external pressure has intimate relations to the ultimate pressure and the pumping speed. As the external pressure decreases, the ultimate pressure decreases and the puming speed increases. For this reason, we use sometimes two pumps of the same kind, connected in series, for the purpose of promoting the ultimate vacuum and the pumping speed.

We will state a method which enables a pump to obtain nearly the same ultimate vacuum and nearly the same pumping speed as those which are obtained by the two connected pumps in series. The principle of the method consists in using the low pressure, which is obtained by the pump itself, as the external pressure.

In Fig. 1, A is a vessel to be evacuated, P is a vacuum pump, B is a empty chamber which is connected with the suction valve (tube) and the exhaust valve (tube) of P by tubes. C_1 and C_2 are the three-way cocks. Firstly, by C_1 connect A and B with the

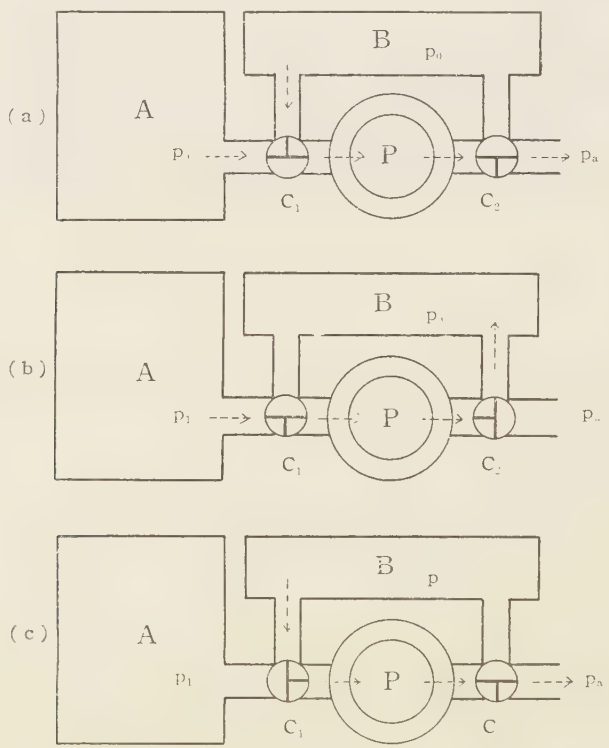

Fig. 1.

suction valve of P, and by C_2 connect the external air with the exhaust valve of P, as Fig. 1 (a), and make the pump operate. Then A and B are exhausted. When A and B are exhausted to nearly the ultimate vacuum, turn the cocks C_1 and C_2 as Fig. 1 (b) as to cut the connection of B with suction valve of P and to cut the connection of external air with exhaust valve of P and to connect the exhaust valve of P with B. Then the gas of A is exhausted into B. As the pressure of B is low, nearly equal to the ultimate pressure of the pump, the pumping speed increases remarkably and the ultimate vacuum promotes considerably. When the exhausted gas accumulates in B, turn C_1 and C_2 as Fig. 1 (c), and exhaust the gas to the outside.

In piston vacuum pump, between the external pressure p_a and the ultimate pressure p_0, the relation $p = \frac{\triangle V}{V} p_0$ exists. Accordingly, using this method and taking p as the external pressure, we get the pressure $p_0' = \frac{p_0^2}{p_a}$ as the ultimate pressure. S' is almost independent of pressure, but S depends on pressure and becomes larger as the ultimate pressure lowers at the constant external pressure as stated before.

In oil rotary pump, the ultimate pressure is determined principally by the quantity of gas contained in the oil. The quantity of gas contained in the oil depends upon the external pressure, and generally the ultimate pressure becomes low as the external pressure decreases. Accordingly, by using this method, we can promote the ultimate vacuum considerably. In oil rotary pump also, S' is almost constant, independent of pressure, S depends on pressure and becomes smaller and smaller as the pressure decreases and becomes 0 at the ultimate pressure. S at a fixed pressure becomes larger as the ultimate pressure becomes lower.

As the ultimate pressure of a diffusion pump is given by (2.3), if u, L and D are constants, p_0 becomes lower as p_L decreases. As pumping speed per unit area is given by (3.9), when the pressure of the high vacuum side or ν is fixed, the speed becomes larger as the pressure of the low vacuum side or $n'(L)$ decreases.

In a molecular pump, the ultimate pressure lowers as the auxiliary pressure or the external pressure decreases. If we can take the flow of gas as the molecular flow, $\frac{p_0}{p_a}$ is a constant, depending on the construction of pump, the working state, the kind of gas and temperature. Accordingly p_0 becomes lower as p_a decreases. By using this method, we can obtain the ultimate pressure $p \frac{p}{p_a}$ for the external pressure p_a, and larger pumping speed.

5. A Method of Promoting dually the Ultimate Vacuum and the Pumping Speed

There are cases where the ultimate vacuum and the pumping speed are promoted by the co-operation of three pumps of the same kind, connected in series. In these cases, instead of three pumps, we can use one pump and obtain almost the same results as those obtained by three pumps in series. We will state the method in the following by the aid of Fig. 2.

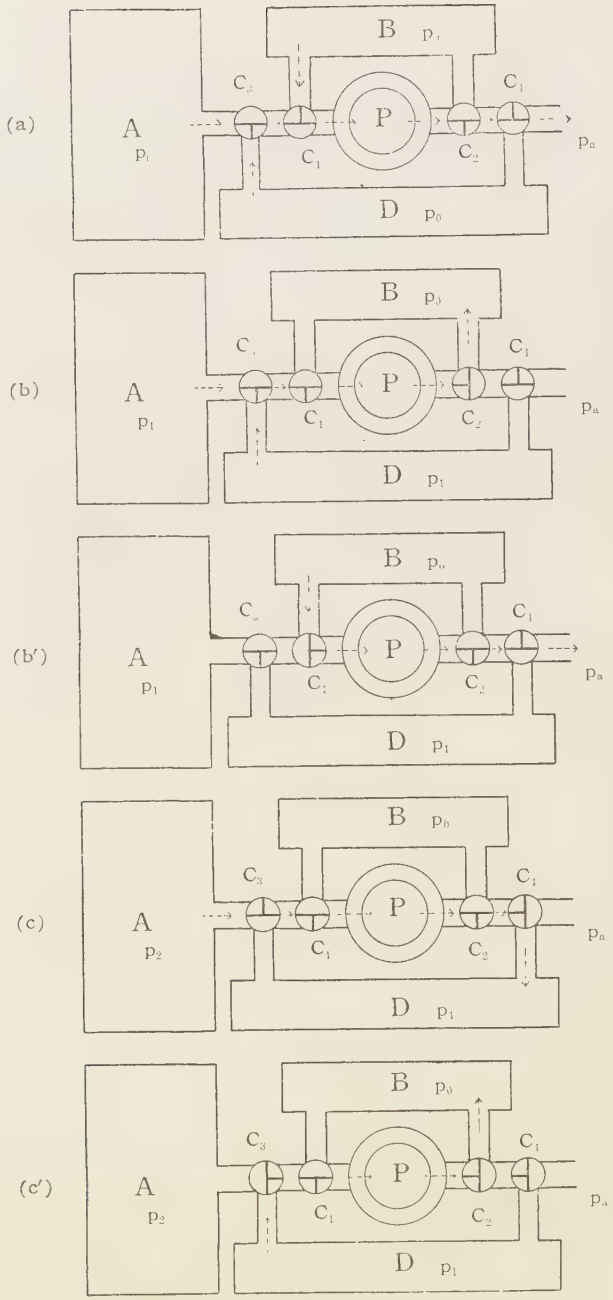
(a)
A
p_1
B p_1
C_3
C_1
P
C_1
C_2
p_a
D p_0
(b)
A
p_1
B p_0
C_3
C_1
P
C_1
C_2
p_a
D p_1
(b′)
A
p_1
B p_0
C_3
C_1
P
C_1
C_2
p_a
D p_1
(c)
A
p_2
B p_0
C_3
C_1
P
C_1
C_2
p_a
D p_1
(c′)
A
p_2
B p_0
C_3
C_1
P
C_1
C_2
p_a
D p_1

Fig. 2.

P, A, B and C_1, C_2 have the same meanings as in Fig. 1. D is the another chamber which can be connected to A, B, P and outside by the three-way cocks C_3 and C_4. Firstly put C_1, C_2, C_3, C_4 as Fig. 2 (a) to connect the suction valve of P with A, B and D, and connect the exhaust valve of P with the outside, and cut the connection of the exhaust valve of P with B and D. Let the pump operate in this state, then A, B and D are exhausted. When the pressure of A, B and D becomes nearly equal to the ultimate pressure p_0, turn C_1 and C_2 as Fig.2 (b), then the gas of A and D is exhausted into B, the pressure of which is nearly equal to p_0. Accordingly the pumping speed increases considerably and in a short time nearly the ultimate pressure p_0 is attained for the external pressure p_0. Turn C_2, C_3, C_4 as Fig. 2 (c), to cut the connection of the exhaust valve of P with B and outside, to connect the suction valve of P with A, to connect the exhaust valve of P with D, then the pump operates for the external pressure p_1, so that the gas in A is exhausted into D and the pressure of A decreases considerably. Thus the ultimate vacuum and the pumping speed promote considerably. When the gas accumulates in D, turn C_2 and C_3 as Fig. 2 (c') to exhaust the gas of D into B. When the gas accumulates in B, turn the cocks as Fig. 2 (b') to exhaust the gas of B to the outside. If we use a pump in which $\frac{p_0}{p_a}$ is a constant, we can obtain nearly the ultimate pressure $p_2 = \frac{p_0^3}{p_a^2}$ by this method.

6. Conclusion

It is stated that the ultimate pressure and the pumping speed of a pump are intimately related to the external pressure, that the ultimate vacuum and the pumping speed promote considerably as the external pressure decreases.

As a method of decreasing external pressure, it is stated the method of using the low pressure which is obtained by the pump itself. It is showed that by this method, a pump can have the ultimate vacuum and the pumping speed almost equal to those of two or three pumps of the same kind, co-operating in series.

We wish to express our sincere thanks to Mr. R. Adachi and to Mr. E. Masaki for their discussions and comments.

References

(1) R. Jaeckel : Z. Naturforschg., **2a**, (1947) 666
(2) W. Gaede : Ann. d. Physik, **41**, (1913) 337

"VARIAMIN BLUE B" AS A NEW COLORING AGENT FOR MONTMORILLONITE CLAY.

Daisei YAMAMOTO

(Received November 26, 1957)

It has been known that the montmorillonite clay added with some aromatic amines e. g. benzidine etc. shows remarkable coloration.

As to the cause and mechanism of the coloration, Hauser et al, Takahashi etc. discussed.

In the course of author's investigation to find a new coloring agent for these clays, Variamin Blue B (4-methoxy-4'-aminodiphenylamine sulfate) showed satisfactory results.

The structure of Variamin Blue B is based on diphenylamine nucleus and it is similar to p-anisidine in the following point that methoxy and amino radicals are replaced to the nucleus at para position (Fig. 1).

It can reasonably be supposed that the montmorillonite clay may undergo a color reaction with this amine because of the fact that montmorillonite complexes of diphenylamine and p-anisidine are able to show coloration.

Experiments which have carried out upon several japanese acid clays (montmorillonite) gave a proof of a rightness of the presumption.

The coloration technique was made by placing about 3–5 grams of the clay on a watch glass, adding 1–2 cc of a saturated solution of variamin Blue B.

The blue coloration was rapid and striking.

Beside montmorillonite clays, a hydrated halloysite is also deeply colored.

This amine may be recommendable as a new coloring agent for it's high sensitivity and easy availabilities.

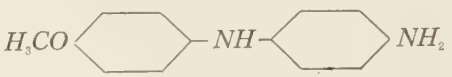

Fig. 1

References

1) Hauser, Leggett, J. Am. Chem. Soc. 62, 1811 (1940)
2) H. Takahashi, Bull. Chem. Soc. Japan 28, 5 (1955)

A STRANGE PHENOMENON IN THE LONGITUDINAL MAGNETOSTRICTION IN WEAK MAGNETIC FIELD.

Tatuo CHIKAZAWA and. Shigeo MATSUMAE

(Received Nov. 30, 1957)

(1) Introducution

When we study the longitudinal magnetostriction of nickel in weak magnetic field by the mutual-dynamic impedance method, we find a strange phenomenon which is caused by oxidation of the specimen. The details are as follows.

(2) Experimental results

The specimen is a round bar of electrolytic nickel, 6mm in diameter and 58 cm in length, containning a small amount of manganese.

After the cold work, the specimen is annealed at about 500°C in air for a long time. The experimental results in this case are shown in Fig. 1. In the figure, points on the X-axis indicate magnitudes of maximum amplitude of alternate demagnetizing field and

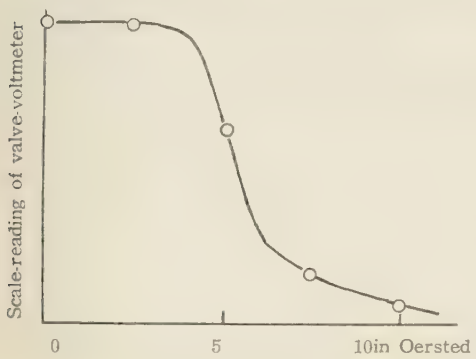

Fig. 1 maximam amplitude of alternate demagnetizing field

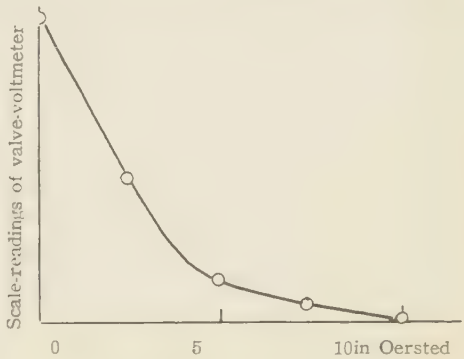

Fig. 2 maximamamplitude of alternate demagnetizing field

the scale-readings of the valve-voltmeter are measured when the exciting alternate field is less than 0.01 Oersted and the polarizing magnetic field is about 0.05 Oersted.

The curve shows the relation between the demagnetizing field-strength and scale-readings of the valve-voltmeter which is roughly proportional to the longitudinal magneto-striction, as the proportional constants are not strictly the same.

When this specimen is further annealed at about 600°C for several hours in hydrogen-atmosphere, the experimental results are shown in Fig. 2.

As seen from Fig. 1 and Fig. 2, the relation between the scale-reading of the valve-

voltmeter and the dimagnetizing magnetic field-strength is quite different in these two cases.

This difference is considered to be caused by the oxidation of the specimen but further study is neccessary to explain it.

ON A COMPLETELY HARMONIC SPACE WITH AN ALMOST COMPLEX STRUCTURE

Takeo OHKUBO

(Received Jan. 15 th 1958)

§1. Consider a Riemannian n-space V_n for which

$$ds^2=g_{ij}dx^i dx^j. \tag{1.1}$$

If $P_0(x_0^i)$ is a fixed point of the V_n and if $s=s(x_0^i, x^i)$ is the length of arc of the geodesic joining it and a variable point $P(x^i)$, then the V_n is called (centrally) harmonic with respect to the basepoint $P_0(x_0)$ if

$$\Delta_2 s \equiv \frac{1}{\sqrt{g}} \frac{\partial}{\partial x^i}\left(\sqrt{g}\, g^{ij} \frac{\partial s}{\partial x^j}\right) \tag{1.2}$$

is a function of s alone; it does not involve the coordinates x^i of the variable point explicitly, but the coordinates x_0^i of the base-point may be involved as parameters. If this holds for all choices of the base-point, the space will be called completely harmonic. If V_n is completely harmonic and $\Delta_2 s$ has the special form $(n-1)/s$, then V_n is called simply harmonic. E. T. Copson and H. S. Ruse[1] showed how to obtain the conditions, in term of the curvature tensor, that a V_n should be completely harmonic. These conditions were infinite in number and involved the covariant derivatives of the curvature tensor.

A. G. Walker[2] (1942) has found another method of obtaining them, using Ruse's invariant ρ. The Ruse's invariant ρ is defined by

$$\rho^2=\frac{|g_{ij}|_{P_0}|g_{ij}|_P}{J^2}, \qquad J=\left|\frac{\partial^2 \frac{s^2}{2}}{\partial x^i \partial x^j}\right|. \tag{1.3}$$

Walker has given the expansion of $\log \rho$:

$$\log \rho=\frac{W_1}{2!}s+\frac{W_2}{3!}s^2+\frac{W_3}{4!}s^3+\cdots\cdots+\frac{W_m}{(m+1)!}s^m+\cdots \tag{1.4}$$

Each of the coefficients is the trace of a certain polynomial in matrices Γ, Γ', Γ'', etc. (of degree $\frac{m-1}{2}$ or $\frac{m}{2}$, whichever is an integer), where

$$\begin{aligned} &\Gamma=(K_{\cdot\cdot\cdot\cdot}\lambda^i\lambda^j), \qquad \Gamma'=(K_{\cdot\cdot\cdot\cdot}\lambda^i\lambda^j\lambda^k), \\ &\Gamma''=(K_{\cdot\cdot\cdot\cdot}\lambda^i\lambda^j\lambda^k\lambda^l), \text{ etc.} \end{aligned} \tag{1.5}$$

(1) See the Bibliography at the end of the paper [1]

(2) See [2]

and λ^i is the unit tangent vector of the geodesic P_0P at P_0. These coefficients must all be evaluated at P_0.

When and only when the space V_n is centrally harmonic with respect to P_0, ρ is dependent only upon s, i. e., independent of λ^i and completely harmonic when it holds about every point of the space. These conditions can be derived from the equation (1.4), i. e., we require that each W_r shall be independent of λ^i. It is easily seen that W_r is of the form

$$W_r = W_{i_1 i_2 \cdots i_r}\, \lambda^{i_1}\, \lambda^{i_2} \cdots \lambda^{i_r}$$

where $W_{i_1 i_2 \cdots i_r}$ assumed symmetric in the suffices, are functions of the foundamental and curvature tensors and their derivatives. As the λ^i satisfy $g_{ij}\lambda^i\lambda^j =$ constant, the required conditions are

$$\left.\begin{aligned} &W_{i_1 i_2 \cdots i_r} = 0, \qquad \text{r; odd number,} \\ &W_{i_1 i_2 \cdots i_r} = k_r \Sigma g_{i_1 i_2} g_{i_3 i_4} \cdots g_{i_{r-1} i_r}, \quad \text{r: even number,} \end{aligned}\right\} \tag{1.6}$$

where the k's are scalars, the sum being taken to give an expression symmetric in suffices. When these conditions are satisfied at P_0, it appears for any point P that ρ is a function of s, and is expressed as a power series in s^2, strictly in es^2 where $e = g_{ij}\lambda^i\lambda^j = \pm 1$ or 0.

When a space is completely harmonic, conditions (1.6) are satisfied at every point of the spasce. We see easily that, in general, the form of ρ as a function of es^2 must be the same for all choices of base-points. It follows that the sealars k_r in (1.6) are all constants.

It is well known that another special class of spaces, that is to say, simply harmonic spaces, consists of those spaces which are completely harmonic and in which $\rho = 1$ for every pair of points. (1.4) implies that $\rho = 1$ only when $W_r = 0$ for all λ's. Therefore the conditions for a simply harmonic space are that the equations: $W_r = 0$, $r = 1, 2, 3, \cdots\cdots$ must be satisfied at all points of the space and for all direction λ^i.

Let λ^i be any direction and put $\Lambda = g_{ij}\lambda^i\lambda^j$. As the matirces $\dot{\Gamma}$, $\ddot{\Gamma}$, $\dddot{\Gamma}$ etc. are all zero matrices for a symmetric space we have the following theorems.

Theorem A. *A symmetric space is harmonic if, for all N, the trace of Γ^N is of the form $k_N\Lambda^N$, where Γ^N is the N-th power of Γ and k_N is independent of the λ's.*

Theorem B. *The necessary and sufficient conditions for a symmetric V_n to be harmonic are that the latent roots of Γ should be of the form*

$$0,\ \alpha_1\Lambda,\ \alpha_2\Lambda, \cdots\cdots\cdots,\ \alpha_{N-1}\Lambda$$

where the α_i is independent of the λ's.

Theorem C. *The necessary and sufficient conditions for a symmetric space to be simply harmonic are that all the latent roots of Γ should be zero for all λ's.*

A problem of characterizing all harmonic spaces H_n has been only partially solved. Harmonic 2- and 3-spaces are trivial, and for real harmonic 4-spaces the

following theorems have already been established.

(1) Every harmonic 4-space H_4 with signature 2 is a space of constant curvature, and the proposition also holds for $n>4$.

(2) There exist H_4's which are symmetric, but are not spaces of constant curvature. All such spaces are known; some have definite metrics and others have zero signature.

(3) There are H_4's which are recurrent, but are not symmetric. All such spaces are known and have zero signature.

(4) Every real H_4 with definite metric is symmetric.

(5) Every simply harmonic 4-space with definite metric is a flat space and the proposition also holds for $n>4$.

(6) Every simply harmonic recurrent 4-space has the metric of a form

$$ds^2=\alpha(x,y)dx^2+2\gamma(x,y)dxdy+\beta(x,y)dy^2+2dxdz+2dydt.$$

Only a few properties of harmonic spaces H_n with $n>4$ are known. Some of them are following:

(7) A harmonic space H_n conformal to a flat space is a space of constant curvature.

(8) A Riemannian space V_{2p} admitting a null strictly parallel p-plane is simply harmonic.

(9) The product of two simply harmonic K*-spaces is also a simply harmonic K*-space.

(10) If a harmonic K*-space is decomposable, it is a simply harmonic K*-space which is flat-extension of a certain simply harmonic K*-space.

(11) If a homogeneous space E of a Lie group G has a locally spherically transitive isotropy subgroup H, and a positive definite Riemannian metric invariant under G, then it is completely harmonic.

(12) The following spaces, (1) spheres, (2) real projective spaces, (3) complex projective spaces, (4) quaternionic projective spaces, and (5) the Cayley projective plane admit positive definite Riemannian metric which are harmonic.

In following sections we observe an even dimensional Riemannian manifold which admits an integrable real-analytic almost complex structure a_j^i and also is exact. We shall show that a space of constant holomorphic curvature[1] in such a space is completely harmonic.

§2. We observe in a manifold of dimension $n=2m$ a coordinate neighborhood U_x of which points are written by n real coordinates $x^1, x^2, \cdots\cdots, x^n$. Under an almost complex structure J of class C^h in a differentiable manifold M^n, we understand a tensorfield a_j^i of class C^h with respect to x^i, satisfying $a_j^i\ a_k^j=-\delta_k^i$. Then we have linear mapping $b=Ja$ which is represented by $a^i=a_j^i b^j$, where a^i and b^i are the components of vectors a and b respectively. We put

(1) See [3] and [4]

$$x^\mu + ix^{\bar\mu} = z^\mu,\ \mu, \nu, \cdots = 1, 2, \cdots\cdots, m;\ \bar\mu = \mu + m. \tag{2.1}$$

A contravariant vectorfield in the manifold M^n is written by the components $a^1(x)$, $\cdots\cdots$, $a^n(x)$ in a local coordinate system (x^i), and by $a^1_{(y)}, \cdots\cdots, a^n_{(y)}$ in a y-coodinate system (y^i). Then we have in $U_x \cap U_y$, $a^k_{(y)} = \dfrac{\partial y^k}{\partial x^l} a^l_{(x)}$ (k, $l, \cdots\cdots = 1, 2, \cdots\cdots, n$). We call the complex masses

$$A^\mu_{(z)} = a^\mu_{(x)} + ia^{\bar\mu}_{(x)} \tag{2.2}$$

the complex components of the vectorfield with respect to z-coordinate system, where (z^μ) is the complex coordinate system belonging to x^k. To a vector a with the complex components $A^\mu_{(z)}$ we make correspond the vector $b = J_{(z)}a$ with the components $B^\mu_{(z)}$ by means of

$$B^\mu_{(z)} = iA^\mu_{(z)}. \tag{2.3}$$

In the above we have shown the mapping by $J_{(z)}$, where the index (z) shows that the mapping is defined by using the coordinate system (z). Such a mapping of vectors should be independent of a choice of local coordinate system. $J_{(z)}$ and $J_{(w)}$ are equal, if and only if Cauchy-Riemann's differential equations holds between z^μ and w^ν. We say that a complex structure is given on M^n, if M^n is covered with such complex coordinate system that all coordinates transformations $w^\nu = w^\nu(z)$ are complex-analytic, where (w^ν) is the complex coordinate system belonging to y^k. Then we have[1];

For a coordinate system belonging to one complex structure, the multiplication of the complex vector components with $i(=\sqrt{-1})$ is a linear mapping admitting $A^2 = -I$ independent of the coordinate system. And also we have:

If the multiplication of the complex vector components with i in z-coordinate system and in w-coordinate system respectively is the same mapping, these both coordinate systems (in their intersection) are connected by a complex-analytic transformation.

Therefore a complex structure is well determined by the belonging mapping. In the other words, to one complex structure belongs a well determined almost complex structure. Such almost complex structures derived from a complex structure are called *integrable.*

From the above, we see that an almost complex structure belongs to at most one complex structure, while an integrable almost complex structure does to just one precisely.

When an almost complex structure J is defined by a^i_j and the torsion tensor by $t^i_{kl} = a^i_{hk}a^h_l - a^i_{hl}a^h_k$ where $a^j_{kl} = \dfrac{\partial a^j_k}{\partial x^l} - \dfrac{\partial a^j_l}{\partial x^k}$, we have:

Theorem. A necessary and sufficient condition that a real-analytic almost complex structure is integrable, is vanishing of the belonging torsion tensor.

We now consider the manifold M^n with a positive definite metric and assume the almost complex structure on M^n is real-analytic and integrable.

(1) See [5]

Furthermore we assume the almost complex structure a_j^i is orthogonal, or the length of any vector is invariant. Then we have

$$g_{ik}\, a_j^k + g_{jk}\, a_i^k = 0. \tag{2.4}$$

Then we assume that a differential form $\omega = a_{ij}\, dx^i \Lambda dx^j$ where $a_{ij} = g_{ik}\, a_j^k$, is exact, namely

$$d\omega = 0 \quad \text{or} \quad D_l\, a_{ij} + D_i\, a_{jl} + D_j\, a_{li} = 0, \tag{2.5}$$

where D_i represents the covariant derivative with respect to g_{kl}.

§3. Now we assume that in a 2m dimensional real analytic manifold which has an almost complex analytic structure defined by a_j^i of class C^ω a positive definite metric

$$ds^2 = g_{ij}\, dx^i\, dx^j$$

is given and that the structure a_j^i is orthogonal and without torsion. Furthermore we assume that the differential form ω is exact. By these assumptions we have:

a) $a_{ij} = g_{ik}\, a_j^k = -\, a_{ji}$

b) $d\omega = 0$ or $D_l\, a_{ij} + D_i\, a_{jl} + D_j\, a_{li} = 0$

c) $t_{ji}^k = 0$

c) implies that $(a_{j,k}^i - a_{k,j}^i)a_l^j - (a_{j,l}^i - a_{l,j}^i)a_k^j = 0$ or $(D_k a_j^i - D_j a_k^i)a_l^j - (D_l a_j^i - D_j a_l^i)a_k^j = 0$. After some calculations we get the relation:

$$D_i\, a_k^j = 0. \tag{3.1}$$

If we take an unit vector u^i, as well readily seen, the vector $v^i = a_j^i u^j$ is also unit and orthogonal to u^i. Then we have a *holomorphic sectional curvature* with respect to u^i defined by

$$k = -\, R_{ijkl}\, u^i\, v^j\, u^k\, v^l$$

where R_{ijkl} is the curvature tensor. If the holomorphic sectional curvature is always constant with respect to any vector at every point, the curvature tensor has the form:

$$R_{ijkl} = \frac{k}{2}\,(g_{i[k]}\, g_{jl} + a_{i[k]}\, a_{jl} + a_{ij}\, a_{kl}). \tag{3.2}$$

This space is symmetric in Cartan's sense.

Now we shall prove that it is a completely harmonic. In our space, the matrix Γ defined in §1 has the following form:

$$\Gamma_l^i = R_{jkl}^i\, \lambda^j\, \lambda^k = \frac{k}{4}\,(\Lambda \delta_l^i - \lambda^i\, \lambda_l + 3 l^i\, l_l), \tag{3.3}$$

where we put

$$l^i = a_k^i\, \lambda^k \quad \text{or equivalently} \quad l_i = a_{ij}\, \lambda^j, \tag{3.4}$$

λ^i being any direction and $\lambda_i = g_{ij}\lambda^j$. Then we have

$$\Lambda = l_i l^i = g_{ij}\lambda^i\lambda^j \text{ and } l_i\lambda^i = \lambda_i l^i = 0. \quad \cdots\cdots (3.5)$$

From the equations (3.3), (3.4) and (3.5) we get after some calculations:

$$\Gamma^i_k l_i = \Lambda k l_k \text{ and } \Gamma^i_k \lambda^k = 0 \quad (3.6)$$

and

$$\left.\begin{aligned} \Gamma^i_l \Gamma^l_j &= \frac{k}{4}\Lambda\Gamma^i_j + \frac{3k^2}{4}\Lambda l^i l_j, \\ \Gamma^i_l \Gamma^l_j \Gamma^j_k &= \left(\frac{k}{4}\right)^2 \Lambda^2 \Gamma^i_k + \frac{15k^3}{4^2}\Lambda^2 l^i l_k, \text{ etc.} \end{aligned}\right\} \quad (3.7)$$

Now by mathematical induction we shall prove that the N-th power of the matrix Γ has the following form:

$$\Gamma^N = \Lambda^{N-1}\{\alpha(\Gamma^i_j) + \beta(l^i l_j)\}, \quad (3.8)$$

where α and β are certain scalars.

In fact when $r = 2$, we have $(3.7)_1$. If we assume that (3.8) holds good, we have

$$\begin{aligned} \Gamma^{N+1} &= (\Lambda^{N-1}\{\alpha(\Gamma^i_k) + \beta(l^i l_k)\}\Gamma^k_j) \\ &= \Lambda^{N-1}\left\{\frac{k}{4}\Lambda\alpha(\Gamma^i_j) + \frac{3k^2}{4}\Lambda\alpha(l^i l_j) + \beta k\Lambda(l^i l_j)\right\} \\ &= \Lambda^N\{\alpha'(\Gamma^i_j) + \beta'(l^i l_j)\}, \end{aligned}$$

where we put $\alpha' = \frac{\alpha k}{4}$ and $\beta' = \frac{3k^2}{4}\alpha + \beta k$.

In the other hand we see that all the matrices $\dot{\Gamma}, \ddot{\Gamma}, \dddot{\Gamma}, \cdots$ are zero matrix, since the space is symmetric. Consequently the trace of the matrix $\Gamma^N (N = 1, 2, 3, \cdots)$ is the form $k_N \Lambda^N$, k_N being independent of λ^i, and from the Theorem A in §1 we conclude that our space is completely harmonic. Thus we have

Theorem. If a 2m dimensional real analytic manifold which has an almost analytic structure defined by a^i_j of class C^ω and a positive definite metric $ds^2 = g_{ij}dx^i dx^j$ satisfying $d\omega = 0$ and (2.4), has the constant holomorphic sectional curvature, then the manifold is completely harmonic.

Bibliography

[1]. E. T. Copson and M. S. Ruse, Harmonic Riemannian spaces. Proc. Roy. Soc. Edinburgh, 60, (1940), 117-133.

[2]. A. G. Walker, Note on a distance invariant and the calculation of Ruse's invariant. Proc. Edingburgh Math. Soc. (2), 7 (1942) 16-26.

[3]. K. Yano and I. Mogi, Sur les variétés pseudokählerienes à courbure holomorphique constante. Comptes Rendus, 237 (1953) 962-964.

[4]. K. Yano, Quelques remarques sur les variétés à structute presque complexe. Bull. Soc. Math., France, 83 (1955), 57-80.

[5]. A. Frölicher, Zur Differentialgeometrie der komplexen Strukturen. Math. Ann. 129(1955), 50-95.

ON THE THEORY OF PARITY DOUBLET

Seibun SASAKI

(Recieved Aug. 31, 1958)

Summary

We have considered the roles of the parity doublets of the Bosons in the interactions with the Fermions. To consider the parity doublets in ordinary Yukawa type interactions causes the effects of the parity non-conservations not only in the weak interactions relating to the decays but also in the strong interactions containing hyperons and kaons. If we adopt the derivative couplings for pions with Fermions, same situations are also true for pions produced by the interactions other than NN-π type. The degrees of parity mixture for pions are expected to depend on the histories by which they are produced. It is desirable to perform the absorption experiments to the deuterium with various pions produced in different processes (i. e. with various pions having different histories). Assuming the parity doublet for the Bosons, θ and τ mesons are interpreted as the different modes of disintegrations of the kaons.

§ 1. Introduction

As is well known, the wave function of the Boson with spin zero, $\varphi(\vec{x}, t)$, satisfies the Klein-Gordon equation

$$(\square - \kappa)\varphi(\vec{x}, t) = 0 \qquad (1)$$

where

$$\square = \frac{1}{c}\frac{\partial}{\partial t}$$

$$\kappa = \frac{mc}{\hbar} \qquad (m = \text{mass of the Boson})$$

In the following, we will adopt the natural units ($\hbar = c = 1$).
Then, κ may be considered as the mass of the particle. Hereafter, we will refer the letter κ to the mass of the particle.

As the transformation $(\vec{x}, t) \to (-\vec{x}, t)$ makes the operator $(\square - \kappa^2)$ invariant, we get from the equation (1)

$$(\square - \kappa)\varphi(-\vec{x}, t) = 0 \qquad (2)$$

Thus, $\varphi(\vec{x}, t)$ and $\varphi(-\vec{x}, t)$ satisfy the same Klein-Gordon equation of motion. Therefore, we get the following three types of the transformation characters for $\varphi(\vec{x}, t)$:

I) $\varphi(\vec{x}, t)$ is scalar
then $\varphi(\vec{x}, t)=\varphi(-\vec{x}, t)$

II) $\varphi(\vec{x}, t)$ is pseudoscalar
then $\varphi(\vec{x}, t)=-\varphi(-\vec{x}, t)$

III) $\varphi(\vec{x}, t)$ is the mixture of scalar and pseudoscalar.

From the considerations of the free fields of the particles only, we can not decide which one of these three actually occurs in nature. It must be determined by comparing the experimental results with the theoretically constructed interactions which satisfy the requirments of the relativity for each of the three cases respectively. As the pion and the kaon are believed to be the Boson with spin zero, we will bring in mind the above situations for the pion.

That the pion is of spin zero seems to be indisputable by comparing the reactions $\pi^+ + D \rightarrow p + p$ and $p + p \rightarrow \pi^+ + D$.[1]
It was a rather troublesome problem, for a long time, to decide whether the parity of the pion is even or odd. There are many discussions about the problem and gradually, of course indirectly, evidences have increased in which odd parity pions are preferable to even parity ones. Since 1951, when Panofsky et al[2] performed the capture experiment of the negative pion in the hydrogen and the deuterium and observed that the process*) $\pi^- + D \rightarrow n + n$ certainly occured in nature, pseudoscalar seemed to become a decisive type for the pion and nowadays the possibility of the pion being of scalar type seems to be almostly ignored.
Recently, new particles such as hyperons and kaons have been discovered and they have caused various questions and discussions about the natures of the interactions between elementary particles. Of course, some of them might be compound particles but we have not touched the possibility of their being compound in this report. Now, if all the particles are elementary, the question is still open in which we may ask whether the parities of them decided by the way mentioned above are unique or not. After Lee and Yang[3] pointed out that the conservation of parity does not hold in weak interactions, the problem of the interactions between elementary particles have had to be re-examined from the new stand point of view.

Concerning the problem of the non-conservation of parity, the theory of the neutrinos have appeared as the important problem. Neutrinos come from the beta-decay must have almostly vanishing masses. But the question whether the neutral half-odd spin particles ejected from the $\pi-\mu$ decay and $\mu-e$ decay are identical with the neutrinos emitted from the beta-decay can not solved by examining only the energy spectrum of the charged secondary particles.[4]

Therefore, it becomes a matter of hypothesis to identify the secondary half-odd spin particles come from the meson decay, and the propriety of the hypothesis must be decided from the experiments other than the measurement of the integrated energy spectrum. Provided that the mass of the neutrino is zero, the solution of the problem appears as the form of the two component theory of the neutrino,[5] connected with the

*) n, p and N stand for the neutron, the proton and the nucleon respectively.

problem of the non-conservation of the parity. This theory agrees excellently with many experiments. As two component theory of the neutrino causes necessarily the violation of the parity conservation, if this theory is correct, we can conclude that in every processes containing neutrinos the parity conservation of the theory must be destroyed.

Lately, it is found that the same situations exist in some of the elementary processes without neutrinos (of course, weak).

Let $\bar{P}$ be the average of the magnitudes of the polarization of the hyperon and α be the anisotropy coefficient for the completely polarized hyperons, then in the hyperon decay processes it is found that[6]

$$\alpha\bar{P}=0.44\pm0.11$$

and this value is remarkably different from the value obtained by Gatto[7]

$$|\alpha|<0.18\pm0.02$$

assuming the invariance under the charge conjugation. Therefore, we can say that the conservation is also destroyed in the hyperon decay. Thus we must conclude that:

Parity is not conserved in all of the weak interactions. (*I*)

Further problem comes out, asking why the parity does not conserve in such phenomena. Two directions along this line offered recently are:

i) to assume another wider invariance property (CTP-invariance, for example).

ii) to consider such as the parity doublet of the particle, remaining the formalism itself invariant under the parity conjugation.

We have already pointed out that when we consider the pseudospinors, it becomes meaningless to distinguish even and odd parities for the Boson.[4] (Of course, under the assumption of the parity conservation.)

We think that it is valuable to consider the parity mixture for the Boson from the second stand-point and to examine how far we can explain the experimental results. As for the second stand-point, Lee and Yang[8] have discussed the case where the particles with the odd strageness are of parity doublet, and further, Green and Hurst[9] have shown that the experimental results can be uniquely explained if we assume the parity doublet for μ, Λ and Σ particles.

In this report, we assume parity mixtures to the Boson with spin zero leaving the spinors ordinary. Firstly, we will examine whether the possibilities that the parity of the pion is not odd do not exist at all, and then discuss the results obtained from the assumptions of parity mixture for the pion and the kaon.*

*) Roughly speaking, CTP-invariance of the Hamiltonian may be assured from the hermiticity of it. Therefore if we make the Hamiltonian hermite, we may consider that the CTP-invariance is guaranteed in the theory. Today, the propriety of the CTP-invariance seems to be undoubtful, and to take the stand-point (ii) reduces very often to examine whether the results obtained agree with the results obtained from the stand-point (i). In this paper, we will not touch the stand-point (i), but this does not mean our denial of (i). It only means that it is our purpose to examine whether we can approach to the stand-point (i) starting from the stand-point (ii).

§ 2. Parity of the Pion
(Re-examination of the Panofsky's Experiment)

Firstly, we will consider the Panofsky's experiment[2] which is believed to give a direct proof that the parity of the pion is odd. Panofsky et al observed the capture process of the negative pion in the deuterium and found that the process

$$\pi^- + D \rightarrow 2n + \pi^0$$

does not occur, and the processes

$$\pi^- + D \rightarrow 2n \quad \cdots\cdots (3)$$

$$\pi^- + D \rightarrow 2n + \gamma \quad \cdots\cdots (4)$$

occur with the ratio of 2 : 1. It is the very former, non-radiative capture process that informs us that the parity of the pion must be odd. Provided that the conservation of parity holds in the process (3), it is based on the fact that the negative pion is, when captured by the deuterium, at the K-shell of the pi-mesic atom, and the deuterium at its ground state, i. e. ^3S-state while two neutrons in the final state must be at the parity odd state due to Pauli's exclusion principle. Therefore, the negative pion which causes the process (3) could not be of scalar type. But it is worth while to notice that if the conservation of parity is held in this process (of course, there is no evidence against the parity conservation in thisprocess), the process (3) becomes forbidden for the scalar pion. That is to say, so long as the process (4) exists and so long as the scalar pion can cause the process (4), it seems to us that the possibility of the scalar pion being scalar should not be abandaned only from the reason that the scalar pion could not cause the process (3). Even though the pion is the mixture of scalar and pseudoscalar (i. e. parity doublet) it could be easy to explain the Panofsky's experimental results by the suitable choice of the mixing ratio.

Brueckner et al[10] considered the possibility of the scalar pion being captured from the P-state of the mesic deuterium atom, but the capture probability became too small to interprete the ratio 2 : 1 of (3) to (4). Their conclusions, from our stand point of view, however, could be reinterpreted as follows. Namely, almost all of the scalar pions do interact with the deuterium through the reaction (4) and result in reducing the ratio of the process (3) to (4) for the pseudoscalar pions some percents according to the ratio of the impurity of the scalar pions to the pseudoscalar ones*)**).

*) Throughout this paper we use the perturbation theory. Quantities calculated are, therefore, of the lowest order in the perturbation theory.

) Using the perturbation theory, the probabilities for the neutron and the radiative absorption of the pion in the deuterium were calculated by S. Tamor and R. E. Marshak, (Phys, Rev. ***80* 766 1950) and S. Tamor, (Phys. Rev. ***82*** 38 1951) as follows:

pion theory	S (S)	PS (PS)	PV (PS)
neutron absorption	0	2.7×10^{-3}	0.25
radiative absorption	0.012	6.6×10^{-4}	0.12
ratio	0	4.1	2.1

(unit $0.9\times10^{16}g^2/\hbar c.\ sec^{-1}$).

From these values we can see that the pion should almostly be of the PV (PS) type.

We will estimate in the following how much contaminations are allowed in order to reconcile them with Panofsky's results. Let α be the ratio of the process (4) to the process (3). α is the experimentary observable quantity. Be the existing ratio of the scalar pions to the pseudoscalar ones x, and be the ratio of the probability of the process (4) to the process (3) for the pseudoscalar pion $(1-z : z)$.
Let $N[\pi^- + D \to 2n]$ and $P[\pi^- + D \to 2n]$ etc. be numbers and probabilities respectively for the processes within the square bracket, and further let ξ be the ratio of $P[\pi_s + D \to 2n+\gamma]/g_s^2$ to $P[\pi_{ps} + D \to 2n+\gamma]/g_{ps}^2$.

Then we get the relation

$$\alpha = \frac{N[\pi + D \to 2n+\gamma]}{N[\pi + D \to 2n]} = \frac{P[\pi_{ps} + D \to 2n+\gamma] + x\,P[\pi_s + D \to 2n+\gamma]}{P[\pi_{ps} + D \to 2n]}$$

Using the definitions of x and ξ, we obtain

$$\alpha = \left(1 + x\xi\, g_s^2/g_{ps}^2\right)\alpha_0;\quad \alpha_0 = z/(1-z)$$

or

$$x = \frac{g_{ps}^2}{g_s^2}\,\frac{1}{\xi}\left(\frac{\alpha}{\alpha_0} - 1\right). \qquad (5)$$

where g_{ps} and g_s are the coupling constants of the pseudoscalar and the scalar pion with the nucleon respectively. The value of α is approximately 1/2 (experiment of Panofsky et al). Using the value 1/3 for z obtained by Tamor, x will be found to be very small. This seems to mean that the contamination of the scalar pion is, if any, very small. We will return back to this point later.

In the above considerations, we made no attention to the mesic absorption containing the charge exchange effect. Taking the mass difference between π^- and π° as about 4.7 Mev., Q-value for the mesic absorption become about 1 Mev. and we may expect that this process is unprobable. Indeed, the probability for this process is about the order of 1 % of that of the radiative absorption.* Thus, we seem to be allowed to ignore the possibility for this process. We can say as a conclusion that it is difficult to abandan the small contaminations of the scalar pion only from the existence of the neutron absorption process $\pi^- + D \to 2n$.

§ 3. Considerations About Other Phenomena and the Deduction to the Forms of Interactions

As is well known, in the nucleon and the pion interacting system, pseudovector coupling of the pseudoscalar pion (PV (PS)) is equivalent to the pseudoscalar coupling of it (PS (PS)) if we choose the coupling constants suitably, and the vector coupling of the scalar pion (V (S)) is vanishingly small unless we choose the coupling

*) R. E. Marshak: Meson Physics, p. 156

constant unreasonably large, because of the mass difference of the proton and the neutron being very small (~1.3 Mev.)*). As a rule, we can say that the vector coupling of the scalar particle is small as compared with its scalar coupling (S (S)), but when the mass difference of the two Fermions taking part in this process is not so small, V (S) can not be neglected both for the pion and the kaon. (In the following, we will use the abbreviations S (S) etc. not only for the pion but also for the kaon.) Therefore, when we take the position that all of the spin zero Bosons are of parity doublet, it will be possible to examine the suitability of our stand-point by investigating the actual phenomena, and further to get some informations about the forms of the interactions participated.

I. Deuteron Potential (Non-Relativistic)

In the non-relativistic approximations, deuteron potentials are

(a) spherical symmetric and repulsive for the symmetrical scalar pion,

and (b) spherical symmetric term plus tensor term and attractive for the pseudoscalar pion.

Therefore, if we assumed that all of the pions are of scalar type, of course, we could not explain the formation of the deuteron, but we can expect that the small contaminations of the scalar pions do not affect the attractive character of the potential come from the pseudoscalar pions provided that the degree of the impurity is small enough.

II. Gamma-Decay of the Neutretto $\pi^\circ \to \gamma + \gamma$

According to the calculations of Sasaki, Oneda and Ozaki[11] and Fukuda and Miyamoto[12], the life-time of the process is shorter for S (S) than for the pseudoscalar neutretto provided that $g_s = g_{ps}$. For the V (S), the matrix element of the process involving the interaction $\bar{p}p\pi^\circ$ vanishes as was mentioned above. The scalar neutretto, with exclusively V-coupling, must, therefore, decays through the other strong interactions than $NN\pi^\circ$. An example of the decay diagram is shown in Fig. 1. Because the coupling $\Lambda^\circ \Sigma^\circ \pi^\circ$ is effectively small, the life-time for the diagram is expected to be longer than that for the pseudoscalar neutretto. (c. f. III)**)

III. Pion Production

The data on the pion production seem to fit in the PV (PS) pion, and the possibility that the scalar pions are produced through the S-coupling seems to be negligible***).

*) In general, the equivalence of PS (PS) and PV (PS) does not hold for the interactions containing the charge exchange effect. In this case, V (S) does not vanish too. Besides, PS (PS) and PV (PS) have quite different characters in the renormalization theory. Above argument concerning the equivalence theorem should be understood as conventional, and be allowed only when the lowest order perturbation theory is used.

**) We assume that the disintegration of the Boson into the Bosons go through the intermediary of the usual Yukawa type interactions, and do not make the direct interactions between the Bosons.

***) One of the reasons against the S-coupling of the scalar pion is that it predicts a zero cross section for the neutretto in the n-p collision, in conradiction with the fact that the same numbers of the neutrettos come from the n-p collisions.

The latter can be seen from the comparison with Panofsky's experiment. That is, if the S-coupling of the scalar pion had the same order coupling constant as the PV-coupling of the pseudoscalar pion effectively, the results of the experiments could not be understood. On the other hand, the V-coupling of the scalar pion seems to meet no such a grave difficulty. Cross section for the scalar pion production through the interaction $NN\pi$ will become very small. Thus, we can adopt the derivative couplings for both the scalar and the pseudoscalar pions, and this is very fine for the symmetricity of the theory. We get the following conclusion:

Interactions between the parity doublet pion and the hyperons are of derivative type, and so the pion behaves almostly as having the pseudoscalar property in nature. (II)

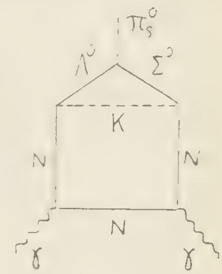

Fig. 1 An example of the gamma-decay of the scalar neutretto with exclusively V-coupling.

When we consider the higher order processes, we must take account of the diagrams such as shown in Fig. 2. Attributing the scalar couplings to the interactions $V\Sigma\pi$, $\Sigma\Sigma\pi$ and $\Xi\Xi\pi$ (all are strong interactions) must be avoided from the same reason as above.

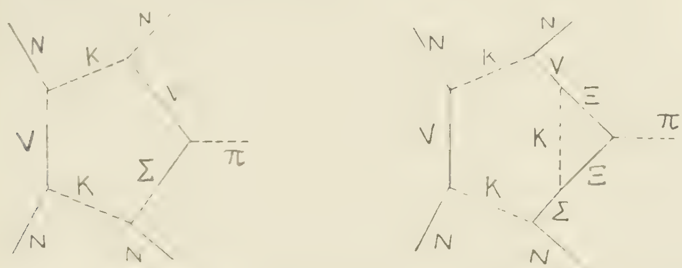

Fig. 2 Examples of the higher order pion production diagrams containing hyperons

IV. $\theta^{\pm}$ and $\tau^{\pm}$ Mesons[13]

These particles are defined as the Bosons which decay into two pions and three pions respectively. The decay schemes are as follows:

$$\left.\begin{array}{l}\theta^{\pm}\rightarrow\pi^{\pm}+\pi^{0}\\ \tau^{\pm}\rightarrow\begin{cases}\pi^{\pm}+\pi^{+}+\pi^{-}\\ \pi^{\pm}+\pi^{0}+\pi^{0}\end{cases}\end{array}\right\}\cdots\cdots\quad \text{life}\sim10^{-8}\,\text{sec.} \qquad (6)$$

The second of the τ modes of the decays is usually called τ', but we will include it into the category of τ. If the pion and the kaon have fixed parities and the parity conservation holds for these processes, then θ and τ must have the parity even and odd respectively, and will be different particles[*)]. Recently, Fujii and Marshak[14]

have attempted to determine the parity of the kaon assuming the global symmetry and using the lowest order perturbation theory. In their calculations for the absorption processes of the kaon in the hydrogen and the deuterium the same situations occur to which we have already met in examining the Panofsky's results. Their conclusions are as follows:

If the kaon is scalar, the absorption from the 2P orbital is about a factor 10 smaller than the optical transition rate in both hydrogen and deuterium. From the 1S orbital, the absorption takes place quickly. If the kaon is pseudoscalar, the absorption from the 2P orbital and the optical transition rate are comparable. In addition, for the absorption of the scalar kaon, the mesic mode is the chief process for hydrogen, while the non-mesic and the radiative absorption modes should compete with the mesic mode with the rate of one to ten. For the pseudoscalar kaon, the mesic mode is dominant both in hydrogen and deuterium.
Therefore, if we could perform these experiments carefully enough, we could determine whether the kaon is of fixed parity or not. Unfortunately, we are not at such a situations. We will proceed assuming that the kaon is parity doublet, just as was done for the pion. (The propriety of this assumption seems much more certain than for the pion.)

From our stand-point of view, the kaon decay into the pions are classified as follows:

$$\theta^{\pm}\begin{cases} K_e \to \pi^{\pm} + \pi_e \\ K_e \to \pi_e + \pi_e \\ K_0 \to \pi_e + \pi_0 \end{cases} \qquad \cdots\cdots (7)$$

$$\tau^{\pm}\begin{cases} K_e \to \pi_e + \pi_e + \pi_e \\ K_e \to \pi_e + \pi_0 + \pi_0 \\ K_0 \to \pi_e + \pi_e + \pi_0 \\ K_0 \to \pi^{\pm} + \pi^{\pm} + \pi_0 \end{cases} \qquad \cdots\cdots (8)$$

In the schemes (7) and (8), π_e and K_e denote the pion and the kaon with the parity even (scalar), and π_0 and K_0, with parity odd (pseudoscalar), respectively.

As was shown in the conclusion (II), the pion and the hyperon interact with the derivative coupling. Then, it is easily found that the contamination ratio of the scalar pions to the pseudoscalar pions is different for different hyperons with which the pions interact. We will set this fact as our third conclusion, that is:

The contamination ratio of the scalar Bosons to the pseudoscalar ones is different for the different Fermions the Bosons interact with. (*III*)

This means that the contamination ratio is not constant but is different corresponding to the different interactions involving the pions. (The same, of course, can be said for the kaon, too.) We will be able to test the suitability of our assumptions

*) Historically, the existence of the tau-meson was confirmed firstly, as the four particles playing a role in the decay process are all charged. In ref. 13), we have calculated the life times of θ and τ attributing fixed parities to them, and concluded that θ and τ have even and odd parities, respectively.

by examining the absorption process in hydrogen and deuterium using the pions come from the different schemes of interactions (in other words, the pions having different parents).

Now, we will estimate the ratio of the process (4) to (3). The pions appeared in the schemes are the decay products of the kaon. Since the ratio considered is determined by the impurity ratio of the pions, we will treat the problem by counting the latter ratio using the diagrams. Fig. 3 (a) and (b) are the diagrams responsible for the decay modes θ and τ respectively. In Fig. 3, we have considered the lowest order of the perturbation theory. As was mentioned previously, the pions come from the interaction $NN\pi$ are almostly pseudoscalar. So, if we neglect the interaction $NN\pi_e$, then it may be enough to consider the second and the fourth diagrams in (a) and the first and the seventh in (b).

Let the ratio K_e to K_0 be y and the ratio π_e to π_0 come from the $V(\Sigma)N\pi$ interaction be x'. The ratio π_e to π_0 at the interaction $NN\pi$ is x which is equal to the value in the expression (5). Let β be the observational ratio of τ to θ. Then, we get the relation,

$$\beta=\frac{yx'+1+2x(y+x')+x^2(yx'+1)}{y+x'+x(yx'+1)} \quad \cdots\cdots (9)$$

or, if we put $x\rightarrow 0$,

$$\beta=\frac{yx'+1}{y+x'} \quad \cdots\cdots (9')$$

Thus, we are able to know one of y and x' from the other one. Relation (9') is plotted in Fig. 4. The value of β, $\beta=2.5$, is due to the experimental results of Alexander, Johnston and O' Ceallaigh[15].

Next, let $R(\theta)$ and $R(\tau)$ be the contamination ratio of the scalar pions to the pseudoscalar ones for the decay modes θ and τ, respectively. $R(\theta)$ and $R(\tau)$ are expressed as follows:

$$R(\theta)=\frac{x'+x(2yx+1)}{2y+x'+x}$$

$$R(\tau)=\frac{yx'+2x(2x'+y)+x^2(2+3yx')}{2yx'+3+2x(2y+x')+x^2} \quad \cdots\cdots (10)$$

or putting $x\rightarrow 0$,

$$R(\theta)=\frac{x'}{2y+x'}$$

$$R(\tau)=\frac{yx'}{2yx'+3} \quad \cdots\cdots (10')$$

If the pions appeared from the θ and τ decay modes are mixed up and can not be

separated, then the mixing ratio of scalar and pseudoscalar, $R(\theta, \tau)$, should become

$$R(\theta, \tau)=\{R(\theta)+\beta R(\tau)\}/(1+\beta) \quad \cdots\cdots (11)$$

when we want to have the ratio $N[\pi^-+D\rightarrow 2n+\gamma]/N[\pi^-+D\rightarrow 2n]$ for the absorption experiments in the deuterium using the pions come from the kaon decay, it is enough to substitute these values for x in the expression above (5). These ratios are:

$$\alpha(\theta)=\alpha_0+\eta(\theta)=\alpha_0+\alpha_0\xi\,\frac{g_s^2}{g_{ps}^2}\,\frac{x'}{2y+x'}$$

$$\alpha(\tau)=\alpha_0+\eta(\tau)=\alpha_0+\alpha_0\xi\,\frac{g_s^2}{g_{ps}^2}\,\frac{yx'}{2yx'+3}$$

$$\alpha(\theta, \tau)=\alpha_0+\eta(\theta, \tau)=\alpha_0+\alpha_0\xi\,\frac{g_s^2}{g_{ps}^2}\left(\frac{x'}{2y+x'}+\beta\,\frac{yx'}{2yx'+3}\right)\frac{1}{1+\beta}\,.$$

It seems to be more interesting to examine the ratio η/α_0. As we can suppose that the difference of the strength of the couplings of π_e and π_0 with the hyperons is effectively contained in R's, we may put $g_s^2\sim g_{ps}^2$ in our tentative considerations. Then,

$$\begin{aligned}\eta(\theta)/\alpha_0&=\frac{\xi x'}{2y+x'}\\ \eta(\tau)/\alpha_0&=\frac{\xi yx'}{2yx'+3}\\ \eta(\theta, \tau)/\alpha_0&=\xi\left(\frac{x'}{2y+x'}+\beta\,\frac{yx'}{2yx'+3}\right)\frac{1}{1+\beta}\,.\end{aligned} \quad \cdots\cdots (12)$$

These values are of the order of several percents and we might expect that the careful experiments might judge our stand-point.

In the above considerations, we suppose that the probability for each of the processes shown in the decay schemes (7) and (8), is nearly equal because the life-times of the θ and τ modes of decays are almostly the same. Therefore, it seems to be reasonable to consider that the observed frequency ratio for the θ and τ modes of decay has its origin in the number of the processes containing to each of the modes of decay. Further, we have assumed that the K_0's and the K_e's have the same branching ratios to the other modes of decay such as $K_{\mu 2}$, $K_{\mu 3}$ and K_β, when these particles should be regarded as the identical particles with the kaon considered above.

§ 4. The Interaction Hamiltonian

In general, the interaction Hamiltonian takes the form

$$H_{int}=\bar{\psi}_a\,(g_s\varphi_s+\gamma_5 g_{ps}\varphi_{ps})\,\psi_b+h.c. \quad \cdots\cdots (13)$$

for the non-derivative interactions

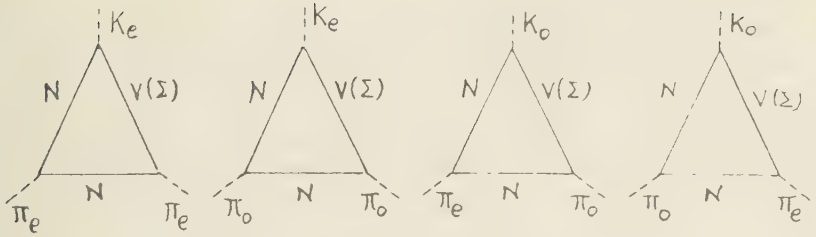

Fig. 3 (a) Diagrams for the decay mode θ.

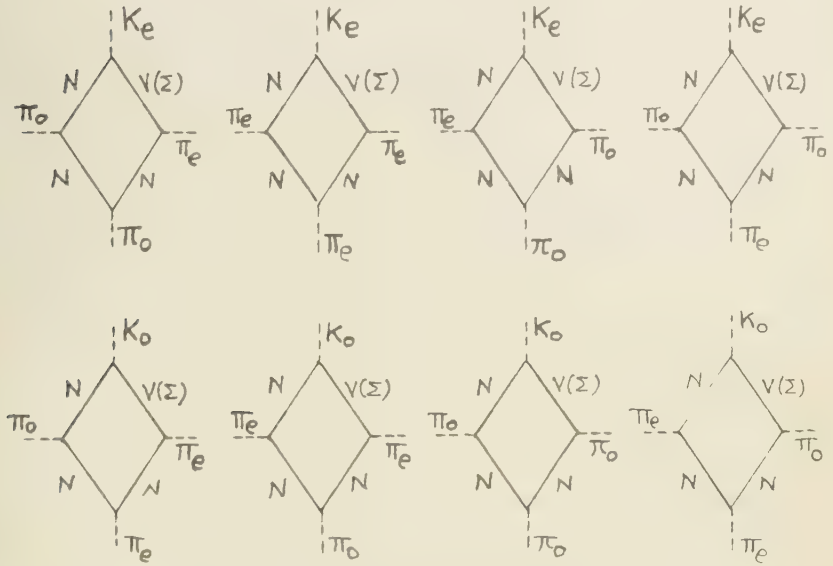

Fig. 3 (b) Diagrams for the decay mode τ.

and

$$H_{int}=i\bar{\psi}_a\partial_\mu\left(g_s\varphi_s+\gamma_5 g_{ps}\psi_{ps}\right)\gamma_\mu\psi_b+h.c. \quad \cdots\cdots (14)$$

for the derivative interactions,

where the meanings of the notations ars as follows:

ψ_a and ψ_b	:	the wave functions for the Fermions,
$\bar{\psi}=\psi^+\gamma_0$; ψ^+	:	hermitian conjugate to ψ,
φ's	:	the wave functions of the Bosons,
$h.c.$	:	hermitian conjugate

and g_s and g_{ps} are the coupling constants which are in general different for the derivative and the non-derivative interactions.

According to our assumptions, the Bosons with spin zero are of parity mixture,

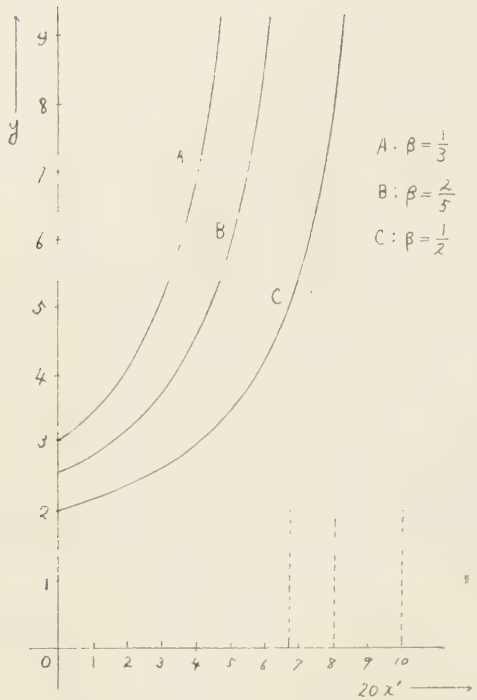

Fig. 4 Curves of $y=\frac{1-\beta x'}{\beta-x'}$

that is, they will appear in nature as the form $(a\pi_s+b\pi_{ps})$ where a and b are the mixing ratios of the scalar and the pseudoscalar Bosons respectively. Then, we must construct the state vectors by considering the $(a\pi_s+b\pi_{ps})$ as a unit. Define the creation and the annihilation operators for the $(a\pi_s+b\pi_{ps})$ particle, and then we will get any states from the vacuum by applying the required number of creation operators just defined. Expanding the wave function of each particle to the plane wave, we get the matrix element of the form:

$$\sim \bar{u}_a(ag_s+\gamma_5 bg_{ps})Ku_b+h.c.$$

where $K=\begin{cases}1 \text{ for the non-derivative coupling,}\\ \gamma_\mu k_\mu \text{ for the derivative coupling,}\end{cases}$

and K is the energy-momenfum four vector of the Bosons.

$\bar{u}$ and u stand for the spinors as usual.

Since the observale quantities are ag_s and bg_{ps}, and not the a, b, g_s and g_{ps}, in the following we will put ag_s and bg_{ps} as simply g_s and g_{ps}, respectively, and will call them as the coupling constants. (This argument is not regorous, because the mixing ratio a and b should be determined from the coupling constants. It is good enough to choose both a and b equal to unity.) Then, the matrix element we must consider becomes

$$\sim \bar{u}_a(g_s+\gamma_5 g_{ps})Ku_b+h.c. \qquad (15)$$

We can put the interaction Hamiltonian in the alternative form, that is, as the factor in the bracket of the expression (13) and (14) can be rewritten as

$$g_s\varphi_s+\gamma_5 g_{ps}\varphi_{ps}=\frac{1}{2}(g_s\varphi_s+g_{ps}\varphi_{ps})(1+\gamma_5)$$
$$+\frac{1}{2}(g_s\varphi_s-g_{ps}\varphi_{ps})(1-\gamma_5)$$

we have

$$H_{int}=\frac{1}{2}\left[g_1\bar{\psi}_a(1+\gamma_5)\psi_b\varphi_1+g_2\bar{\psi}_a(1-\gamma_5)\psi_b\varphi_2\right]+h.c. \qquad (16)$$

for the non-derivative coupling,

and

$$H_{int}=\frac{i}{2}\left[g_1\bar{\psi}_a(1+\gamma_5)\gamma_\mu\psi_b\partial_\mu\varphi_1+g_2\bar{\psi}_a(1-\gamma_5)\gamma_\mu\psi_b\partial_\mu\varphi\right]+h.c. \quad (17)$$

for the derivative coupling,

where

$$g_1\varphi_1=g_s\varphi_s+g_{ps}\varphi_{ps}$$
$$g_2\varphi_2=g_s\varphi_s-g_{ps}\varphi_{ps} \quad (18)$$

In all of the above expressions, the coupling constants are in general complex. In the latter form of the Hamiltonian, we consider φ_1 and φ_2 as the wave functions for the Bosons, and following the same procedures as in the former case, we can get the matrix elements for the Hamiltonians (16) and (17)

$$\sim g_1\bar{u}_a(1+\gamma_5)Ku_b$$
$$\sim g_2\bar{u}_a(1-\gamma_5)Ku_b. \quad (19)$$

Now, consider the space reflection (parity operation) P:

$P:\ x\to x',\ \vec{x}'=-\vec{x},\ x'_0=x_0$

then we get

$$P\varphi_1P^{-1}=\varphi_2$$
$$P\varphi_2P^{-1}=\varphi_1 \quad (20)$$

That is, in this case, the parity operation for φ_1 and φ_2 corresponds to the exchange of φ_1 and φ_2. If the Bosons of spin zero are of the parity mixture of the form (18), then the interaction Hamiltonian takes the form (16) or (17), and this form of the interaction is the same as the one proposed by Green and Hurst[9] for $\pi\mu\nu$ interaction (derivative interaction) assuming the parity doublet for the Fermions. We get thus our fourth conclusion:

To assume the parity doublet for the Fermions has the same results as to assume the parity doublet for the Bosons. (IV)

It may possibly be the total arrangement that is important in nature, and the detailed character of the individual particles such as the transformation properties under the space reflection might be not an important matter for her*.)

Operators $(1+\gamma_5)/2$ and $(1-\gamma_5)/2$ have the meaning of the projection operators defining the left and the right circular waves[16], provided that the mass of the Fermion is zero. As these operators have not such a meaning when the Fermion has a finite mass, we may understand that the expressions (16) and (17) are favorable for the interactions containing the neutrinos, while for the interactions which does not involve the neutrinos, it is more reasonable to employ the expression (15).

Before closing this section, we will consider about the possibility that the

*) We have already pointed out this point of view for the $\pi\mu\nu$ case. (c.f. ref. 4)

interactions of the kaons with the hyperons are the mixture of the derivative and the non-derivative interactions. For the derivative interactions, the equivalence theorem also holds in the lowest order perturbation theory. As ψ and $\bar{\psi}$ satisfy the equations

$$\gamma_\mu \partial_\mu \psi + m\psi = 0, \quad \partial_\mu \bar{\psi} \gamma_\mu - m\bar{\psi} = 0$$

we get

$$H_{int.\ derivative} - i\bar{\psi}_a (G_s \varphi_s + \gamma_5 G_{ps} \varphi_{ps}) \psi_b + h.c. + \text{terms higher than } G^2$$

where

$$G_s = (m_a - m_b) g_s / \kappa$$
$$G_{ps} = (m_a + m_b) g_{ps} / \kappa$$

and m_a and m_b are the masses of the Fermions a and b, and κ is the mass of the Boson. The ratio of the parity mixture for the derivative coupling is, therefore, determined from the ratio G_s/G_{ps}. If the interaction of the kaon with the hyperon is the mixture of the derivative and the non-derivative interactions, it is good enough to make substitutions

$$G_s \to G_s' = G_s + i g_s'$$
$$G_{ps} \to G_{ps}' = G_{ps} + i g_{ps}'$$

in the formular derived for the derivative case. g' means the coupling constant for the non-dervative coupling. The mixing ratio for K_e and K_0 will be of the order of $|G_s'|^2/|G_{ps}'|^2$. As this ratio is usually smaller than unity, the interaction responsible for the production of the kaon will be non-derivative. As these arguments are based on the lowest order perturbation theory and the validity of it for the strong coupling case is quite doubtful, the conclusion has only a poor reliance.

§ 5. Hyperon Decay

Consider the processes

$$\Lambda^0 \to p + \pi, \quad \Sigma \to N + \pi.$$

As is mentioned at the end of the section one, these processes show the angular asymmetries. For the process $\Lambda^0 \to p + \pi^-$ this asymmetry seems to be undoubtful, but for the process $\Sigma \to N + \pi$ we could not assert the angular asymmetry. As we have not considered the other properties of the hyperon than they have spin one-half, no distinction is made between Λ^0 and Σ^0 but for the difference of their mass values. We will content ourselves with getting the reasonable value of α for the process $\Lambda^0 \to p + \pi^-$. Calculations become quite the same as were performed by Taguchi and Kawabe[17], and so we will omit the details of the calculation. The results are, using the matrix element (15):

$$\alpha = \frac{2AR_e(g_s^* g_{ps})}{|g_s|^2 + A^2|g_{ps}|^2}$$

where

$$A = \frac{m_a + m_b}{m_a - m_b} \sqrt{\frac{(m_a - m_b)^2 - \kappa_\pi^2}{(m_a + m_b)^2 - \kappa_\pi^2}}$$

Adopting the values

$m_b =$ mass of the Λ^0 particle $= 1115.2$ Mev.

$m_a =$ mass of the proton $= 938.2$ Mev.

$\kappa_\pi =$ mass of the pion $= 139.6$ Mev.

then we get, assuming $|g_s| \sim |g_{ps}|$,

$$\alpha \fallingdotseq 0.89 \quad (A = 0.616)$$

This value is consistent with the experiments[6].

For the process $\Sigma \to N + \pi$, the value of α become ~ 0.99 and this value does not seem to fit the experiments of ref. 6).

Of course, we can choose the ratio $|g_s| : |g_{ps}|$ so that the value of α may reconcile with the experiments, leaving the degree of the polarization P of Σ equal to that for Λ^0. We get the values of the ratio $|g_s| : |g_{ps}|$ along this line as follows

$$|g_s| : |g_{ps}| \sim \begin{cases} > 2.3 \text{ or } < 0.31 \text{ for } |\bar{P}\alpha| = 0.36^*) \\ > 13.5 \text{ or } < 0.08 \text{ for } |\bar{P}\alpha| = 0.07^{**}) \end{cases}$$

As there is no reason that the degrees of the polarization for the production processes of Λ^0 and Σ, i. e. $\pi + N \to K + \Lambda^0$ and $\pi + N \to K + \Sigma$ should be equal and, in addition, as we have not considered the isotopic spin etc. for the hyperons, these values can not be considered as meaningful.

It is worth while to notice here that, as the result of the conclusion (III), the contamination ratio of the scalar and the pseudoscalar pions from this decay will be different from the one obtained from the usual pion-nucleon interaction, just as the case of the kaon decay.

§ 6. Relation to the Interaction Model and the Future Problem

Various discussions have been done about the interaction models between π; μ, ν; e, ν; p, n. This is the problem that when we draw a picture as shown in Fig. 5, which lines should be binded by the solid lines expressing the existence of the direct interaction. We will examine each of lines separately.

pn–π : There is no doubt to bind this by the solid line.

pn–$e\nu$: This is the interaction responsible for the Beta-decay.

*) The value obtained by Crawford et al.

**) The value obtained by Eisler et al.

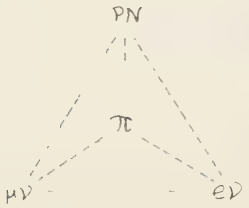

Fig. 5

There are attempts to interprete the beta-decay phenomena by introducing the heavy Boson (B-particle) between pn and $e\nu$. It is the future problem whether it is possible or not to derive the polarization effects for the beta-decay of the oriented nuclei by assuming the parity doublet for the B-particle.

pn–$\mu\nu$: In our stand point of view, this interaction is not always necessary. Interaction between pn and $\mu\nu$ may occur through the intermediary of the pions, and the effect of the parity non-conservation will appear for this interaction.

π–$\mu\nu$: Interactions responsible for the decay of the pions.

π–$e\nu$: Probably unnecessary.

$\mu\nu$–$e\nu$: Interactions responsible for the decay of the muon. Due to the two component theory of the neutrinos, the interaction $\pi\mu\nu$ plays a role of the complete polarizer of the muon, and for the muon thus created, the well known formula for the angular distribution of the emitted electron is derived

$$\sim 2x^2[(3-2x)-\xi\cos\theta\,(1-2x)]dxd\Omega \qquad (21)$$

where

$x =$ electron momentum/maximum electron momentum

$\theta =$ angle between the electron momentum and the spin direction of the muon in the center of mass system of the muon,

$d\Omega =$ solid angle of the electron momentum ejected

and

$$\xi = \frac{g_V g_A^* + g_A g_V^*}{|g_V|^2 + |g_A|^2}$$

g_V ang g_A being the coupling constants for the vector and the axial vector interactions of the Fermi type.

If we want to interprete the phenomena in nature assuming the Yukawa type interactons only without assuming any of the Fermi type ones, and if there is no-direct $\pi e\nu$ interactions, we must suppose the other Boson, with the intermedlary of which the process $\mu \rightarrow e+\nu+\nu$ can occur, because we can not take the pion as the intermediate Boson for this process. We will call this Boson as the B′-particle. Then, this is again the future problem whether it is possible or not to derive the formular (21) by assuming the parity doublet theory for the B′-particles.

There may be the possibility to make the process $\mu \rightarrow e+\nu+\nu$ possible with the intermediary of the pion, assuming the interaction $\pi e\nu$, but if we allow this interaction, the competition will occur between the two processes $\pi \rightarrow \mu+\nu$ and $\pi \rightarrow e+\nu$. As the latter is, in general, predominant than the former, it seems unfavorable to allow the competition of these two processes.

If we forbid both of the two interactions $\pi\mu\nu$ and $\pi e\nu$, the decay of the muon

can occur through the intermediary of the nucleon pair, and again the competition between these two processes will appear. In this case, however, the former will win only for the derivative coupling of the pseudoscalar pion. (The value of the ratio $P(\pi \to \mu + \nu)/P(\pi \to e + \nu)$ is of the order of $\sim 10^{-1}$ for the pseudoscalar pion. Otherwise, it takes the values $1.4 \sim 1.5$[18].) It is interesting to note here that, if we take this third case and if we assume the parity doublet for the pion, then, due to the contamination of the scalar pions, the ratio of $P(\pi \to e + \nu)$ to $P(\pi \to \mu + \nu)$ will have the tendency of increasing. The rate of increasing should be expected to become larger for the pions come from the kaon and the hyperon decays than for the pions created in the pion nucleon interactions.

We get the following classes of the interaction pictures:

i) If we allow the Fermi interactions, the models are as shown in Fig. 6. We can not say anything about the competition between $\pi \to \mu + \nu$ and $\pi \to e + \nu$. The interaction between pn and $\mu\nu$ will occur through the intermediary of the pion.

ii) If we allow every Fermi interactions, then the interaction model will become as is shown in Fig. 7. There are no direct $\pi\mu\nu$ and $\pi e\nu$ interactions.

iii) If we do not allow anyone of the direct Fermi interactions, the model is as is shown in Fig. 8. The possibility of the case iii) is still in question.

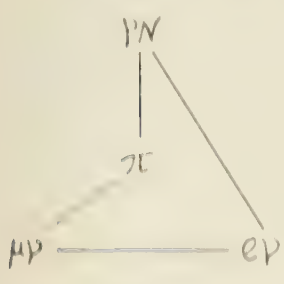

Fig. 6

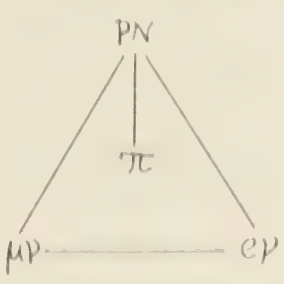

Fig. 7

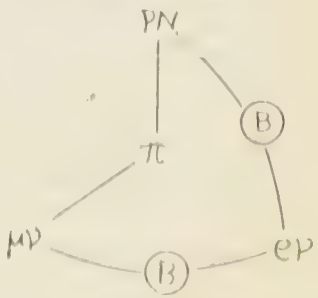

Fig. 8

§7. $\pi \to \mu + \nu$ Decay

I. Introduction of the Theory of Umezawa and Visconti[19]

Assuming the mass of the neutrino being zero, its wave equation becomes

$$i\omega\partial_0\psi = 0$$

where ψ is the neutrino wave function. This equation can be rewritten as

$$(\sigma k)\, u^{\pm}(k) = \pm i\omega u^{\pm}(k)$$

where

ω: the energy of the neutrino ($\omega > 0$)

σ: the 4×4 spin matrix

and $u^+(k)$ and $u^-(k)$ are the positive and the negative frequency part of the ψ, respectively.

Defining the operators

$$\Lambda_+ = \frac{1+\gamma_5}{2}, \quad \Lambda_- = \frac{1-\gamma_5}{2}$$

then we get

$$(\vec{\sigma}\vec{k})\, u_1^{\pm}(k) = -\omega u_1^{\pm}(k)$$
$$(\vec{\sigma}\vec{k})\, u_2^{\pm}(k) = +\omega u_2^{\pm}(k)$$

where

$$u_1^{\pm}(k) = \Lambda_+ u^{\pm}(k)$$
$$u_-^{\pm}(k) = \Lambda_- u^{\pm}(k)$$

Thus, we can interprete $u_1^{\pm}$ and $u_2^{\pm}$ as follows:

u_1^-: left handed state particle

u_1^+: left handed state anti-particle

u_2^-: right handed state particle

u_2^+: right handed state anti-particle

respectively, in which "right handed state" ("left handed state") means that the direction of the spin is, in that state, parallel (anti-parallel) to the direction of its momentum. Therefore, if the neutrino has a vanishing mass, we know that the neutrino can be separated into two components in which $\vec{\sigma}$ and $\vec{k}$ are parallel or antiparallel, by applying the projection operators Λ_1 and Λ_2.

II. $\pi \to \mu \to e$ Decay

Since the pion has a spin zero, if the neutrino has a spin parallel (anti-parallel) to its momentum, then the spin of the muon must be parallel (anti-parallel) to its momentum in the center of mass system of the pion. Thus, for the zero mass of the neutrino, we will have the completely polarized muon.

Because of the existence of the operators Λ_1 and Λ_2 in our matrix elements (19), these situations are just the cases for our choice of the interaction Hamiltonians. Thus, for the massless neutrinos, our theory is equivalent to the two component theory of the neutrinos in the case of $\pi \to \mu \to e$ decay. The muon come from this decay will be completely polarized, and so, by assuming the Fermi interaction between μ, ν and e, ν, we can derive the well known formular (21)[19].

§ 8. Conclusions

We will list up the conclusions obtained by assuming the parity doublet for the Bosons with spin zero.

I. The Pion

The pion should be considered to interact with the Fermions by the derivative coupling, otherwise the contamination ratio of the scalar pions to the pseudoscalar ones becomes too large to explain the experimental resuls. As the effects of the derivative interactions, the mixing ratio should be different as the Fermions the pions interact with are different. The observed mixing ratio will be negligible if the pions are created through the interaction NN–π, but it may be expected to become larger when they are produced by the interactions such as the hyperon decays or the kaon decays.

The pions used in the Panofsky's experiment are the ones obtained from the wolfram target bombarded with the 330 Mev. proton beam. Therefore, the contamination becomes very small because the interactions responsible to the production are expected to be NN–π. So far, almost all of the experiments concerning the pions have used the ones produced through the interaction NN–π, and so we could not expect to find any sorts of the different ratio of the contaminations of the scalar pions to the pseudoscalar ones. The experiments using the pions which have the other origins are desirable to get some informations about the nature of the pions.

II. The kaon

The interaction type of the kaon with the Fermions seems to be favorable for the non-deirvative coupling contrary to that of the pion. The mixing ratio of the scalar kaons to the pseudoscalar kaons will be much larger than the ratio for the pions. The θ and τ particles can be considered as the same particles having several channels of disintegrations.

Up to now, the kaon seems to have not been able to be produced from the decay of other particles, the mixing ratio of the scalar kaons and the pseudoscalar kaons will be almostly constant.

III. The Relation to the Other Theory

To consider the parity doublet results effectively to the violation of the parity conservation as are shown in this paper and in the work done by Green and Hurst[9]. There are two ways for considering the effects of the parity mixture. One of them is to consider the parity doublet for the Fermions as was done by Green and Hurst, while the other lies in taking account the parity mixture for the Bosons. But these two ways give the same answer for the interpretation of the actual phenomena in the case of the Yukawa type interactions.

We will note here as our final remark that if we want to explain all the phenomena which show the disruption of the parity conservation by mixing the Bosons with different parities, we must treat the Fermi interactions by introducing some intermediate particles such as the B-particles or B'-particles.

ACKNOWLEDGEMENTS

The author wishes to express his heartful thanks to Prof. Ozaki for his kind discussions and helps, and to Prof. Narida for his encouragement in the performance

of this work. Without their aids, this investigation would not have been possible. The author is indebted to the late Mr. Yoshihiro Yoshida for his calculational aid in the early stage of this research.

References

(1) Clark, Roberts, Wilson: Phys. Rev. 83 649 (1951)
Durbin, Loar, Steinberger: Phys. Rev. 83 646 (1951)
(2) Panofsky, Aamodt, Hadley: Phys. Rev. 81 565 (1951)
(3) T. D. Lee and C. N. Yang: Phys. Rev. 104 254 (1956)
(4) S. Ozaki, S. Oneda, S. Sasaki: Progr. Theor. Phys. 5 491 (1950)
(5) T. D. Lee and C. N. Yang: Phys. Rev. 105 1671 (1957)
A. Salam: Nuovo Cimento 5 299 (1957)
L. Landau: Nuclear Physics 3 129 (1957)
(6) F. S. Crawford et al: Phys. Rev. 108 1102 (1957)
F. Eisler et al: Phys. Rev. 108 1353 (1957)
(7) R. Gatto: Phys. Rev. 108 (1957)
(8) T. D. Lee and C. N. Yang: Phys. Rev 104 822 (1956)
(9) H. S. Green and C. A. Hurst: Nuclear Physics 4 589 (1957)
(10) Brueckner, Serber, and Watson: Phys. Rev. 81 575 (1951)
(11) S. Ozaki, S. Oneda and S. Sasaki: Soryushiron Kenkyu IV 7 (1949), Vol. 1 No. 1 110 (1949)
(12) Fukuda and Miyamoto: Progr. Theor. Phys. 4 347 (1949)
(13) S. Sasaki, S. Oneda and S. Ozaki: Progr. Theor. Phys. 4 524 (1949); 5 25, 165, 305(1950)
S. Ozaki: Progr. Theor. Phys. 5 373 (1950)
(14) A. Fujii and R. E. Marshak: Nuovo Cimento, in press.
(15) G. Alexander, R. H. W. Johnston and O'Cealleigh: Nuovo Cimento 6 478 (1957)
(16) H. Umezawa and A. Visconti: Nuclear Physics 4 224 (1957)
(17) T. Taguchi and R. Kawabe: Progr. Theor. Phys. 19 586 (1958)
(18) M. Ruderman and R. Finkelstein: Phys. Rev. 76 1458 (1949)
(19) T. Kinoshita and A. Sirlin: Phys. Rev. 107 593 (1957)

SOME STUDIES ON VOLCANIC ACTIVITY OF VOLCANO SAKURA-JIMA (PART 2), ON THE EXPLOSION SOURCE "MAGMA RESERVOIR" AND THE PROCESS OF VOLCANIC ACTIVITY

Yasuhiro SUGIMOTO and Munetoshi NAMBA

(Recieved Jan. 20th 1958)

Abstract

The writers assumed that volcano Sakura-jima has two energy sources or magma reservoirs and analysed the process of volcanic activity by taking into accounts of type A of volcanic tremors which are recorded from Apr. to Dec. in 1957 at Hakamagoshi by kagoshima L. M. O.

The process of volcanic activity is expressed as follows:

1) Firstry, a volcanic activity should be occurred in the first reservoir;

2) Its activity transports to the second reservoir;

3) And next, the volcanic energy may be gathered in the third reservoir which is under the active crater, and at last a surface activity occurrs.

4) When a surface activity bocomes to be an end, the volcanic earthquakes occurr near second reservoir owing to the decreasing of the pressure at the upside of the volcanic vent tube.

5) And next, the source descends to the first reservoir and at last the volcano returns to a dormant period.

§ 1 Foreword.

Volcauo sakura-jima erupted at Minamidake old crater on 13th (14h 53m 30.3s) Oct. 1955.[1]

Earthquake accompanied by an explosive eruption which was recorded on Wiehelt seismometer at Kagoshima L. M. O., about 10 km west the active crater, and its maximum amplitude is 439μ, P–S is 2 sec., the first motion is East and "pull", and the eruption made an East-West crack which is comfirmed by the photograph and the actual observation[1,7].

The eruption emitted out many ejecta about 500,000 tons, and it was computed the kinetic energy of ejecta to be about 10^{19} erg and that of the volcanic earthqnake to be about 10^{18} erg employing Gutenberg-Richter's formula and Benioff's by Mr. Y. Yasui, Kagoshima L. M. O[8]..

After that time, explosion occurred 15 time till the end of Oct. 1955 and it dormanted between Nov. and Dec.. And after that the surface explosive eruptions took place about 10 times in every month, but the eruption becomes weak and occurred only once in tow or three months since Apr. 1957 which is seemed to be a

dormant period.

The eruption of Oct. 1955 followed by no lava flow, and this eruption has some forrunner phenomena just like to that in 1941.[2,3]

Therfore, they discussed on the process of volcanic activity and on the explosion source or magma reservoir taking in to acounts of P–S of whole type A and other records in every cases of volcanic activity in Sakura-jima.

§ 2 On the Explosion Source or Magma Reservoir.

Mr. R. Nakamura of Kagoshima L.M.O. has tried a crassification of the volcanic earthquakes and tremors that was recorded on a microseismometer of 450 times at Hakamagoshi, about five kilometers west from the crater as the following types:[7]

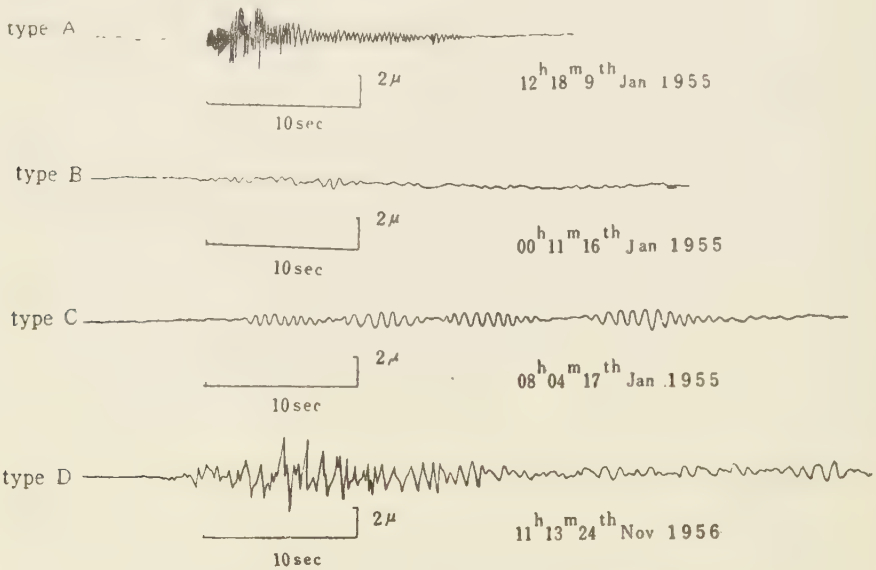

Fig. 1. The modes of volcanic tremors and earthquakes at Hakamagoshi, by R. Nakamura, Kagoshima L.M.O.

Type A is deep volcanic earthquake of 0.1 sec. or less in period, and according to the method of investigation of Prof. T. Minakami, it has its hypocenter about one kilometer or beyond.

Type B is a solitary micro and shallow erathquake which is the main part of the volcanic tremors.

Type C is a spindle shape ossilation, scarcely occurred since the eruption of Oct. 1955.

Type D is accompanied by an explosive smoking since the eruption of Oct.. It has comparatively short period or comparatively large one, about three seconds.

This writers discussed on the magma reservoir of Aira volcano in first report

part 1.[9] It may be considered that the resrvoir situates at 10 km under the sea level near An'ei islands and its diameter is about 6.5 km as a sphere. And now they discussed on the explosion sonrce or magma reservoir and the process of volcanic activity taking into accounts of whole volcanic tremors of type A which is recorded between Apr. 1957 and Dec. 1957 at Hakamagoshi by Kagoshima L. M. O. (table 1, Fig. 2) employing high sensibility microseismometer.

Table 1. List of P–S intervals of type A at Hakamagoshi in 1957, observed by Y. Yasui, Kagoshima L. M. O.

Date	P–S sec 6~5	5~4	4~3	3~2	2~1	1~0	Total
Apr. 15					2		2
19					1	1	2
20					1		1
23					3		3
27					2		2
28					1		1
30			1		2		3
May. 3					1	1	2
5						1	1
8						1	1
14	1		1		1		3
17					1		1
18		1			3		4
20			1				1
22			1				1
23			1		1		2
24					1		1
30		1			1		2
Jun. 3					1		1
9					1		1
17					1		1
19						1	1
21					2		2
29						1	1
Jul. 11				1			1
18				1			1
30					1		1
Aug. 4	4						4
9					1		1
10					1		1
11					2		2
12					1		1
13						1	1
14					2		2
15		1		1			2
23				2			2
28					2		2

Date		P–S sec 6~5	5~4	4~3	3~2	2~1	1~0	Total
Sep.	1					1		1
	12						1	1
	14					1		1
	15				1	1	1	3
	16				1			1
	17		1	1	1			3
	18					1		1
	24			2				2
	28						1	1
	29						1	1
	30					1		1
Oct.	1					1		1
	4			1				1
	6					2	1	3
	8					1		1
	12						1	1
	14					1		1
	15					1		1
	16						1	1
	19	1						1
	20	1						1
	23		(P-S ? 1)					1
	25					1		1
	26					1		1
	27			1				1
	31					1		1
Nov.	1					1		1
	5					1		1
	6			1			1	2
	7			1				1
	13			1				1
	15				1			1
	18						1	1
	20				1			1
	22		(P-S ? 2)					2
	29					2		2
Dec.	1					1		1
	5					1		1
	7					1		1
	8			1				1
	10			1				1
	15						1	1
	27		(?)					
	30	1	1					2

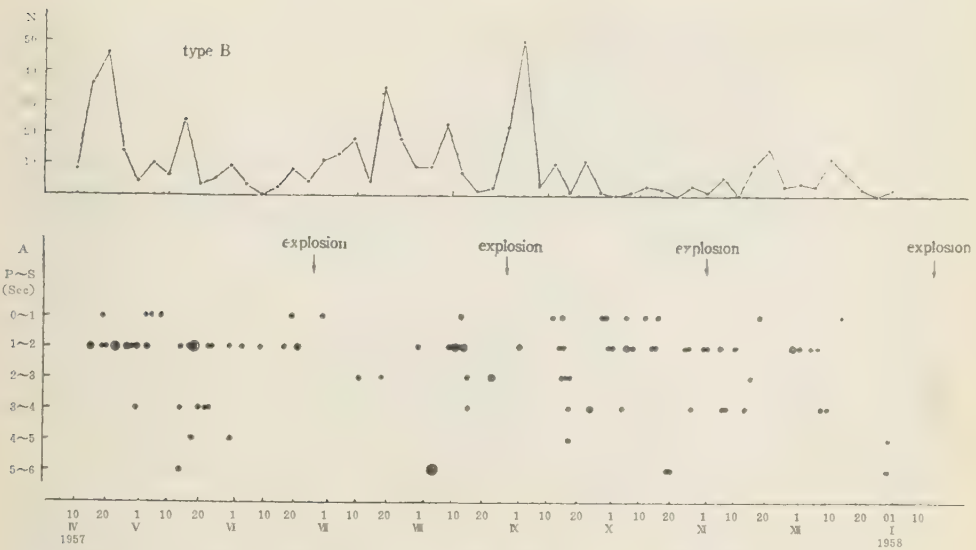

Fig. 2. Frequency distribution of P–S intervals of type A (lower) and that of type B (upper) observed at Hakamagoshi by Y. Yasui, Kagoshima L. M. O.

As is shown by Fig. 2, P–S 1–2 sec., 0–1 and 3–4 sec. are main part of the P–S (table 1, Fig. 2).

Volcanic earthquake occurrs at the upper part of magma reservoir when a volcanic gas passing through there[10]. Threfore, by the above view, the writers comfirmed that there must be two magma reservoirs under volcano Sakura-jima. The first reservoir must be at about 10 km under the sea level near An'ei islands, about 2 km NE off Sakura-jima, and the second one has a depth of 3 km from the sea level under Nakadake old crater and it is about 1.5 km in diameter.

On the other hand, a focal distance D is calculated 3 or 4 km per second of P–S by Mr. Y. Yasui[16]. This writers used 3.5 km in every second of P–S as the mean values of the above, and they adopted it to the following expression:
$D=3.5\times(P-S)$ km.

It is assumed that the hypocenter of 1.5 sec. P–S is at about 2.5 km under the bottom of the crater, and of 3.5 sec. P–S is at about 7 km under the sea level of North-East coast of Sakura-jima. In generaly, the volcanic earthquake occurrs between 1.5 km to 7 km under the sea level as well as the case at volcano Aso[13], Mihara and Usu.

From the above, it may be computed that the center of first magma reservoir must situate at about 10 km under the sea level with 6 or 7 km in diameter, and the second one must be at about 3 km under Nakadake crater and it has a diameter of 2 or 3 km. Fig. 3, 4)

According to the above mention, the main cause of the explosion in Oct. 1955 must be the increasing of magma pressure in the second reservoir, because of the type A of about 1.5 sec. was mostly predominated before the explosion of Oct. 13th

Fig. 3. Map of Volcano Sakura-jima.

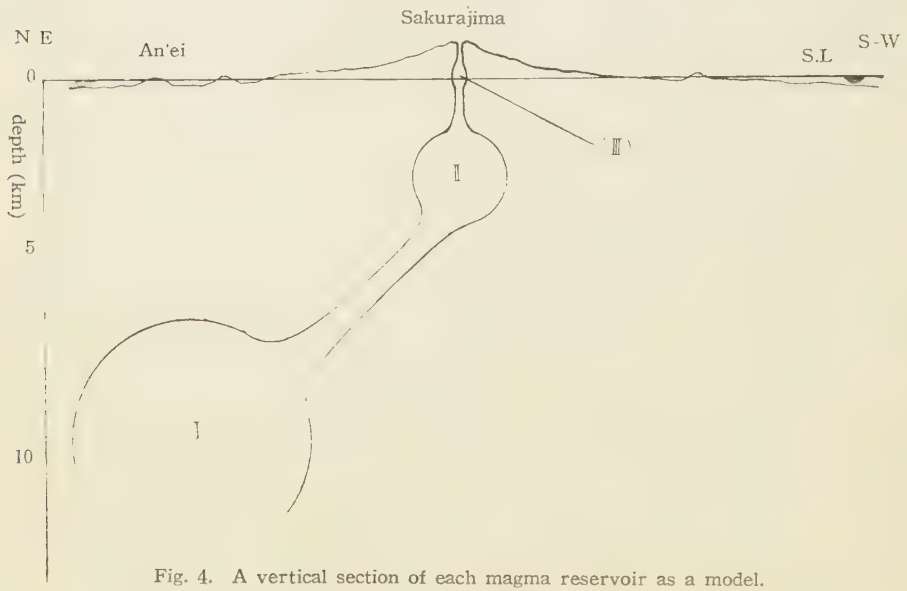

Fig. 4. A vertical section of each magma reservoir as a model.

1955. (table 2) It will therefore be easily suporsed by above reason that the explosion must not be occurred in so large scale.

Table 2. The readings of volcanic earthqukes (type A) at Hakamagoshi, (Ishimoto type: 450 times), observed by Y. Yasui.

Seismicity	Occurrence time	P–S (sec)	amplitude (μ)	period (sec)	P–F (sec)
		h m s			
0	1955 Jun. 3, 12 56 00	1.9	3.3	0.8	70
0	3, 14 20 00	1.5	0.8	0.7	55
0	Dec. 8, 14 39 54	0.5	3.2	0.1	10
0	1956 Jan. 12, 11 09 28	2.4	2.6	0.2	20
0	13, 00 40 00	1.0	1.1	0.2	20
0	13, 02 37 00	3.0	0.6	0.1	15
0	Mar. 21, 04 27 00	—	0.3	0.2	55
0	24, 20 45 00	—	0.3	0.2	30
0	Apr. 5, 02 50 00	—	0.3	0.3	25
0	26, 03 50 00	—	0.5	0.1	25
0	May. 10, 00 09 33	1.6	4.1	0.1	40
0	17, 11 53 53	1.6	15.7	0.1	40
0	18, 15 03 38	1.4	26.0	0.1	06
0	18, 15 20 02	1.1	2.2	0.1	05
0	24, 10 10 07	2.0	1.8	0.1	40
0	Jun. 10, 14 35 42	3.3	17.4	0.1	—
0	12, 20 54 15	1.6	6.6	0.1	25
0	27, 10 24 29	2.0	6.6	0.1	20
0	Jul. 1, 00 36 09	2.0	5.9	0.1	25
0	16, 21 28 00	1.5	0.6	0.2	15
0	18, 02 00 24	0.5	0.8	0.3	20
0	18, 21 56 54	1.0	0.6	0.1	15
0	Aug. 11, 19 57 00	1.5	2.2	0.1	15
0	Sep. 20, 01 20 07	—	0.9	0.1	10
0	Oct. 18, 19 22 00	1.3	tremor	—	10
0	22, 16 23 00	1.6	tremor	—	25

§ 3 On the Process of Volcanic Activity.

Kagoshima L. M. O. pointed out that the time-lag between the peek of tremors of type B and an explosion is 30 or 40 days, and that the period of wave-motion was enlarged to about 0.8 sec[11]. The investigation of Prof. T. Minakami said that the hypocenter of type B must be very shallow than the hypocenter of type A[12]. As the writers believd that the energy of a surface explosion must be charged by a deep magma reservoir, the main origine of type A must be the first magma reservoir.

One of the writers analysed each P–S of type A which was observed at Hakamagoshi from April to December in 1957. (Table 1, Fig. 2) The relation between the number of P–S and laspe time refer to an explosion are figured in Fig. 5, taking into accounts of whole type A. And now, he analysed the daily variation of each

P–S as is shown by Fig. 5.

A surface activity occurred about a month later than the peak of P–S of 4–6 sec., the cause of which is due to the activity of the first magma reservoir, and it has occurred about half a month after the peak of P–S of 1–2 sec., the cause of which is due to the activity of the second reservoir. (Fig. 5)

The volcanic energy probably ascends upward and comes togather at the third reservoir (a quasi-reservoir) during about half a month after the activity of the second reservoir, then it breaks out the bottom of the Minamidake crater as a surface eruption.

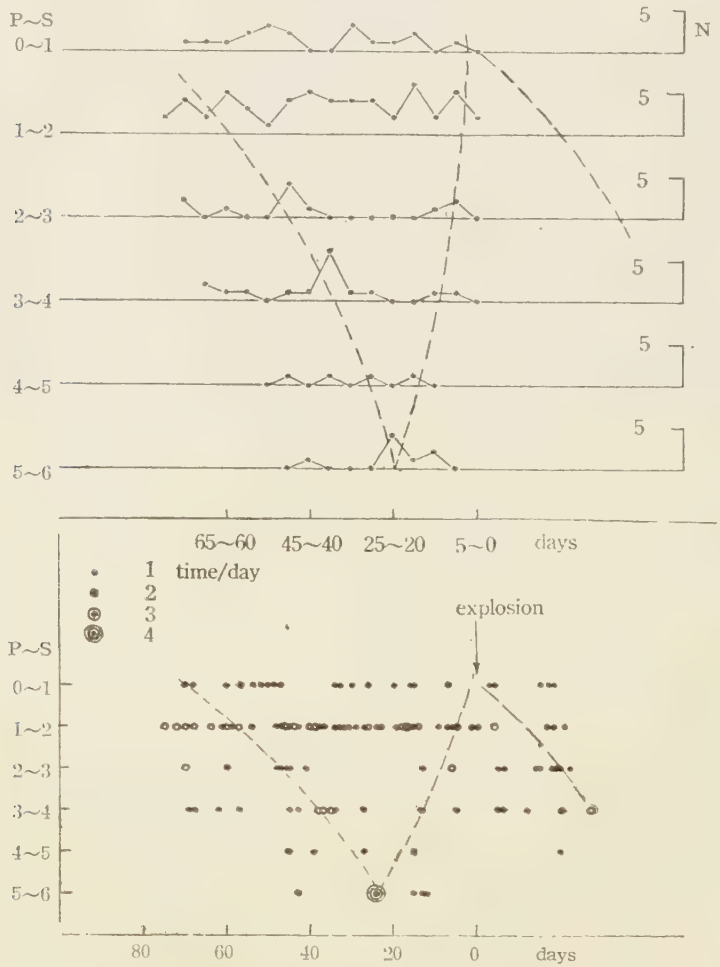

Fig. 5. Frequency distribution of P–S intervals of type A before each explosion.

Prof. T. Minakami pointed that the type B appears on 10 or 15 days before an explosion. This process is also held at volcano Aso. After a surface explosion ceases the center of activity seems to descend from surface to subteranean due to the pressure decreasing of the surface parts, and therfore earthquake disapear in the third reservoir, and next occurrs in the second reservoir and at last they appear at the first one, then a dormant period begine.

In 1955 Sakura-jima acted mainly due to the second reservoir, because the type A of 1.5–1.9 sec. P–S were happend as shown by table 2, and now the activity of the first reservoir began since early of 1956, and the activity of Sakura-jima became violent. Therefore by the explosion since Apr. 1956 the lots of original ejecta were emitted, and some of them are picked up by Prof. H. Tsuya and Mr. Tanabe at Nakadake on Apr. lst 1956[5,7]. Pumices are observed at Kurokami region on Apr. 24th 1956[4,5], and also the people felt a vertical motion of volcanic earthquake at Naka-no-shima, An'ei islands on Nov. 22nd 1956[6]. Sensible earthquakes type A were observed at Yuno and Arimura on Jan. 19th 1956[6,15].

In generaly, the scale of vertical motion becomes rather larger than the horizontal motion since the explosion of 1955[7].

From this phenomena, it may be seemed that the volcanic activity has occurred not only near shallow part but also arround the first reservoir. The activity in the first reservoir probably becomes energitic as well as in the second one, and the activity in the second reservoir since 1956 should made some effects on the magma pressure of the first one.

Above mentioned process almost agrees with the case of volcano Aso at which avolcanic earthquake occurrs before its surface activity[10].

Now the writers deduced a new process of a volcanic activity, that is the activity center returns to the first reservoir from the surface owing to the decreasing of the volcanic pressure due to the surface activity; shortly, the volcanic activity at first begins at the first reservoir and again at last it ceases at there. (Fig. 5)

This writers explains scematicaly a process of volcanic activity mentioned above as follows:

1) At first, a volcanic activity should be occurred in the first reservoir.

2) Its activity transports to the second reservoir.

3) Then next, the volcanic energy may be gathered in the third reservoir which is under the active crater, and soon after, an explosion takes place as a surface activity.

4) After a surface activity becomes weak, micro-earthquakes occurre near the second reservoir owing to the decreasing of the magma pressure in the upside of it.

5) And again, the first magma reservoir some earthquakes occurr, and at last volcano again returns to a dormant period.

§ 4 On the Relation between the Surface Activity and the Amount of Precipitation.

The writers analysed a relation between surface activity in an active stage of volcano Sakura-jima and amount of precipitation at Kagoshima in 1956.

The resulting correlation is expressed as the following equation

$$N_{max}=8\times e^{-0.0115R}$$

where N_{max} is maximum frequency of explosion in every five days, R is the amounts of precipitation in every five days in mm.

It may be said that an explosion in an active stage of the volcano comparatively often occurrs on a fine day or after a rainy day .(Fig. 6)

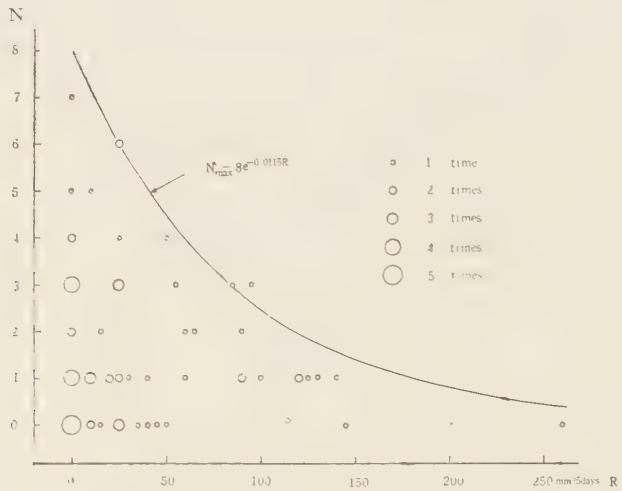

Fig. 6. Numbers of cases with N explosions and R amounts of precipitation in every five days (1956)

Then the writers analysed the daily variation about 170 or more of its explosions, and obtained that 63% of them occurred in the day time, that is the volcano is explosive at the most changeble houre of the atmospheric pressure. This means that the volcanic explosion may often occurrs after the maximum of semidiurnal variation of the atmospheric pressure. This fact is simillary observed at volcano Aso and other volcanoes[15].

§ 5 Conclusions.

The writers discused on the volcanic earthquakes and microtremors at Volcano Sakura-jima as follows: –

1) Volcano Sakura-jima has two explosion sources "magma reservoirs or magma domes". The first reservoir situates at about 10 km under the sea level near An'ei islands and its diameter is about 6 or 7 km. The second one situates under Nakadake, its depth is about 3 km and its diameter is about 2 or 3 km.

2) The main cause of the explosion in Oct. 1955 is the increasing of magma pressure in the second reservoir.

3) The process of volcanic activity of Volcano Sakura-jima are probably rolled

on as follows in scematicaly;

i) The second reservoir becomes active due to some energy which has been sent up from the first erservoir.

ii) Then its energy was sent up under the active crater at which there may be the third reservoir (a quasi-reservoir), and an explosion occurrs as a surface activity.

iii) When the volcano comes near a dormant period of the surface crater, type A earthquakes again awake in the second reservoir due to the decreasing of magma pressure in the third one or upper part of the vent tube.

iv) And then again some shocks are happened in the first reservoir, and after them, at last, the volcano entirely returns to its dormancy.

4) The explosion scarcely occurrs during the heavy precipitation. And an explosion often occurrs in the day time. This agrees to the case at volcano Aso that an explosion often occurrs after maximum atmospheric pressure in the fore noon. This is perhapse due to the changeability of the atmospheric pressure in the day time.

The detailed studies on the above facts must be continued through more long times. If volcanic earthquakes are observed at North-East and North coast of Kagoshima Bay the process of the volcanic activity above mentioned will be investigated more clearly.

In conclusion, the writers express their hearty thanks to Mr. Y. Yasui, chief of the observing section of Kagoshima L. M. O. who allowed them to use the records in his observetory and to Prof. S. T. Nakamura who gave his kind encouregement, and also to Mr. M. Sato for his figurings.

This paper was read on Feb. 28th, 1958 at the seminar of this facluty.

References

1. Kagoshima L. M. O.: Urgent report of the explosion at Volcano Sakura-jima No. 1 (1955).
2. 〃 〃 〃 〃 No. 2
3. 〃 〃 〃 〃 No. 3
4. 〃 〃 〃 〃 No. 4
5. 〃 〃 〃 〃 No. 5
6. 〃 〃 〃 〃 No. 6
7. Kagoshima L. M. O.: Report on the eruption of Volcano Sakura-jima in 1955 and 1956, Memoirs of Fukuoka M. O., No. 13 (1957).
8. Y. Yasui: The eruption smokes of Volcano Sakurajima (1), "Kenkyu-jiho", Vol.9, No. 3 (1957).
9. Y. Sugimoto and M. Namba: Some studies on Volcanic activity of Volcano Sakura-jima (part 1), Kumamoto J. of Science, A, Vol. 2, No. 4 (1957)
10. M. Namba: A consideration on the process of earthquake frequency followed by a volcanic explosion, Chikyu-Butsuri Vol. 7, No. 3 (1943)
11. A. Imasato, Y. Yasui, Y. Noda, H. Yamakata and R. Nakamura: On the Characteristics of the Occurrence of Volcanic Tremors and Quakes of volcano Sakurajima. Bull. Volcanol. Soc. Japan II, Vol. 2, No. 1 (1957)
12. T. Minakami, K. Mogi and the others: On the investigation of explosive activities of Sakura-jima and various earthquakes originating from the volcano (1), Bull. Volcanol. Soc. of Japan, II, Vol. 2, No. 2 (1957)

13. K. Sasa: On the distribution of the hypocenter of Volcano Aso, Chikyu-Butsuri Vol.3, No. 1 (1939).
14. The letter from Y. Yasui to M. Namba on Jan. 28th, 1956.
15 M. Namba: The effect of atmospheric pressure on volcanic explosion, Chikyu-Butsuri Vol. 6, No. 3 (1942)
16. The letter from Y. Yasui to M. Namba on Jan. 12th, 1958

NOTE ON THE TAKARA-JIMA ANNULAR ECLIPSE EXPEDITION

A. ONUKI, S. SASAKI, T. CHIKAZAWA, T. MATSUMOTO
S. MITSUSHIMA
Institute of Science, Kumamoto University
and
H. KOZUMA
Research Laboratory, Shin Nippon Chisso Co.

The observation of the annular eclipse on April 19th, 1958, was planned and executed under the co-operations of Kumamoto and Kagoshima Universities. The details of the results obtained will be published in future. Here, we report only brief and preliminary notes on this expedition.

Takara-jima ($\varphi = 29°8'7\ N$, $L = 129°12'\ 4\ E$), the small island in the Tokara Retto in Kagoshima Prefecture, was selected as the place of the observation, because the position of the island is exactly on the predicted central line of the eclipse. Expedition party (composed of 6 members; the leader, Ass. Prof. A. Onuki) started from Kagoshima on April 16th by the "Keiten-maru" (260 tons), a training boat belonging to Kagoshima University.

Four-inch equatorial telescope and 800 mm Canon equatorial telescope with color filters were used for observations, while the intensity of the sky-light during the eclipse was measured by the "whole sky camera" as was done in the former expedition[1]. These instruments were set on the play-ground of the Takara-jima Middle School, which is built in the northern side of the island and is about 70 meters high above the sea-level and 700 meters from the sea shore.

The weather was almost fine when the eclipse began, but became worse gradually, and at the moments of the third and the fourth contact, the sun was covered by a thin speck of clouds which made the contact time determination more or less difficult. These observed times of contact were compared with the NHK radio and were corrected within 0.1 sec. The corona and the shadow band[1] were not recognized as was previously expected.

Schema of measuring plan is shown in Table 1. In Fig. 1, the changes of the air temperature, humidity, and the atmospheric pressure are plotted. The plates in the following pages are the several of the photographs taken by the 800 mm Canon lens.

The careful examination of the results obtained in this expedition are now in progress, and will be published in future, but by some unfortunate reasons, it was found that the four-inch plates are not available for the exact determination of the contact times.

We returned to Kagoshima on April 22nd. On its way, the crew members of the "Keiten-maru" had engaged in the oceanographic observation in the chain of the I. G. Y. program.

We thank the authority of Kagoshima University for granting the use of the "Keiten-maru", also we express our heartful thanks to the peoples and especially to the schoolboys of the Takara-jima island for their kindness offering any sorts

of facilities for our purposes of the observations. And also we express our thanks to Shin Nippon Chisso Co. who kindly helped us in many aspects.

J. S. T.	Photo No.	Photo No.	J. S. T.	Photo No.	Photo No.
h m s			h m s		
10 54 22	0		12 46 47	12	5
12 42 0	1		47 15		6
15	2		48 15		7
30	3		49 0	13	
45	4		15	14	8
43 0	5		30	15	
15	6	1	45	16	
30	7		50 0	17	
45	8		20	18	9
44 0	9		30	19	
15	10	2	45	20	
30	11		51 0	21	
45 15		3	15	22	
46 15		4	30	23	

Table 1. Schema of measuring plan.
First column shows Japanese Standard Time.
Second column shows the photo no. taken by 800mm Canon.
Third column shows the photo no. taken by 4-inch equatorial telescope.

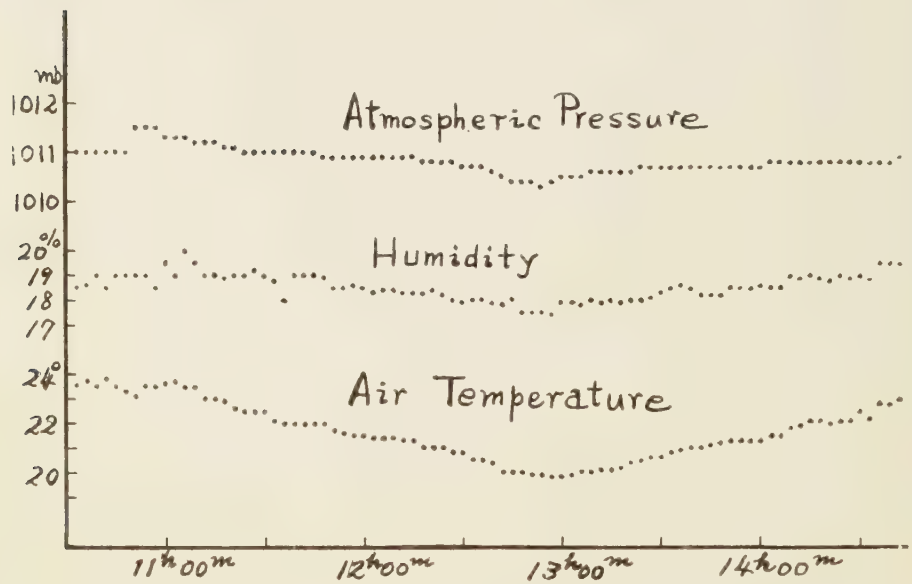

Fig. 1 The changes of the air temperature, humidity, and the atmospheric pressure.

Reference

1) A. Onuki: Kumamoto Journal of Science A2 378 (1956)

Photo No. 0 $10^h\ 54^m\ 22^s$
April 19, 1958. at TAKARA-JIMA:
Phys. Inst. Kumamoto University

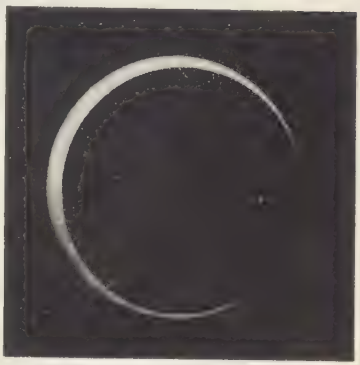

Photo No. 6 $12^h\ 43^m\ 15^s\ 1$
April 19, 1958. at TAKARA-JIMA:
Phys. Inst. Kumamoto University

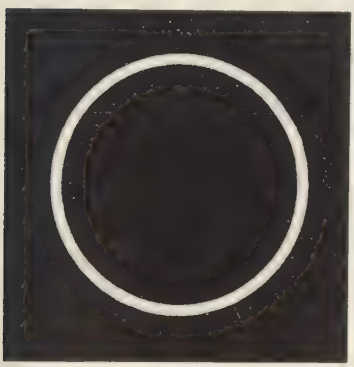

Photo No. 12 $12^h\ 46^m\ 47^s\ 5$
April 19, 1958. at TAKARA-JIMA:
Phys. Inst. Kumamoto University

Photo No. 16 $12^h\ 49^m\ 45$
April 19, 1958. at TAKARA-JIMA:
Phys. Inst. Kumamoto University

THE EFFECT OF DEMAGNETIZATION ON THE LONGITUDINAL MAGNETOSTRICTION IN WEAK MAGNETIC FIELD (II)

Gunki KOYASHIKI and Shigeo MATSUMAE

(I) Introduction

The longitudinal magnetostriction in weak magnetic field is greatly affected, when the specimen is demagnetized with the alternate magnetic field, as already described[1][2][3]. We study this phenomenon in Fe and Fe–Ni alloy. The experimental results are as follows.

(II) Experimental Results and Discussions.

The apparatus and the process of the experiment are the same as in the previous papers.

For example, the specimens are round bars of Fe and Fe–Ni (50%) alloy, 1.5 mm in diameter and 22 cm in length. The specimens are annealed at 900°C for 2 hours and cooled in the furnace to the roomtemperature.

At first, the specimens are demagnetized with the alternate magnetic field of about 7 Oersted in the case of Fe and about 6 Oersted in the case of Fe–Ni (50%) alloy, and then the tensive stresses of 1.2 kg/mm^2 for Fe and 0.6 kg/mm^2 for Fe–Ni (50%) alloy are applied. The experimental results are shown in Fig. 1 (a) and Fig. 3 (a).

But, in Fe, when it is demagnetized with the alternate magnetic field having the maximum amplitude of about 8 Oersted, the longitudinal magnetostriction decrea-

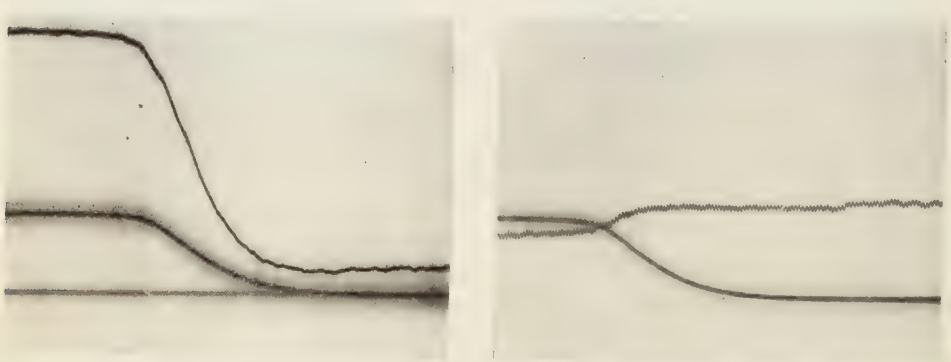

(a) Before demagnetizing

(b) After demagnetizing with the alternate magnetic field

Fig. 1 Oscillograph-records of the longitudinal magnetostriction of Fe in weak magnetic field under the tensive stress of 1.2 kg/mm^2.

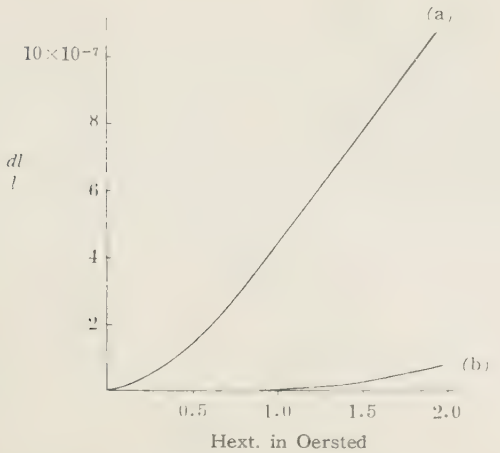

Fig. 2 $\frac{dl}{l}$–Hext curves of the oscillograph-records
(a) Before demagnetizing
(b) After demagnetizing

ses and becoms almostly vanishes, as shown in Fig. 1 (b) and Fig. 2. And in Fe–Ni (50%) alloy, when it is demagnetized with the alternate magnetic field having the maximum amplitude of about 7 Oersted, the longitudinal magnetostriction does not decrease so much as in Fe, as shown in Fig. 3 (b) and Fig. 4.

Such tendency which the longitudinal magnetostriction is affected greatly by demagnetization is observed in Fe, Ni and other Fe–Ni alloys.

From these facts, the longitudinal magnetostriction in weak magnetic field is considered to be caused by the unstable magnetic domain or the unstable domain-boundary produced by the proper internal stress in the specimen.

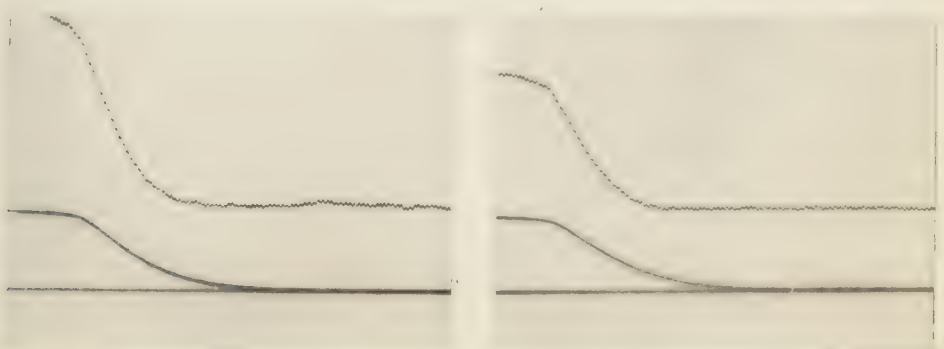

(a) Before demagnetizing

(b) After demagnetizing with the alternate magnetic field

Fig. 3 Oscillograph-records of the longitudinal magnetostriction of Fe Ni (50%) alloy in weak magnetic field under the tensive stress of 0.6 kg mm-

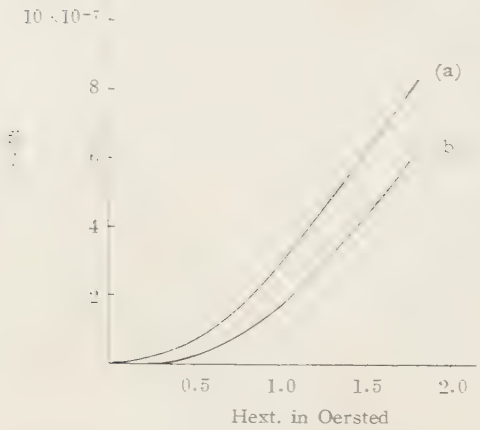

Fig. 4 $\frac{dl}{l}$–Hext curves of the oscillograph-records
(a) Before demagnetizing
(b) After demagnetizing

References

(1) S. Matsumae: "The Effect of Demagnetization on the Longitudinal Magnetostriction in Weak Magnetic Field" Kumamoto Journal of Science Vol. 2. No. 4. 1956.
(2) S. Matsumae: "The Effect of the Internal Stress on the Longitudinal Magnetostriction in Weak Magnetic Field" Kumamoto Journal of Science Vol. 2. No. 2. 1955.
(3) S. Matsumae: "The Effect of the Heat-Treatment on the Longitudinal Magnetostriction in Weak Magnetic Field (II)" Kumamoto Journal of Science Vol. 2. No. 2. 1955.

昭和33年12月15日印刷
昭和33年12月20日発行

非売品

編輯兼発行者　熊本大学理学部
印刷者　佐伯善次
印刷所　佐伯印刷所
熊本市大江町九品寺138
電話㊋2355・㊎2958番